Morphodynamic hazard analysis for river restoration and flood mitigation measures

Dissertation

submitted to and approved by the

Department of Architecture, Civil Engineering and Environmental Sciences
University of Braunschweig – Institute of Technology

and the

Faculty of Engineering
University of Florence

in candidacy for the degree of a
Doktor-Ingenieur (Dr.-Ing.) /
Dottore di Ricerca in Risk Management on the Built Environment *)

by
Annette Schulte-Rentrop
Born 28 July 1976
from Münster/Westf., Germany

Submitted on	18 September 2009
Oral examination on	6 November 2009
Professorial advisors	Prof. Andreas Dittrich
	Prof. Enio Paris

2009

*) Either the German or the Italian form of the title may be used.

ACKNOWLEDGEMENTS

There are many people in my life to whom I owe my gratitude and who supported and accompanied me during the last years and until the delivery of this work.

First of all, I would like to thank my first tutor Prof. Andreas Dittrich for giving me the opportunity for this work at his institute, for his helpful recommendations and suggestions and for letting me participate in his expertise throughout these years.

Moreover, I would like to thank my second tutor Prof. Enio Paris for supervising my thesis from the Italian side. He always found the time for discussion and I appreciated very much his fruitful recommendations and motivation.

Special thanks go to Prof. Matthias Schöniger who kindly admitted to step in as part of the commission on short notice. Frau Schulze sagt Danke!

Furthermore I would like to thank Prof. Nils Reidar Olsen from NTNU Trondheim for giving me the opportunity to work as guest scientist at his department. I owe him and his associates deep gratitude for expertise, availability and help to progress which, without them, would have not advanced as it finally did.

My gratitude goes also to my former colleagues at the Leichtweiß-Institut, especially Dr.-Ing.s Katinka Koll, Jochen Aberle and Bernd Ettmer and to Matthias, Irene and Heidrun for helpful discussions, motivation and nice time apart from science and theory.

In addition, I owe my thanks to Prof. Claudio Borri and Prof. Udo Peil for their effort as coordinators of the International Graduate College 802. It is due to their initiative that I could do my research while in parallel getting to know a beautiful country with great cultural background and wonderful people. I am missing these weeks and months very much and will keep these friendships and intense memories in my mind. My special thanks go to Nadine, Katharina, Nancy and Camilla for letting me live this wonderful time in Via Massaia.

Special thanks go to Dr.-Ing. Matthias Reinighaus, Matti Dechentin and his student for making it possible that I could finish my thesis in time despite technical problems.

My deepest gratitude goes to my parents and sister for having accompanied me through all the years and for their permanent support, motivation and love since I can remember. The same goes to my friends. I am looking forward to spend more time with you all.

Last but not last, I owe my thankfulness to Steffen for his imperturbable patience, motivation, help and love.

KURZFASSUNG

Im Zuge des Klimawandels und der Umsetzung der EU-Wasserrahmenrichtlinie werden neue nachhaltige und naturverträgliche Hochwasserschutzkonzepte wie Reaktivierung von Flussauen oder naturnahe Umgestaltung von Fließgewässern erforderlich. Allerdings ist es bis heute aufgrund der komplexen Wechselwirkungen zwischen Flussgeometrie, Strömung, Vegetation und Sedimenttransport nicht möglich, die Wirksamkeit und Nachhaltigkeit von naturnahen Maßnahmen bereits im Planungsstadium abzuschätzen. Morphodynamische Prozesse spielen jedoch bei der Verlässlichkeit von naturnahen Hochwasserschutz-maßnahmen eine ausschlaggebende Rolle.

In der vorliegenden Arbeit wird ein neues Konzept zur Abschätzung von lokalen morphodynamischen Prozessen entwickelt, welches bei der Planung von nachhaltigen, naturnahen Hochwasserschutzmaßnahmen herangezogen werden kann. Die detaillierte Aufarbeitung zum Stand des Wissens und der Technik verdeutlicht die komplexen dreidimensionalen Wirkungszusammenhänge zwischen Flussgeometrie, Strömung, Sedimenttransport und Vegetation. Es wird aufgezeigt, dass es bislang kein verlässliches Planungswerkzeug gibt, mit dem die Entwicklung von naturnahen Flusssystemen mit Vegetation in hoher räumlicher Auflösung abgeschätzt werden könnte. Herkömmliche Ansätze bestehend aus 1D- oder 2D-Modellen und GIS-Anwendungen weisen signifikante Unsicherheiten hinsichtlich der Rauheitserfassung sowie der Berechnung der Hydrodynamik und der Sohlschubspannung auf und sind daher für hoch aufgelöste Fragestellungen bei komplexer Flussgeometrie mit Vegetation nicht geeignet. Darüber hinaus werden verfügbare Ansätze kaum auf ihre Anwendbarkeit im jeweiligen Flusssystem hin überprüft oder mit Felddaten validiert.

Der Hauptbeitrag der vorliegenden Arbeit liegt auf einer neuen schrittweisen Methode zur Identifikation, Analyse und Bewertung der Gefährdung durch morphodynamische Prozesse in naturnahen, kiesführenden Fließgewässern. Mithilfe der Risiko-Identifikation wird das Flusssystem hinsichtlich der hydromorphologischen Randbedingungen detailliert charakterisiert. Hierauf aufbauend werden die Risikoelemente und potenziell gefährdende morphodynamische Prozesse im Flussabschnitt qualitativ ermittelt. Die so erlangten Kenntnisse über das Flusssystem ermöglichen eine fundierte Gefährdungsanalyse. Die Gefährdungsanalyse besteht aus 2 Schritten. Um die komplexen dreidimensionalen Prozesse detailliert zu erfassen, wird im ersten Schritt ein neuartiger gekoppelter 1D/3D-Modellansatz zur Simulation der Hydrodynamik entwickelt, der die Rauheitswirkung von Vegetation über einen physikalisch-basierten Ansatz berücksichtigt. Im zweiten Schritt werden zur Abschätzung der morphodynamischen Reaktion für jedes Risikoelement geeignete analytische Stabilitätsansätze und ein neuer Ansatz zur Bestimmung des Transportverhaltens mitgeführter Sedimente herangezogen. Langfristige Betrachtungen werden mithilfe der Regimetheorie ermöglicht. Zentrale Bedeutung des Konzeptes liegt auf der Kalibrierung und Validierung der verwendeten Methoden und der Prüfung der Ergebnisse auf Plausibilität durch Felddaten.

Die neu entwickelte Methode wird im zweiten Teil der Arbeit anhand eines Fallbeispieles am Oberrhein überprüft. In diesem Rheinabschnitt sind zahlreiche Umgestaltungsmaßnahmen

inkl. Naherholungsgebiet und Hochwasserrückhaltefläche mit Auewald geplant. Die Methode wird am Ist-Zustand mit Felddaten kalibriert. Die Validierung erfolgt anhand der hydrodynamischen Simulation eines rezenten Hochwasserereignisses und zeigt die Güte des Modellansatzes auf. Das geprüfte Konzept wird auf den Planungszustand angewendet und die morphodynamische Entwicklung für drei relevante Abflüsse in mehreren Szenarien abgeleitet. Für Unsicherheitsbetrachtungen werden Vergleichsrechnungen mit einem 2D-Modell durchgeführt.

Die Ergebnisse zeigen, dass es mithilfe der neuen Methodik möglich ist, die morphodynamischen Prozesse in komplexen, naturnahen Fließgewässern mit Vegetation plausibel abzuschätzen. Dies ist mit herkömmlichen Methoden bislang nicht gelungen. Das entwickelte Konzept kann einen wichtigen Beitrag zur Wirksamkeit und Nachhaltigkeit von naturnahen Hochwassermaßnahmen leisten und zur Planungsoptimierung eingesetzt werden.

TABLE OF CONTENTS

LIST OF FIGURES

LIST OF TABLES

1 INTRODUCTION

1.1 INTRODUCTION

Ever since, people had to cope with fluvial hazards. Due to settlement in fruitful floodplains and the use of rivers for shipping and transport, people were regularly affected by inundations and morphological adjustments. Finally, within the centuries, improving knowledge and technologies have led to widespread management of rivers for human purposes accompanied by extensive channelization and regulation activities with the aim to prevent flooding and severe channel shifting, and in order to assure safety, navigability, agriculture, drinking water and most recently, power generation, instead. Many river measures were successful at that time they were constructed feeding the hope to be capable to alter the river systems' behaviour to human needs. However, in the course of the decades, it turned out that the impact on the fluvial equilibrium had been severely underestimated becoming evident in the occurrence of a new kind of problems: The lack of inundation space which had been created by dike construction and cutoff of meanders, dramatically increased the travel velocity of flood waves as well as the total volume of floods with the consequence that in combination with a multiplication of industrial values in the floodplains, flood risk re-increased tremendously in many catchments. These circumstances have become evident already in the last century by many flood catastrophes such as the exceptional flood in 1966 in Tuscany/Italy which caused the death of 14 people, the loss of more than 5,000 properties, severe damage to around 24,000 houses in more than 50 towns and uncountable losses of cultural heritage and arts (see Figure 1.1, Caporali et al., 2005). Nevertheless, inundation

Figure 1.1: Effects of the 1966 flood in Santa Croce/Firenze, Italy (source: Caporali et al., 2005).

Figure 1.2: Fluvial erosion risk (VANR, 2008).

might be accompanied by severe morphological changes of the river due to increased fluvial forces leading to channel shifting, scouring and consequently exceptional sediment transport and deposition. E. g. VANR (2008) reports that over the period of 1995 – 1998 alone, flood losses in Vermont/USA were caused less by inundation, but mainly by fluvial erosion totalling nearly $57 Million (Figure 1.2).

In addition to fluvial hazards aggravated by river and catchment regulations, a second aspect may be amplifying flood risk in future, which is climate change. In recent years, the number of floods has increased significantly worldwide as well as number of people affected and economic losses. Currently flooding causes over one-third of the total estimated costs of natural disasters and accounts for two-thirds of people affected by them (Blackwell and Maltby, 2005). The increase in the occurrence of disastrous inundation events is revealed as demonstrated by the recent widespread flooding on many Central European rivers such as in July 1997 when the River Odra flooded more than 5,000 km², damaged 70,000 buildings and 3,800 bridges in Poland alone, or in August 2002 when tremendous flooding in Austria, Czech Republic, Germany, Russia, Romania, Spain and Slovakia caused 100 fatalities, economic losses exceeding 15 billion € and the evacuation of about 400,000 people while some 4 million residents in Germany were affected. Also the occurrence of floods in the highly regulated and densely populated catchment of the River Rhine has augmented significantly in the last 10 years reflected in exceptional events in the Upper Rhine of 1994, 1999 and 2007. In the case of a 200 years' event, losses are estimated by State Ministry of the Environment Baden-Württemberg (2007) to 6 billion € disregarding human casualties (Figure 1.3).

Figure 1.3: Industrial area in the Upper Rhine floodplain near Ludwigshafen (Rother, 2002).

Figure 1.4: Reactivation of former floodplains for sustainable flood protection (Pruijssen, 1999).

In light of the reported challenges, river managers, politics and planners have claimed urgent need for new sustainable flood protection technologies, which also take the river system's nature into account as manifested also in the EU Water Framework Directive. Among those are so-called "room for the river" measures comprising flood retention areas, reactivation of former floodplains and rehabilitation of regulated modified river sections as illustrated in Figure 1.4. However, sustainable management and the reliability of rehabilitated river sections and retention areas are a challenge. Until now, there is no adequate methodology available, which determines and estimates the hazardous processes likely in natural river systems and which can be implied into flood risk management strategies. Current planning procedures for flood protection often deal with the stream in a steady state condition focussing on inundation as sole hazard only while assuming that the river is not subjected to morphological changes. As already highlighted above, this assumption is

hardly valid especially in rehabilitated or nature-close river sections where multiple degrees of freedom are present. Alterations in sediment load, flow regime/discharge, and roughness pattern such as vegetation which are initiated by river engineering works may it be for navigation, flood protection or recreation can subsequently lead to rapid morphological response which can be so severe that they become hazardous for adjacent areas and municipalities as it had been experienced by people centuries ago. As a consequence, the demand for an interdisciplinary, long-term strategy for nature-close flood protection measures and river restoration projects which account for typical characteristics of natural streams such as variable geometry and vegetation remains high (Thompson and Clayton, 2002; Alkema and Cavallin, 2003; Gilvear, 1999).

1.2 MOTIVATION AND SCOPE OF RESEARCH

With the awareness of this dangerous situation, responsibilities need precise information about the risk resulting from natural morphodynamic development within natural flood protection measures and restored river reaches in addition to inundation studies. However, appropriate apriori methodologies concerning the planning, assessment and evaluation of those projects and the estimation of related local morphodynamic hazards are scarce. This is due to the fact that interdisciplinary river management approaches are rather new. River geo-ecology, climate change, and the need for new holistic flood protection strategies have turned into public and political concern only recently. Accordingly, methodologies which are applicable to practical problems on the local river reach scale are usually restricted to inundation modelling prior or extensive monitoring programmes after the measure's implementation while analysis tools with focus on morphodynamic processes are just under development, certainly also due to the complexity of the given task. In order to perform sustainable nature-close river measures, a procedure is required that reveals local fluvial hazards and potential consequences as early and as reliably as possible, most desirably in the design phase.

The prognosis of channel adjustments of natural rivers with floodplains demands distinct consideration of both the bed shear stress and the three-dimensional flow field as initiated by geometry variations, macrostructures and vegetation. Although vegetation is omnipresent and crucial for the success and sustainability of flood retention measures, available modelling tools account for the representation of vegetation only marginally. Here, floodplain roughness is mainly described by standard upscaled empirical roughness coefficients chosen via literature tables. The shortcomings of these approaches may be underlined by the fact that flow forces occurring in vegetated areas are commonly derived by assuming a vertical velocity distribution equivalent to that of non-vegetated channels although this assumption is not valid. The reported simplifications can lead to high uncertainties and physically incorrect results to the effect that morphodynamic hazards in vegetated streams cannot be successfully prognosticated until today.

In the light of these problems, the objective of this dissertation is the development of a method for the estimation of local morphodynamic hazards likely to occur in nature-close flood protection measures and restoration projects. A strategy is proposed which enables to identify for a given river project, the risk induced by morphodynamics, to analyse potential hazards and in alter stage, to determine related structural damages in the case of failure. The strategy may indicate the need for plan optimization according to the acceptance criteria provided by the plans and thus could complement

currently available flood risk management strategies. To this aim, a novel technique for morphodynamic hazard analysis is derived based on combined-multidimensional modelling. The technique aims at adequately considering the local 3D turbulent flow field, the physically-sound representation of vegetation resistance and analytical formula which enable to investigate morphodynamic behaviour for single Elements at Risk in detail. The iterative procedure of the Risk Management approach is chosen as a useful framework for tackling this objective. To assure system understanding and thus a sound prognosis, the methodology demands the generation of adequate input data for modelling, appropriate model calibration and validation as well as the investigation of outer limits of boundary conditions to reveal the range of processes likely. Furthermore, the obtained prognosis is cross-checked for plausibility with field observation of the river in question. As morphological response is dependent on various processes as well as on the river's own properties, the present study focuses on regulated gravel-bed rivers in the actual state and the planned restoration state including:

- armoured river beds
- regulated discharge and sediment dynamics
- cross-sectional widenings and floodplains with loose bed material
- features exhibiting distinct flow resistance incorporated by
  - vegetation (grass, soft and hardwood forest)
  - macrostructures (islands and gravel banks)
  - buildings

1.3 OVERVIEW

The dissertation is structured as follows. Chapter 2 gives an introduction into the general concept of Risk Management with a detailed description of the major steps. Then, the concept is applied to Risk Management of morphodynamic processes in rivers. Chapter 3 presents the state of the art in science and modelling concerning hydraulic processes in natural gravel-bed rivers with vegetation. Focus is placed on morphological response, the driving and dependent variables, the special role of vegetation and current approaches to quantify these processes. Based on the overview gained in Chapter 2 and 3, a new approach for Hazard Analysis is derived for the scope of the present study. This approach is applied in Chapter 4, 5 and 6 to a case study reach with the aim of demonstrating its applicability to the estimation of morphodynamic hazards for natural flood protection measures. In particular, Chapter 4 presents the phase of Risk Identification including system definition and governing boundary conditions while in Chapter 5, the new modelling concept is calibrated on the actual river state and validated with field data. Consequently, in Chapter 6, the validated model is used to determine morphodynamic hazards for the study reach in the planning state. In order to show the advantages of this method in comparison with standard tools, Chapter 7 offers test calculations with a 2D model which are briefly compared with the results obtained with the proposed approach. Finally, Chapter 8 summarizes the achievements of the present research, the conclusions to be drawn and presents an outlook of further research which is still necessitated in this field.

2 THE CONCEPT OF MORPHODYNAMIC RISK ANALYSIS FOR RIVER RESTORATION AND FLOOD MEASURES

The present chapter aims at offering an introduction ino the general concept of Risk Management. The three major steps of Risk Identification, Risk Assessment and Risk Mitigation are described in Chapter 2.1 while in Chapter 2.2., the risk chain is transferred and applied to the scope of the present study of fluvial morphodynamics.

2.1 THE RISK MANAGEMENT FRAMEWORK – AN OVERVIEW

The term "Risk Management" has been gaining importance within the last years. Strategies of Risk Management are useful whenever a certain event with a certain probability of occurrence can lead to damages and losses of a system and if measures must be found to manage these situations. This term has become widely used in the course of climate change, natural disasters and related consequences and is an indispensable tool above all in the fields of engineering, economics, insurance industries and health care. However, the terms used in Risk Management are not clearly defined throughout the disciplines. Proske (2004) states that more than 30 definitions of "risk" can be found in literature. In order to clarify the vocabulary used in the present work, this chapter provides key definitions and the general procedure of the Risk Management framework. The definitions follow the recommendations of Pliefke et al. (2006, 2007), see also Urban (2007) and Salvatori (2008).

The general Risk Management framework is summarized in Figure 2.1. It consists of three major and consecutive phases: Risk Identification, Risk Assessment and Risk Treatment.

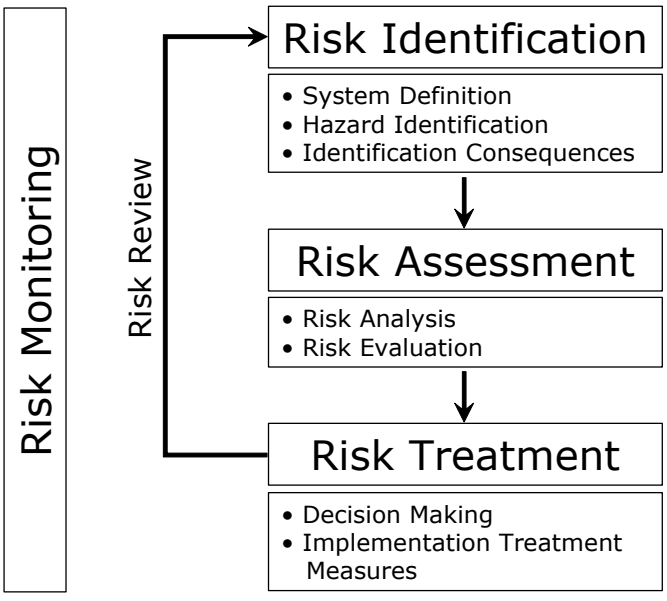

Figure 2.1: The major phases of the Risk Management framework (Pliefke et al. 2006, 2007).

2.1.1 Risk Identification

The initial phase "Risk Identification" is the most important process within the Risk Management framework as here, the context of the problem is identified and clarified. It provides a detailed qualitative insight into the system investigated and into potential sources of harm that are treated further in the Risk Management framework. First, the system's properties and behaviour are analysed and the boundaries of its model domain are defined. According to the system's complexity, the system may be further decomposed into a number of components or elements that are treated separately within the Risk Management procedure. Moreover, the design criteria and the desired performance of the system are determined. Based on this detailed understanding, it analyses how the system's functionality can be affected. In other words, all sources and processes (*hazard*s) must be detected which are potentially able to harm the system. These hazards can be potential dangerous situations, events or sources of failure. Different techniques for identifying hazards have been developed in various engineering areas such as chemical industries or the nuclear power industry. Widely applied techniques are e. g. Preliminary Hazard Analysis (PHA), Failure Mode and Effect Analysis (FMEA), Hazard and Operability Studies (HAZOP) and Risk Screening (HAZID). But hazards may also be appropriately identified on the basis of past experiences gained from systems and events with similar boundary conditions (see also Faber, 2005; Merz, 2006; DIN EN IEC 60812:2006).

2.1.2 Risk Assessment

The next phase within the Risk Management framework concerns the Risk Assessment. It consists of two sub-phases, namely the *Risk Analysis* phase and the *risk evaluation* phase. The *Risk Analysis* phase finally aims to quantify the risk in monetary units per time unit (e.g. [€/year]). The term "risk" in common meaning describes danger, threat or the possibility to be harmed. In Risk Management, however, the term "risk" is clearly defined as the result of the interaction between *hazard* and *vulnerability*. In order to assign a monetary value to hazards – those identified in the Risk Identification phase - and related *consequences* (damages and losses), they must be estimated quantitatively. Consequently, the *Risk Analysis* phase requires the development and application of suitable mathematical models and the definition of possible scenarios to be investigated. The first step within the *Risk Analysis* is the *Hazard Analysis* where the intensity and frequency of each hazard are estimated according to the data, mathematical models available and scenarios chosen (see Plate, 2001), see Figure 2.2. The hazard source in flood risk management is usually represented by discharge. However, discharge does not only affect the system by its volume flow but is transformed into other relevant parameters among which the most common remains "water height" (or "inundation height"). The parameters flow velocity and bed shear stress are mostly neglected in flood studies but can gain major importance according to the scope of investigation, to the scale and to the system of interest. The common unit of hazard is [intensity/time unit], e. g. water height or flow velocity/discharge event.

After the quantification of hazards, their impact on the system and related consequences must be estimated for each scenario. This is performed within the next two phases depicted in Figure 2.2: the *Damage Assessment* phase (non-monetary assessment) and the *Loss Assessment* phase (monetary assessment). Pliefke et al. (2006, 2007) define *(structural) damage* as a physical, biological or chemical effect on a system (or element within the system, such as people, buildings, infrastructure,

ecosystems) that is caused by a hazard with a given intensity. It is expressed by measures (such as degree of water logging, pollutant concentration, erosion depth etc.). *Damage* does not only depend on the intensity of the hazard, but, of course, also on the system's structural properties. The relation between hazard intensity and damage of a system is called *structural vulnerability*. It represents the degree of susceptibility of a system towards a hazard. The unit of structural vulnerability is [damage measure/intensity measure], e. g. river bed erosion depth/discharge or degree of water logging of a wall/water depth.

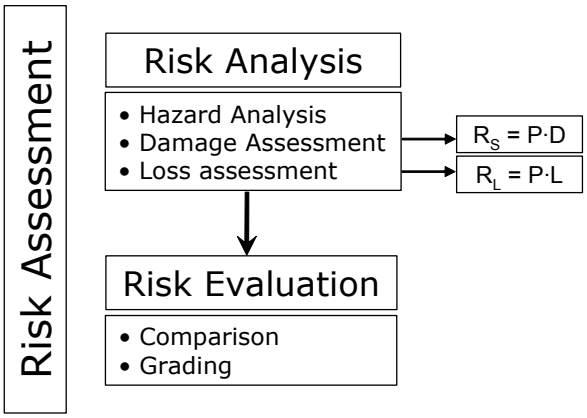

Figure 2.2: The sub-phases of Risk Assessment (Pliefke et al. 2006, 2007).

After having completed the *Damage Assessment phase*, the so-called *structural risk* R_s can be derived as follows:

$$R_S = P \cdot D \qquad 2\text{-}1$$

where R_s = structural risk [damage measure/time unit], P = probability of occurrence for a hazard of a certain intensity, D = damage at the given hazard intensity.

According to this definition, *structural risk* does not indicate the costs related to the hazard but a physical measure. Monetary terms are only introduced in the next phase of Risk Assessment, the *Loss Assessment* phase. The *Loss Assessment* phase aims to assign costs to the damages estimated before. The term *loss* accumulates all direct and indirect consequences in monetary terms that might result from a structural damage. It covers the value of the system itself (or the elements within) and its functionality. *Direct consequences* are events that occur simultaneously to the time the disaster takes place (such as loss of life, costs of reparation, rebuilding, loss of harvest or profits). In contrast, indirect consequences occur with a time shift as a result of the direct consequences. They represent the long-term effects (e. g. increased maintenance costs, modification of economic and social equilibriums, psychic traumata etc.) Furthermore, each consequence class can be subdivided into tangible consequences that are monetarily quantifiable, and intangible consequences where it is not possible to assign a monetary value in a direct way (e.g. injuries and fatalities, destruction of cultural heritages or ecosystems etc.) Both direct and indirect consequences can be further classified in human, economical, ecological, cultural, social and historical (CSH) losses.

The assignment of a loss value to a given damage state and hazard intensity, respectively, is called *system vulnerability* (in contrast to *structural vulnerability* where a non-monetary damage measure is assigned to a hazard intensity). The common unit for structural vulnerability is [loss measure/intensity

measure, e.g. €/inundation height]. Examples for loss-hazard relationships can be found e. g. in Merz (2006).

After the completion, the *total risk* can be derived (see also Gouldby and Samuels, 2005) according to

$$R_L = P \cdot L \qquad 2\text{-}2$$

with R_L = total risk [loss measure/time unit], P = probability of occurrence of a hazard of a given intensity, L = loss occurring at the given hazard intensity.

After having quantified the total risk the final part of the Risk Assessment process is induced, the so-called *Risk Evaluation*. The purpose of *Risk Evaluation* is to make different risks comparable and to start a prioritization of risks. A prioritization can include for example a grading of higher risks towards lower risks and thus may easily illustrate which scenarios might be negligible and which scenario must be considered for treatment. Hence, the *Risk Evaluation* is crucial for efficient decision making and successful management of risks.

2.1.3 Risk Treatment

After all risks have been identified, analysed and evaluated, it must be decided how to *treat* the risks. In general, there are four major classes of Risk Treatment as shown in Figure 2.4: the risk might be *accepted, rejected, transferred*, or *mitigated*.

Risk Acceptance is common if the quantified risk is judged as less relevant and subsequently does not require further treatment. Given this, also risk *acceptance* can be a solution, e. g. in the case that measures to handle the risk are ineffective or too costly. In the case the risks are *not* in accordance with the specified risk acceptance criteria, there are several options for treatment. First, risk can be *rejected*, e. g. in the case that the risk is not acceptable and/or strategies are missing for an adequate risk reduction. Mostly, *Risk Rejection* requires the abandonment or the severe modification of a project (in flood risk management, for example, the choice of alternative building sites outside flood prone areas or the modification of a river design in the case of potential bank erosion). In the case risk is *transferred*, a third part takes over the risk by providing financial support in the emergency case. The third part is usually represented by the government, insurances or by other financial arrangements.

Finally, *Risk Mitigation* aims to achieve a risk reduction. Regarding the risk definition, risk can be reduced by either reducing the probability of occurrence of the hazard or by reducing the vulnerability of the system. However, reducing the probability of occurrence of natural hazards is very demanding due its complex, natural origin and unknown effects of climate change. Hence, most Risk Treatment measures are limited on the reduction of vulnerability, e. g. by technical prevention (early warning systems, technical measures and structural reinforcement such as dikes, embankments) or by simply reducing the monetary value of a system (e. g. explicit use of flood prone areas as low-cost meadows instead of valuable building grounds for private households or industry). Alternative risk mitigation strategies are measures of *Preparedness* prior to the disaster (such as development of evacuation plans, emergency training etc.) or *Response* and *Recovery* measures after the disaster (e. g. organization of shelters, emergency help, reconstruction or reinstallation of infrastructure).

Figure 2.3: Living with flood risk (Torrente Mugnone, Firenze/Italy).

After having completed the Risk Treatment phase, the whole Risk Management chain usually has to be reviewed (see Figure 2.4) taking into account new information and gained experience. This is required since during the Risk Management procedure new information is revealed that has been neglected, ignored or was simply unknown so far. Moreover, the revision can consider that the risk influencing variables (of hazards or system) are probably not constant with time. They might change during the planning process and after implementation of the project, respectively, or are even initiated

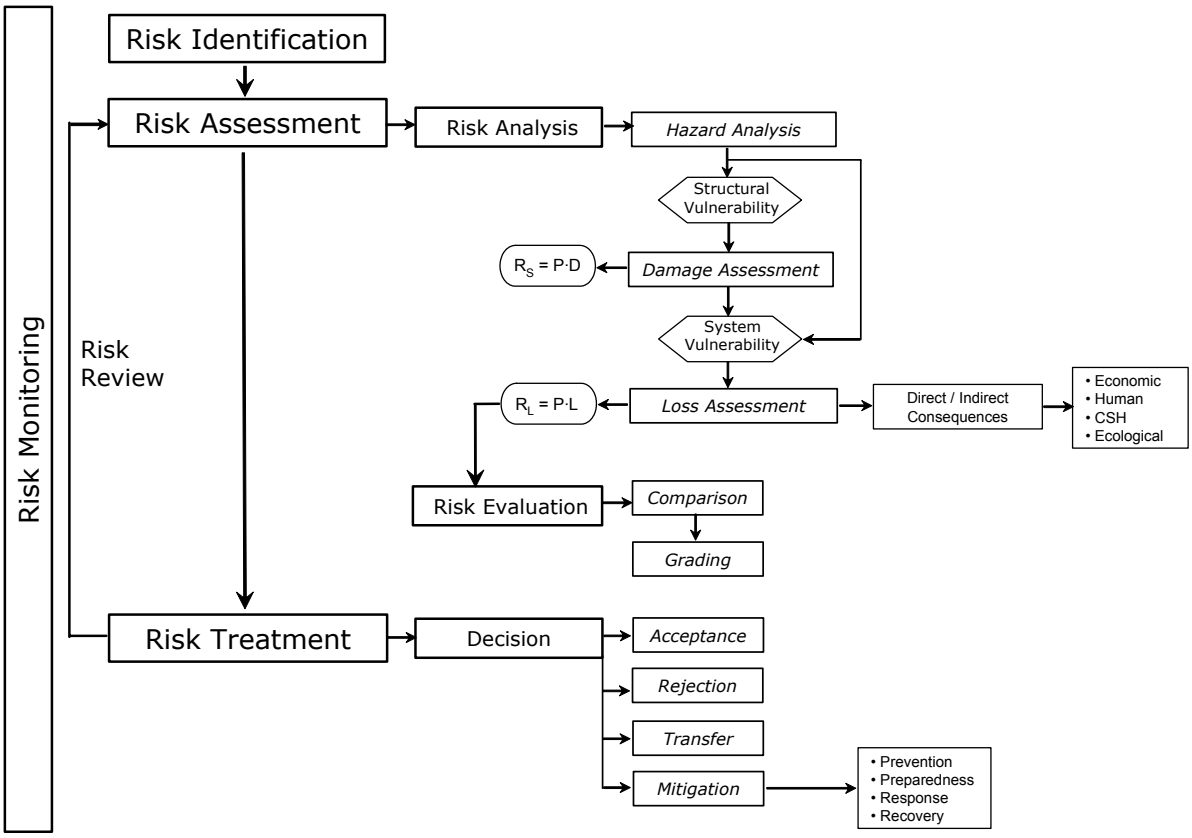

Figure 2.4: The Risk Management framework (Pliefke et al., 2006, 2007).

by new boundary conditions produced by Risk Management measures. To tackle these challenges, permanent information updates via *Risk Review* and *Risk Monitoring* are indispensable. *Risk Review* is necessary if new information must be considered for a risk that has already identified. *Risk monitoring*, instead, involves the revision of the complete Risk Management chain (conducted e.g. also after identification of new hazards). It is a prerequisite for meeting the design criteria or safety standards of a project in the long-term.

The present discussion shows that Risk Management is an open, iterative process. It requires a permanent feedback of information among involved planners and decision makers regarding the system of investigation, potential hazards and measures. Due to this iterative, systematic approach, it was successfully applied in various engineering areas. For example, it can be used as optimization strategy whenever a sustainable design or long-term performance of a given system must be guaranteed in accordance with certain acceptance criteria.

In the present study, the Risk Management procedure is applied for optimising the river design for river restoration and flood protection in the planning stage. The procedure developed for the given task is presented in the next chapter.

2.2 THE RISK MANAGEMENT FRAMEWORK APPLIED TO MORPHODYNAMIC RISK

Chapter 2.1 showed the overall procedure of Risk Management, revealing, however that appropriate applications of the management framework are still missing in flood risk management and river design. If ever applied, the risk chain is limited to large-scale inundation studies while focussing on water depths as key parameter and while mostly neglecting river dynamics. This simple approach is acceptable for homogeneous river sections and modified water bodies where degrees of freedom and morphodynamics are few. However, in natural rivers, morphodynamics can play a significant role due to numerous interactions between flow, sediment, vegetation and changes of river bed geometries. Consequently, morphodynamic processes can distinctly affect the success of river restoration projects or nature-close flood protection measures and might lead to severe consequences in the case of the project's failure. In order to perform a sustainable nature-close river design, a procedure is required that reveals hazardous processes and potential consequences in the river section as early and as reliably as possible, most desirably in the design phase. The systematic, iterative strategy of the Risk Management framework is a useful tool for tackling this objective.

The present study aims to apply parts of the Risk Management chain to river design and flood protection projects. The objective is identifying and assessing risks induced by morphodynamics in order to optimize the river design according to the acceptance criteria given by recreation plans and flood protection. In the present chapter, the common Risk Management chain is discussed regarding the risk caused by morphodynamic development.

As aforementioned, a hazard does not necessarily lead to harm in terms of damages or losses and subsequently to risk. Only if there exists a vulnerable, exposed system and only if there are routes and processes by which the hazard can reach this system, the hazard can lead to consequences and risk in the defined sense. To illustrate the linkage between morphodynamic hazard and morphodynamic risk the common Source-Pathway-Receptor-Consequences (S-P-R-C) model is applied via Figure 2.5. This conceptual model considers that risk is evoked on the one hand by a hazard consisting of a *source* or

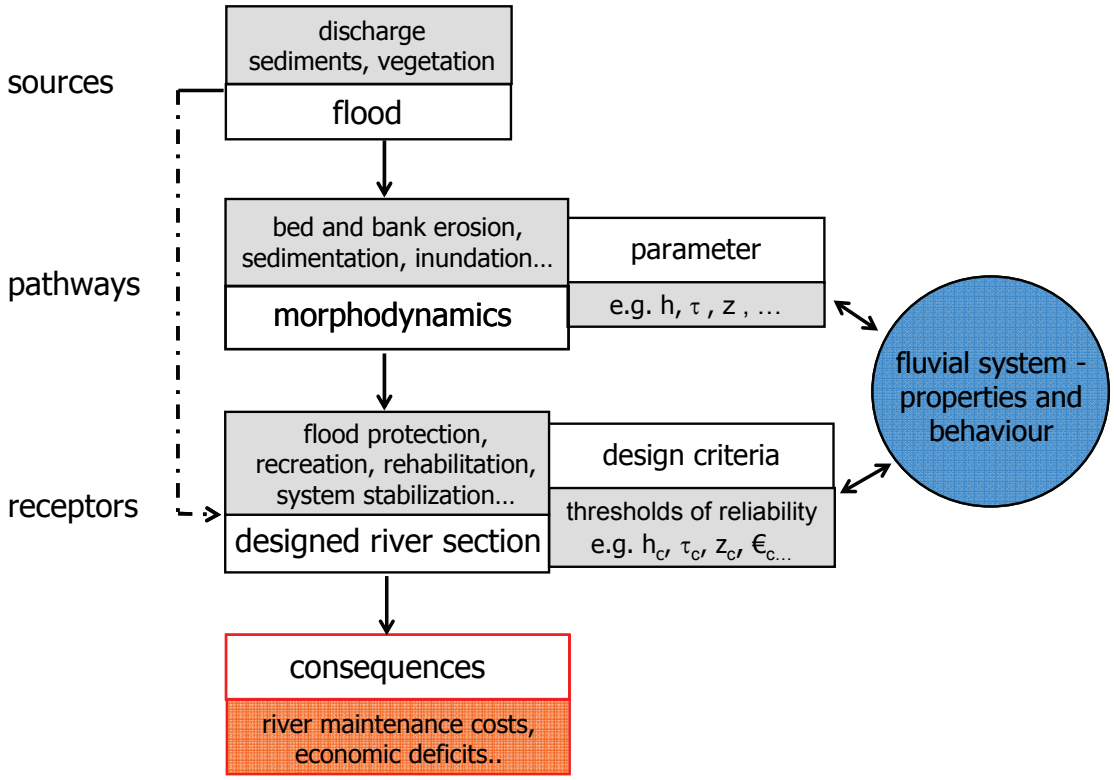

Figure 2.5: The source-pathway-receptor-consequences (S-P-R-C) model applied to morphodynamic risk.

initial key event and a *pathway*. The *pathway* can be defined as the route or medium that a hazard takes to reach the receptor (Gouldby and Samuels, 2005; Urban, 2007) or alternatively as a process which is initiated by the source and which affects the receptor (see also Kortenhaus, 2006; Floodsite, 2008). In the present study, the second definition for *pathway* is used. The *receptor* is the system that can be potentially harmed by the hazard, in the present case the river section to restore or the river design, respectively. The system can be subdivided, if necessary, into smaller elements (Elements at Risk), e .g. morphodynamic features such as river bed, river banks, side channels, islands etc.. The functionality of the river design is endangered by the sources like discharge, sediment transport and vegetation development affecting the system physically via the pathways. The pathways, in turn, are initiated morphodynamic processes, for example bed or bank erosion, initiated sediment transport, sedimentation/silting or inundation. They can lead to failure of the system, for example the river design objectives cannot be met any longer and the proper functioning of the system is endangered. Failure of the system is here defined as the state that the thresholds of reliability (e. g. the river design criteria critical water depth h_c, critical shear stresses τ_c, maximum acceptable sedimentation height z_c, maximum acceptable maintenance costs $€_c$) are exceeded. The consequences in the case of failure can be costly river maintenance, economic deficits and in the worst case, if flood protection is affected, the typical losses related to flood disasters.

The linkage of sources, pathways and receptors to the risk variables in question is schematized in Figure 2.6. Both Figure 2.5 and Figure 2.6 clearly demonstrate that the management of morphodynamic risk is a very challenging task due to the complexity involved. The functionality of the designed fluvial system (or in other words: the probability of failure of the river design) is not only dependent on the hazards' intensity and frequency (which are strongly time-variant themselves), but

also closely linked to the system's own properties and behaviour due to complex dynamic interactions among hazard and system (see Figure 2.5). The characteristics of the fluvial system determine its vulnerability and initiated hazardous processes. Hence, in addition to accurate information about the risk sources, a detailed understanding of the fluvial system is a prerequisite in order to find a sustainable flood design which withstands the hazards.

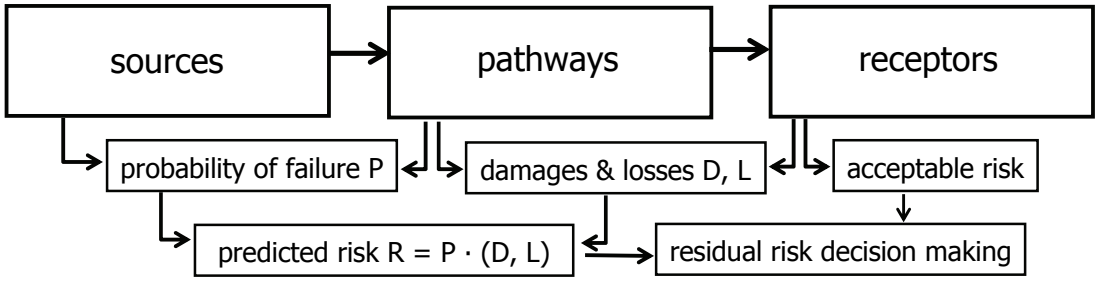

Figure 2.6: The S-P-C-R-Model for determination of risk variables (Kortenhaus, 2006; modified).

The present study focuses on the first part of the Risk Management chain, namely the phases of Risk Identification and Hazard Analysis (see Figure 2.4): For a given river design project, the risk induced by morphodynamics is identified and potential hazards are analysed. Based on that, related structural damages in the case of failure can be determined. The structural damages detected are further used as preliminary input parameters for an optimization plan. In order to develop a suitable concept of morphodynamic hazard analysis for rehabilitation and flood measures in a planning state, it is crucial to first provide an overview of basic morphodynamic processes acting in natural rivers with vegetation and related challenges. Based on this gained knowledge, currently available techniques for estimation of morphodynamics of these systems must be assessed and shortcomings of these techniques should be discussed. The following Chapter 3 aims to meet these demands by providing the state of the art in science and modelling of morphodynamics hazards in natural rivers with vegetation. Finally, the concept of morphodynamic risk analysis whose main features has been schematized above will be picked up again and developed further towards a novel methodology for the scope of the present study.

3 MORPHODYNAMIC HAZARDS – STATE OF THE ART IN SCIENCE AND MODELLING

As presented in the previous chapter, the present study focuses on the first part of the Risk Management chain: the phases of Risk Identification and Hazard Analysis. For a given river rehabilitation plan, the risk induced by morphodynamics is identified and the potential hazards are determined. In order to perform the Risk Identification and Risk Analysis for a given river system as accurately as possible, the origins and facettes of morphodynamic processes must be highlighted according to the actual state of the art. Further, based on this understanding, currently available modelling techniques must be reviewed and evaluated concerning the scope of the present study. The present chapter therefore aims to present the state of the art in science and modelling of morphodynamic processes in rivers. The main focus is placed on the following hydromorphological conditions related with measures of river rehabilitation, natural flood protection and touristic recreation in gravel-bed rivers such as armoured river beds, cross-sectional widenings and floodplains with loose bed material, features exhibiting distinct flow resistance incorporated by vegetation, macrostructures (islands and gravel banks) and buildings.

In the first part of this chapter, the main large-scale aspects of morphodynamics and semi-quantitative techniques for their estimation are presented (Chapter 3.1). In Chapter 3.2, the underlying small-scale hydraulic processes of morphodynamics are presented as the state of the art with special focus on the aforementioned hydromorphological conditions. Chapter 3.3 presents the literature review summarizing currently available quantitative modelling approaches for the estimation of morphodynamic development. Based on the scientific background provided in Chapter 3.1 and 3.2, these approaches are evaluated and discussed regarding the scope of the present study. Based on this discussion, a novel technique for morphodynamic hazard analysis in planning river rehabilitation and flood measures is derived in Chapter 3.4.

3.1 INTRODUCTION IN MORPHODYNAMICS – THE RIVER AS A CONTINUOUS SYSTEM

The morphology of a river is a function of various processes and interactions among which discharge is most obvious in daily life. Discharge is determined by the water cycle which in turn is a complex result of precipitation, infiltration and evaporation processes and which is strongly individual for each fluvial system due to site-specific biologic, geologic, climatic and tectonic conditions. As a consequence, also fluvial morphology is a function of space and time. Kern (1994) visualized these interdependencies in a space-time model, see Figure 3.1. He emphasized that fluvial processes are highly scale-dependent: Processes which are acting in a certain spatial domain are closely linked with a certain time domain. It should be noted that the domains are not isolated from each other, but form an open, continuous system from the catchment scale down to the microhabitat scale while each domain is connected to the upscale domain. This leads to complicated interdependencies.

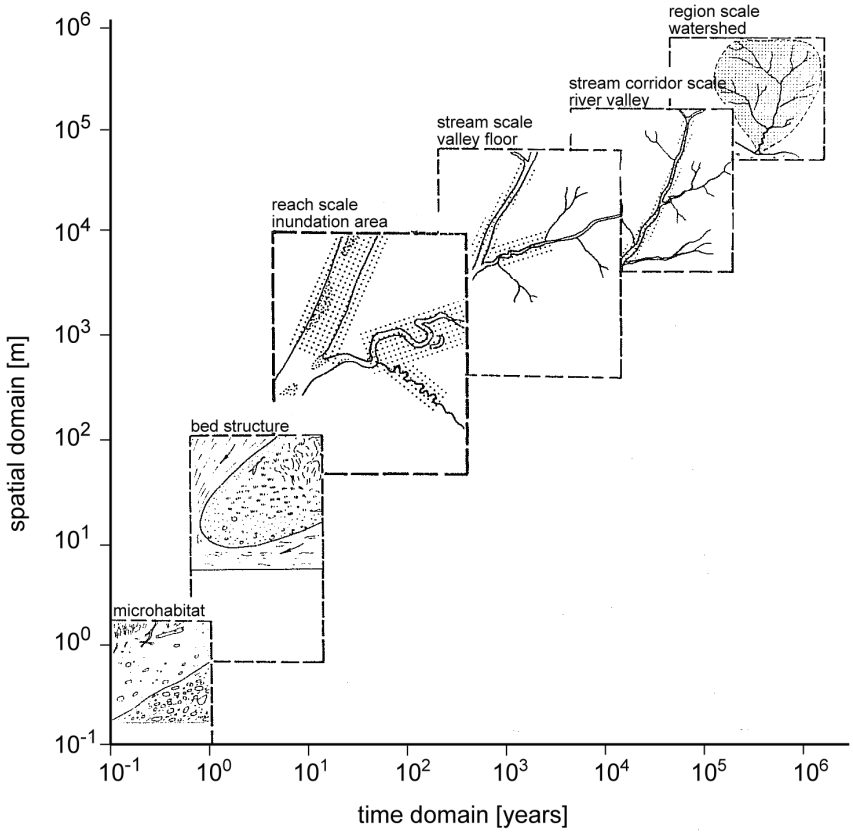

Figure 3.1: System levels in a hierarchical space-time model of morphologic fluvial development (Kern, 1994).

This complexity has also been visualized by Steiger et al. (2005). Figure 3.2 depicts impressively the morphodynamic processes affecting the single hazard "sediment deposition on floodplains". Steiger et al. (2005) highlighted that morphodynamic processes are acting in four dimensions: The hydraulic flow field and resulting channel adjustments are acting in three dimensions. The fourth dimension is time which defines the changes in the 3D system.

The discussion above shows that the estimation of morphodynamic development is a challenging task due to the complexity of the governing interrelationships. It is obvious that an appropriate Risk Management framework and hence, sustainable, successful river measures require a holistic approach. This approach should

- consider large-scale perspectives concerning both time and space
- in parallel focus on details wherever appropriate
- be laid out in accordance with relevant domains and with respect to the river's catchment properties.

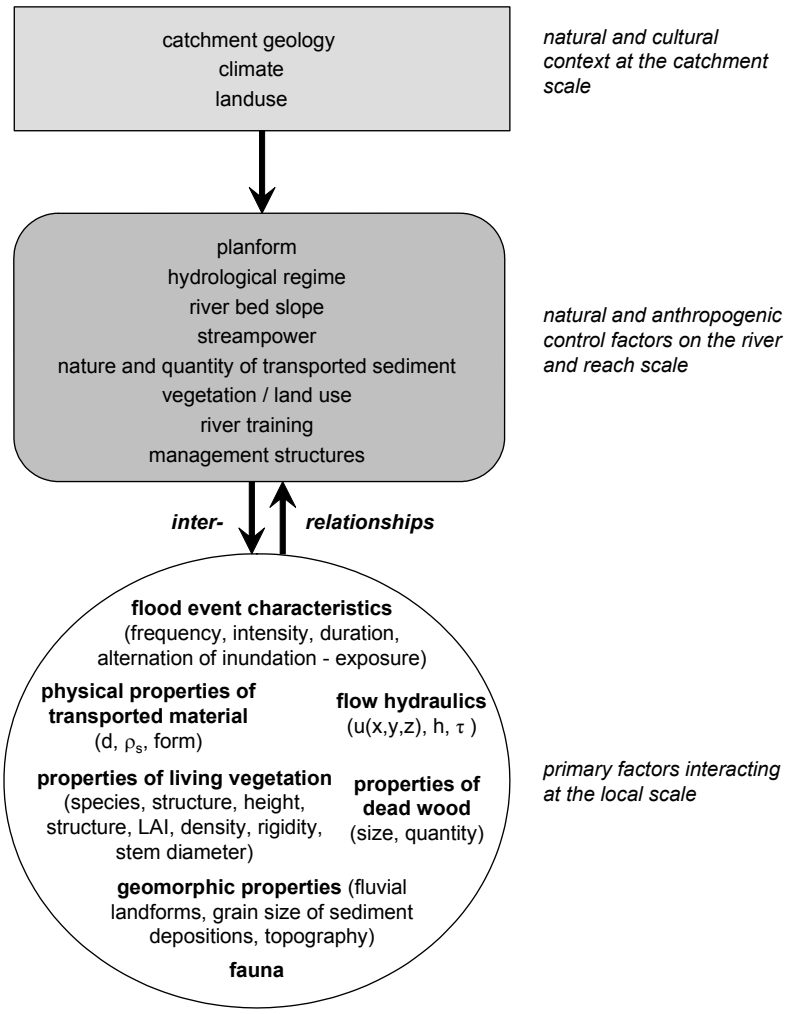

Figure 3.2: Factors controlling riparian mineral and organic matter deposition (Steiger et al., 2005).

So far, various methodologies have been developed to estimate the morphodynamic development of rivers at least in a qualitative and semi-quantitative manner. Following the first and the last of the aforementioned demands, the next sections therefore present the state of the art concerning the (semi-) qualitative estimation of fluvial processes and the main drivers on the river reach scale. The second demand is concerned in Chapter 3.2.

3.1.1 The morphological regime or equilibrium concept

The basic principle for explaining the origin of fluvial adjustments is the theory of the morphological regime or equilibrium. The morphological equilibrium describes the tendency of a river to maintain a “stable” morphological state. Rosgen (2001) showed that there are various definitions and synonyms available in literature for rivers in equilibrium (e. g. Mackin 1948; Leopold et al. 1964; Ahnert, 1973; Shields et al., 2003; Sear et al. 2003). According to Rosgen (1996) the river equilibrium "is the ability of a stream, over time, in the present climate, to transport the sediment and flows produced by its watershed in such a manner that the stream maintains its dimension, pattern and profile without either aggrading nor degrading" (see also Ahnert, 1973; Shields et al., 2003). This

definition is widely accepted today. Thus, a river can be highly dynamic but at the same time geomorphologically stable as long as its long-term temporal average morphological properties (width, depth, slope, sediment input and output) do not change. The crucial point is that this equilibrium can be interrupted, e. g. by strong changes in water or sediment regime on which the river is then reacting with abrupt or progressive channel adjustments (Shields et al., 2003). Chorley and Kennedy (1971), as reported by Kern (1994), defined equilibrium states according to the change of morphological variables over time as well as three characteristic time spans occurring while a river is adjusting to disturbances (Figure 3.3):

- reaction time: time span from the disturbance of the controlling variable until the initialization of morphological change
- relaxation time: time span from the reaction of the river system on the disturbance of the controlling factor until the original or a new equilibrium state is reached
- characteristic form time: time span during which equilibrium is maintained

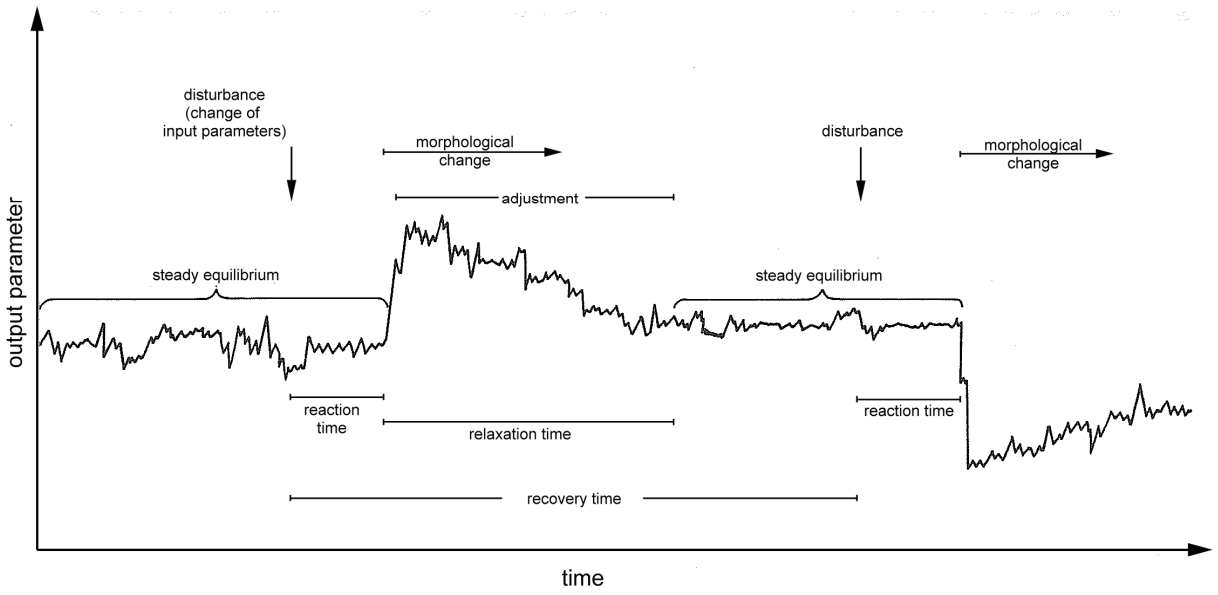

Figure 3.3: System of equilibrium in geomorphology (Kern, 1994).

The theory of morphologic equilibrium has often proofed useful to understand the origin of morphodynamics and to develop tools for predictions of the system's response on disturbances. However, no agreement has been found for decades concerning the factors which dominantly control equilibrium and thus morphodynamics (FISRWG, 2001). A qualitative scheme which is widely accepted today was published by Thorne et al. (1997) (see also Fischenich and Morrow, 2000; Sear et al., 2003) as presented in Figure 3.4. It explains fluvial dynamics and equilibrium conditions as the result of a set of variables:

- driving variables
- boundary conditions
- adjusting variables or channel form.

The driving variables of the fluvial system are the inputs of water and sediment generated from catchment and channel processes upstream, shown in Figure 3.4 as water and sediment hydrographs.

They interact with the independent boundary characteristics such as valley slope and bank material of the river which are inherited by past geomorphological processes. As shown in Figure 3.4, vegetation plays an important role in boundary characteristics since it may significantly affect the flow field and transport pattern (see also Hupp and Rinaldi, 2007). In the frame of these boundary properties, the river reacts on the driving variables with changes of channel form and alterations in sediment transport or in other words, by changes of channel and floodplain morphology. According to Sear et al. (2003) morphodynamic development therefore can be defined as alterations of any of the three descriptors: channel planform, longitudinal profile (slope) and cross-sectional geometry.

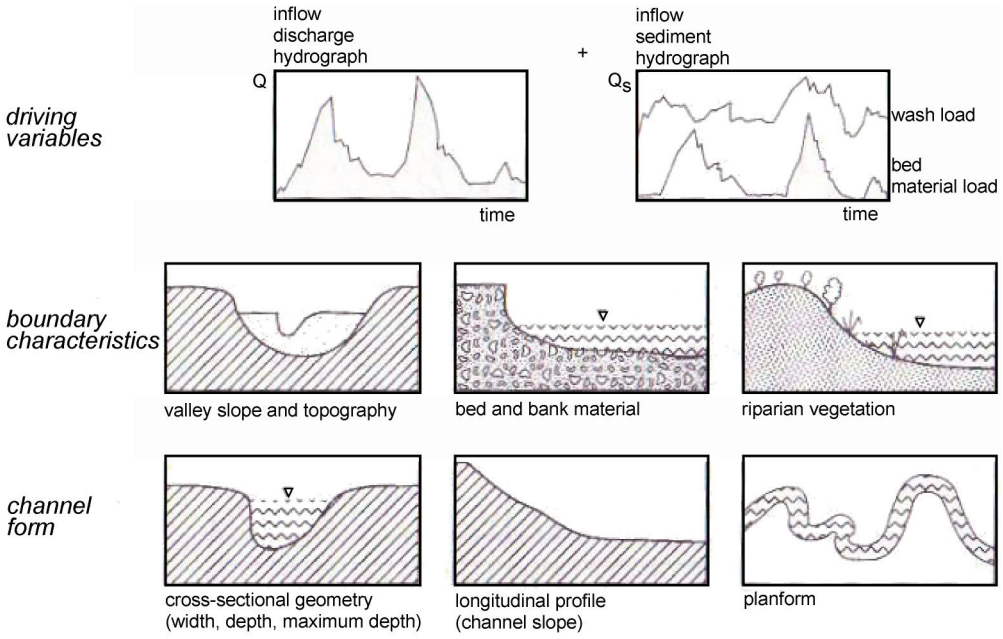

Figure 3.4: Independent and dependent controls on channel form (Thorne, 1997).

In the following Chapter 3.1.2, the driving variables discharge and sediment dynamics as well as resulting channel forms are briefly presented within the scope of the morphodynamic risk management framework. Moreover, qualitative as well as semi-quantitative approaches for their estimation are provided.

3.1.2 Independent and dependent variables of morphodynamics

3.1.2.1 Hydrologic processes – morphodynamic relevant discharges

As known from daily experience, discharge has large impact on fluvial morphodynamics. Most prevalent observations related to flood disasters are inundation, channel shifting, erosion and deposition phenomena. Consequently, it is clear that for morphodynamic hazard management, the river-specific hydrological conditions must be investigated appropriately. Hydrological studies usually comprise the detailed analysis of the discharge regime, discharge frequencies and flow durations (e.g., extreme, high, mean and low events) while required hydrological information is commonly obtained from gauging data and modelling tools, see FISRWG (2001) and Merz (2006) for a review. As the main purpose of the present study is the Hazard Analysis related to morphodynamic behaviour, a

detailed hydrological analysis would go beyond the scope of work. As a consequence, hydrological data is considered as input data for the corresponding area.

During a year, natural alluvial rivers experience a wide range of discharges with different magnitudes. Due to these fluctuations, only the most relevant flow events can be usually considered in morphological studies. At first sight, one might assume that the largest impact on fluvial morphology is exhibited by rare and large flood events. In contrast, many studies revealed that low and more frequent discharge events have major influence on river morphodynamics instead (Wolman and Miller, 1960, see also Zarn, 2008). A widely used concept for defining the most relevant flow events is the determination of the "channel-forming" or "dominant" discharge which presents the most effective discharge for shaping and maintaining the natural channel. This concept comprises that, for a given alluvial channel geometry, a single discharge exists which, given enough time, would produce width, depth, and slope equivalent to those produced by the natural hydrograph. But in practice, the estimation of the channel-forming discharge is a difficult task. In literature, there are numerous definitions available and as many strategies for its calculation (see Shields et al., 2003, for a review). Among these definitions are the *effective discharge*, *bankfull discharge*, and the discharge that corresponds to a given return interval. The *bankfull discharge*, for example, refers to the maximum discharge that the channel can convey without overflow onto the floodplain. In stable alluvial channels, it can correspond to *effective discharge* and shows a flood recurrence interval of approximately 1 to 2.5 years (Leopold et al., 1964; Scherle, 1999, Dittrich, 2007). But it must be noted that flood recurrence intervals of 4 – 10 years for *bankfull discharges* of different river types are not uncommon. The drawback of the channel-forming discharge concept is that the choice of an appropriate method for its calculation is often restricted due to the low quality and availability of hydrologic and hydraulic data which remains a major problem in river studies. Moreover, it must be bared in mind that the concept is only applicable for natural, alluvial channels in equilibrium (Sear et al., 2003; Copeland et al., 2001; Schulte-Rentrop et al., 2005). Thus, for reliable morphodynamic estimations, the outcomes should be always critically checked for plausibility with close respect to the individual characteristics of the river reach in question.

3.1.2.2 Sediment budgets and sediment dynamics

As aforementioned, the morphodynamic development of a river reach is not only governed by hydrological parameters but also by sediment dynamics. The assessment of sediment loads and the transport behaviour exhibited by erosion or deposition is crucial for appropriate Risk Management and has been neglected a long time in the domain of river planning. As shown in Chapter 3.1, a river reach forms a single part of a large continuous system where sediment is transported or deposited at different spatial and temporal scales. Sediment sources that require distinct consideration in morphodynamic estimation are both external sources (e. g. soil erosion from agricultural soils or aerial deposition) as well as internal sources (river bank erosion, bed erosion and scouring). A prerequisite for adequate estimation of morphodynamic processes in a reach therefore is the analysis of the reach-scale sediment budget. The sediment budget analysis is usually performed by comparing the quantity of sediment transported *into* the reach (internal and external sources) with sediment transport capacity and bed stability, respectively, *within* the reach. A methodology based on field measurements, gauge analysis, sediment transport and stability calculations as well as GIS calculations for land erosion has been suggested by Schulte-Rentrop et al. (2005). As well known, the identification of sediment pathways

and the linkage of sediment sources to sinks are not straightforward. Sediment transport behaviour is extremely complicated and is strongly varying according to transport mechanism (bed load, suspended load), sediment characteristics, flow field, discharge dynamics and river maintenance to the effect that, until today, no reliable tool exists which accurately predicts sediment loads or sediment routes through natural, complex, vegetated rivers.

3.1.2.3 Morphological structures

For the reported reasons of complexity, morphological development has been estimated for decades on an informative, qualitative basis only (see Kern, 1994, for a review). An example has been provided in Figure 3.4 summarizing the most relevant sources of channel development qualitatively. A more detailed analysis has been published e. g. by Hütte (1994). Hütte (1994) follows the assumption that, despite the large complexity of physical processes acting on different spatial and temporal scales, rivers seem to re-produce morphological features under similar boundary conditions as a function of grain size, sediment transport, slope and bed width, see Figure 3.5. The parameters shown in Figure 3.5 are closely connected so that the river morphology must be considered as a result of their interactions in addition to past processes and river management. Following Leopold and Wolman (1957), river planform can be classified into four main groups according to sinuosity (total length of channel per unit valley length) and the degree of channel division, namely into straight, meandering, braided and anastomosted beds. Straight river channels are rare in nature and are mainly restricted to areas where the channel is confined by bedrock, cohesive sediments, or trees. In contrast to straight streams, meandering channels exhibit a series of bends and sinuous sections which often can be described by a sinus curve so that the river geometry can be defined by measurable parameters, e. g. channel width, sinuosity, meander wavelength, meander belt width etc.. In contrast to straight and meandering (thus single bed) river types, braided rivers are systems with numerous branches. Prerequisite for braiding is the exceedance of transport capacity by sediment supply, often combined with a dynamic discharge regime (Sear et al., 2003; Kern, 1994). The resulting sediment deposits are frequently inundated and subjected to sediment transport leading to a dynamic network of channels and bars. Braided rivers can occur across a range of valley slopes, depending on the grain size of the transported bed material (see Figure 3.5). But it should be noted that vegetation development on bar surfaces is an important mechanism by which natural dynamic braided systems can become stabilized. This mechanism becomes apparent in so-called anastomosed multi-channel rivers: Here, anastomosed branches show only low dynamics and are separated from each other by stabilized vegetated surfaces of the same elevation as the floodplain. Their main characteristic feature is the deposition and accretion of fine sediments on the floodplain mainly occurring in low gradient valleys. Among the planforms aforementioned, many transitional bed forms such as alternate bars are present, see also Figure 3.6 (Zarn, 1997; Jäggi, 1983).

In addition to the presented mainly informative approaches, the relationship between planform and measurable parameters which could be used for estimation of planform in the case of varying boundary conditions was investigated by many authors, e. g. Jäggi (1983), da Silva (1991), Zarn (1997). Da Silva (1991) finally concluded that planform was a function of the relative bed width $w_{rel} = w/h$ to relative water depth $h_{rel} = h/d$ with grain size d as less sensitive variable. According to da Silva (1991), planform changes if w, Q or d are being varied as presented in Figure 3.6.

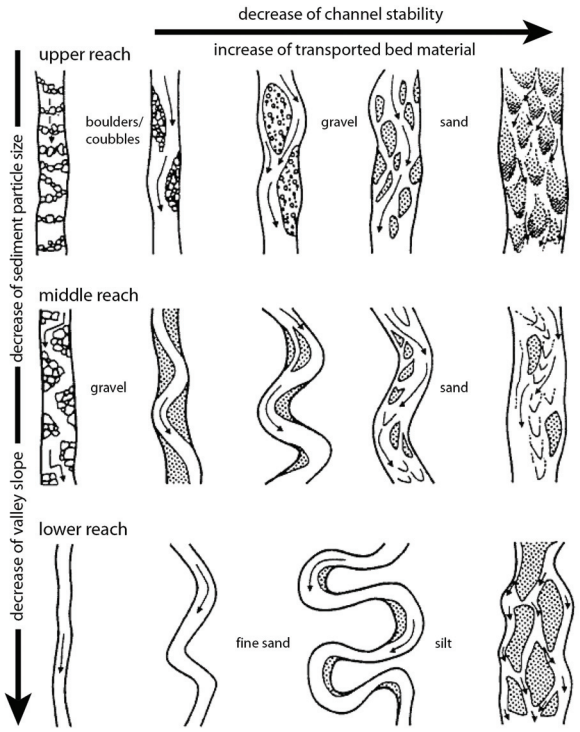

Figure 3.5: Planform evolution of alluvial channels (Rüther, 2006; Hütte, 1994).

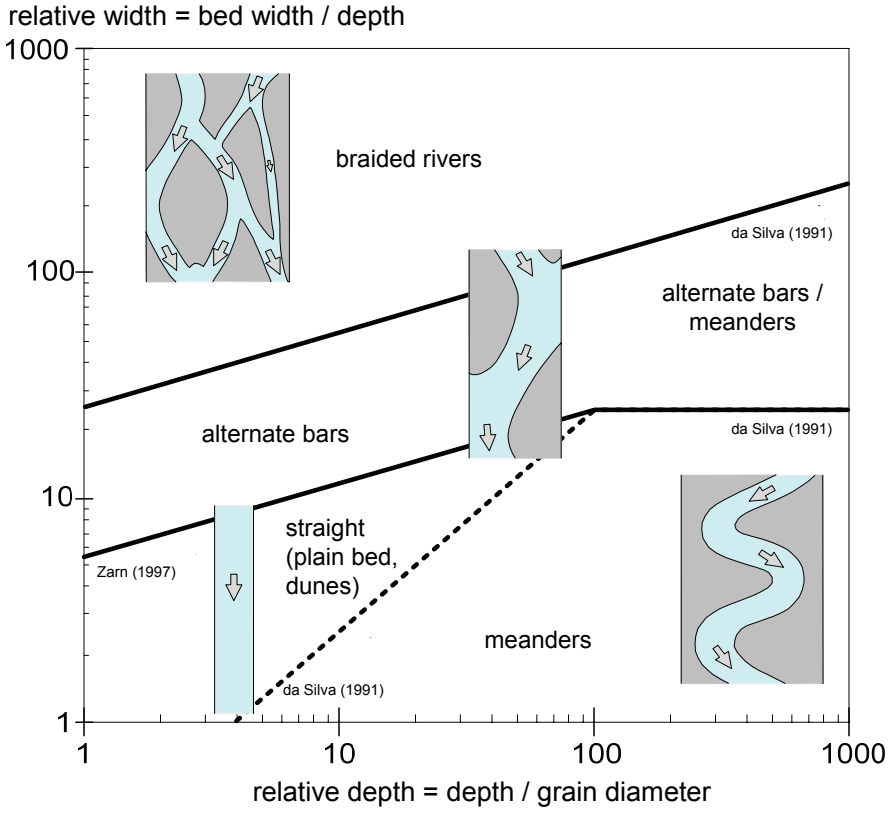

Figure 3.6: Channel form in dependency on width, depth and grain diameter (Zarn, 1997; da Silva, 1991).

The previous section shows clearly that bed load transport, channel slope and channel width are in distinct interdependency. This relationship has been further schematized by Zarn (2008), see Figure 3.7. For example, given a single-thread river section with fixed slope (Figure 3.7 top), bed load transport capacity increases if channel width is increasing until a maximum bed load transport capacity is reached at a critical bed width. If bed width further increases, bed load transport capacity decreases again towards a limit value with planform changing from single-bed to multi-bed pattern. In turn, if bed load transport capacity is required to be constant (e. g. for reasons of maintenance) and bed width increases (Figure 3.7 bottom), slope must be modified accordingly to keep the bed load transport constant.

Also the development of river banks is closely affected by morphodynamics, as can be easily concluded from Figure 3.5 - Figure 3.7. The erosion of river banks can become a serious morphodynamic hazard since it directly affects the safety of adjacent areas. Moreover, it can release enormous amounts of sediments and, thus, play a significant role for sediment budgets, transport behaviour and related river maintenance (see e. g. Schulte-Rentrop et al., 2005). But it should be emphasized that the processes and mechanisms governing bank erosion are as, or even more complicated than those for river bed erosion. According to Sear et al. (2003), there are 3 major bank retreat mechanisms: a) erosive processes which detach and transport single particles or assemblages of particles, b) bank failure mechanisms which lead to collapse of the bank and c) weakening processes on or within the bank that increase erodibility and reduce geotechnical stability (Thorne and Tovey, 1981; Thorne, 1982; Reed et al., 1994). These mechanisms are dependent on various factors affecting

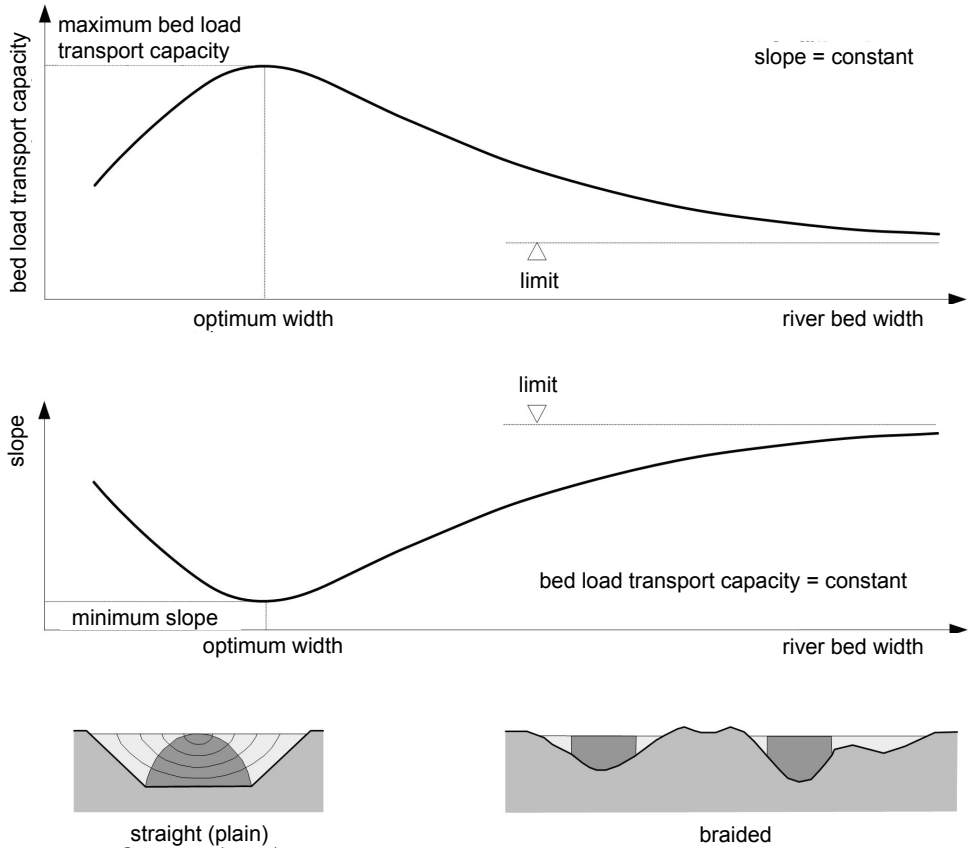

Figure 3.7: Influence of river bed width on bed load transport capacity (top) and slope (bottom) (Zarn, 2008).

stream forces and erosion resistance (Richards, 1982; Thorne, 1982; Knighton, 1996; Scherle, 1999): e. g. discharge regime (flood magnitude and frequency, occurrence throughout the year), climate, ground conditions (ground water level and flow, soil moisture), channel geometry, bank protection measures, biology (root structure and density, plant types, woody debris, burrows), sediment of bed and banks (content of cohesive fractions, friction angle, inhomogenity, layering) and sediment regime. Further recent research on bank erosion processes has focused e. g. on bank material variation (Julian and Torres, 2006; Wallick et al., 2006) or on vegetation cover (Micheli et al., 2004; Wynn and Mostaghimi, 2006) while new techniques on bank erosion rates have been published by e. g. Duan (2005). A review of existing methods for bank erosion management is provided by Piégay et al. (2005). The impact of bank material, sediment layering and vegetation on bank form is schematized in Figure 3.8.

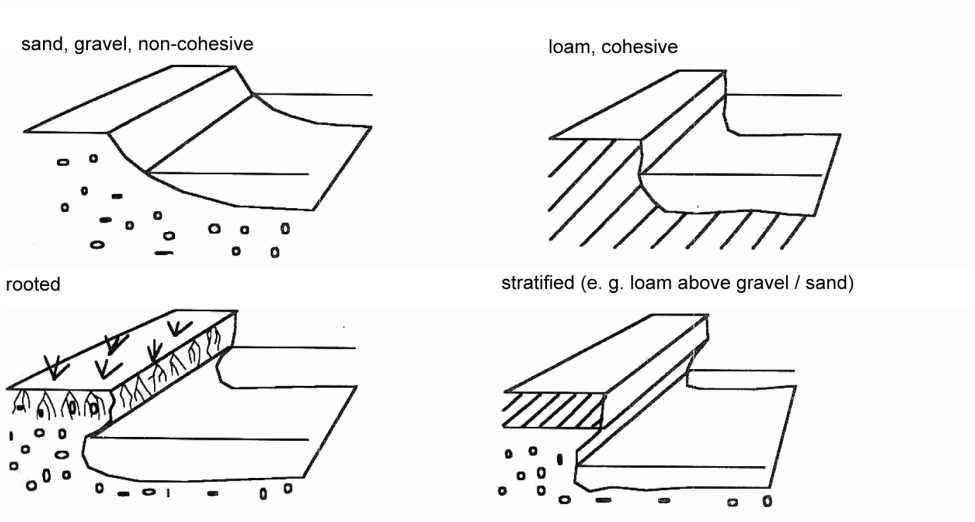

Figure 3.8: Influence of bank material on bank form (Scherle, 1999).

Various methods including sophisticated CFD codes have been developed for the determination of bank stability and erosion rates, see e. g. Schmautz (2003) and Rüther (2006) for a review. A straightforward handy method to roughly estimate bank stability for cohesionless material is the tractive force method, see Figure 3.9. It relates the critical Shields parameter of the bed to the critical Shields parameter on the bank assuming that bank stability is dependent on the friction angle of the bank material and on the cross-sectional geometry represented by the bank slope (see also Ikeda and Parker, 1989; Kovacs and Parker, 1994; Millar, 2005).

$$K = \frac{Fr^*_{c,\beta}}{Fr^*_{c,0}} = \cos\beta\sqrt{1-\frac{\tan^2\beta}{\tan^2\varphi}} \qquad 3\text{-}1$$

$Fr^*_{c,\beta}$ = critical Shields parameter of the bank, $Fr^*_{c,0}$ = critical Shields parameter of the bed, β = friction angle of the bank material, φ = bank slope.

This approach strongly simplifies nature since it neglects other factors than friction angle and is limited to flow parallel to the bank, trapezoidal channels and non-vegetated banks with non-cohesive sediments. But it is important to remark that it has been proofed useful for first rough estimations of

bank stability in engineering practice and has been used in modified versions in guidelines and numerical models (BAW, 2004; Schmautz, 2003, Millar, 2005).

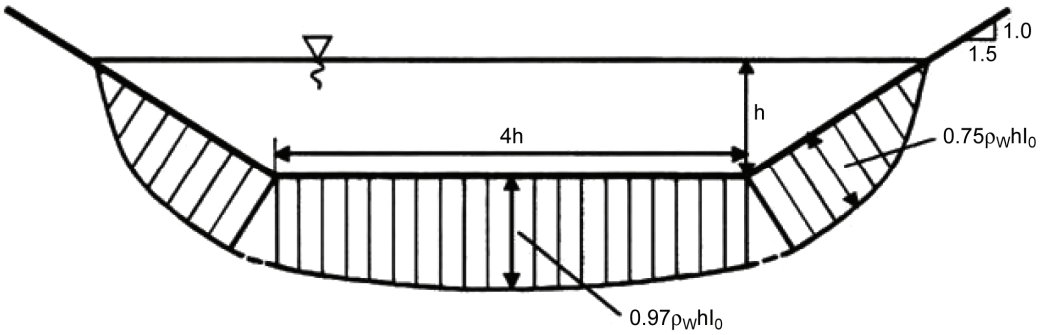

Figure 3.9: Bed shear stress distribution in dependency of bed geometry (Chow, 1959).

3.1.2.4 Hydraulic geometry

As previously shown, there is a distinct interrelationship between driving variables, boundary characteristics and dependent morphologic variables. If the magnitudes of the independent variables are known, this relation can be used to roughly estimate the magnitude of the dependent variables and to provide information on channel stability as well as on the sensitivity to morphological change. This is carried out by so-called hydraulic geometry equations or regime laws, see also Singh (2003). Regime equations usually follow the form

$$Y = a \cdot Q_{c-f}^{c} \qquad 3\text{-}2$$

with: Y = dependent variable, a and c = constants, $Q_{c\text{-}f}$ = channel-forming discharge.

assuming that the channel-forming discharge is the key driving variable (see Chapter 3.1.2.1). Various studies could show that if Y = bed width, Y is mostly proportional to $Q^{0,5}$. If Y = channel depth, the exponent c is dependent on the river's bed material (smaller for gravel bed rivers than for sand-bed rivers). If Y = slope, the exponent c is also varying with bed material, but is higher for gravel bed rivers than for sand-bed rivers. In all cases, bed width and water depth are increasing with increasing $Q_{c\text{-}f}$ whereas slope is decreasing with increasing $Q_{c\text{-}f}$. In order to determine the variables in Eq. 3-2 for a given river of interest, Copeland et al. (2001) propose several methods, e. g.: a) statistical analysis of field data from the investigated stream at stable, alluvial reaches, b) statistical analysis of field data from rivers with similar physiographic conditions or c) by means of generalized statistical regime equations from literature. However, methods a) and b) are often problematic due to data lacks and the nonavailability of reference reaches or similar rivers. Thus, c) is often enfavoured in practical engineering problems (see also Schulte-Rentrop et al., 2005).

The first generalized regime equations have been published by Lacey (1930). A review of hydraulic geometry equations is provided by Yalin (1992) as well as Copeland et al. (2001) for the quantification of bed width and channel depth of gravel-bed rivers. Examples are listed in Table 3-1. Besides bed width and channel depths predictors, there exist numerous approaches for the pre-estimation of meander geometry. These approaches follow the assumption that the ideal meander can be described by a sinus function as schematized in Figure 3.10. Examples for meander geometry

Table 3-1: Coefficients for regime equations based on field data.

author	system pattern	Y	a	c
Simons and Albertson (1960)	straight rivers, d_{50} = 0.03 – 0.8 mm	w_m	2.5	0.5
Kellerhals (1967)	U.S., Canadian, Swiss rivers of low sinuosity with paved beds, low bed load, d = 7–265 mm, I_0 = 0.00017–0.0131	w_b	3.26	0.5
Copeland et al. (2001)	U.S., Canadian rivers	w_b	3.68	0.5
	U.K. rivers	w_b	2.99	0.5
	<5% tree, shrubs or grass-lined banks (U.K.)	w_b	3.7	0.5
	≥5% tree or shrubs (U.K.)	w_b	2.46	0.5
Nixon (1959)	U.K. rivers, d_{50} = 0.1 – 0.6 mm	w_b	1.67	0.5
Simons and Albertson (1960)	straight rivers	h_b	0.43	0.36
Nixon (1959)	U.K. rivers	H	0.55	0.33
Kellerhals (1967)	Field (U.S., Canada, Switzerland, low sinuosity) and lab, paved beds, low bed load, d = 7–265 mm, I_0 = 0.00017–0.0131	h_m	$0.242*k_S^{-0,12}$	0.4

formulations are listed in Table 3-2, see e. g. FISRWG (2001), Copeland et al. (2001), Singh (2003) and Millar (2005)

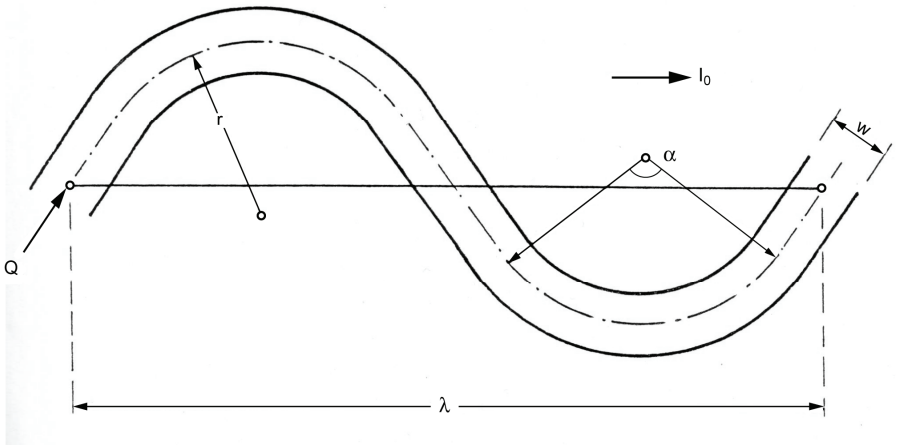

Figure 3.10: Definition of meander shape descriptors (e.g. Copeland et al., 2001).

for a review. According to Copeland et al. (2001), the most reliable hydraulic geometry relationship is wavelength λ vs. w according to λ ~w.

Various studies could show that hydraulic geometry relationships can well approximate the long-term morphology of natural rivers. But as well known in practice and as illustrated in Figure 3.11, rivers do not follow the regime laws precisely due to complexity and natural variabilities in space and time. Furthermore, Table 3-1 and Table 3-2 reveal various formulas for one and the same parameter. As a consequence, dependent on the formula chosen a wide scatter of potential dimensions is obtained.

In order to apply regime equations in river rehabilitation planning successfully, it is recommended to use more than one formula in order to reveal the range of possible results. Moreover, the formula

Table 3-2: Selection of regime equations (see e.g. Yalin, 1992; Singh, 2003).

Author	parameter	Formula
Leopold and Wolman (1957)	λ	$\lambda = 64 \cdot Q_b^{1/2} \otimes$
	λ	$\lambda = 10.9 \cdot w^{1.01}$
	A	$A = 2.7 \cdot w^{1.1}$
	R	$r = 2.3 \cdot w^{1.0}$
	R	$r = 2.3 \cdot \lambda^{1.0}$
Inglis (1941)	λ	$\lambda = 65.5 \cdot Q_1^{1/2}$
	λ	$\lambda = 6.6 \cdot w^{0.99}$
	A	$A = 104 \cdot Q_1^{0.54}$
	A	$A = 1.7 \cdot \lambda^{1.06}$
Dury (1965)	λ	$\lambda = 30 \cdot Q_1^{1/2}$
Yalin (1992)	λ	$\lambda = 6 \cdot w$

should be chosen with close respect to the river's characteristics. Baring this in mind, the regime equations can well indicate reach-average or ideal conditions about which channel morphology fluctuates (Copeland et al., 2001; FISWRG, 2001; Scherle, 1999). Subsequently, they can work as preliminary guide to potential changes and provide helpful information on the river's tendency to severe morphodynamic hazards.

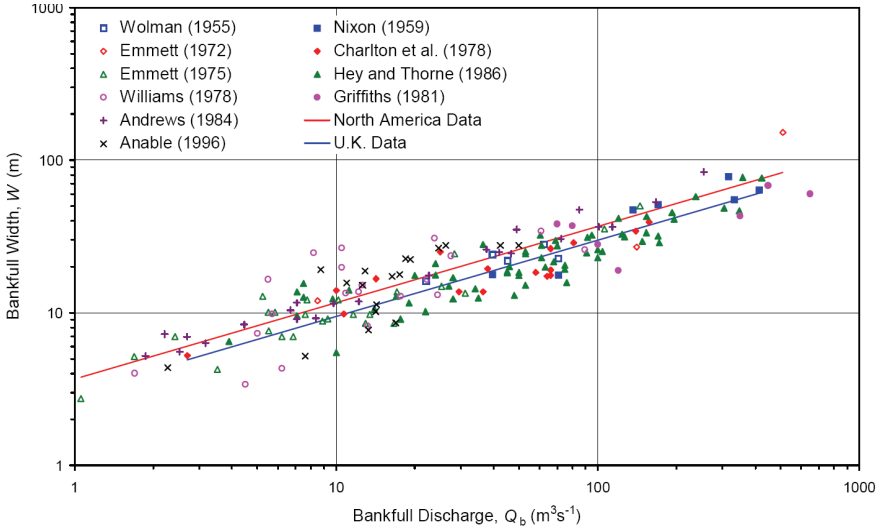

Figure 3.11: Derived regime equations for gravel bed rivers based on field data and scatter of data: North American rivers, w = 3.68 $Q_b^{1/2}$, U.K. rivers w = 2.99 $Q_b^{1/2}$ (Copeland et al., 2001).

3.2 HYDRAULICS OF NATURAL GRAVEL-BED RIVERS

Chapter 3.1 has shown that morphodynamics is determined by multiple processes interacting on different scales within a continuous dynamic system. So far, semi-qualitative approaches have been presented which help to understand morphodynamic interrelationships and to estimate the tendency to morphologic changes on the river reach scale. In order to perform the analysis of morphodynamic hazards for practical applications, it must be considered that the reach-scale behaviour is affected by many local physical processes (scale-time model by Kern (1994), see Figure 3.1) which have to be understood and quantified. The present chapter therefore aims to summarize the state of the art for small-scale hydrodynamic processes in natural streams.

First, a brief background on fluid dynamics in open channels is presented. Afterwards the influence of flow resistance on the flow field due to channel roughness and vegetation is highlighted. Finally the theoretical background for bed stability and sediment transport are presented. The focus is placed on processes mainly apparent in gravel-bed rivers with vegetated floodplains and on local scales which are most relevant for rehabilitation and natural flood protection measures.

3.2.1 Basic equations for the water flow motion in rivers

As discussed in Chapter 3.1, water flow in natural rivers is three-dimensional in nature and highly time dependent. The 3D flow field can be described by the differential equations of Navier Stokes (Eq. 3-4 in combination with the continuity equation Eq. 3-3) for incompressible fluids (ρ_W = constant) as follows (see e. g. Schlichting, 1979; Prandtl et al., 1969):

$$\frac{\partial u_i}{\partial x_i} = 0 \qquad 3\text{-}3$$

$$\frac{\partial u_i}{\partial t} + u_j \cdot \frac{\partial u_i}{\partial x_j} = -\frac{1}{\rho_W} \cdot \left[\frac{\partial p}{\partial x_i} - \rho_W \cdot \nu \cdot \frac{\partial}{\partial x_j} \cdot \left(\frac{\partial u_i}{\partial x_j} \right) \right] + F_i \qquad 3\text{-}4$$

where $u_{i,j}$ = flow velocity, $x_{i,j}$ = spatial scale, ρ_W = density of water, p = pressure, ν = kinematic viscosity, F_i = external forces; i, j = 1,2,3.

The first term on the left side of Eq. 3-4 is the transient or local velocity term (change of velocity with time), the second term is the convective term (the change of velocity with location). On the right hand side of Eq. 3-4 there is the pressure term and the stress term. The term F represents external forces acting on the fluid mass such as gravity or Coriolis forces. The latter is relevant only on large catchment scales and is therefore usually neglected in fluvial hydraulics (DVWK, 1999). In principle, Eqs. 3-3 and 3-4 are universally valid for describing the flow motion and could describe also turbulent flow in the case of sufficient computational resolution. However, the flow motions in open channels exhibit multiple turbulent structures of various spatial and temporal scales. Solving the equations above would require immense computational effort which is mostly neither necessary nor feasible while dealing with practical fluvial problems on the river reach scale. Hence, the turbulent flow motion in rivers is usually described by a simplified version of the Navier-Stokes equations in

combination with turbulence models. This simplification is based on time-averaging such that both the velocity and the pressure term are divided into a time-averaged value ($\overline{u_i}$, $\overline{p}$) and a fluctuating value (u′, p′):

$$u_i = \overline{u_i} + u_i' \tag{3-5}$$

$$p = \overline{p} + p' \tag{3-6}$$

Placing Eqs. 3-5 and 3-6 into Eqs. 2-1 and 3-4 and after some modifications the time-averaged turbulent flow field can be finally written by means of the so-called Reynolds-averaged Navier Stokes (RANS) equations (Eq. 3-8) and the time-averaged continuity equation (Eq. 3-7). The RANS equations are widely used in hydrodynamic modelling of the three-dimensional turbulent flow field in complex river reaches with vegetation and varying geometry, e. g. floodplains or natural streams:

$$\frac{\partial \overline{u_i}}{\partial x_i} = 0 \tag{3-7}$$

$$\frac{\partial \overline{u_i}}{\partial t} + u_j \cdot \frac{\partial \overline{u_i}}{\partial x_j} = -\frac{1}{\rho_W} \cdot \left[\frac{\partial \overline{p}}{\partial x_i} - \rho_W \cdot \frac{\partial}{\partial x_j} \cdot \left(\nu \cdot \frac{\partial \overline{u_i}}{\partial x_j} - \overline{u_i' u_j'} \right) \right] + \overline{F_i} \tag{3-8}$$

The first term in the inner brackets of Eq. 3-8 represents the inner or viscous stresses. The second term in the inner brackets represents the so-called Reynolds stress term obtained with time-averaging. It represents the shear stresses caused by turbulence in the flow and describes the momentum exchange caused by the fluctuations. However, Eq. 3-8 cannot be solved directly due to too many unknown variables. Thus, the Reynolds stress term is usually quantified by additional approximations and turbulence models. The most known is the Boussinesq approximation assuming that the Reynolds stresses influence the flow field like an inner shear stress and can be described by the mean flow field linked with a proportional constant, eddy viscosity ν_T.

$$-\overline{u_i' u_j'} = \nu_T \cdot \left(\frac{\partial \overline{u_i}}{\partial x_j} + \frac{\partial \overline{u_j}}{\partial x_i} \right) - \frac{2}{3} \cdot k \cdot \delta_{ij} \tag{3-9}$$

with k = turbulent kinetic energy, δ_{ij} = Kronecker delta.

The Boussinesq approximation assumes that turbulence is isotrop while the eddy viscosity ν_T is dependent on the flow field, on channel geometry and turbulence properties. For quantification of ν_T, additional turbulence models are required among which the k-ε model is most widely used in fluvial hydraulics. The k-ε model implies that turbulence features can be described by the turbulent kinetic energy k and the dissipation rate ε of the turbulent kinetic energy as:

$$\nu_T = \frac{c_\mu \cdot k^2}{\varepsilon} \tag{3-10}$$

with c_μ as constant.

To fully describe turbulence pattern, both k and ε require further equations and empirical constants which are not presented here furthering detail. Moreover, besides the k-ε model, other turbulence models exist, e.g. the k-ω model or Reynolds stress models (see Nezu and Nagakawa, 1993, for a review).

A prerequisite for reliable morphodynamic estimations is the accurate computation of the bed shear stress. If the flow field is resolved fully in three dimensions, bed shear stress can be directly derived from the near-bed flow field following the boundary conditions for rough walls represented by the logarithmic law

$$u_0^* = \frac{\kappa \cdot u_0}{\ln \cdot \left(\frac{30 \cdot y}{k_S} \right)} \qquad 3\text{-}11$$

where u_0^* = shear velocity close to the bed, u_0 = flow velocity close to the bed, κ = von Kármán constant = 0.4, y = distance from the wall, k_S = equivalent sand-grain roughness.

and can be computed by

$$\tau_0 = \rho_W \cdot u_0^{*2} \qquad 3\text{-}12$$

In order to explicitly account for the bed shear stress due to turbulent flow, τ_0 can be directly linked to the turbulence model while assuming that the production of turbulence is equal to the dissipation near the boundary (see Rodi, 1984). For the k-ε model this linkage yields:

$$\tau_0 = \sqrt{c_\mu} \cdot \rho_W \cdot k \qquad 3\text{-}13$$

In many hydraulic studies, the 3D RANS equations are applied in simplified versions only, to reduce both complexity and computational effort. These simplifications lead to the neglection of variable variations within a certain dimension and are mainly appropriate for less complex river sections or for preliminary estimations of the flow field (DVWK, 1999). For example, quasi-3D models with hydrostatic pressure assumption imply that vertical momentum exchange is negligible compared to the momentum exchange in lateral and longitudinal direction which is justified e. g. for rivers with wide beds. Herein, vertical velocity distribution is assumed to be homogenous with stream lines parallel to each other and vertical acceleration is set to zero. Simplified 3D flow equations can further be solved for defined vertical layers and/or optionally with additional distribution functions (DVWK, 1999) to account for vertical resolution. Very wide and shallow rivers can justify a further simplification of the RANS equations while assuming that the horizontal length scales are much greater than the vertical length scale. In this case, the RANS equations are depth-integrated, the vertical velocity and variations throughout water depth are assumed to be zero and in combination with the hydrostatic pressure approach the two-dimensional so-called shallow water equations are obtained (with i, j = 1,2):

$$\frac{\partial \overline{h}}{\partial t} + \frac{\partial \left(h \cdot \overline{U}_i \right)}{\partial x_i} = 0 \qquad 3\text{-}14$$

$$\overline{h} \cdot \frac{\partial \overline{U}_i}{\partial t} + \overline{h} \cdot \overline{U}_j \cdot \frac{\partial \overline{U}_i}{\partial x_j} = -g \cdot \overline{h} \cdot \frac{\partial \overline{z}_{WL}}{\partial x_i} + \frac{1}{\rho_W} \cdot \frac{\partial}{\partial x_i} \left[\overline{h} \cdot \left(V_{ij} + T_{ij} + D_{ij} \right) \right] + \overline{h} \cdot \overline{F_i} \qquad 3\text{-}15$$

where $\overline{U}_i$ = depth-averaged velocity, g = acceleration of gravity, $\overline{h}$ = mean water depth, $\overline{z}_{WL}$ = depth at water level, T_{ij} = turbulent stress term, V_{ij} = viscous stress term, D_{ij} = dispersion term.

Bed shear stress velocity u_0^* is commonly derived from the depth-averaged velocity $\overline{U}_i$ according to:

$$u_0^{*2} = c_f \cdot \overline{U}_i^{\,2} = \frac{\tau_0}{\rho_W} \qquad 3\text{-}16$$

with c_f as friction parameter.

However, the dispersion terms D_{ij} require further modelling approaches so that they have been neglected for a long time in the 2D equations for reasons of complexity. Only recently, further research is being carried out to implement turbulence considerations in 2D approaches. The shallow water equations can further be simplified by lateral integration yielding the so-called one-dimensional St. Venant equations. The 1D approach assumes that flow pattern are determined by longitudinal variation only while lateral or vertical variations are neglected. The St. Venant equations are widely used but, strictly speaking, their application is limited to simple, homogenous flow geometries, large scale studies or for preliminary hydraulic estimations.

$$\frac{\partial Q}{\partial s} + \frac{\partial A}{\partial t} + q_i = 0 \qquad 3\text{-}17$$

$$\frac{\partial Q}{\partial t} + \frac{\partial \left(k_m \cdot U \cdot Q \right)}{\partial s} + U \cdot q_i = -g \cdot A \cdot \frac{\partial \overline{z}_{WL}}{\partial s} - \frac{\tau \cdot R}{\rho_W} \qquad 3\text{-}18$$

with s = longitudinal river length, k_m = velocity correction parameter, Q = discharge, q = additional flow sources, $R = \frac{A}{P}$ = hydraulic radius, with A = cross-sectional flow area and P = wetted perimeter.

The parameter τ in Eq. 3-18 represents the bulk shear stress which sums up viscose and turbulent shear in one single parameter. The bulk bed shear stress which is evolved by the water body with depth h is computed by:

$$\tau_0 = \rho_W \cdot g \cdot h \cdot I_0 \qquad 3\text{-}19$$

with I_0 = bed slope, with $\sin\alpha = I_0$ if $\sin\alpha \to 0$

The bed shear stress is further related to the bed shear velocity u_0^* for 1D cases according to:

$$u_0^* = \sqrt{\frac{\tau_0}{\rho}} = \sqrt{g \cdot h \cdot I_0} \qquad 3\text{-}20$$

Note that the bed slope I_0 must be replaced by I_e in Eqs. 3-19 and 3-20 in the case of non-uniform conditions.

3.2.2 Flow resistance estimation in rivers

Bed material, bed forms, vegetation and the river geometry exhibit various kinds of resistance to the flow (see Figure 3.12). These characteristics lead to distinct energy losses by eddies which in turn influence the flow field and conveyance capacity of a river. The appropriate description of the hydraulic flow field is crucial, among others, for the proper determination of bed shear stresses and subsequently, bed and bank stability, sediment transport and, thus morphodynamics. Hence, the quality of the morphodynamic hazard determination and the success of a channel design are highly dependent on the quality of resistance estimation obtained. However, as shown in Figure 3.12, flow resistance is exerted by various sources. Although much effort has been taken within the last decades to understand and quantify flow resistance in natural vegetated rivers, many problems could not have been fully solved, or even satisfactorily parameterized, until today. Due to this, many studies with focus on morphodynamics of natural rivers bypass this obstacle by disregarding that conventional resistance approaches cannot reflect the hydrodynamic complexity in natural vegetated rivers at all. In contrast, the present study aims to show a new way considering flow resistance in combination with multi-dimensional modelling as basic key factor for adequate estimation of morphodynamics.

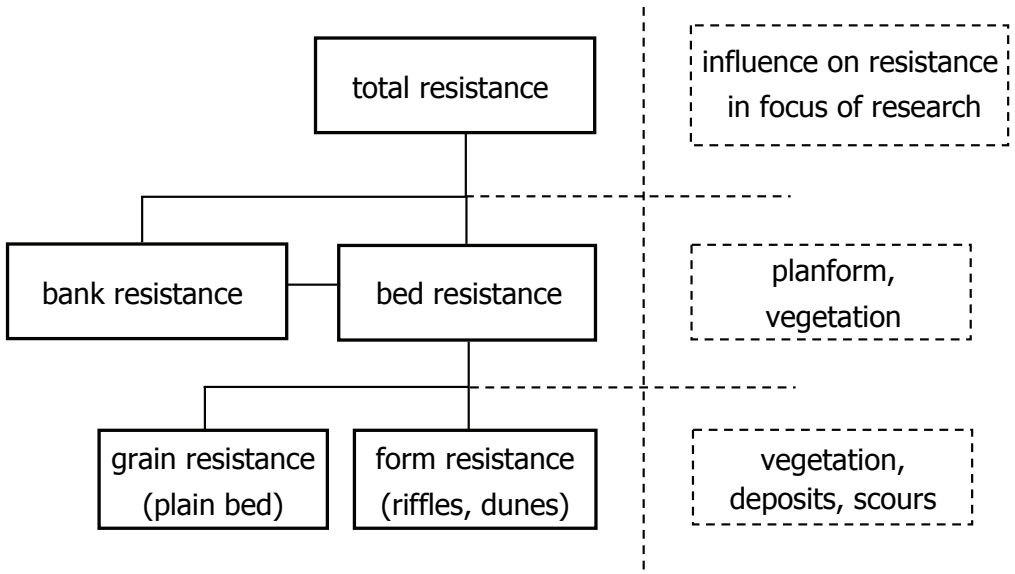

Figure 3.12: Sources of flow resistance in natural rivers with vegetation (DVWK, 1994; modified).

The present chapter presents the state of the art in flow resistance estimation. For reasons of clarity, it is subdivided in two parts: Chapter 3.2.2.1 summarizes the current knowledge of flow resistance estimation for non-vegetated channels. Chapter 3.2.2.2 deals with flow resistance estimation in streams with vegetation since they are of special interest for the present study objective.

3.2.2.1 Basic approaches for the vertical flow field and flow resistance

The 3D RANS equations can be further used in a simplified version to derive the vertical distribution of flow velocity which is standard practice today for turbulent flow over rough beds. It is assumed that the flow can be described by a two-dimensional flow and by a fully developed boundary

layer. The vertical velocity profile can then be well approximated by a logarithmic function which is written for fully turbulent flow (for details please refer to Schlichting (1979), Dittrich, 1998 or Mertens (2006)) with

$$Re^* = \frac{u_0^* \cdot k_s}{\nu} \geq 70 \qquad 3\text{-}21$$

with Re* = grain Reynolds number

according to:

$$\frac{u(z)}{u_0^*} = 2.5 \cdot \ln(\frac{z}{k_s}) + 8.5 \qquad 3\text{-}22$$

The characteristic logarithmic velocity profile for turbulent flow over rough rivers bed and the related vertical shear stress profile are shown in Figure 3.13.

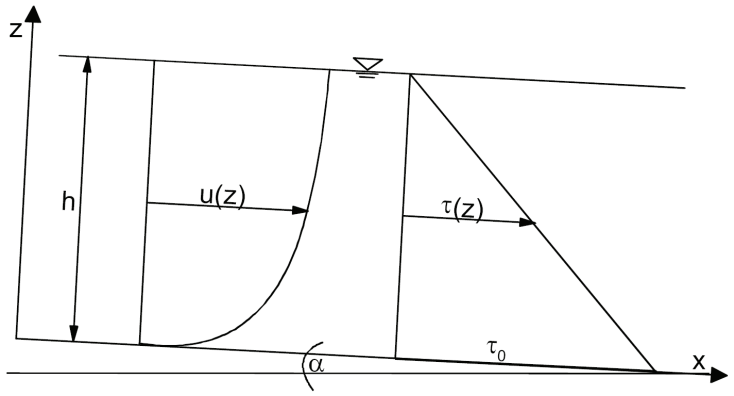

Figure 3.13: Vertical profiles of flow velocity and shear stresses.

Strictly speaking, Eq. 3-22 is valid only in the zone close to the wall where $z/h < 0.2$ (Schlichting, 1979) and must be modified if the flow field close to the water surface is of special interest (see e.g. Dittrich, 1998). However, the influence of the free water surface on the total vertical flow field is negligibly small so that for bulk considerations the velocity profile is approximated sufficiently well with the logarithmic law.

The mean flow velocity u_m can be obtained by the formula of Colebrook and White (1937), Eq. 3-23. The term B in Eq. 3-23 represents the impact of the channel form on the flow field.

$$\frac{u_m}{u_0^*} = 2.5 \cdot \ln(\frac{R}{k_s}) + B = \sqrt{\frac{8}{f}} \qquad 3\text{-}23$$

where B = 6.5, 6.27, 6.02 for semi-circle, trapezoidal and wide rectangular cross-sections (R ~ h); f = Darcy-Weisbach friction factor.

Eq. 3-23 draws a relation between the vertical velocity distribution and flow resistance of the channel which is parameterized by the variable f, called the Darcy-Weisbach friction factor. The

friction factor is mainly dependent on roughness structure and channel geometry. It is physically sound, dimensional homogenous and widely applicable.

In addition, alternative resistance approaches exist which follow a totally different scientific background and which are widely used for bulk uniform flow. E. g. Brahms and de Chézy developed a friction formula that is based on dimensional considerations. They relate u_m as proportional to the bulk bed shear velocity yielding:

$$u_m = C \cdot \sqrt{R \cdot I_0} \qquad 3\text{-}24$$

with C = Chézy roughness coefficient.

The Chézy coefficient depends on channel roughness (height, form, and spacing of roughness elements) as well as on size and shape of the cross-sectional flow area A. An alternative, widely used approach is the empirical equation of Gauckler-Manning-Strickler (GMS) which is obtained by substituting the Chézy coefficient by $C = k_{St} / R^{1/6}$ such as follows

$$u_m = k_{St} \cdot R^{2/3} \cdot \sqrt{I_0} \qquad 3\text{-}25$$

with the Strickler roughness coefficient k_{St} or its reciproce value, the Manning coefficient n, $k_{St} = 1/n$.

The advantage of the GMS approach is its straightforward handling and applicability what has led to one of the most applied friction formulas in fluvial hydraulics worldwide. The choice of the GMS friction factor is facilitated by the outcome of numerous studies and experience carried out in the last decades where values and methods for its estimation for natural and artificial roughness are provided (Chow, 1959; DVWK, 1990; USACE, 2000). The GMS or Manning equation also provides the hydraulic background for various computational and modelling tools, see Chapter 3.2. However, a significant negative aspect from the fluid mechanics perspective is that this friction factor is dimensionally non-homogenous and that it cannot be explicitly linked with the roughness properties. As bulk approach it only reflects the resistance exhibited by the whole channel summarizing shape, form and bed roughness.

Despite their different theoretical background, Eqs. 3-23, 3-24, and 3-25 are related such that the resistance coefficients can be transformed easily into each other as:

$$\sqrt{\frac{8}{f}} = \frac{R^{1/6}}{n \cdot \sqrt{g}} = \frac{k_{St} \cdot R^{1/6}}{\sqrt{g}} = \frac{C}{\sqrt{g}} \qquad 3\text{-}26$$

A basic assumption for the aforementioned formula is that flow resistance is distributed homogenously over the channel cross-section. However, this condition is rarely the case in natural channels since roughness is mostly distinctly varying along the wetted perimeter e.g. in the presence of heterogeneous geometry and floodplain vegetation which alter the velocity distribution significantly. In order to account for roughness variation along a cross-section, various 1D methods have been developed, e.g. the subdivision method of Einstein and Horton (1933) or the n-summation approach of Cowan (1956). More detail can be found in standard hydraulic textbooks, see e.g. Yen (2002) for a review. It must be pointed out that many bulk approaches do not account for the roughness change neither with channel width nor with water depth. However, bed width may

significantly influence the roughness exhibited by the banks on the flow field and roughness may vary considerably with water depth especially if channel banks are covered with vegetation. If the local flow field is of interest and flow conditions are highly three-dimensional, such as in rivers with heterogeneous geometry, river bends, narrow beds with considerable bank influence and vegetation, multi-dimensional treatment and other resistance formula may be required. Special friction approaches for vegetation resistance are presented in the following.

3.2.2.2 Flow field and flow resistance in streams with vegetation

Introduction

The major controlling factor of morphodynamics in natural rivers is vegetation. Vegetation is covering the river banks, river islands, and inundation areas. It significantly impacts river bank stability, biodiversity and water purification. Moreover, vegetation exhibits major flow resistance due to the fact that its stems and foliage form obstacles to the streaming water, sometimes – in the case of emergent vegetation – over the whole water depth. Hence, the flow resistance of the river bed is often exceeded by the flow resistance due to vegetation in natural rivers. In order to find a reliable design of rehabilitation and nature-close flood protection measures such as the reactivation of floodplains or retention areas, the impact of vegetation resistance on the flow field, conveyance capacity and, thus, morphodynamic hazards must be parameterized and quantified as accurately as possible.

Compared to non-vegetated river sections, vegetation is significantly altering the flow field leading to intensified energy losses, intensified sedimentation and erosion processes, and thus a reduction of conveyance capacity. Figure 3.14 illustrates the hydraulic effects of bank vegetation in a trapezoidal channel exemplarily according to the experiments with natural willows published by Felkel (1960) and as reported by Rickert (1986). In the non-vegetated channel, the isotachs are almost parallel to the channel boundary whereas, in the vegetated channel the flow field is extremely complex with isotachs parallel to the vegetation boundary: Here, maximum velocities do not occur, unlike homogenous channels, near the water surface, but are shifted towards the river bed. Moreover, flow velocities are significantly reduced both in the vegetated areas and the non-vegetated middle section. This phenomenon is evoked by high energy losses induced by macroeddies resulting from the velocity discrepancy between vegetated area and non-vegetated area, see Figure 3.15. The primary mechanism of momentum exchange between main channel and vegetated area is governed by spiraled secondary currents. Near bed fluid is accelerated into the direction of the floodplain while this transfer is counterbalanced by fluid transport from the floodplain in the direction of the main channel which occurs close to the water surface at lower velocities. In the case vegetation is present at the interface between main channel and vegetated area, the flow field is additionally influenced by wakes due to the vegetation elements (Schnauder, 2004). In the experiment of Felkel (1960), this intensive mass- and momentum transfer has led to a conveyance capacity reduction of more than 60 % in the vegetated channel compared to the non-vegetated channel. It is obvious that these processes have resulted within the last centuries in wide spread elimination of vegetation from the streams for flood protection purposes and river regulation.

A common phenomenon related with the described flow pattern along vegetated river banks is the development of fine material sediment ridges (German: “Rehne”) which can reach heights up to few meters (Schindler, 2008) see Figure 3.16. Sediment ridges mostly occur in the presence of structured

cross-sectional profiles, vegetated banks and adjacent floodplains which due to the presented interrelationships lead to distinct deposition of transported material.

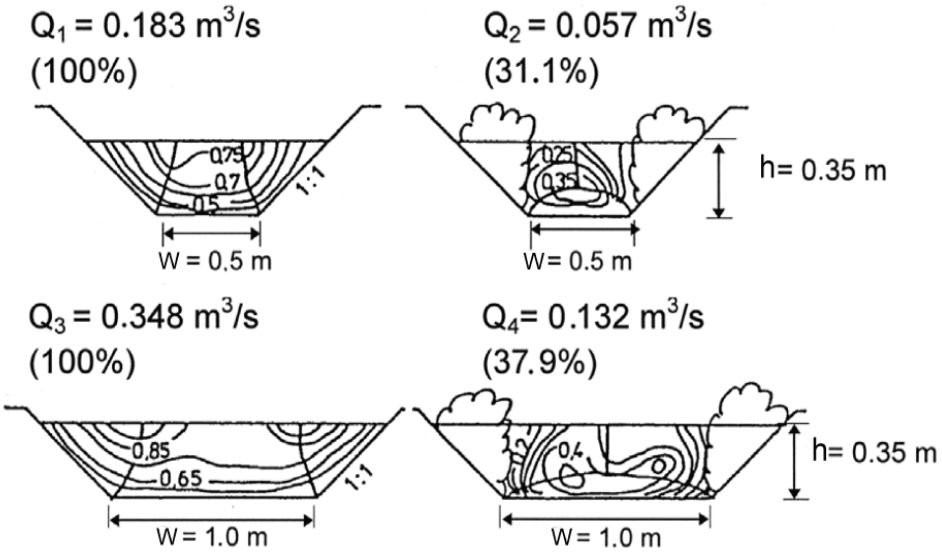

Figure 3.14: Modified isotachs due to riparian vegetation (Rouvé, 1987).

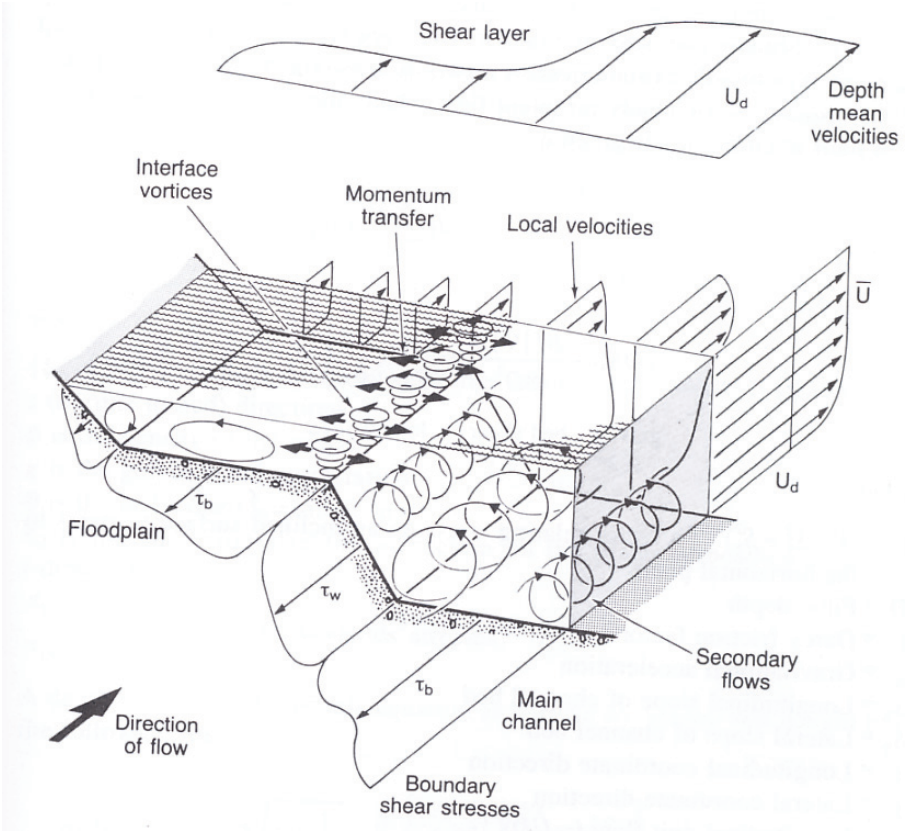

Figure 3.15: Velocity and bed shear stress distribution as well as macro-turbulent flow structures at the interface between main channel and floodplain (Shiono and Knight, 1991).

Figure 3.16: Sediment ridges as frequent phenomenon in compound channels with vegetated banks (photo: Geitz).

Schindler (2008) reports that sediment ridges can frequently be observed also in rivers with fixed banks. In natural rivers, however, they are usually destructed again by morphodynamics, e.g. by channel shifting.

The hydraulic effect of vegetation turns out to be even more complex if the plants characteristics are taken into account. Surface roughness of the plants, vegetation stiffness, presence of foliage, distribution of vegetation in longitudinal, lateral and vertical direction and on water depth all play a significant role for the resulting flow field and subsequently for morphodynamic processes in vegetated areas. A classification of the flow situation on or over vegetated floodplains has been published by Bölscher et al. (2005), as shown in Figure 3.17. The classification comprises four conditions exhibiting specific vertical velocity distribution each: submerged conditions, emerged conditions, emerged conditions with canopy and bottom flow as well as submerged conditions with

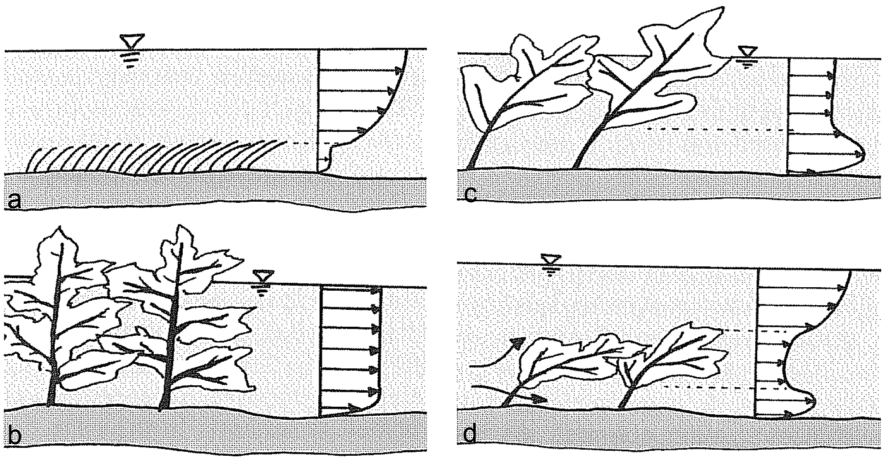

Figure 3.17: Flow conditions according to vegetation type (Bölscher et al., 2005).

canopy and bottom flow. It is obvious that – in the presence of vegetation – the vertical velocity profile does not follow the logarithmic law Eq. 3-22 any more and that for the proper estimation of the local flow field and bed shear stresses new approaches would be required. However, the estimation of the interaction vegetation – flow – morphodynamics could not be parameterized satisfactorily until

today and remains a field of research. Dittrich and Järvelä (2005) even concluded that a physically based understanding of the hydraulic, mechanical and biological controls is still missing. In order to determine the flow field in vegetated areas for practical applications, some simplications have to be drawn for hydraulic modelling that encounter for this complexity satisfactorily. An overview of approaches for vegetation resistance is presented in the following.

Approaches

So far, a considerable amount of research has been carried out related to vegetated flow. For many decades, vegetation roughness has been taken into account by simply adjusting the channel or floodplain roughness coefficient. Vegetation is then reduced to boundary roughness and its effect is added to one bulk friction factor such as the Darcy-Weisbach or Manning value which combines all sources of flow resistance in the channel. These conventional approaches have been widely applied to practical problems while the roughness coefficient is usually chosen by tables available in literature (such as Chow, 1959; DVWK, 1990; USACE, 2002). Among these, straightforward methods are e. g. the Cowan summation method (1956) or the n-VR method (Palmer, 1945; Kouwen et al., 1969; Rhee et al., 2008). However, these bulk approaches are suitable only for one-dimensional conditions. A detailed analysis of the significant hydraulic effect of vegetation on the flow field and thus on local morphodynamic processes is not possible (James et al., 2004; Wilson et al., 2005, 2006). One way to consider these interactions more appropriately is the separation of the total flow resistance of a vegetated channel into surface roughness (e. g. roughness height of the bed) and form resistance exerted by vegetation (see Petryk and Bosmajian, 1975; Pasche and Rouvé, 1985). Vegetation resistance can be calculated by a separate approach and then linearly superimposed with the surface roughness to determine the overall resistance, via (e. g., Yen, 2002; Dittrich and Järvelä, 2005):

$$f = f_s + f_P \tag{3-27}$$

where f_s = bed / surface roughness, f_p = form resistance of the plant.

Accordingly, the bed shear stress can be divided linearly into (e. g. Meyer-Peter and Müller, 1949; Patt et al., 1998):

$$\tau_0 = \tau_{0S} + \tau_{0P} \tag{3-28}$$

where τ_{0S} = shear stress exerted by the bed, τ_{0P} = shear stress exerted by the plant.

In order to calculate f_p, most computational approaches consider the case of emergent conditions where vegetation is taller than the water depth and rigid enough to withstand the flow (see Figure 3.17b), e.g. the approach of Lindner (1982):

$$f_P = \frac{c_v \cdot h}{2} \tag{3-29}$$

$$c_v = \frac{d_P}{a_x \cdot a_y} \cdot c_D \tag{3-30}$$

where d_P = stem diameter, c_v = vegetation factor.

In this case, the vertical velocity profile does not follow the logarithmic law any more, but is almost constant over depth. For bulk flow, classical friction laws such as Darcy-Weisbach or GMS may be

used (Bölscher, et al., 2005). However, if the local flow field is of interest, more sophisticated methods are required.

Recently, alternative physically based approaches have been developed to relate resistance to measurable characteristics of vegetation and flow, as already present in the Lindner formula. A widely used method is the determination of the vegetation resistance by associated drag forces. Herein, the plant is represented by a rigid cylinder which exhibits a resistance force to the flow. The drag force F_D is defined as

$$F_D = \rho_W \cdot \frac{u_{ref}^2}{2} \cdot f_P \qquad 3\text{-}31$$

where u_{ref} = reference velocity in cell, f_p = friction coefficient of the elements, C_D = drag coefficient.

with the friction coefficient:

$$f_P = \frac{A_P}{a_x \cdot a_y} \cdot C_D \qquad 3\text{-}32$$

where A_p = area projected to the flow, a_x, a_y, distance between stems in and lateral to flow direction, C_D = drag coefficient.

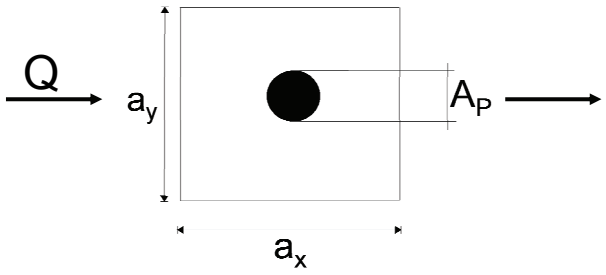

Figure 3.18: Vegetation element in the flow field with area projected to the flow A_P and stem distances.

Figure 3.19: Example for emergent rigid vegetation: floodplain forest along the Upper Rhine (photo: Bernhardt).

Taking the emergent flow type of Bölscher et al. (2005) in Figure 3.17 and floodplain forest in the succession stage depicted in Figure 3.19 into account, it can be concluded that mature floodplain forest can be well approximated by rigid cylinders. The suitability of this assumption could also be confirmed by experimental and field studies of e. g. Vischer and Oplatka (1998), Armanini et al. (2005), Schoneboom et al. (2008). However, the determination of the drag coefficient C_D is not straightforward since it is varying with flow and turbulence characteristics, rigidity, projected flow area, channel geometry and degree of submergence (Li and Shen, 1973; Lindner, 1982; Dunn et al., 1996, Nepf, 1999). For reasons of complexity, the drag coefficient is therefore usually reduced in practice to a bulk value which represents the total plant array of cylindrical rigid stems. Dittrich and Järvelä (2005) report bulk C_D values between 0.6 – 2.4, DVWK (1991) and Järvelä (2004) recommend 1.5 for practical applications. Stoesser et al. (2003) yielded reasonable results with C_D values around unity given that the afore defined boundary conditions are valid.

3.2.3 Bed stability and sediment transport in gravel-bed rivers

3.2.3.1 Bed stability

Another important morphodynamic hazard which goes hand in hand with the hydraulic flow field and resistance pattern is river bed erosion. As Chapter 3.1 shows, bed erosion is omnipresent also in geomorphologically stable rivers. But, in contrast to rivers in non-equilibrium, river bed erosion is then mostly a local phenomenon only and is closely associated with deposition of transported sediments to the effect that the overall sediment budget of the river section remains more or less constant. However, if changes in the driving variables in the system are severe (e. g. in the course or river training measures), river bed erosion can turn into a significant hazard associated with high amounts of released sediments and subsequently high costs of maintenance, as reported e. g. in Schulte-Rentrop et al. (2005). It is obvious that for sustainable river planning the river bed's potential reaction on planform and hydrologic modification must be estimated accordingly.

Bed stability, the tendency to river bed erosion and mechanisms of sediment transport are individual for each river system and are variable with regime of discharge and sediments, maintenance activities as well as bed and bank material. For example, the stability characteristics of rivers with rather homogenous bed material differ significantly from those of rivers with non-homogenous material. The first, e. g. many sand-bed rivers show a fully moveable bed while the latter often tend to more stable beds. The increase in bed stability is mainly caused by armouring processes due to selective erosion which is a widely observed phenomenon in gravel-bed rivers. Selective erosion occurs if smaller grains are transported away while the larger sizes remain on the bed. The space inbetween is filled up by smaller grains and "glued together" to the effect that bed stability increases successively. Both the maximum bed stability as well as the armour layer's thickness is determined by the maximum available grain sizes. Beneath the armour layer, a lower layer remains which consists of the original grain size distribution. In contrast to beds with loose material which are moveable at most discharges, armour layers remain stable at low and moderate flow conditions. Only at high flow events, flow forces usually can exert the resistance forces of the armour layer to the effect that the upper layer is destructed and sediment transport is initiated. In this case, large amounts of fine sediments beneath are released from the lower layer leading to severe bed incision. The phenomenon of armouring is especially enfavoured in gravel-bed rivers where discharge and sediment transport from upstream is limited by weirs and locks, such as in the Upper Rhine. This discussion shows that a detailed investigation of the system characteristics is necessary in order to estimate the bed development and related morphodynamic hazards adequately.

In common practice, river bed erosion is quantified by solving the problem of incipient motion. The classic approach for incipient motion is based on the force balance between flow forces and resistance forces of single sediment grains on the bed, see Figure 3.20. Flow forces can be described by the shear stresses on the bed τ_0 (e. g. acc. to Eqs. 3-13, 3-16 or 3-19). Flow resistance of the particle - the so-called critical shear stress τ_{0c}- instead is a function of various sedimentological (e. g. grain diameter, grain form, friction angle), morphological (e. g. water depth/roughness height, bed slope, bed structure) and hydraulic parameters. The ratio between shear stresses of the flow and the

resistance force by gravity of the submerged grain is called Shields-Parameter Fr* (also called sedimentological Froude number). Lifting forces by turbulence are neglected (Mertens, 2006):

$$Fr^* = \frac{u_0^{*2}}{\rho' \cdot g \cdot d_{ch}} = \frac{\tau_{0c} \cdot d_{ch}^2}{(\rho_S - \rho_W) \cdot g \cdot d_{ch}^3} \sim \frac{\text{attack of flow}}{\text{resistance of particle}} \qquad 3\text{-}33$$

with d_{ch} = characteristic sand grain diameter, ρ_S = sediment density.

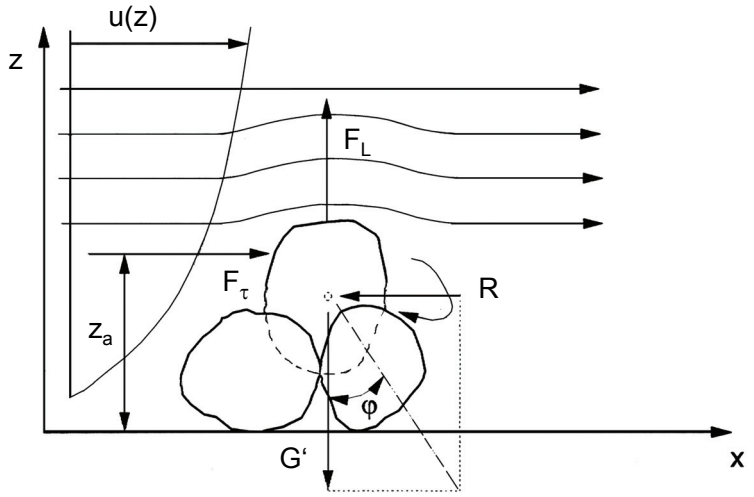

Figure 3.20: Forces acting on a sediment particle: F_L = lifting forces, F_t = shear forces, R = resistance force, G' = weight under submergence, z_a = wall distance, φ = friction angle (Dittrich, 1998).

Fr* is a function of the grain Reynolds number Re* and becomes constant at fully hydraulically rough flow conditions (Eq. 3-21). A well-known equation for incipient motion has been published by Shields (1936) with $Fr_c^* = 0.06$:

$$\tau_{0c} = 0.06 \cdot (\rho_S - \rho_W) \cdot g \cdot d_{50} \qquad 3\text{-}34$$

Strictly speaking, the Shields approach is valid only for rivers with homogenous, loose material and fully moveable bed. Armouring processes are not considered.

So far, numerous approaches for τ_{0c} have been published. Most of them follow the Shields approach Eq. 3-34, but with different sedimentological Froude numbers and characteristic grain diameter d_{ch}, see also Dittrich (1998) for a review. It is obvious that dependent on the chosen approach, distinctly varying values for τ_{0c} are obtained for one and the same system. As a consequence and considering the aforementioned individual stability conditions of each river, the stability approaches should be applied with close respect to the fluvial system. In order to account for individual bed characteristics in stability estimation, Koll and Dittrich (1998) classified stability approaches into four groups and validated them with field data (see Table 3-3): river beds a) without armour layer and loose material, b) with immature armour layer, c) of maximum bed stability and d) with mobile armour layer. It is worth noting that, in many hydraulic studies, stability approaches are

still used without being critically cross-checked for plausibility and regardless whether they can adequately describe the system behaviour. As a result, obtained results can deviate significantly from reality and might inhibit sustainable river planning.

Table 3-3: Summary of approaches available for bed stability (taken from Koll and Dittrich, 1998) with d_{mD} = mean grain diameter of the armour layer, d_{mA} = mean grain diameter of the original sample, ρ = density of water, $s = \rho_s/\rho_w$.

situation of armour layer	relationships	authors
loose material	uniform bed material $\tau_{oc} = 0{,}06 \cdot (\rho_s-\rho) \cdot g \cdot d_{50}$	Shields 1936
	non-uniform bed material $\tau_{oc} = 0{,}047 \cdot (\rho_s-\rho) \cdot g \cdot d_m$	MP/M 1949
	$\tau_{oc} = 0{,}035 \cdot (\rho_s-\rho) \cdot g \cdot d_{50}$	Wilcock et al. 1996
immature armour layer	$\tau_{oc} = 0{,}047 \cdot (\rho_s-\rho) \cdot g \cdot d_{mD}$	Gessler 1965
	$\tau_{oc} = 0{,}035 \cdot (\rho_s-\rho) \cdot g \cdot d_{50D}$	Parker and Klingemann 1982
maximum bed stability	$\tau_{oc} = \lambda \cdot 0{,}047 \cdot (\rho_s-\rho) \cdot g \cdot d_{max}$ $\lambda = \left(\frac{d_{mD}}{d_{max}}\right)^{0{,}64} \cdot \left(\frac{d_{mA}}{d_{max}}\right)^{0{,}33}$	Günter (1971)
	$\tau_{oc} = Fr_{*c} \cdot (\rho_s-\rho) \cdot g \cdot d_{mD}$ $Fr_{*c} = \frac{0{,}6^2}{a \cdot Fr_g^{\,2}}; \; Fr_g^{\,2} = \frac{u_m^{\,2}}{(s-1) \cdot g \cdot d_{mD}}$ $a = \left(\frac{d_{90}}{d_{50}}\right)^{1/3} \cdot \left(\frac{d_{mA}}{d_{50}}\right)^{1/2}$	Schöberl 1979, 1991
	$\tau_{oc} = 0{,}045 \cdot (\rho_s-\rho) \cdot g \cdot d_{90A}$	MP/M 1949
	$\tau_{oc} = Fr_{*c} \cdot (\rho_s-\rho) \cdot g \cdot d_{50Dmax}$ $Fr_{*c} = 0{,}05 \cdot \left[0{,}4 \cdot \left(\frac{d_{50D\,max}}{d_{50}}\right)^{-1/2} + 0{,}6\right]^2$	Chin 1985

3.2.3.2 Bed load transport

Bed load transport is defined as rolling or saltating transport of sediments close to the bed. Generally speaking, bed load transport is initiated if the critical shear stress of the bed material is exceeded by the shear stress of the flow. Numerous sediment transport equations have been developed within the last decades for sand and gravel material. According to Mertens (1995) these approaches can be roughly classified into three groups: a) deterministic approaches describing the relationship between transport relevant input parameter and sediment transport; b) stochastic approaches describing sediment transport by means of probability functions and c) statistic approaches using regression

analysis based on sediment transport data. Besides, various other classifications exist (Malcherek, 2009; Specht, 2002). In the following, two widely applied bed load transport formulas for gravel-bed rivers may be briefly presented.

Meyer-Peter and Müller (1949) investigated the relationship between bed load transport, discharge and energy slope under stationary flow conditions on the basis of data from 139 flume experiments. The experiments considered homogenous bed material (gravel with d_m = 5.2 and 28.65 mm) as well as non-homogenous material (sand and fine sand with d_m = 0.4 – 4 mm) while bed slopes ranged between 0.04 – 2 %. Based on their experiments, Meyer-Peter and Müller (1949) obtained the following deterministic relation with a critical Shields parameter Fr_c* of 0.047:

$$m_B = 8 \cdot \left(Fr_m^* \cdot \left(\frac{k_{St}}{k_r} \right)^{1.5} - Fr_c^* \right)^{1.5} \cdot \sqrt{\frac{\rho_S - \rho_W}{\rho_W} \cdot g \cdot d_m} \qquad 3\text{-}35$$

with m_B = bed load rate, Fr^*_m = 0.047 – Shields parameter with d_m as d_{ch}.

Moreover, Meyer-Peter and Müller modified the Gauckler-Manning–Strickler equation according to:

$$k_{St} = \frac{u_m}{R_b^{2/3} \cdot I_r^{1/2}} \qquad \text{with } R_b = \frac{Q_{bed}}{Q} \cdot h \qquad 3\text{-}36$$

where Q_{bed} = part of discharge forcing the bed: ($Q_b/Q \approx 0.95 – 1.0$ if $k_{St} \approx k_r$ and /or $w/R \geq 15$).

In contrast to the original form (Eq. 3-25), Meyer-Peter and Müller (1949) implemented the so-called hydraulic radius of the bed R_b in order to consider the influence of the river banks on the bed flow forces. Moreover, using the friction slope I_r instead of I_0, they take into account that bed forms might lead to increasing critical shear stresses. I_r is thus describing the part of the energy slope which is relevant for transport after elimination of bed form influence.

$$I_r = \left(\frac{k_{St}}{k_r} \right)^{3/2} \cdot I_0 \qquad \text{where } k_r = \frac{26}{\sqrt[6]{d_{90}}} \qquad 3\text{-}37$$

with k_r = grain Strickler parameter, d_{90} = grain size of 90 % finer.

The Meyer-Peter and Müller equation was further modified by Hunziker (1995) for fractional bed load transport in gravel-bed rivers. His approach is based on experimental results of Meyer-Peter and Müller (1949), Gessler (1965) and Günter (1971). Here, grain sizes of 0.3 – 6 mm with d_m = 1.59 – 2.71 mm and bed slopes of 0.14 – 5 % were considered. Hunziker (1995) reported that the approach of Meyer-Peter and Müller overestimated the energy losses caused by form friction (R_b und I_r, see Eq. 3-36 and 3-37) yielding overestimated effective shear stresses and subsequently too high bed load transport rates. Alternatively, Hunziker implemented the equation for form losses of Yalin and Scheuerlein (1988) with Fr_c* = 0.05 yielding:

$$m_B = 5 \cdot \left(Fr_m^* \cdot \left(\frac{k_{St}}{k_r} \right)^{1.5} - Fr_c^* \right)^{1.5} \cdot \sqrt{\frac{\rho_S - \rho}{\rho} \cdot g \cdot d_m} \qquad \text{3-38}$$

$$\text{where } k_r = \frac{23.5}{\sqrt[6]{d_{90}}}$$

There are several drawbacks related with bed load transport equations which make their application to nature extremely difficult. First, many approaches are fully or semi-empirical and have been developed from flume experiments and literature data with clearly defined laboratory conditions. Hence, their direct application to nature is rather limited. Secondly, it must be pointed out that bed load transport formulas are restricted to rivers with fully moveable bed in morphological equilibrium where transport capacity - the bed load transport rate which occurs at a given discharge without erosion nor deposition at fully moveable bed - is reached. However, these conditions are often not fulfilled especially in gravel-bed rivers where armouring processes occur. Moreover, other approaches have been derived for one special case study so that their validity is limited to that investigated system or they are too data-intensive for practical engineering problems. In fact, an omnivalid equation for bed load transport is still missing until today. Last but not least, as a result from the previous discussion, it turns out that the application of bed load transport equations to vegetated streams, vegetated gravel islands and floodplains is not possible. Transport mechanisms among flow, sediments and vegetation are not yet fully understood and remain in the focus of current research, see e. g. Zinke and Olsen (2007). Thus, as similar to stability approaches, also bed load transport equations should be applied only if boundary conditions are justifying their use.

3.2.3.3 Suspended load

The second important transport mechanism which determines morphodynamics in rivers is the transport of suspended sediments. In contrast to bed load transport which is limited to coarse particles (coarse sand and gravel) close to the bed, suspended load is transport of mainly finer sand and silt fraction within the water column. Suspended sediment transport is crucial for morphodynamic development of areas with low flow velocities such as on floodplains or harbours since in contrast to bed load transport which is inhibited there, suspended particles can reach those areas of low flow velocities by advective transport and turbulence.

The tendency of suspended particles to deposition is mainly a function of their characteristic settling velocity which, in turn, is a function of particle size, gravity and resistance forces of water. The settling velocity u_s in stilling basins can be quantified e.g. by the equation of Stokes for spheres with $d < 100$ µm by:

$$u_s = \frac{1}{18} \cdot \frac{(\rho_s - \rho_w) \cdot g \cdot d}{\nu} \qquad \text{3-39}$$

or according to Zanke (1977) for spheres with $100 < d < 1{,}000$ µm by

$$u_s = 10 \cdot \left(\frac{\nu}{d} \right) \cdot \sqrt{1 + \frac{0.01 \cdot (\rho_s - \rho_w) \cdot g \cdot d^3}{\nu^2}} - 1 \qquad \text{3-40}$$

The vertical profile of suspended load can be computed e. g. by the Rouse approach (1938) including the Rouse number Z as

$$c(z) = c_0 \cdot \left(\frac{h - z}{z} \cdot \frac{z_0}{h - z_0} \right)^{\frac{u_s}{\beta \cdot \kappa \cdot u_0^*}} = c_0 \cdot \left(\frac{h - z}{z} \cdot \frac{z_0}{h - z_0} \right)^{Z} \qquad 3\text{-}41$$

where c(z) = suspended load concentration at vertical level z, z_0 = reference depth, c_0 = concentration at z_0 , β = reciprocal turbulent Schmidt number.

with

$$Z = \frac{u_S}{\beta \cdot \kappa \cdot u_S^*} \qquad 3\text{-}42$$

The Rouse number Z expresses the ratio of gravity (settling velocity) and turbulent diffusity which is based on the von Kármán constant κ and the reciprocal turbulent Schmidt number (β ~ 1). As a consequence, the vertical concentration of suspended sediments is dependent on c_0 , z, settling velocity and flow forces close to be bed. The concentration profile according to Rouse is close to zero at the water surface and increases in vertical direction towards the river bed at high mixing and high turbulent diffusity. Highest concentration is reached close to the river bed. The Rouse number Z determines the form of the concentration profile following the relationship that the lower Z the more uniform is the vertical concentration.

Similarly to bed load transport, numerous equations for suspended sediment transport can be found in literature (e. g. van Rijn, 1984a; Zanke, 1982). In computational fluid dynamics, suspended sediment transport is usually quantified by the advective-diffusion equation, see e. g. Olsen (2004a) or Malcherek (2009) for details. It must be pointed out that the aforementioned equations are applicable only to non-vegetated streams. For vegetated areas, however, Zinke and Olsen (2007) showed that until today it is not possible to reliably describe suspended sediment dynamics by currently available hydrodynamic models due to the complex bio-hydraulic-sedimentological interactions.

3.2.3.4 Sediment transport lengths

Transport distances of sediments are of fundamental importance for morphodynamic development of rivers and related harzardous processes. The routes and distances transported sediments might take are required to be determined in many fields of river maintenance, e. g. for bed incision prevention in instable rivers, for the regulation of severe sedimentation processes in harbours and shipping routes as well as for river restoration projects where the morphology governing parameters are altered.

Obviously, sediment transport distances are the results of transport mechanismen and various interactions in a river. As a consequence, their determination is rather challenging up to now. In the last decades, several studies were conducted with the aim to develop equations for transport lengths, however with insufficient results. The approaches can be classified in indirect methods where the transport velocity of particles are determined and in direct methods which focus directly on transport lengths as parameter in question. Due to the reported complexity of sediment dynamics, most approaches are either empirically or stochastically based requiring a large amount of field data with the effect that their application in field practise is rather limited. The problem is further aggravated by

the fact that approaches follow different physical assumptions yielding contradictive results among each other. E. g. the studies of Stelczer (1981) and Church und Hassan (1992) concluded that transport distances are only a function of grain diameter while Ljubomirova und Seveleva (1968) assume them independent of grain size and solely dependent on water depth and flow velocity. Test calculations carried out in the present study exemplarily with the approaches of Ljubomirova und Seveleva (1968) as well Stelczer (1981) for the Rhine-section Weil-Breisach showed unrealistic deviations reaching magnitudes of 10^6 between the equations for common discharge events which indicates their limited practicability. As a result, expertise mostly agrees that transport lengths are hardly determined by theoretical approaches in morphodynamic studies in terms of hard figures and could alternatively be described only by means of probability functions (Gautier, 2004).

A practicable alternative to gain an insight in sediment dynamics is provided by tracer studies which are conducted in the river investigated e. g. by colored, marked or radio-controlled stones. Although extensive, tracer studies yield promising results and are very helpful for enhancing system understanding, e.g. Gautier, (2004), Mc Ewan et al. (2000), Faulhaber and Riehl (2000), Gölz and Trompeter (2000).

3.2.3.5 Bed level changes and alternative approach for sediment transport behaviour

The processes of bed erosion and sediment transport (via bed and suspended load) finally govern the morphodynamic development of rivers via changes of the bed topography. In fluvial hydraulics, bed level changes are commonly quantified with the help of the sediment continuity equation (so-called Exner equation). The Exner equation describes sediment continuity by the difference of inflowing and outflowing fluxes for each section (river section or bed cell, dependent on the dimensionality considered). If sediment balance in the section is not met, the system is reacting with deposition or erosion and thus yielding bed level changes. A simple form of the Exner equation is:

$$\frac{\partial z_0}{\partial t} = \frac{\mathrm{Flux}_{in} - \mathrm{Flux}_{out}}{A} \qquad 3\text{-}43$$

with Flux_{in} = inflowing sediment flux, Flux_{out} = outflowing sediment flux, A = base area.

Flux_{in} is comprising bed and suspended sediment load which is being deposited in the section of interest. Flux_{out} is comprising material leaving the section after being eroded from the bed (and transported as bed load or in suspension), as well as bed load and suspended load which is transported into the section and leaving it again without being deposited.

Within the last years, the Exner equation has become standard tool in fluvial hydraulics. However, the approach can yield reasonable results only if mechanisms of bed erosion, deposition and sediment transport are quantified adequately. As repetitively mentioned, this remains a challenge especially in vegetated river systems where the proper physical description of sediment-flow-vegetation interaction is still not solved.

An alternative approach for sediment transport behaviour was developed by Wang and Dittrich (1992). They derived a theory of suspended sediment motion based on numerical solutions of the diffusion equation and Eq. 3-42 with different boundary conditions. Wang and Dittrich (1992) applied the relationship to a 2D open channel flow assuming the vertical flow component to zero at the water

surface, bed load concentration close to the bed as constant and uniformly distributed suspended sediment concentration at the entrance of the channel. Investigated was the development of the sediment concentration profile by variation of the incoming sediment concentration at the entrance of the channel and by variation of the Rouse number. The numerical solutions indicated that suspended sediments with Z values < 0.06 distribute uniformly and depend on the incoming concentration only while sediments with Z values > 0.1 depend on turbulence intensity and bed load concentration. At Z values larger than 5, concentration was found to be little affected by turbulent diffusity but mainly dependent on the tractive force of flow. Thus apparently, the tendency to transport in suspension is increasing with decreasing Rouse number (with decreasing ratio of settling velocity to shear stress velocity). Since Wang and Dittrich (1992) could well confirmed their numerical investigations with field data, their approach distinguishes sediment transport behaviour according to Table 3-4:

Table 3-4: Sediment transport behaviour in dependency of the Rouse number Z (Wang and Dittrich, 1992).

Rouse number	predominating transport mechanism
Z > 5	bed load transport
Z = 3 ~ 5	transition zone
0.1 < Z < 3	suspended transport
Z < 0.06	wash load

Dittrich et al. (2007) successfully applied this approach to estimate the sediment transport behaviour in side channels of vegetated flood retention areas in the Upper Rhine. Settling velocity of the sediments in Eq. 3-42 was derived from field data while the shear stress velocity u_s^* was quantified by means of a fully 3D hydrodynamic numerical model with a physically based approach for vegetation resistance. Dittrich et al. (2007) concluded that with this combined tool, a reasonable estimation of morphodynamic development in vegetated nature-close rivers is possible.

3.3 LITERATURE REVIEW ON METHODS FOR THE PROGNOSIS OF MORPHODYNAMIC PROCESSES IN NATURAL RIVERS

The previous chapter shows that, due to the complexity of interacting processes, the proper estimation of morphodynamic development in river restoration and nature-close flood measures is not straightforward. The present chapter aims to summarize existing approaches available in literature which focus on the pre-estimation of morphodynamics and which could be applicable in the early planning stage of a project. Moreover, they are discussed referring to the following scope of this study.

In literature, several strategies can be found concerning the planning, assessment and evaluation of nature close river measures and induced morphodynamics. Taking a closer look however, approaches which could be used for the given study objective are scarce. This is due to the fact that the interdisciplinary approach in river management is rather new. New insights in climate change, its impact on flood risk, the resulting need for sustainable, holistic flood protection strategies as well as

the demands of the EU Water Framework directive have become in public and political awareness only recently. Given that, current literature is mainly addressing the public, stakeholders, politics and river managers in forms of guidelines (e. g. Rutherfurd et al., 2000; FISRWG, 2001) or project reports (e. g. Wolters et al., 2001), however often with generalized recommendations concerning tools and procedures. Other studies investigated the topic only from clearly defined aspects as forestry, vegetation dynamics or ecology while dealing with the physico-hydraulic interactions between flow and floodplain development only marginally (Hughes, 2003; Blackwell and Maltby, 2005; Armbruster et al., 2006; Geerling, 2008). Thus, the assessment of river rehabilitation measures *before* its implementation is still problematic and is usually being performed afterwards via intense monitoring techniques (RRC, 2002; Caruso, 2006). Accordingly, methodologies which are applicable to practical problems on the river reach scale, are just under development, certainly also due to the complexity of the given task as shown in the previous chapter. Downs and Thorne (1998, 2000), Fischenich and Morrow (2000), FISRWG (2001), Copeland et al. (2001), Sear et al. (2003), Shields et al. (2003), Meixner et al. (2003) were doing the first step towards a pre-estimation of morphodynamic development within the river planning procedure in flood protection and river rehabilitation.

3.3.1 Guidelines

Guidelines for assessing restoration projects and fluvial geomorphology have been published by Rutherfurd et al. (2000), Copeland et al. (2001), FISRWG (2001) and Sear et al. (2003) for Australia, the US and the UK where the current knowledge was summarized. The authors proposed stepwise methodologies towards sustainable river design. This methodology mostly includes - besides the project planning phase itself - a detailed river analysis concerning hydrologic, hydraulic, sedimentological and geomorphologic studies which is based on detailed data collection, field investigations and the application of regime theory, reference reaches and hydraulic modelling for design verification with catchment-wide and long-term perspective. However, although these guidelines have been developed for river rehabilitation strategies where vegetation would be omnipresent, representation of vegetation was treated only marginally, if ever by bulk roughness approaches such as Manning's n and the Cowan method. Moreover, most reports neglected that for reliable estimations, hydraulic formula must be chosen carefully with respect to the river's boundary conditions. Thus, mainly conventional approaches such as the Manning's equation and the Shields equations were suggested to account for conveyance capacity, stability and flow resistance disregarding the variability of fluvial systems. Shields et al. (2003) published a methodology for the assessment of river design similar to the guidelines above. However, Shields et al. (2003) emphasized that their approach was strictly limited to single-thread channels of simple geometry while calling for more sophisticated modelling approaches in the case of heterogeneous flow fields in complex rivers.

A detailed guideline for the management of riparian forests was published by Meixner et al. (2003) as final report of the EU-funded project RipFor (Hydraulic, Sedimentological and Ecological Problems of Multifunctional Riparian Forest Management). They provided a state-of-the-art collection of measurement techniques and theoretical approaches for evaluating the actual situation of a river reach as well as future scenarios concerning hydrological, hydraulic, morphological, vegetation and ecological aspects and according to the goal of investigation, location in the river system and spatial scale. The tools have been applied and verified both in field and lab studies. Meixner et al. (2003)

recommended the use of conventional straightforward methods for simple geometries but referred to sophisticated approaches, if required by more complex boundary conditions (e.g. improved roughness formulas for bed and vegetation as well as multi-dimensional modelling).

Besides guidelines, various lab and field studies have been carried out in order to estimate morphodynamic development of natural rivers. The key predictive tool is herein the use of hydraulic modelling.

3.3.2 One-dimensional modelling

As previously shown, straightforward one-dimensional models are widely and successfully applied in hydraulic studies especially to water level calculations or flood wave propagations on the upper river reach and catchment scale (e. g. Minh Thu, 2002; Kidson et al., 2006; Lopéz-Avilés, 2007). Recent research in 1D morphodynamic modelling has mainly concerned the coupling with sediment transport, bed level changes (Catella et al., 2005; Daly and Porporato, 2005; Salant et al., 2006; Schweizer et al., 2007; Verhaar et al., 2008; Bertoldi et al., 2009), meander shifting (Solari and Seminara, 2005), bank stability and landslides (Mahdi, 2007).

Downs and Thorne (1998, 2000) used 1D models for assessing planned rehabilitation and flood protection measures in the sandy-gravel bed River Idle in Great Britain. Since the authors were not satisfied with currently available modelling approaches they applied three different 1D models separately for defined purposes. Instead of the conventional Manning's n method, they developed a combined model (HMODEL2 and FCFA) with a physically-based approach for the Darcy-Weisbach friction factor that takes gravel bed and rigid vegetation as boundary roughness elements into account. Furthermore, the 1D model HEC-RAS was used to simulate the impact of the measures on regional flood defence. The authors concluded that the combined modelling approach was sufficiently well performing for their purpose. But they found several shortcomings due to the models' inability to account for, e. g. strong secondary currents and for a proper representation of the vegetation resistance.

Thomas and Nisbet (2006) investigated the impact of floodplain woodland on flood level, flow velocity and storage volume for a 2.2 km short reach of the River Parrett in the UK. They used a 1D model (HEC-RAS) in comparison with a 2D model (River2D) for water levels and velocity distribution. Three scenarios of different vegetation density were considered. Vegetation roughness was estimated in the 1D model with Manning's roughness and in the 2D model with k_s, respectively via look-up tables for a 100-year event without calibration. For both models, the same roughness height was chosen. Topographic input data were derived from high resolution LIDAR data. The authors concluded that the approach could sufficiently well illustrate the impact of vegetation of flood retention. Calculated water levels were in good agreement for both models with deviation of less than 5% while distinct differences were observed concerning the flood peak travel time.

An alternative one-dimensional approach for main channel and floodplain flow has been developed by Yoshida and Dittrich (2002) with special respect on vegetation. Yoshida and Dittrich (2002) simulated the flood wave propagation for a 42 km long section of the River Rhine with a 1D unsteady-state hydraulic model. Flow friction was quantified by subdividing the Darcy-Weisbach coefficient into bed roughness of main channel and floodplains, the drag force caused by riparian forest and momentum exchange between main channel and floodplain (see also Chapter 3.2.2.2) was modelled

using the approach of Pasche and Rouvé (1985). Input parameters for vegetation drag were taken from field studies. Bed roughness of main channel and floodplain was calibrated with a second 1D steady-state model and verified with gauging data. Yoshida and Dittrich (2002) found the modelling result to be in good agreement with observations, but called for a better parametrization of vegetation properties in future hydraulic modelling.

Chatterjee et al. (2008) used a 1D model and a coupled 1D-2D model to evaluate flooding and emptying processes in polders (emergency storage areas) along a 18.6 km long reach of the River Elbe. Flow resistance was represented by a bulk Manning's roughness and chosen according to literature data and calibration. The 1D model was stepwise calibrated and validated against gauging data for the river bed and the floodplain separately. To evaluate uncertainties related to roughness choice, grid resolution and number of cross-sections used, a detailed sensitivity analysis was carried out. The authors concluded from the results that a 1D model could sufficiently well predict water levels and conveyance capacity in the area whereas a 1D-2D approach was recommended for investigation of flow dynamics in the polder. Moreover they observed high sensitivities to changes in the roughness values for the 1D model rather than for the 1D-2D model.

3.3.3 Two-dimensional modelling

In addition to the simplified 1D treatment of fluvial hydraulics, 2D shallow water equations have been increasingly used in the last years and were found to suitably approximate the flow pattern in rivers with large width-to-depth-ratio. 2D flow representation results from depth-averaging of the RANS equations under the conditions that vertical flow acceleration is negligibly small compared to lateral and longitudinal flow acceleration. Depth-averaging is usually linked with the hydrostatic pressure assumption including that horizontal pressure gradients can be approximated as a function of water depth (see Chapter 3.2.1). One drawback of depth-integration is the necessity to introduce additional correction parameters in the shallow water equations which account for the neglected vertical velocity component. However, according to DVWK (1999), Lane (1998) and Lane et al. (1999) their explicit formulation have been neglected for long time and only recently steps were undertaken to represent 3D effects in the 2D equations (Wu et al., 2004; Minh Duc et al., 2005; Perucca et al., 2009; Knight et al., 2007; Tang and Knight, 2008).

2D shallow water equations have been successfully used on the upper river reach scale for evaluating e. g. inundation processes (Bates and de Roo, 2000; McMillan and Brasington, 2007) and ecological habitats (Crowder and Diplas, 2000; Pasternack et al., 2004). Current research is focusing on improving sediment transport formulation and meandering processes (Abad et al., 2008; de Moor et al., 2007; Li and Millar, 2007). However, although most 2D models have been developed for investigating inundation processes on floodplains where distinct roughness features are omnipresent, many of them treat resistance induced by structural elements and vegetation only marginally (see also Yu and Lane, 2006a). First attempts to explicitly account for floodplain roughness have been published by e. g. Beffa and Connell (2001), Kowalski et al. (2006), Yu and Lane, (2006 a,b), Bennett et al. (2008). Bennett et al. (2008) used the 2D model of Wu et al. (2005) with sediment coupling, dispersion consideration and the drag force approach for comparing laboratory flume experiments with modelling results. Two vegetation zones of different shapes were introduced into a trapezoidal channel to investigate bed level changes. They observed that the spatial pattern of bed changes was generally

well predicted by the numerical model but deviations occurred directly upstream and downstream of the vegetated zones.

Toda et al. (2005) investigated the interaction between floodplain flow, sediment-related nutrient deposition and vegetation development via field observations and a 2D shallow water equation model. Flow resistance was formulated with the Manning's equation via linear superposition of a constant friction parameter for the river bed and a drag formula for riparian vegetation for groups of cylinders. Toda et al. (2005) found that the model reproduced the tendency of deposition fairly well, but concluded that further model development is required to obtain quantitatively satisfying results for practical applications.

In the course of technological advances, remote sensing data and aerial photography are increasingly used as topography data source in geomorphology and have largely contributed to an improvement of predictability. They are also widely applied today in studying morphodynamics as input data for multi-dimensional modelling as well as for GIS based analysis. E. g. Geerling (2008) used LIDAR data to track and reconstruct channel and floodplain changes for a Dutch reach of the River Rhine. Geerling (2008) investigated the linkage between measured sedimentation rates, vegetation structure to hydraulic changes by comparing digital elevation models and aerial photographs of vegetation structures for different years by a GIS system. The effect of changing topography and vegetation structure on flow velocity, flow direction and water level was analysed by 2D hydraulic modelling for different years. Vegetation roughness was estimated from literature data as Chézy roughness according to the vegetation types provided from aerial photography. However, it is not clear how bed roughness was chosen and if and how the hydraulic model was calibrated. The approach suggested by Geerling (2008) is useful for describing qualitatively the impact of vegetation, flow and floodplain sedimentation but it is not applicable for the task of the present study since a sound physical linkage of interacting processes is missing.

3.3.4 Three-dimensional modelling

At the small scale, recent research has shown a move away from 2D models to fully 3D models. With the solution of the RANS equations in three dimensions, 3D models aim to reduce the uncertainties related to 2D models which represent complex flow processes with simplified 2D velocity fields and empirical assumptions only. 2D models reach their limit of reliability when natural morphodynamics are of interest on the local scale induced by overbank and inundation flows, variable geometry and distinct roughness elements which lead to highly three-dimensional flow pattern and which require the accurate resolution of the near bed flow field. However, the development of 3D models has been challenged a long time by the complexity of numerical methods required and the representation of physical interactions involved. Many studies still concentrate on solving technological problems such as grid generation and improvements of numerical stabilities. Subsequently, 3D models are mainly applied to test studies on the laboratory scale for their improvement and validation (e. g. Choi and Kang, 2006; Li and Zeng, 2009) and only less to real fluvial systems. Stoesser et al. (2003) reported that, due to both process and numerical complexity, many 3D tools exhibit a high need for re-calibration for different flow conditions, especially concerning turbulence closure which complicates their application in practical cases. Thus, only few

tools appear suitable for engineering problems on the river reach scale. e.g. Fischer-Antze (2005) and Stoesser et al. (2003).

Fischer-Antze (2005) carried out a real case study by using the 3D numerical model SSIIM for investigating morphodynamic processes along a 8 km long Austrian reach of the Danube River. The model SSIIM from Trondheim University (Olsen, 2004b) has been originally developed for sediment movements in water intakes including bed load and suspended sediment transport. SSIIM uses the finite volume method for solving the 3D RANS equations with a standard k-ε model while the pressure term is computed with the SIMPLE method. Fischer-Antze (2005) evaluated the model performance for the River Danube regarding unsteady flow, sediment transport and morphological changes while the sediment transport module was modified by incorporating a non-uniform sediment transport formula considering hiding-exposure effects. Vegetation resistance was of minor importance in this reach. Among others, the model was calibrated and validated regarding flow pattern in a steady state mode for two discharge events and was compared on plausibility with analytical formulas. Flow simulations of the research events revealed that 3D flow field and 3D bed level changes were found in good agreement with measured values. A sensitivity and an error analysis were carried out showing that 78 % of the erosion-deposition pattern were computed at the correct position when a measurement tolerance of 10 cm was introduced. Fischer-Antze (2005) reported that both the use of the hiding-exposure approach and the non-hydrostatic pressure approach included were found to significantly enhance modelling performance. Sources of uncertainties were related to the threshold for incipient motion and sediment parameters of the transport formula used as well as to the availability of bed level data. Further research was recommended in modelling sediment sorting processes, in numerical grid properties such as wetting and drying algorithms, in flow through vegetation and groyne fields and finally the availability of topographical data.

In order to enhance model reliability for real case studies concerning flow through vegetation, Zinke and Olsen (2007) carried out 3D numerical modelling of sediment deposition in a partly vegetated open channel with a modified version of the 3D model SSIIM (Olsen, 2006). The model solves the RANS equations for water flow and the convection-diffusion equation for suspended sediments. Moreover, the drag force on the vegetation was included as sink term in the RANS equations. In contrast to Fischer-Antze (2005) and Van den Bosch (2003), the change of turbulence characteristics due to vegetation was also taken into account by introducing drag-related source terms in the k-ε model following Baptist et al. (2007). Suspended sediment transport was modelled according to van Rijn (1984b). The models performance was tested against literature data of flume experiments for different model set ups. The authors found that the model was successfully used to estimate deposition profiles and that the introduction of turbulence source terms in the turbulence model was enhancing model performance. Zinke and Olsen (2007) concluded however, that until today the mobilization of sediments inside vegetation areas, vegetation flexibility and the impact of branches and leaves can still not be reflected adequately by currently available modelling techniques and that in addition to this, more sophisticated turbulence approaches were required in order to fully determine the flow field in partly vegetated channels. Despite this, 3D modelling approaches are recently under development that aim to reduce turbulence representations again (e. g. Li and Zeng, 2009).

Prior to the aforementioned studies, Stoesser et al. (2003) induced first steps towards a 3D modelling strategy for engineering purposes with special regard to vegetation resistance. They applied

a 3D numerical code for flow computations in a 3500 m reach of the Upper River Rhine. The model uses the finite volume method to solve the 3D RANS equations with a standard k-ε model and has implemented the drag force approach for vegetation resistance. The drag force term was introduced as sink term in the RANS equations only so that the k-ε model used for turbulence closure did not need any separate recalibration. Sediment transport was not regarded for in the model. Bed roughness was modelled with the equivalent sand grain roughness k_s. The 3D model was applied to flow in the vegetated two-stage channel of the Upper River Rhine, Germany for a 100-year event. Both bed roughness and vegetation resistance parameters were derived from field data taken from the study reach in terms of sieve curves of the bed material and vegetation mapping, respectively. In contrast to many other 1D and 2D studies aforementioned, Stoesser et al. (2003) took into account that the roughness parametrization from field work might contain errors and might affect model performance and/or grid resolution and vice versa. To illustrate uncertainties and related ranges of results, Stoesser et al. (2003) used four different roughness formulas and obtained k_s values ranging from 0.31 – 0.67 m dependent on the formula chosen for a single bed material sieve curve. To provide increased confidence in the resistance values, the 3D model was initially used to compute a low flow event without inundation of the floodplains in order to verify the bed roughness k_s whereas a high flow event with inundation of the floodplains was computed to verify vegetation parameters (see also Yoshida and Dittrich, 2002; Chatterjee et al., 2008). The resistance values were then used for the 100-year flood simulation. In order to evaluate the obtained flow velocities in the vegetated floodplains, field measurements of the same event (100-year) were used. Floodplain velocities were measured with a tracer technique and very good agreement was found between measured and computed flow velocities. Based on the 3D model, Stoesser et al. (2003) were also capable to evaluate the three-dimensional pattern of flow velocity and turbulent kinetic energy in both channel and floodplain which are relevant for transport phenomena of bed and suspended load. Their model approach was later successfully applied on the river reach scale by e. g. Stoesser and Dittrich (2007), Dittrich et al. (2007) and Schulte-Rentrop and Dittrich (2007).

3.3.5 Evaluation of multi-dimensional modelling tools

Within in the last years, the suitability of multi-dimensional numerical methods for geomorphological problems was tested by comparing 2D and 3D models (e. g. Lane et al., 1999; Shen and Diplas, 2008). Lane et al. (1999) compared a 2D and a 3D model for flow simulations in a confluence area of a gravel-bed river. The 3D model solved the fully 3D RANS equations with finite volume discretization and a non-standard k-ε model while the 2D model used the depth-averaged form of the RANS equations, a standard depth-averaged k-ε model and an optional correction coefficient for secondary flows. Both models showed the Manning's roughness approach for roughness closure. The models were applied with identical boundary conditions and input data in a steady state mode to simulate the field study. Lane et al. (1999) found a significantly enhanced performance for the 3D model over the 2D tool regarding bed shear stresses, mixing processes, spatial distributions of hydraulic parameters and in the case that the correction coefficient option was not used in the 2D mode. The 2D approach strongly over-estimated mean flow velocities and bed shear stress while the least over-predictions were obtained with an unreasonable high n value compared to the field and the

3D model. Here, bed shear stress was calculated taking the depth-averaged velocity and the total water column into account. Using an alternative common 2D approach where the log law is assumed to be valid over the total depth and depth-average velocity was assumed to be equivalent to flow velocity at 40 % of the water depth above bed, over-predictions of bed shear stresses reached magnitudes of even 10^5 N/m². The 3D model instead was capable of resolving the vertical flow profile appropriately taking the near bed velocity field into account for bed shear stress considerations and log law applications. The 3D results were in good agreement with field observations. However, Lane et al. (1999) reported high sensitivity to Manning's n values for the 2D model and high sensitivity to the quality of topography input for the 3D model. In summary Lane et al. (1999) concluded that "there is significant merit in the move towards 3D models but research is required to incorporate methods developed in other fields for dealing with boundary conditions uncertainty."

The outcomes of Lane et al. (1999) are supported by Van den Bosch (2003), Baptist (2005) and Shen and Diplas (2008) who compared the performance of a 2D model and a 3D model with field measurements. Van den Bosch (2003), Baptist (2005) both used the model Delft3D-FLOW that simulates both 2D and 3D unsteady flow with a hydrostatic pressure approach (quasi-3D) and transport phenomena. In the 2D mode, vegetation was represented by increased roughness value in terms of the Chézy formula while in the quasi-3D mode, the classical drag force approach was used. Similarly to Lane et al (1999), it was found that the quasi-3D model predicted a more realistic horizontal velocity redistribution which were in good agreement with field observations and plausible bottom shear stresses in areas with vegetation. In contrast, the 2D model yielded unrealistic results with strongly increased bottom shear stresses in the vegetated areas compared to the non-vegetated areas (see also Baptist, 2005). The model used by both authors computes bed shear stress according to:

$$\tau_0 = \frac{\rho \cdot g}{C} \cdot u^2 \text{ with } C = 18 \cdot \log\left(\frac{12 \cdot h}{k_s}\right) \qquad 3\text{-}44$$

Eq. 3-44 show that the Chézy coefficient decreases in the case vegetation is represented as increased equivalent sand grain roughness k_S. Since the 2D approach additionally considers the depth-averaged flow velocity in Eq. 3-44, this results in strongly over-estimated bed shear stresses (see also Lane et al., 1999; Li and Millar, 2007). In the quasi-3D version of the model instead, vegetation roughness is taken into consideration via the drag force term as inserted into the RANS equation, so that C remains relatively small reflecting bed roughness only. The 3D model further computed the bed shear stress as directly related to the velocities in the nearest bed cell in contrast to the depth-averaged values of the 2D mode (see Lane et al. 1999). However, it must be pointed out that the quasi-3D model used by van den Bosch (2003) and Baptist (2005) solves the vertical component with a hydrostatic pressure approach only. This approach is a shortcoming compared to the shear stress closures used by Stoesser et al. (2003), Olsen (2006) and Shen and Diplas (2008) where bed shear stress is directly related to the turbulent kinetic energy and vertical mixing processes are explicitly accounted for.

3.3.6 Discussion and conclusion

The literature review reveals that there exist numerous approaches for estimating fluvial hydraulics. However, most approaches exhibit serious drawbacks regarding the scope of the present study. The objective is to develop a tool for estimation of morphodynamic hazards for river rehabilitation and

flood measures in the planning stage. 1D approaches are successfully applied to large-scale hydraulic studies and if ever applied to local scales their reliability is limited to rivers with simple geometry and homogenous roughness distributions. Detailed resolution of the flow field, local variations of bed shear stress due to geometry variations and vegetation as they are omnipresent in rehabilitated river reaches and natural flood protection measures cannot be regarded at all (see e. g. Downs and Thorne, 1998, 2000). However, studies revealed that 1D models can give good approximations for water levels and conceyance capacities on the local scale. For floodplain studies, 2D approaches show several advantages since they are capable of resolving lateral and longitudinal flow pattern and thus can give more detailed information of flow directions in variable geometries. Despite promising results, a number of problems still remain. Most 2D models and quasi-3D models assume vertical hydrostatic pressure distributions and require corrective dispersion coefficients for calibration which does not enfavour their use for practicable applications in complex systems. Moreover, physically sound resistance approaches for vegetation are hardly considered and often treated only marginally. In most approaches, floodplain roughness is represented by an upscaled Chézy roughness or Manning's n chosen via tables and literature data. However, vegetation is a crucial factor determining the success and sustainability of flood retention and recreation measures and thus requires distinct consideration in the morphodynamic hazard tool. In addition, bed shear stresses are often computed in 2D approaches by means of depth-averaged velocities while mostly assuming a logarithmic velocity distribution as relevant for the flow forces on the bed although this logarithmic assumption is severely violated in vegetated areas (see Figure 3.17). Several studies show that the simplifications related to roughness parametrization and the vertical velocity field lead to unrealistic over-predictions of bed shear stresses in vegetated areas. Thus morphodynamic processes likely to occur in restored river sections with floodplains cannot be evaluated properly. These aspects are aggravated by the inappropriate use of input data in many hydraulic modelling studies. Only recently, high resolution remote sensing data are increasingly used to incorporate topography and vegetation structure information. LIDAR data show significant advantages due to their high accuracy, relatively easy collection and the possibility of repeat flights over floodplains to report geomorphological changes. However, it was often reported that these advantages may be compensated partially by less powerful interpolation techniques which affect data accuracy again. Moreover, LIDAR data is often used in an inadequate manner for roughness specification. It is mainly directly transferred to empirical bulk Manning's or Chézy values for channel and floodplains using tables and literature values to the effect that the detailed terrain information looses its high physical information potential. It is highly questionable whether high quality input data can compensate the uncertainties with bulk friction parameters or generalized assumptions involved. Moreover, using field data does not imply the automatic neglection of any further model calibration and verification which is however practice in hydraulic modelling. Each model exhibits its own uncertainties concerning e. g. mathematical descriptions involved, grid resolution and boundary conditions used in addition to the uncertainties related to field data measurements. This was impressively shown by Stoesser et al. (2003) or Yu and Lane (2006a, b). Yu and Lane (2006a, b) investigated the performance of a 2D model for flood inundation in urban areas with vegetation and structural elements (houses, walls) and reported strong uncertainties related to the commonly proceeded upscaling of the Manning's coefficient gained from LIDAR data according to mesh resolution. Their study revealed that blockage effects and surface routing processes induced by structural elements were not predicted correctly by upscaled Manning's value since the model setup

was not able to account for the complex flow properties which both resulted in bad representation of water levels and velocities. Yu and Lane (2006a, b) questioned whether the simple transfer of LIDAR data into uniform Manning's n for floodplain vegetation via look-up tables without taking into account the discretization of the model and any physical basis was appropriate.

Recent research has concerned the development of 1D and 2D morphodynamic models with focus on sediment transport, bed level changes and meandering. As previously shown these models are only applicable to rivers in morphologic equilibrium, exhibiting moveable bed and banks and natural discharge variations. These conditions are not present at the sites of the present study. The main channel of the River Rhine is a heavily modified system with controlled discharge dynamics, armour layer and fixed banks. Here, the application of transport formula is neither reasonable nor useful since the equations have been developed for fully moveable beds and do not account for processes linked with armour layers. Also, they are less favorable for retention areas and recreation measures with vegetation, structural elements and loose bed material. Still today, it is not possible to reliably predict bed levels changes and sediment transport when vegetation is involved because the interaction between plants, flow and sediment is still not fully understood yet, see e. g. Zinke and Olsen (2007), Dittrich and Järvelä (2005). Computing sediment transport in this river section would be a rather guess and not helpful for hazard assessment.

In contrast, fully 3D models provide many advantages for the present objectives. The main aim is the detailed determination of morphodynamic hazardous processes affecting river restoration and natural flood measures on the local scale in the planning process. For this task, the proper representation of complex flow pattern present in natural river systems is crucial. The literature study has shown that compared to 2D and 1D approaches, fully 3D models yield much more reliable results concerning complex turbulent flow fields in natural river sections. They can represent hydrodynamic processes induced by abrupt cross-sectional widenings, overbank and floodplain flows, curvatures, distinct roughness elements such as vegetation, floodplain forest, houses, walls and infrastructures in detail. Bed shear stresses and flow directions can be reliably simulated due to the distinct representation of the near-bed velocity field and turbulence characteristics in a physically sound manner what cannot be achieved by lower dimensional approaches.

A drawback of fully 3D tools, however, is that they are very data and time demanding and their handling is not straightforward at first sight. Since they are capable of reflecting hydraulic processes fully in three dimensions, they show high requirements regarding the quality and quantity of input data, boundary conditions and numerical grids. Moreover, if commonly used, their computational time is hardly competitive compared to 1D and 2D models. In order to fully benefit from detailed modelling, the use of a 3D numerical tool would require modifications for morphodynamic process estimation and reliable risk assessment in practical engineering problems.

3.4 APPROACH DERIVED FOR MORPHODYNAMIC HAZARD ANALYSIS FOR RIVER RESTORATION AND NATURAL FLOOD MEASURES

Sustainable nature-close flood protection measures and river restoration projects call for explicit consideration of river dynamics in addition to inundation studies alone. Morphodynamic processes distinctly impact the success of these projects and might lead to severe damages and losses in the case of the projects' failure. In order to achieve sustainability, a methodology is required which identifies potential hazards and related consequences already in the planning state, further enables plan optimization and thus support decision makers to meet the acceptance criteria in the long-term. To tackle this objective, the systematic iterative Risk Management procedure is judged as useful basis framework and has been modified according to the scope of the present study.

For reasons of complexity, the new strategy concerns the first part of the Risk Management chain: the phases of *Risk Identification* and *Hazard Analysis*. For a given river project with certain acceptance criteria provided by recreation plans and flood protection, the strategy aims to identify the risk induced by morphodynamics and to determine and analyse the hazards being able to endanger the designed river section. The structural damages in the case of failure are further required as preliminary input parameters for an optimization plan. Chapter 3 clearly demonstrates that current methods and modelling approaches show severe shortcomings concerning the reliable estimation of morphodynamics in natural rivers with vegetation. Hence, the new strategy should be able to tackle these shortcomings. Based on the foregoing explanations and discussions, a combined approach of multi-dimensional modelling and analytical approaches is developed and implemented in the Risk Management framework following the basic principles of FISRWG (2001), Copeland et al. (2001) and Sear et al. (2003). An overview of the procedure is presented in Figure 3.21. The methodology of identification and analysis of morphodynamic hazards is then applied to a case study region to test its performance.

3.4.1 Risk Identification

The phase of morphodynamic risk identification including *System Definition* plays a key role in the new approach as depicted in Figure 3.21. As reported in Chapter 3.1 and 3.2 the reliable estimation of a river's future behaviour requires a detailed understanding of the fluvial system. Thus, the procedure of System Definition proposed herein aims at a detailed characterization of the river system's hydromorphology on the corresponding spatial and temporal scales. It regards historical development, actual state and trends for the river catchment, for the river reach to be restored and for its future design. In order to consider the river's heterogeneity on the local scale, the river reach is segmented into its Elements at Risks (EaRs), i. a. the morphological units. This step enables a detailed investigation of the river's individual features in the subsequent Hazard Analysis. Dependent on the project, the System Definition might cover information about (see also FISRWG, 2001, Copeland et al., 2001 and Sear et al., 2003):

- main hydrological and gauging data: climate, regime, flood frequencies, flood duration, (sub)catchment sizes, tributaries, lakes

- morphology: geology, river classifications, length and cross-sectional profile, hydraulics, sediment and discharge continuum, bed and bank material, morphological tendencies
- river engineering and structures, maintenance, typology according to EU WFD
- landuse, economic and social-geographical information
- Elements at Risk (i. a. morphological units) of the project area in the actual state and in the future design (bed, banks, macrostructures such as bars, islands, vegetation, groynes, buildings, floodplain)

The detailed picture obtained by the System Definition allows to proceed with the *Hazard Identification* where the potential hazards which might harm the project units or EaRs can be identified (see Figure 3.21). This step is important since without an accurate hazard listing a sustainable river system that withstands these hazards cannot be achieved. The Hazard Identification is carried out based on scenarios with clearly defined hydromorphological boundary conditions. The investigation based on scenarios can be very helpful in the case that the river project is very complex and/or potential hazards are too numerous. Typical scenarios may be chosen according to e. g. discharges to investigate, river bed (mobile or fixed), or different vegetation densities on the floodplains. To identify the hazards, the present work further uses a modified version of the PHA approach (see also Rausand, 2004). The PHA (Preliminary Hazard Analysis) is commonly conducted on a qualitative basis in the early stage of a project with the purpose to detect potential hazardous situations, related consequences and scenarios that are investigated further in the risk chain. The output is recorded in a table that lists each hazard, its origin, failure modes, potential consequences, severities and possible measures for Risk Treatment (see also Rausand, 2004; Merz, 2006; Faber, 2005; Gowen et al., 1992). Hence, this procedure enables to systematically investigate which hazards

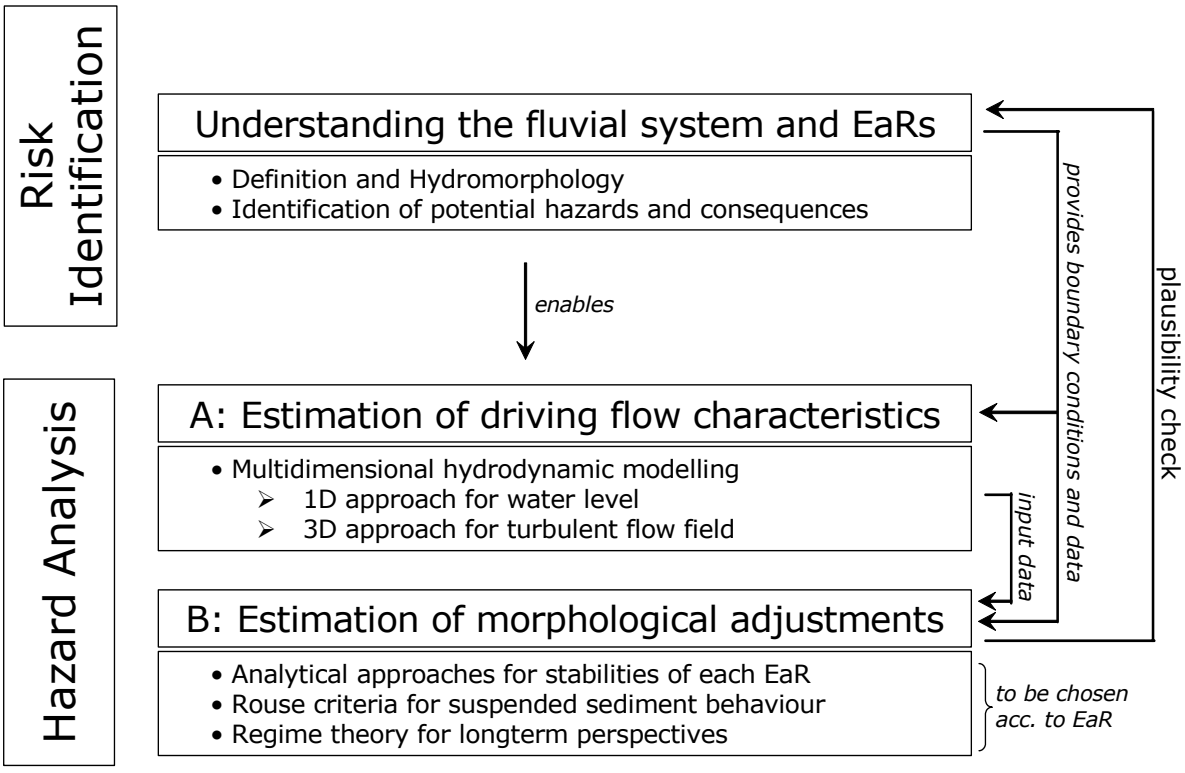

Figure 3.21: New approach for Hazard Analysis of morphodynamic processes in natural rivers with vegetation.

and scenarios are relevant and which tools are appropriate in order to analyze them as reliably as possible. Due to its qualitative character, the PHA methodology is judged very useful for the scope of the present study to obtain a first overview of hazardous situations and consequences in the river project. In general, the PHA results are used as input for more sophisticated quantitative Hazard Identification methods like FMEA or HAZOP initializing the Risk Management procedure with frequency estimations and damage/loss assessments. In the present study instead, the PHA methodology is applied as a straightforward informative "brain storming tool" following Merz (2006), Rausand (2004) and Faber (2005).

With termination of the Risk Identification phase, the relevant knowledge concerning the System under Analysis, potential hazardous events, possible damages and losses should be available. This knowledge enables to proceed with the consecuting phase of *Hazard Analysis*.

3.4.2 Hazard Analysis

Here, the hazards' intensity and frequency are quantified. In fluvial hydraulics, the analysis tools may cover e. g. modelling techniques, field measurements, laboratory experiments, stability and sediment transport assessments, regime theory, application of reference reaches or a combination of those. In order to achieve reliable estimations, these tools should be chosen carefully according to hazards, scenarios and the system's properties. Due to the reported severe shortcomings of current modelling techniques (see Chapter 3.3), a new approach of *Hazard Analysis* is derived for morphodynamics of natural, vegetated river systems and nature-close flood protection measures. The Hazard Analysis consists of two basic steps as illustrated in Figure 3.21. In step A, the driving hydrodynamic flow field is calculated by means of combined multi-dimensional hydrodynamic modelling. In the second step B, the river's reaction on the simulated driving forces in form of morphodynamic development and adjustment is estimated.

Step A of the Hazard Analysis comprises the use of a fully three-dimensional hydrodynamic numerical model. It was decided to use the 3D model SSIIM 2.0 (Olsen, 2008). The use of SSIIM 2.0 is enfavoured due to the following reasons:

- the fully 3D approach enables the calculation of the 3D hydraulic flow field in complex geometries on the local scale with a non-hydrostatic approach
- origins of flow resistance are considered separately and in a physically sound manner: the total flow resistance is subdivided into both bed roughness and flow resistance due to vegetation; vegetation resistance is modelled via a physically-based drag force approach to account for accurate mass and impulse transfer
- bed shear stress is directly derived from turbulent kinetic energy in the nearest bed cell
- the 3D resolution enables to consider variable roughness pattern of vegetation with depth
- SSIIM 2.0 exhibits a sophisticated non-orthogonal unstructured grid including wetting and drying algorithm

The first four demands have been already discussed extensively in the previous chapters. However, the last demand is of similar importance. The strongly heterogeneous flow geometry of natural river systems including floodplains and recreation zones require a powerful numerical grid. This grid must

reliably cover the topography at different discharges and water levels of interest and must, at the same time, exhibit high numerical stability. The non-orthogonal unstructured grid of SSIIM 2.0 meets these criteria since the numbers of cells per cross-section is adaptive to flow width in contrast to common structured grids where the number of cells must be kept constant over the cross-section. Secondly, the combination of a wetting-drying algorithm with the unstructured grid improves the quality of numerical modelling. Last but not least, this combination allows the generation of only one computational grid for various discharge scenarios. This is an important advantage for practical applications compared to common grids which must be modified for each discharge event.

In the present methodology, the 3D model is further combined with a straightforward 1D model (HEC-RAS 3.1.3, USACE, 2005), see Figure 3.21. Free-surface calculations in combination with wetting and drying algorithms in three dimensions for natural rivers with vegetation are still a field of research. To reach numeric stability, a fixed water level is usually given as boundary condition. Therefore it was decided to use a 1D model in addition to pre-estimate the water level for a given scenario which is in turn implemented as boundary condition of the 3D model. This step is legitimate since according to the literature review low-dimensional models yield good approximations of water levels and discharge capacity in natural rivers despite their low performance when detailed flow pattern are of interest. The corresponding three-dimensional flow field is further calculated by the 3D model using the 1D water level as input data (see also DVWK, 1999). In contrast to many other studies, a detailed calibration and validation procedure of both the 1D and the 3D model against field data is carried out in order to guarantee plausibility. The uncertainties related to the pre-estimated 1D water level are discussed later in the study as well. The 1D-3D model combination has significant advantages compared to the sole 3D model use without the water level pre-estimation which are supporting its use in practical engineering problems: In addition to the enhancement of numerical stability aforementioned, the computational time of the 3D model is distinctly shortened with the water level implemented as boundary condition without distinctly reducing its 3D information potential. Finally, a 1D model used prior to a 3D model can give additional rough hydraulic information in advance. Used as a preliminary calculation tool a straightforward 1D model can help to investigate the system's behaviour at various boundary conditions in addition to the detailed 3D numerical model calculations which are performend for a limited number of chosen cases.

Step B of the Hazard Analysis comprises the estimation of morphodynamic development as reaction on the driving forces which have been simulated in Step A by the 1D-3D approach, see Figure 3.21. The literature review revealed that many studies use generalized approaches for sediment transport or river bed erosion while neglecting the individual hydraulic characteristics of the EaRs which in turn can affect the approaches' validity. In contrast, the present methodology estimates the morphodynamic reaction of each EaR separately. This is carried out by analytical approaches according to the governing boundary conditions. These analytical approaches are chosen explicitly for each EaR and validated by field data. They comprise stability formula for various bed material (e.g. armour layer vs. loose bed material) and different vegetation types, an approach for suspended sediment transport behaviour (approach of Wang and Dittrich, 1992) and formula for bed load transport. The results obtained with the analytical approaches are then interpreted in close regard to the simulated bed shear stresses from the step A (Figure 3.21). Based on this assessment, the subsequent morphodynamic reaction per scenario and EaR can be derived. The results can further be cross-checked with regime equations.

It is important to know that, as shown in Chapter 3.3, a fully 3D model is highly demanding regarding the quality of input data and boundary conditions. In order to fully benefit from the accuracy of a 3D model, these data requirements must be fulfilled. Also at this point, the potential of the Risk Management framework is demonstrated: The data basis produced for system understanding in the Risk Identification can be directly used for model forcing and detailed investigation in the Hazard Analysis (Figure 3.21).

3.4.3 Plausibility check

Figure 3.21 further presents the final and maybe the most crucial process in hydrodynamic modelling which is, however, often missing in many studies, namely the *Check for Plausibility*. Since morphodynamic processes in natural rivers with vegetation are very complex, it is not possible to reliably predict – in terms of "forecasting" – the interaction among flow, vegetation and sediments processes until today. In order to test the outcomes of the hydraulic tools and to assure their reliability, they should be checked in any case against field observations. Data and information for this plausibility check is again being provided by the Risk Identification phase.

In the following Chapters 4, 5 and 6 the new methodology for morphodynamic hazard analysis is applied to a case study region to test its performance. The case study region is located in the Upper Rhine north of Basel/CH. In this river reach, numerous river restoration projects are planned. In order to test the feasibility and sustainability of these rehabilitation plans and to reveal needs for optimization, the new methodology is used and assessed.

4 CASE STUDY UPPER RHINE: IDENTIFICATION OF RISK INDUCED BY MORPHODYNAMIC HAZARDS

4.1 INTRODUCTION

In the following, the novel methodology for the analysis of morphodynamic hazards is applied and tested for a case study region in the Upper Rhine/Germany. The study area is located north of Basel/CH close to the municipality of Neuenburg between Rhine-km 198 – 201. The actual morphological state near Neuenburg is depicted in Figure 4.1. This region had been chosen as study area for the following reasons.

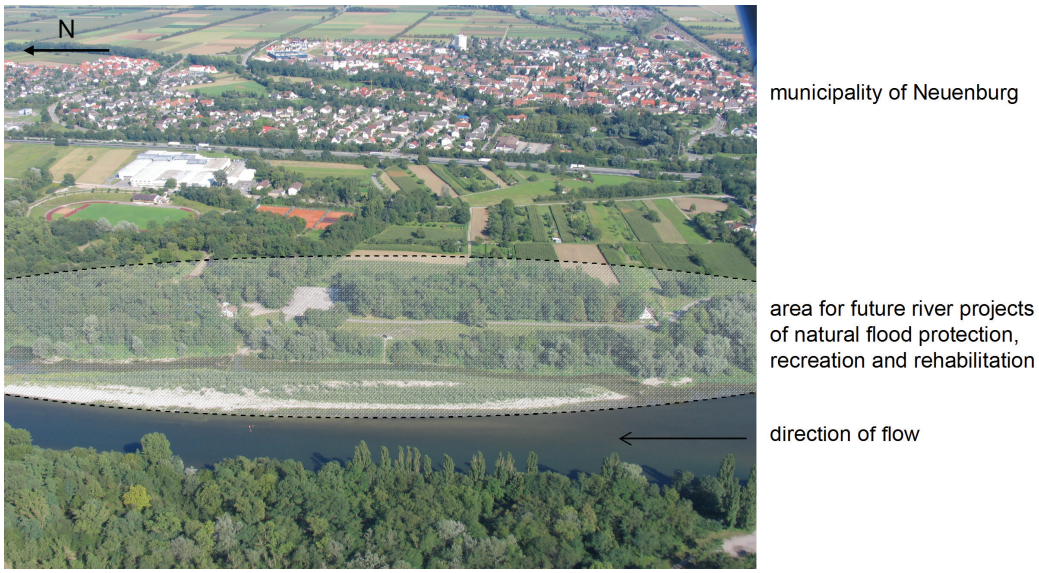

Figure 4.1: Study site Neuenburg with indicated area of future recreation projects, Rhine-km 199.5 (provided by ILN, modified).

➢ First, the river section Neuenburg exhibits an interesting morphological situation both in the actual and the planning state. The Upper Rhine had been subjected for many decades to severe river regulations such as channelization and construction of groynes and dikes which has led to a heavily modified system. However, flood risk has severely increased in the last decades and tourists did not frequent the river banks due to the monotonous regulated stream. In order to improve flood protection and touristic attraction, the Land Baden-Württemberg and the municipality of Neuenburg have evolved river plans which comprise nature-close flood protection measures as well as a local river restoration and recreation concept. The flood protection measure of the Land Baden-Württemberg forms part of an important supraregional flood protection programme and comprises a large flood retention area on the German Rhine side while the local municipality concept comprises the flattening of river banks, touristic infrastructure and the integration of an existing vegetated gravel island (see Figure 4.1). Thus, compared to the actual heavily regulated state, the future river design will change

the boundary conditions significantly towards heterogeneous flow geometries and extensive vegetated areas. The performance of the new Hazard Analysis tool can be tested for these complex situations.

- The river projects provoke high financial investments for both their implementation and maintenance in order to guarantee flood protection and touristic attraction for the region. In the case of failure, potential damages and losses might be considerable so that the proper functioning of the measures is of fundamental importance for flood protection, human life and economy. The Hazard Analysis tool can be used to test the sustainability of these rehabilitation plans and to further reveal needs for optimization.
- The testing of the new methodology requires a sound data basis for model forcing and plausibility checks. The Upper Rhine area has been studied and monitored over many years by universities and river authorities so that data and field observations are available. Moreover, two severe flood events appeared in recent years (1999 and 2007) which have been documented by several institutions. This information is well suited for system understanding and model validation.

In the following, the Risk Identification procedure for the case Neuenburg is presented. It aims at characterizing and analysing the river system on the relevant spatial and temporal scales in order to understand its behaviour and to detect potential sources of harm. These scales might concern the historical development, actual state and current trends for the catchment and/or the upper scale regions and for the river reach itself. In addition, the future design must be analysed accordingly. To gain a better overview, the Risk Identification for Neuenburg is therefore structured as depicted in Figure 4.2: In System Definition I (Chapter 4.2), the Rhine catchment upstream of Neuenburg is briefly presented as well as its regional hydromorphology. Furthermore, the impact of river regulations on flood risk is reported and the Upper Rhine flood protection concept of the Land Baden-Württemberg is introduced. In System Definition II (Chapter 4.3), local morphodynamics of the project site Neuenburg are analysed for the actual state as well as the future river projects of Neuenburg (so-called planning state) including their desired functionality. The proper understanding of the system gained so far enables to further investigate how the system's functionality might be affected. Subsequently, the Hazard Identification is carried out in the consecutive Chapter 4.4.

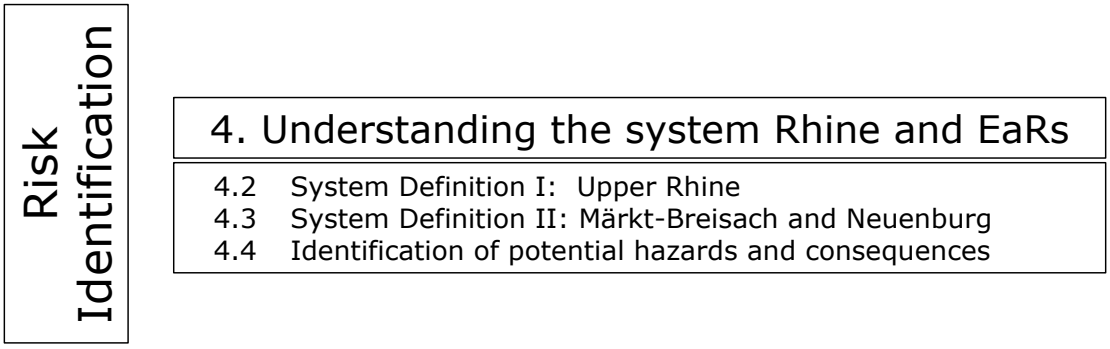

Figure 4.2: Structure of the Risk Identification procedure in the present chapter.

4.2 SYSTEM DEFINITION I – HYDROMORPHOLOGY OF THE UPPER RHINE

The River Rhine is the largest river in Germany. It has its origin in the Swiss Alps and has a length of 1,324 km at the catchment outlet in Lobith (NL), see Figure 4.3. The total catchment area comprises 197,000 km² covering nine countries: Germany (106,000 km²), Switzerland, France and the Netherlands (20,000 – 30,000 km² each), Austria, Luxemburg (2,500 km² each) and small parts of Belgium, Liechtenstein and Italy (IKSR, 2005). Today, the Rhine basin is one of the most important waterways worldwide with important industrial congested areas and about 50 mio inhabitants throughout the catchment. As aforementioned, the course of the River Rhine has been subjected to heavy modifications within the last centuries. In order to understand the morphological behaviour of the River Rhine nowadays and to estimate the behaviour of the project area in future, the next sections present the natural morphology of the River Rhine apparent centuries ago in equilibrium and its historical development due to human intervention. Moreover, the impact of the measures on the current flood and morphologic situation is shown.

4.2.1 The study area: Upper Rhine

4.2.1.1 Natural hydromorphology

The undisturbed River Rhine can be roughly subdivided into 6 stretches (see Figure 4.3): the Alpine Rhine, High Rhine, Upper Rhine, Middle Rhine, Lower Rhine and Delta Rhine where the river is divided into several branches that flow into the North Sea (Umweltbüro Essen, 2004; IKSR, 2005). The project area Neuenburg is located in the Upper Rhine. Therefore, the focus is placed on this as well as on its upstream stretches while the downstream parts are presented as short overview only.

The natural typology of each Rhine stretch is strongly determined by climate, hydrology, geology, soils and the properties of their tributaries. The Alpine Rhine covers the region from the source and headwaters until Lake Constance. Here, the original morphology is partly straight, partly meandering with a single bed and an average slope of 1 – 3 ‰. The Alpine Rhine exhibits high bed load transport (fine gravel and sandy fractions) due to large sediment sources in the catchment, though alpine lakes mostly inhibit that these sediments are transported further downstream. The High Rhine covers the outlet of Lake Constance (Rhine-km 0) to Basel (CH, Rhine-km 170). Until Rhine-km 45, the morphology is strongly influenced by Lake Constance given a single bed, low slope (0.3 ‰) and negligible bed load transport as the lake acts as a sink for upstream sediments. With downstream distance from the lake (Rhine-km 45 – 170), morphodynamics intensify including intensive bed load transport (coarse material, gravel) due to higher slope of 1.3 ‰ and the impact of the tributaries. The main tributaries of the High Rhine are: Thur (Rhine-km 65), Töss (Rhine-km 70), Wutach (Rhine-km 100), Aare (Rhine-km 102), Birs (Rhine-km 166) (Umweltbüro Essen, 2004; IKSR, 2005).

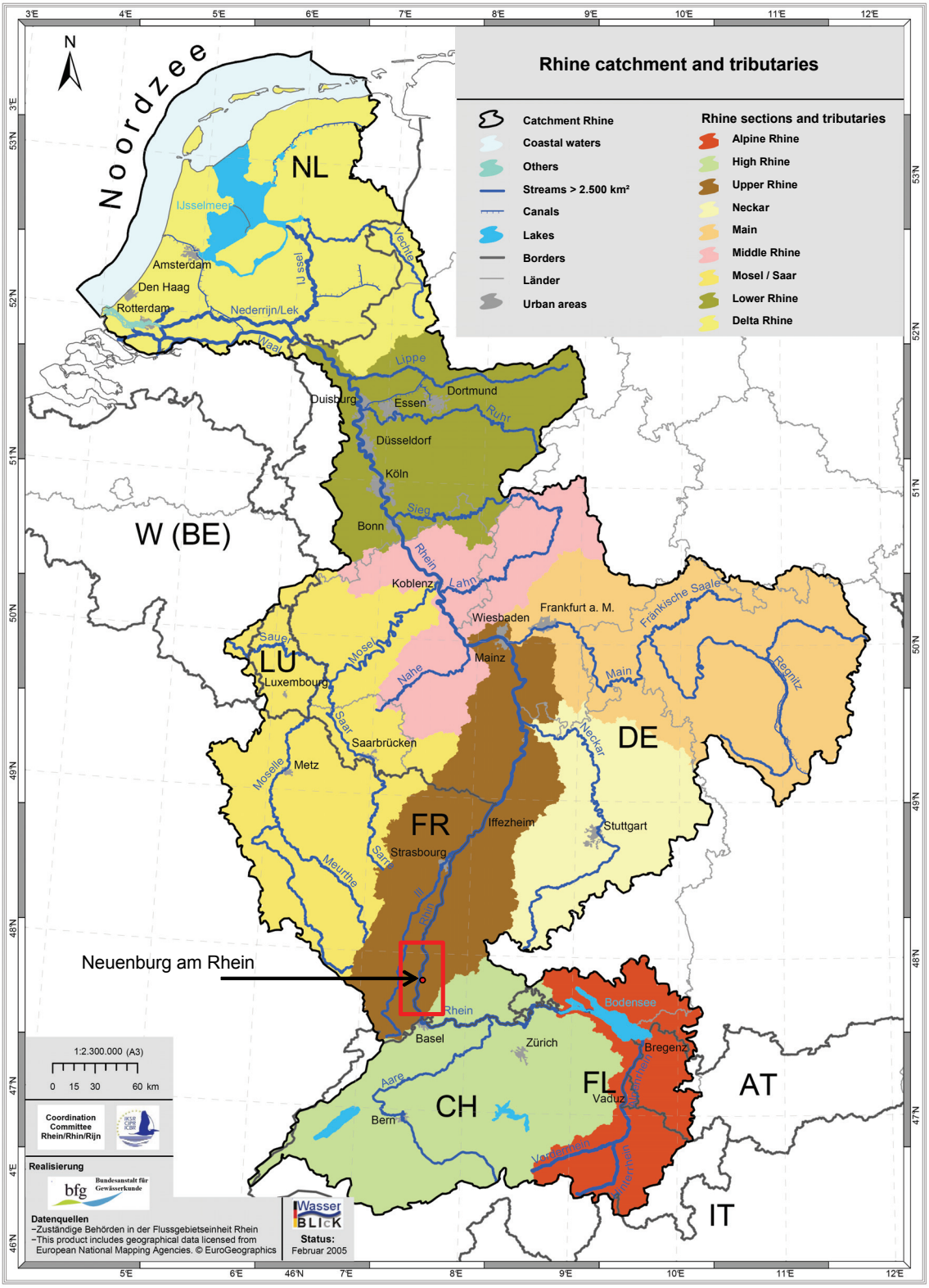

Figure 4.3: The catchment of the River Rhine and the location of the study area (IKSR, 2005).

The Upper Rhine - where the study area of the present work is located – covers the section from Basel (Rhine-km 170) to Bingen (Rhine-km 530). Until Strasbourg (Rhine-km 290), the original Upper Rhine morphology was part of the furcation zone with low slopes of about 0.25 ‰, a wide floodplain up to 3,500 m comprising braided arms, numerous islands partly covered with vegetation (see Figure

4.4) and a total bed width of up to 2 km. Bed load transport was predominated by alluvial, coarse gravel material of the river bed. Downstream of Strasbourg, the Upper Rhine is turning into a single-stretched meander with intensive morphodynamics and accumulative tendencies (sand and coarse gravel). The main tributaries of the Upper Rhine are: Kander (Rhine-km 175), Elz (Rhine-km 265), Kinzig (Rhine-km 298), Ill (Rhine-km 311), Murg (Rhine-km 345), Neckar (Rhine-km 420) and Main (Rhine-km 495) (Umweltbüro Essen, 2004; IKSR, 2005; Regierungspräsidium Baden-Württemberg, 2005).

Figure 4.4: Landscape of the River Rhine near Basel in the year 1810 (State Ministry of the Environment Baden-Württemberg, 2007).

Further downstream, there is the Middle Rhine (from Bingen, Rhine-km 530, to Cologne, Rhine-km 690, with the famous small, deep river valley with cliffs and rocky islands and the Lower Rhine (from Cologne, Rhine-km 690, to Kleve, Rhine-km 865) where the river course is changing from a straight, single bed channel without floodplains towards a lowland river with numerous branches and oxbows. The Delta Rhine finally discharges into the North Sea. Here, morphology comprises meanders, numerous branches and wide floodplains with oxbows and a sandy bed. Further downstream the morphology is predominated by an estuarian character (Umweltbüro Essen, 2004).

The runoff regime of the River Rhine is determined by glacial, nival and pluvial influences changing the occurrence of the mean flood peaks along the river course from summer floods due to ice and snow melt in the upstream parts down to floods in winter due to rain in the most downstream parts (Umweltbüro Essen, 2004). The runoff regime from upstream (Rheinfelden Rhine-km 20.4) to downstream (Rees, Rhine-km 837.4) is illustrated in Figure 4.5. However, both the Rhine regime and discharge volume are strongly influenced by its tributaries as depicted in Figure 4.6. As a consequence, the interaction of the Rhine flood wave with the flood waves of the tributaries can lead to dramatic flood situations in the river catchment (see Chapter 4.2.1.3).

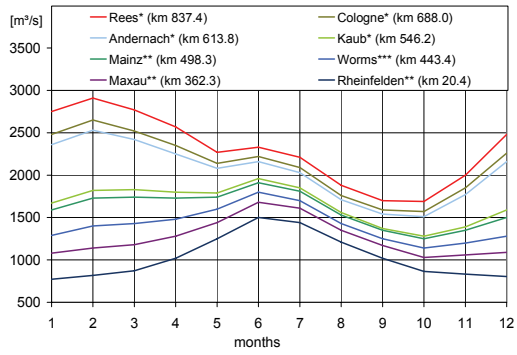

Figure 4.5: Runoff regimes of the River Rhine based on mean monthly time series, *: 1931 –2003 **: 1931 – 2004, * (1930 – 2004) (Landesanstalt für Umweltschutz, 2006, 2007).**

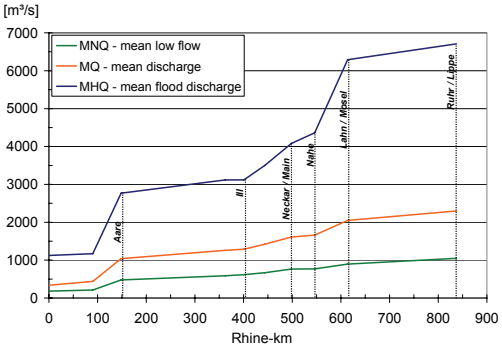

Figure 4.6: River Rhine discharge based on mean monthly values (1931 – 2003/2004) (Landesanstalt für Umweltschutz, 2006, 2007).

4.2.1.2 Historical development

By many centuries, the River Rhine and its catchment have been subjected to man-made interventions leading from the natural state described before to a heavily modified system. First river engineering works focussing on shipping measures have been carried out already in Roman times. With increasing settlement of people near the river in the Middle Ages, morphodynamic and flood risk were increasing significantly due to frequent inundations, large sediment depositions and channel shifts in the valley resulting in the need for strong protection measures. Hence, Switzerland conducted extensive regulations of the Alpine Rhine including bed stabilization and dam construction until late in the last century (IKSR, 2003). In addition, the Upper Rhine has been subjected to extensive river regulation measures for flood protection, drainage and shipping purposes starting in the beginning of the 18th century (see Figure 4.7) (IKSR, 2003; GWD Südlicher Oberrhein/Hochrhein, 1997). Settlements on the fruitful floodplains were regularly affected by floods and morphodynamic changes of the river course accompanied by various diseases including Typhus and Malaria. The first Rhine measures were carried out between 1817 and 1880 acoording to master plans of the engineer Johann Gottfried Tulla in the furcation zone of the Upper Rhine downstream of Basel. These so-called “Rhine corrections” were comprising the reduction of the flow length by cut-offs with the objective to deepen the river bed which in turn should reduce inundation frequencies and lead to an improvement of agricultural land on the floodplains by lowering the groundwater table. Thus, the water was concentrated in one single bed of 200 – 240 m width. This bed has essentially remained the same until today (State Ministry of the Environment Baden-Württemberg, 2007). Without a doubt, the Rhine regulations have led to an improvement of living conditions and flood protection in adjacent areas at that time. However, the impact of theses measures on the river’s morphodynamic equilibrium was strongly underestimated leading to severe river bed incision down to 7 m locally and accompanied by intensified sediment transport and large sediment depositions in former times (IHP/OHP, 1996). To guarantee navigation, groynes have been constructed in the early 19th century which concentrated the flow in a permanent channel of 75 – 100 m width and 2 m depth (State Ministry of the Environment Baden-Württemberg, 2007). The groyne fields as well as the confined, deeply incised river bed play a significant morphologic role in the River Rhine also today (IKSR, 2003).

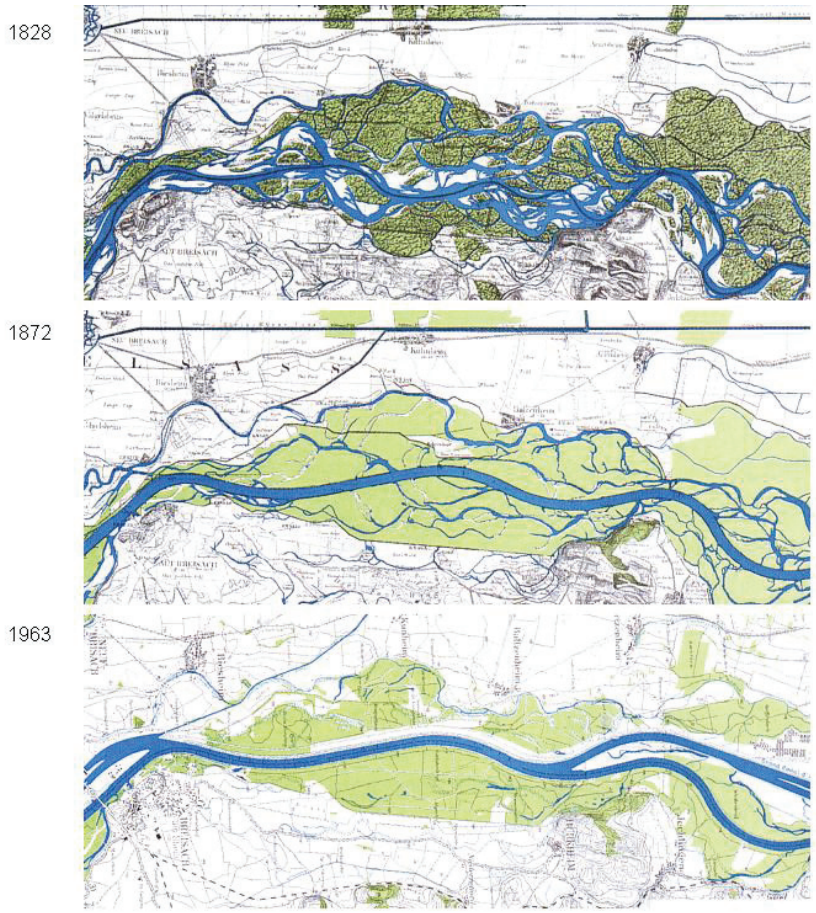

Figure 4.7: The systematic development of the Upper Rhine in the furcation zone near Breisach (State Ministry of the Environment Baden-Württemberg, 2007).

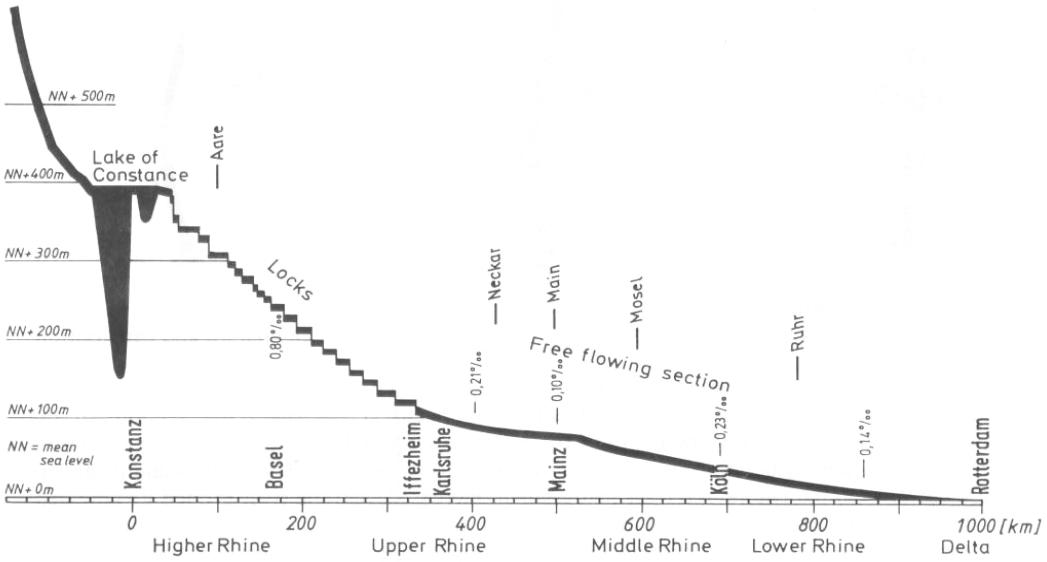

Figure 4.8: Longitudinal profile of the River Rhine today (IHP/OHP, 1996).

Further drastic interventions in the Upper Rhine were realized after the Second World War for water power production and further improvement of navigation. The Grand Canal d'Alsace has been constructed by France downstream of Basel (1928 – 1959) parallel to the Rhine bed which required

the construction of four weirs in the canal. Additional barrages were built downstream of Breisach, partly in loop solution, as well as dikes for water level maintenance. All in all, these measures impeded the interstitial interactions so that the groundwater table which was already strongly affected by river bed erosion dropped further. Nowadays, severe erosion is occurring downstream of the last lock at Iffezheim. In order to control bed incision, about 170,000 m³ of coarse gravel is supplied artificially each year since 1969 (IHP/OHP, 1996). River regulations and their impact on slope and natural discharge are impressively illustrated in the Rhine longitudinal profile as depicted in Figure 4.8.

4.2.1.3 Impact of river regulations on flood risk

The river regulation measures carried out in the Upper Rhine successfully improved flood protection at that time. In the 20th century, however, flood risk has re-increased tremendously downstream of the last barrage Iffezheim. According to Integriertes Rheinprogramm (1996) and State Ministry of the Environment Baden-Württemberg (2007) this is due to several reasons. Firstly, population growth and industrialization have led to severe modifications in landuse such by large-scale deforestation, extensive agricultural use and urbanization/surface sealing. With this change, the discharge volume in the River Rhine increased significantly. The situation was aggravated by dike constructions and cut-off of floodplains impacting the retention volume in addition. Figure 4.9 illustrates how regulation measures reduced former inundation area by approximately 870 km² leaving just 10 percent of the original area available to the river. This has led to a significant increase of both the discharge volume and the flood peak.

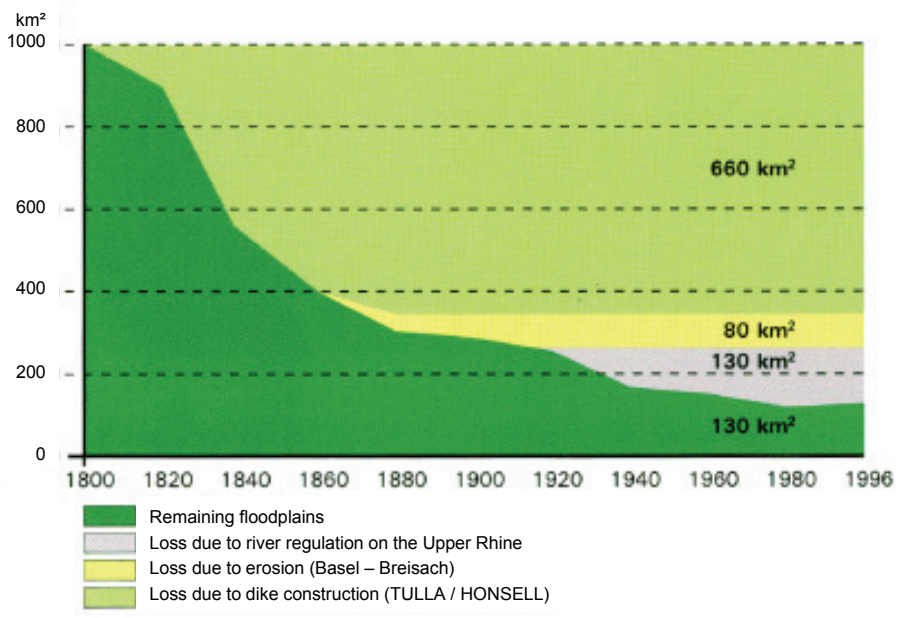

Figure 4.9: Loss of inundation area due to river regulation of the Upper Rhine (Integriertes Rheinprogramm, 1996).

Secondly, the river corrections caused a considerable acceleration of the flood wave. The reduction of 81 km flow length between Basel and Worms (from 354 km down to 273 km) has resulted in a reduction of the flood peak travel time between Basel and Mannheim of nearly 30 h (from a total flood

peak travel time of 110 h at end of the 19th century down to 80 h today) (Alsace Nature et al., 2003). As a consequence, flood peaks of the Rhine tributaries which in former times did not meet the flood peaks of the Rhine have now a higher likelihood to hit the Rhine flood wave as the Rhine water flows much faster than before (see also Figure 4.6). Thus, the probability of a huge flood has increased significantly. The severe indundations in 1992, 1999 and 2007 attest these circumstances.

However, the magnitudes of floods have been accompanied by increasing stream forces and increasing severity of morphodynamic hazards. It can be assumed that the mean flow velocity of a severe flood in the Upper Rhine tended to be moderate in former times since the river was discharging into wide floodplains. Now, after the Rhine corrections, flow velocities reach 4 – 5 m/s instead as reported by Hartmann et al. (2000) for a high flood in 1999. As flow forces are proportional to the velocity squared, flow forces increase significantly as well to the effect that intensified river morphodynamics and related hazards can initiate severe bank erosion, huge amounts of transported sediment and large inundations.

Finally, flood and morphodynamic risk in the Rhine catchment has not only increased by an increase of its probability of occurrence or its magnitudes, but also by an increase of vulnerability. With improving shipping and living conditions near the river, more and more people were settling in the fruitful valleys. Today, 700,000 people live in 95 towns in the Upper Rhine floodplain including the large congested urban areas Ludwigshafen, Mannheim, Karlsruhe and Worms with important industry and 350,000 jobs. The loss that might result from a great flood with a return period of 200 years between Iffezheim and Bingen is estimated by Bund-Länder-Arbeitsgruppe (1995) to more than 6 billion € disregarding human casualties (see also State Ministry of the Environment Baden-Württemberg, 2007). Being aware of this dangerous situation, the Land Baden-Württemberg and France took action in flood risk management by evolving the Integrated Rhine Programme.

4.2.2 Flood risk management in the Upper Rhine

4.2.2.1 The Integrated Rhine Programme

As aforementioned, the Rhine regulations have led to a tremendous increase in flood risk for the areas downstream of Iffezheim. The Integrated Rhine Programme (IRP) for flood control pursued by the federal state of Baden-Württemberg envisages creating space for inundation. It was firstly agreed in 1982, reviewed in 1996 and comprises the reactivation of floodplains on the Baden-Württemberg side of the Rhine where space is available due to foresty and agricultural use. The goal is to attain the level of security against floods that existed prior to the construction of barrages in 1955, in other words the reinstallation of flood protection against a 200 year's event, especially for the Rhine stretch between Iffezheim and Worms and the conurbations of Karlsruhe and Mannheim/Ludwigshafen. To achieve this, the high water peaks must be reduced by 700 m³/s at the gauging station Maxau (Karlsruhe, Rhine km 362.3) requiring a total retention volume of 167.3 mio m³ on the German Rhine as illustrated in Figure 4.10 (State Ministry of the Environment Baden-Württemberg, 2007). To tackle this challenge, the IRP developed a strategy with several retention measures comprising dike relocations, emergency operation of both power stations and weirs as well as the reactivation of former floodplains.

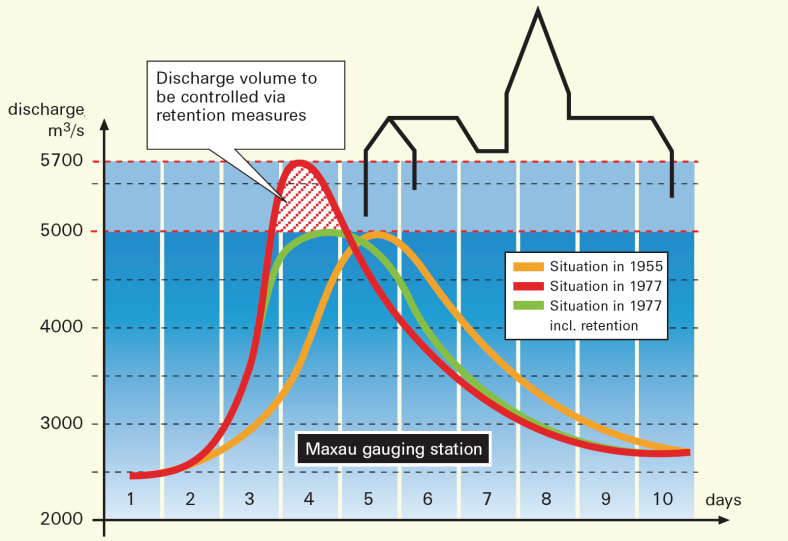

Figure 4.10: Impact of the IRP on flood wave development computed forthe gauging station Maxau/Karlsruhe, Rhine-km 362.3 (State Ministry of the Environment Baden-Württemberg, 2007).

4.2.2.2 The new flood protection strategy of nature-close flood retention areas and related challenges concerning morphodynamic hazards

An important objective of the Integrated Rhine Programme is to attain a sustainable flood control which is compatible with environmental requirements. Thus, besides the adequate operation of technical flood protection, key factors are nature-close measures such as the preservation and restoration of former floodplains. A future flood retention area called retention area Weil-Breisach is planned in the former furcation zone of the Upper Rhine between the barrage of Kembs (Rhine-km 173.975) in the vicinity of the municipalities Märkt and Weil and the barrage of Breisach (Rhine-km 224.800) see Figure 4.11a. This measure consists of several sub-areas providing a retention volume of 25 mio m³ on 450 ha in total which is required for a flood protection against a 200 years' event (a discharge of 4500 m³/s) (Regierungspräsidium Freiburg, 2009). However, the former floodplains are located several meters above the current Rhine bed due to the strong channel erosion reported. Thus, to gain the required volume and to reactivate the floodplains, parts of the current Rhine floodplains will be lowered by excavation of gravel as illustrated in Figure 4.11b and c. These measures will be conducted on a length of 43 km. Dependent on the available land, the side expansion can reach some tens up to hundreds of metres, e. g. in rural areas with gravel pits. In addition to the discharge volume obtained, the vegetated widenings should provoke a significant reduction of the flood travel velocity by its flow resistance. This is of fundamental importance for the areas downstream since the possibility can be reduced that the Rhine flood wave might meet the flood waves of its tributaries at the same time. The retention area Neuenburg is part of this large retention project and is located at Rhine-km 198 – 201.

A general picture of a lowering area planned in the Integrated Rhine Programme for flood retention purposes is given in Figure 4.12. It is obvious that the planning and sustainability of these nature-close flood protection measures is a severe challenge due to the high complexity of interrelationships among discharge, sediment transport and vegetation. The former floodplain is excavated down to 0.5 m above groundwater level in order to provide best conditions for floodplain forest development and finally flood retention. In addition, spillways are planned which will direct water onto the lowering area via side channels in order to improve flow interactions between main channel, floodplain and interstitial.

However, in order to sustain the retention volume required for flood protection it is important to control bed load and suspended sediment transport in the system. For example, in- and outlet and the side channel itself must be designed in such a way that flow velocities within are high enough to guarantee suspended sediment transport and to avoid sedimentation in the side channel. In order to limit potential bed load transport onto the lowering area that could affect the measure in addition, the inlet is planned 1.0 – 1.5 m higher than the Rhine bed. Like that, sediment transported as bed load can be hindered to enter the inlet. The functionality of the side channel is crucial for the success of the flood protection measure. On the lowering areas, instead, the deposition of fine nutrient-rich material is required in the early stage of the project for the vegetation succession towards a natural floodplain forest and for the stabilization of the loose gravel material. Thus, the design of the lowering areas should create moderate flow conditions with low velocities for sediment deposition directly after excavation. Moreover, stream forces on the lowering areas can be reduced to a certain degree by the vegetated groyne fields located between lowering area and main channel. The Leinpfad, a fixed steep embankment with a maintenance road, will be displaced to the outer border of the area some years after excavation when the bed of the lowering area will be stabilized by sorting processes, selective erosion, and the roots of upcoming vegetation. It will be used as maintenance way and for recreation purposes. All in all, morphodynamic activities should be limited to local zones in the side channel.

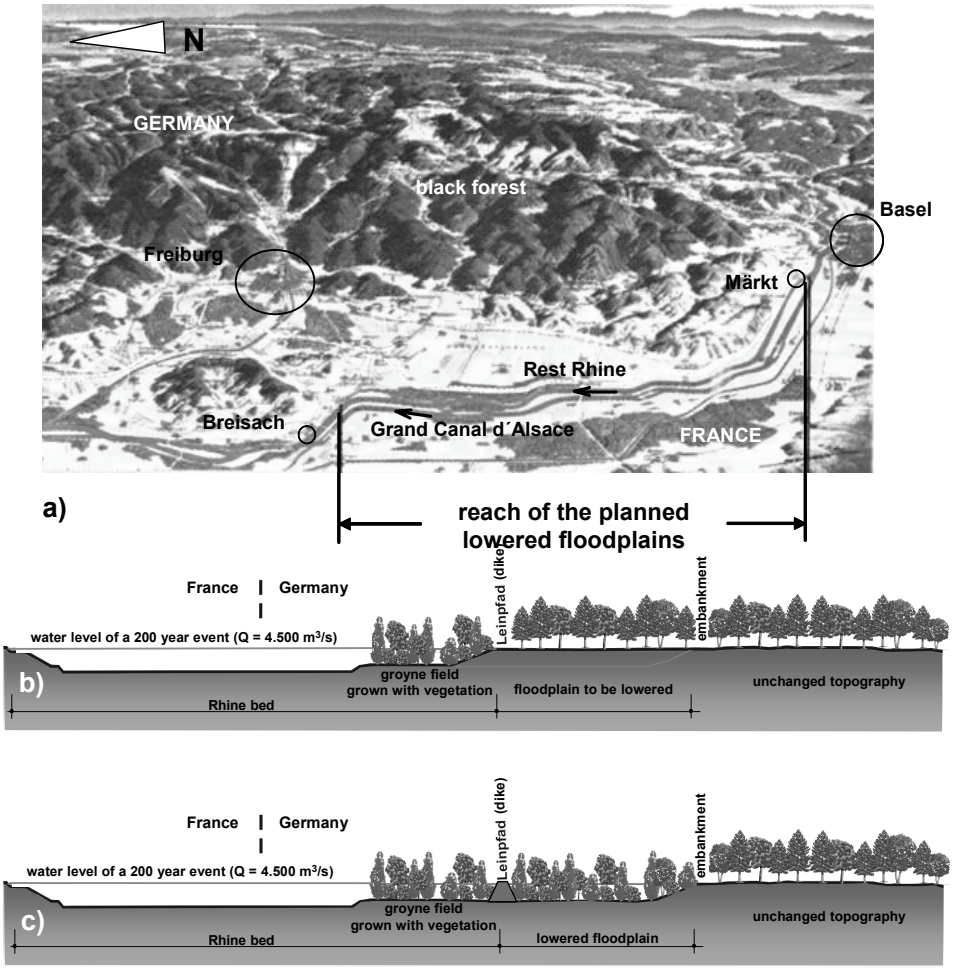

Figure 4.11: Creation of inundation space by lowering former floodplains (provided by GWD).

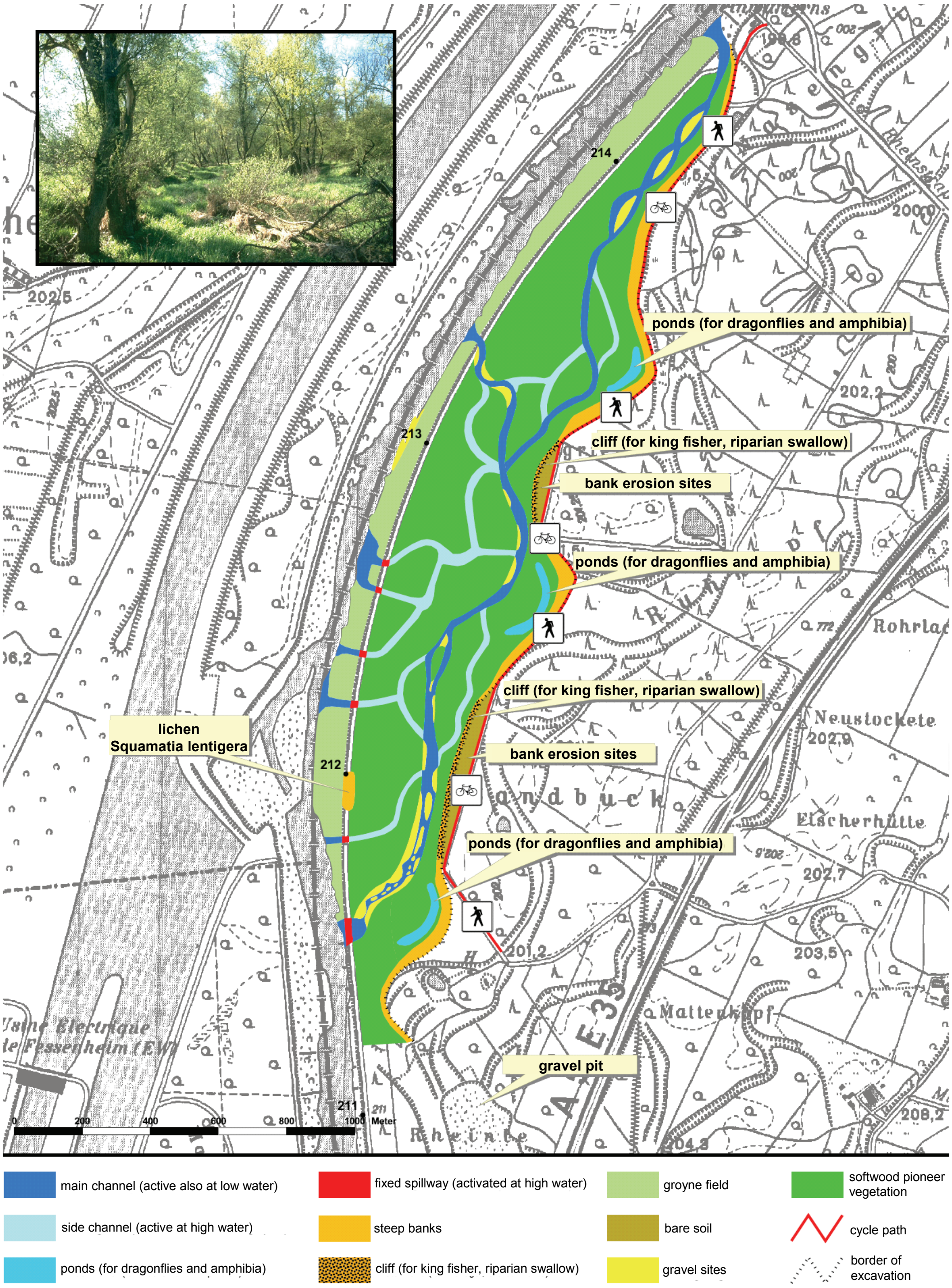

Figure 4.12: Landscape and restoration plan for a flood retention area in the Upper Rhine (provided by ILN).

4.3 SYSTEM DEFINITION II – HYDROMORPHOLOGY OF THE STUDY SECTION WEIL-BREISACH (RHINE-KM 173.975 – 224.800) AND NEUENBURG

The project area Neuenburg is located in the Rhine section between the barrages Kembs/Märkt and Breisach (Rhine-km 173.975 – 224.800), see Figure 4.13. This Rhine section shows special characteristics concerning hydrology and morphology due to the strong regulations carried out in the last centuries (see Chapter 4.2.1.2). Based on the general overview of the Upper Rhine and related flood risk gained so far, the present chapter provides the hydromorphological system characterization of the study area as reference for the morphodynamic hazard analysis. It comprises information on the driving variables (discharge, sediment regime), the boundary variables (sediment material and vegetation cover) and the dependent variables (morphology of the main channel, development of foreland and groyne fields) of the actual state. Finally the hydromorphology of the planning state is analysed as well as its design and desired functionality.

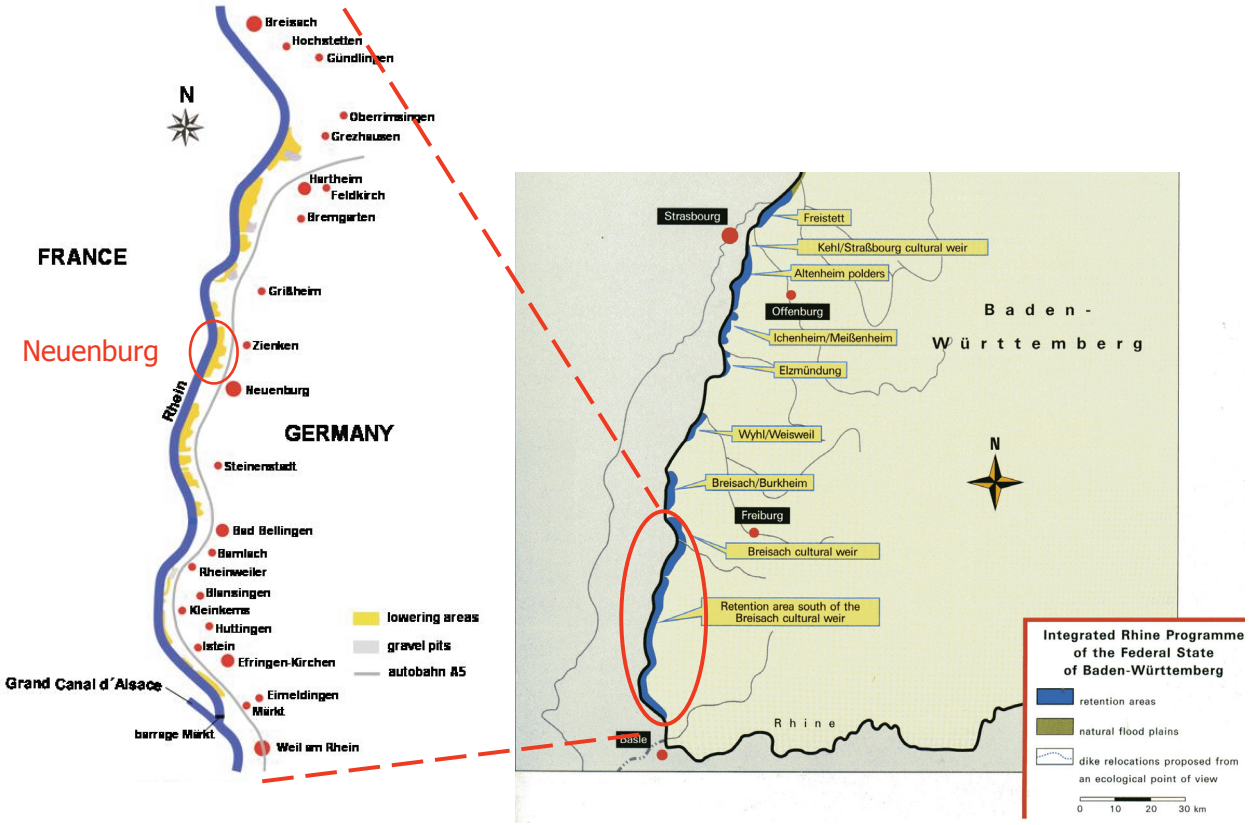

Figure 4.13: Study reach Neuenburg in the framework of the Integrated Rhine Programme (State Ministry of the Environment Baden-Württemberg, 2007, modified).

4.3.1 Driving variables: discharge characteristics and sediment regime

The morphodynamic situation of the Rhine section Weil-Breisach is strongly determined by its discharges and sediment regimes leading to highly modified hydrologic conditions due to the Rhine modifications at the present time. Figure 4.14 shows the duration curve at the gauging station Basel-Rheinhalle (Rhine-km 165.1, black line) upstream of the barrage Märkt/Kembs and the duration curve

at the gauging station Hartheim (Rhine-km 214.0, grey line) downstream of barrage Kembs. At the barrage Märkt/Kembs, most discharge is diverted into the Grand Canal d'Alsace for energy production

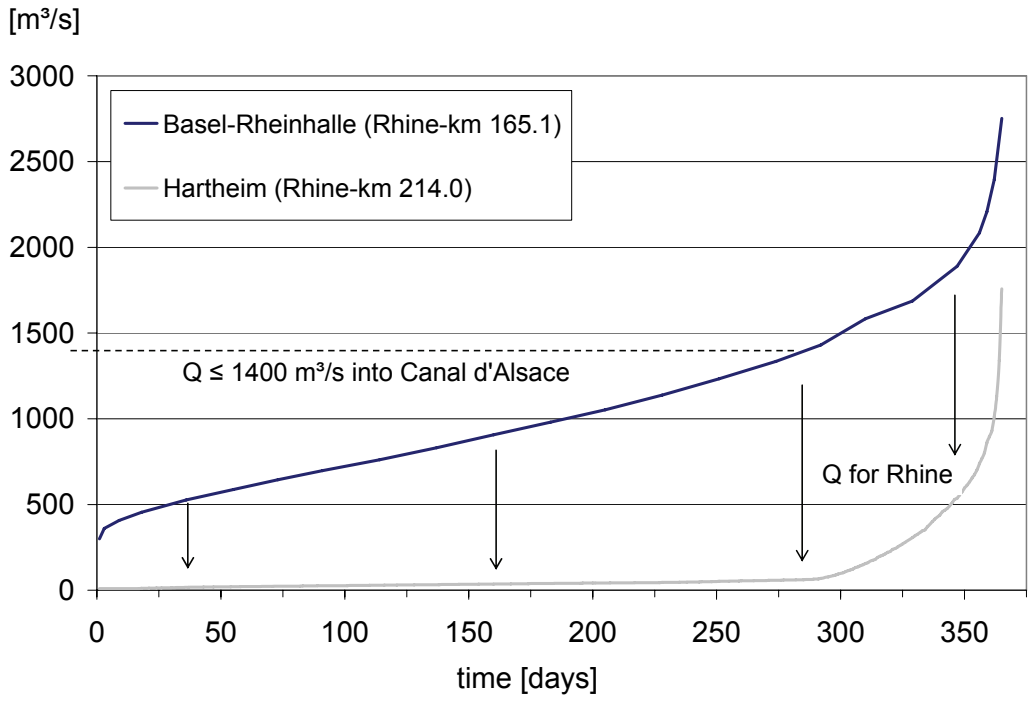

Figure 4.14: Mean duration curves at the gauging station Basel-Rheinhalle, Rhine-km 165.1 – natural regime (period 1891 – 2007, BAFU, 2008) and at the gauging station Hartheim – regulated regime (period 1953 – 1999, provided by ILN, 2004).

while only 30 – 40 m³/s is available to the River Rhine resulting in low water conditions statistically at 300 days per year. Only if a flood with a Q > 1400 m³/s occurs upstream of Kembs, more water is diverted into the Rhine. Figure 4.14 shows impressively the modification of the natural discharge regime of the Rhine.

The second important driving parameter is the sediment regime consisting of bed load and suspended sediment. In the study area, the sediment budget is severely affected by river regulation measures of this section and upstream. Bed load transport is almost totally disrupted since the locks in the High Rhine and in some tributaries as well as the weir Kembs hold back the bed load transported from upstream. As a result, bed load transport into the Rhine section Weil-Breisach is negligible for most time of the year. It is enabled only at extreme flood events in the case the sluices at barrage Kembs are being opened for flood protection as during the flood of 1999. Here, sediment could pass the barrage and possibly initiated the development of gravel banks and islands upstream of the "cascade of Istein". Schälchli et al. (2000) and Hartmann et al. (2000) state that a total sediment passability in the High Rhine could lead to bed load transport rates of approx. 10,000 m³/a downstream which represent 1/3rd – 1/5th of the original bed load rate present prior to the corrections in the 19th century.

In contrast to bed load, suspended sediment load is transported into the Rhine almost all the year without any interruptions leading to constantly high transport rates. Figure 4.15 and Table 4-1 present field measurements of suspended sediments (monthly values based on daily measurements) as well as the corresponding mean monthly discharge exemplarily for the measuring station Weil (Rhine-km 173.0). Suspended sediment concentration range between 17 – 43 g/m³ and vary obviously with

discharge. According to Hartmann et al. (1998) suspended sediment load is as high as prior to the Rhine corrections (relatively to the low discharge conditions).

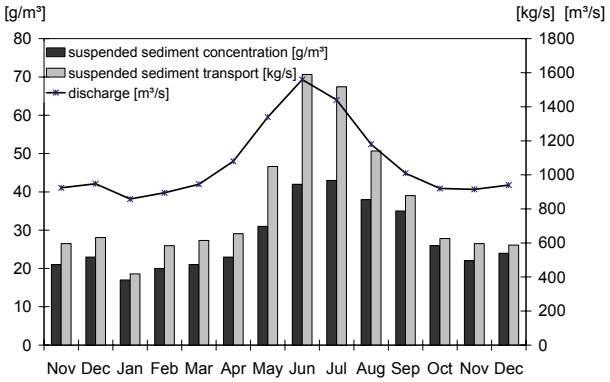

Figure 4.15: Mean suspended sediment concentration and transport measured at Weil, Rhine-km 173.0, period 1971 – 2003 (Landesanstalt für Umweltschutz, 2006).

Table 4-1: Mean suspended sediment data measured at Weil, Rhine-km 173.0 (Landesanstalt für Umweltschutz, 2006).

data on suspended sediments (period 1971 – 2003)	
concentration [g/m³]	29.0
transport [kg/s]	38.11
loads [t/a]	1,201,631

A complete picture of the discharge and sediment characteristics apparent in the study section as well as zones with vegetation development in the planned retention areas draws Figure 4.16.

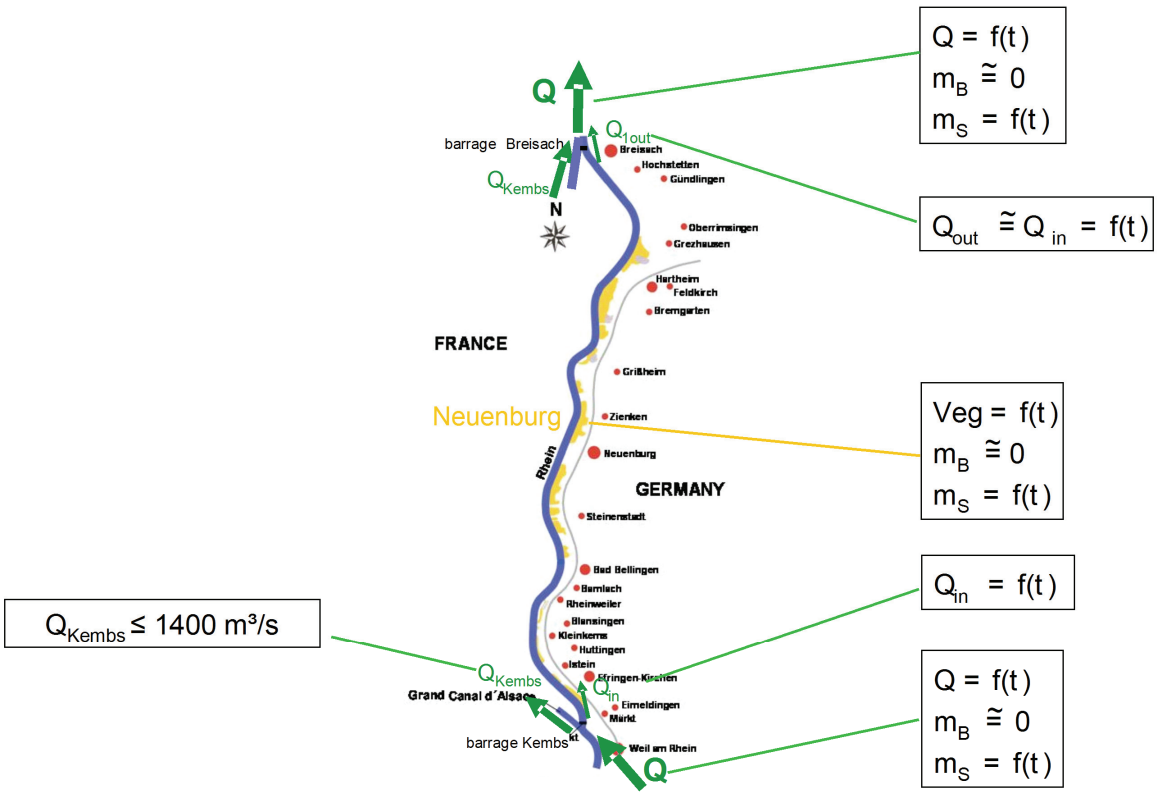

Figure 4.16: Boundary conditions of discharge and sediment regime as well as future locations of flood retention areas with floodplain forest (m_B = bed load, m_S = suspended load, Veg = vegetation growth).

As aforementioned, sediment dynamics in the River Rhine are mainly determined by fine particles transported in suspension while bed load transport can be neglected most of the year. The

characteristics of these suspended particles are crucial for the morphodynamic development of the river reach and the sustainability of the planned rehabilitation measures since they are easily deposited in areas with low flow velocity, for example in vegetated areas and cross-sectional widenings as planned in the Integrated Rhine Programme. It must be emphasized that the sedimentation behaviour of suspended sediments is very complex and highly dependent on various parameters such as turbulence, velocity, discharge, particle size, topography, vegetation type and vegetation densities.

4.3.2 Boundary variables and morphological structures

4.3.2.1 The Rhine section Weil-Breisach – an overview

Figure 4.17 shows a scheme of a typical current Rhine stretch between the barrages Kembs and Breisach. The Grand Canal d'Alsace is located left of the Rhine channel and is separated from the river by the French foreland while on both sides, the Rhine channel is bordered by the Leinpfad. The foreland on the German side is located several meters above the Rhine bed. Due to the lowered groundwater table, the vegetation has changed completely in comparison to the natural state prior to the regulation measures. The original soft and hardwood floodplain forest has vanished in favour of pine trees, shrubs, dry meadows and gravel pits. However, silted oxbows are still present on the foreland as relicts of the furcation zone of the last centuries.

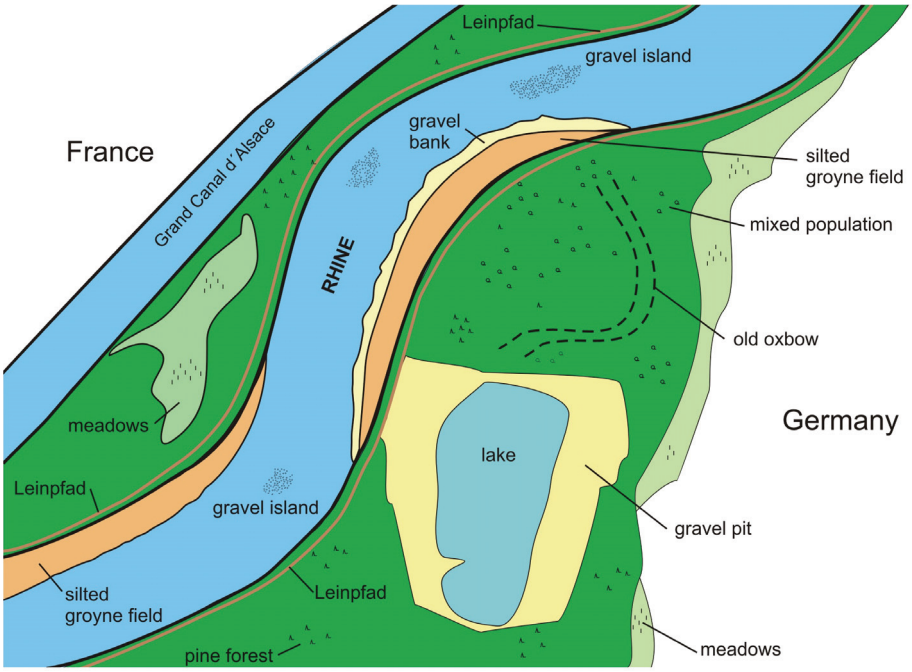

Figure 4.17: Morphology of a typical section in the Upper Rhine between the weirs Kembs and Breisach (provided by Dittrich, modified).

In the course of the regulations in the last century, a plain and dense armour layer has developed in the Rhine main channel by selective erosion. It covers the complete bed and reaches a critical state only at high discharge events of 3600 m³/s or even more (Dittrich et al., 2007). The armour layer is covering a second lower layer of finer material. The sieves curves of armour layer and lower layer

from a gravel bank at Rhine-km 210.50 are depicted in Figure 4.18, the characteristic grain sizes of the material samples taken are listed in Table 4-2. The armour layer consists of material with d_m = 107 mm and d_{max} = 161 mm while Gebler (1992) reports stones with 200 – 300 mm locally. The documentation of the sampling site is provided in Figure A.1.1, Appendix. The Rhine bed and low-water channel are shown in Figure 4.20 and Figure 4.21, respectively. Information on the material present on the former Rhine floodplains can be obtained by sieve curves of three gravel pits Bremgarten, Grissheim and Hartheim close to the project area provided by Hartmann and Dittrich (1995). Corresponding sieve curves and characteristic grain sizes of the location with finest material and of the location with coarsest material as well as mean values of all three sites are depicted in Figure 4.19 and Table 4-2 for the documentation of the sites see Figure A.1.2 –A.1.4, Appendix.

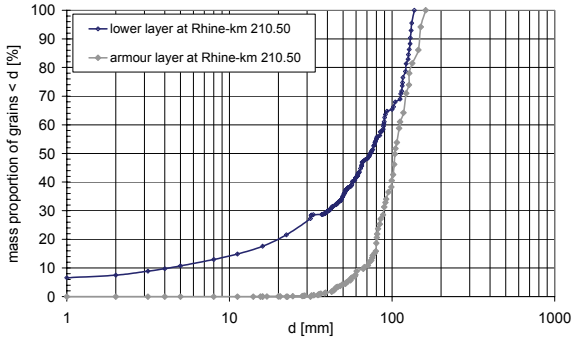

Figure 4.18: Sieve curves of typical armour layer and lower layer taken from a gravel bank at Rhine-km 210.50.

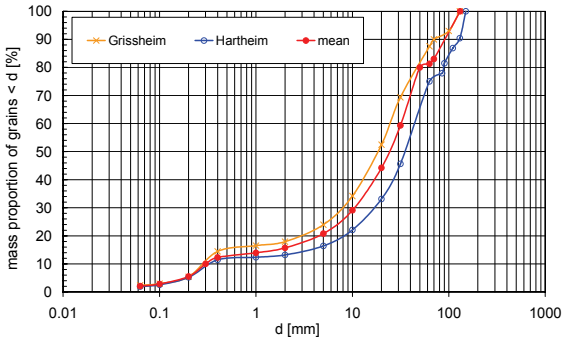

Figure 4.19: Sieve curves of typical loose bed material taken from gravel pits on the former Rhine floodplains.

Figure 4.20: Rhine bed with armour layer (provided by Dittrich).

Figure 4.21: Rhine main channel at low water conditions (provided by Dittrich).

Table 4-2: Characteristic grain diameters of sediments representative for the study site.

d_{ch} [mm]	armour layer (Rhine bed)		loose bed material (floodplains)		
	lower layer	upper layer	Grissheim (min)	mean	Hartheim (max)
d_{50}	73	104	18	25	35
d_m	79	107	30	37	49
d_{max}	137	161	130	131	153

In the last centuries, groyne fields have been built in the River Rhine to improve navigation. In the course of the decades, these groyne fields have silted up and are covered with vegetation nowadays. Aerial photographs presented in Figure 4.22 exemplarily for Rhine-km 192 show impressively how siltation and vegetation development have succeeded over a period of about 40 years. Information of sedimentation characteristics and vegetation pattern for the groyne fields in the project area are provided by Hartmann et al. (1998) who carried out field measurements of sedimentation rates on the silted groyne field at Rhine-km 191.30. The cross-sectional profile and related sampling locations P1 and P2 are documented in Figure A.1.5, Appendix, the corresponding sieve curves for station P1 are shown in Figure 4.23. The material apparent on the groyne fields consists of loose, non-consolidated

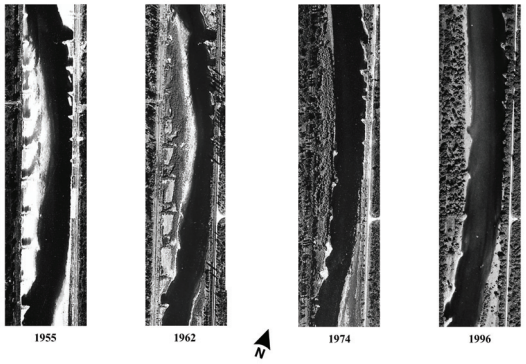

Figure 4.22: Development of groyne fields via sedimentation and vegetation succession over the period 1955 – 1996 (provided by ILN, 2008).

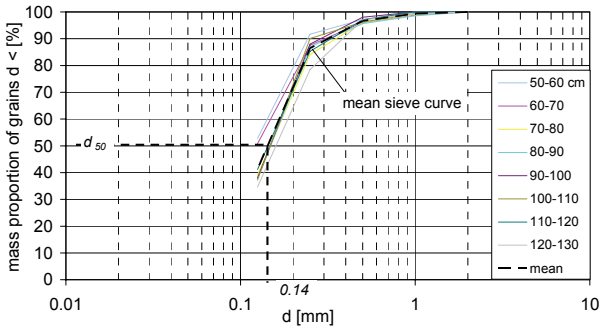

Figure 4.23: Sieve curves of fine sediments deposited on the groyne fields (Hartmann et al., 1998).

sand. Since the samples are homogenous with depth, a mean sieve curve is derived in the present thesis for all samples (d_{50} = 0.14 mm). Furthermore, Hartmann et al. (1998) report that the measured sedimentation rates did not show any significant relationship between suspended sediment transport rate and discharge. This outcome underlines the complexity of the interactions flow/sediment/vegetation which was already discussed in Chapter 3. Alternatively, an indication for the general sedimentation behaviour can be obtained by long-term field observations which are available for the same region, see Hartmann et al. (1998). Observations over the last 40 years show a mean sedimentation rate of 1 m on the groyne fields giving a yearly sedimentation rate of 2.5 cm. However, this value does not take into account that the sedimentation rate is dependent on topography or sedimentation height, respectively (the higher the sedimentation height / topography the lower might be the sedimentation rates since the area is flooded less frequently). But in any case, these data provide at least an overall good estimation of the long-term sedimentation characteristics present in the Rhine section.

In addition to sedimentation data, Hartmann et al. (1998) provide information on vegetation pattern along the groyne fields. A detailed vegetation mapping was carried out including measurements of plant diameter and stem distances yielding that vegetation types and densities differ according to maintenance frequency. The typical vegetation on the German Rhine side consists of a mixed population with mean stem diameters of 3.89 m and mean stem distances of 6.07 m both in cross-sectional and longitudinal direction as well as thinned poplar hardwood forest due to forestry with stem diameters of 0.5 m and 6.0 m both in longitudinal and cross-sectional direction. The latter type is

presented in Figure 4.24. Due to missing maintenance on the French Rhine side, in turn, natural willow poplar forest has developed over the last 50 years with typical stem diameters of 1.0 m and mean stem distances of 5.66 m in cross-sectional and 10.34 m in longitudinal direction, see Figure 4.25.

Figure 4.24: Thinned poplar hardwood floodplain forest, small pole stage forest; German side, Rhine-km 184.5 (Hartmann et al., 1998).

Figure 4.25: Natural willow poplar forest; French side, Rhine-km 192.0 (Hartmann et al., 1998).

Based on the characterization of the Rhine section Weil-Breisach, the System Definition now focuses on the local morphological situation of the case study area Neuenburg. The following chapters present the conditions apparent in the actual state (Chapter 4.3.2.2) as well as the planned design of recreation and flood protection measures (Chapter 4.3.2.3).

4.3.2.2 Morphological aspects of Neuenburg in the actual state

The study site Neuenburg is located in the Rhine section Weil-Breisach in the vicinity of the municipality Neuenburg between Rhine-km 198.410 and Rhine-km 200.970. The morphology exhibits the characteristics of the whole Rhine section Weil-Breisach with an average slope of 0.8 – 1.0 ‰, fixed banks, stretched meanders, originally trapezoidal cross-sections and silted vegetated groyne fields on alternating sides representing the natural floodplains at the present time. Also at Neuenburg, the flow and sediment transport conditions are strongly regulated as reported for the River section Weil-Breisach and schematized in Figure 4.16. In addition to the overall picture, the river site Neuenburg shows two important site-specific morphological features determining the flow field and the local water level: an old harbour located at Rhine-km 199.200 and a gravel island located further downstream between Rhine-km 199.330 and 199.750, see Figure 4.26. The old harbour is filled with sediment, covered with vegetation and forms an immediate cross-sectional widening along the straight, channelized river course. The gravel island located further downstream has developed to its existing extent after the flood of 1999 most likely by local destabilization of the armour layer, by erosion of gravel bars and islands upstream as well as by bed load having passed through the sluices of barrage Kembs which had been opened for flood protection at this event (Dittrich, 2008). The gravel island is nowadays covered with vegetation and remained stable also during the high flood in 2007. A site map of the Neuenburg situation including the island, the harbour and the municipality is given in Figure 4.26 and Figure 4.27.

Figure 4.26: Location of the municipality Neuenburg, gravel island and old harbour (provided by ILN, modified).

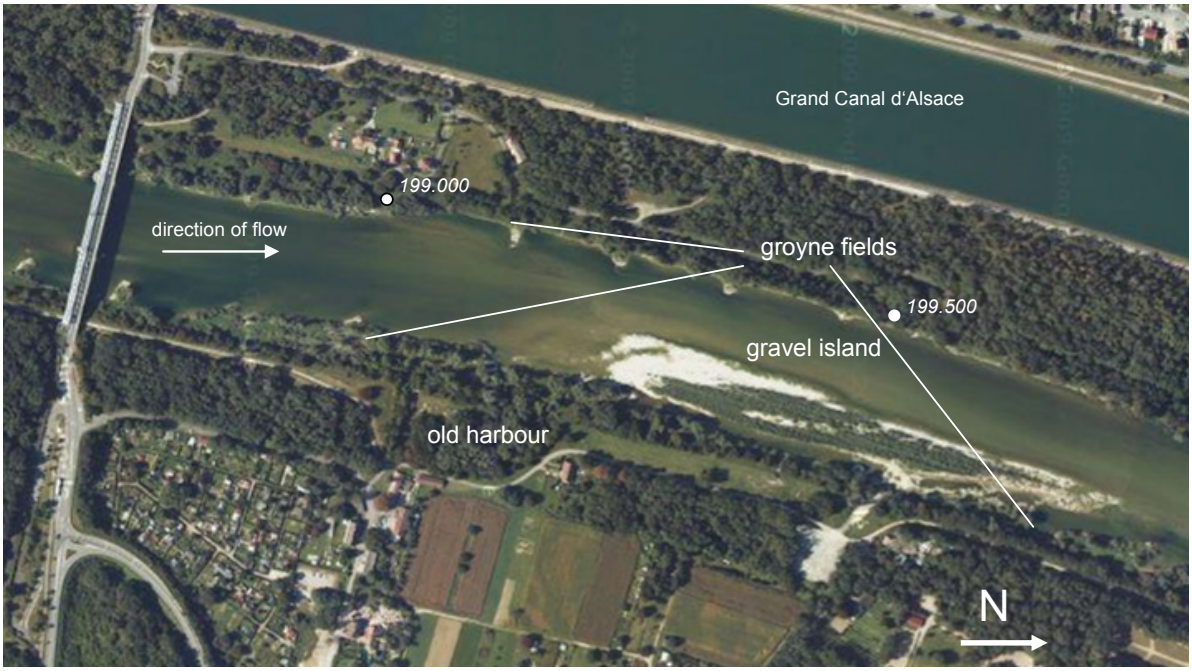

Figure 4.27: Current morphological features at the study site Neuenburg (photo: googlemaps, 2009, modified).

4.3.2.3 Morphological aspects of Neuenburg in the planning state and challenges related to risk

The new river design of the site Neuenburg will be comprising several measures for both flood protection and recreation purposes. The measures cover a large lowering area for flood retention and recreation measures for leisure activities and tourism upstream and in the vicinity of the gravel island.

The analysis of morphodynamic hazards endangering these measures, the estimation of design sustainability and suggestions for design optimization are the objectives of the present study.

- The flood retention area is planned downstream of the gravel island on the German Rhine side at Rhine-km 199.500 with a longitudinal expansion of more than 2.5 km in the framework of the Integrated Rhine Programme. The retention area will be created by excavating the former floodplain down to few decimetres above groundwater level in order to obtain the retention volume as well as nature-close conditions for the development of floodplain forest by natural succession which is required for retention purposes. To optimize natural succession with the desired vegetation types of willows, poplars and hardwood forest, terraces of different altitudes are planned (see Figure 4.28 and Table 4-3). Like that, the flood protection measures will also contribute to the rehabilitation of aquatic interactions among main channel, floodplain, groundwater and interstitial, nature-close morphodynamics and biodiversity. However so far, the plannings do not consider sediment management on the retention area although related morphodynamic hazards might play a key role in the functionality and sustainability of flood protection. As aforementioned, sediment dynamics provoke remarkable challenges to keep the acceptance criteria:

On the one hand, deposition of fine sediment on the lowered floodplains is desired for natural bed stabilization at first for the following reason: Directly after excavation loose bed material is present on the lowering area and must be stabilized to avoid severe bed dynamics at high discharges. The deposition of fine, nutrient rich material initiates the settlement and development of pioneer vegetation which in turn enhances the stability of the loose material by roots in the case of flooding. Furthermore, this pioneer vegetation should be the first step towards a natural floodplain forest succession which is further required for reliable flood retention.

On the other hand, playing in contrast to the desired sedimentation processes, sedimentation rates must be limited to avoid a decrease of the retention volume in the long-term. To achieve these demands and to reduce maintenance activities, among others, a side channel is planned to constantly flush out fine sediments, see also Table 4-3. The inlet of the side channel will be situated at the downstream end of the gravel island 1.5 m above the river bed which should inhibit siltation of the inlet by eventual bed load transport. However, the functionality of the side channel design has not been tested so far. As reported previously, it is not possible to forecast sedimentation rates in vegetated areas. But observations have shown mean deposition rates of fine sediments in the vegetated groyne fields of 1 m in 40 years. Accordingly, the river design plans of Neuenburg roughly assume a maximum deposition height of 1 m of fine sediments on the lowering area with fully developed floodplain forest 50 years after excavation. Topographic levels and dimensions of the lowering area are summarized in Table 4-3.

The construction costs for all measures along the Upper Rhine within the Integrated Rhine Programme are estimated by State Ministry of the Environment Baden-Württemberg (2007) to 775 mio €. In the case of a 200-years flood, losses disregarding human casualties might reach about 6 billion € along the Upper Rhine valley until Mannheim/Ludwigshafen and further downstream. It is obvious that if the retention areas Weil-Breisach do not work properly in combination with the other IRP measures, severe damages and losses can be expected not only locally at the study site Neuenburg, but much more at the congested urban areas downstream. The overview given above highlights however that numerous processes can affect the functionality of the flood protection

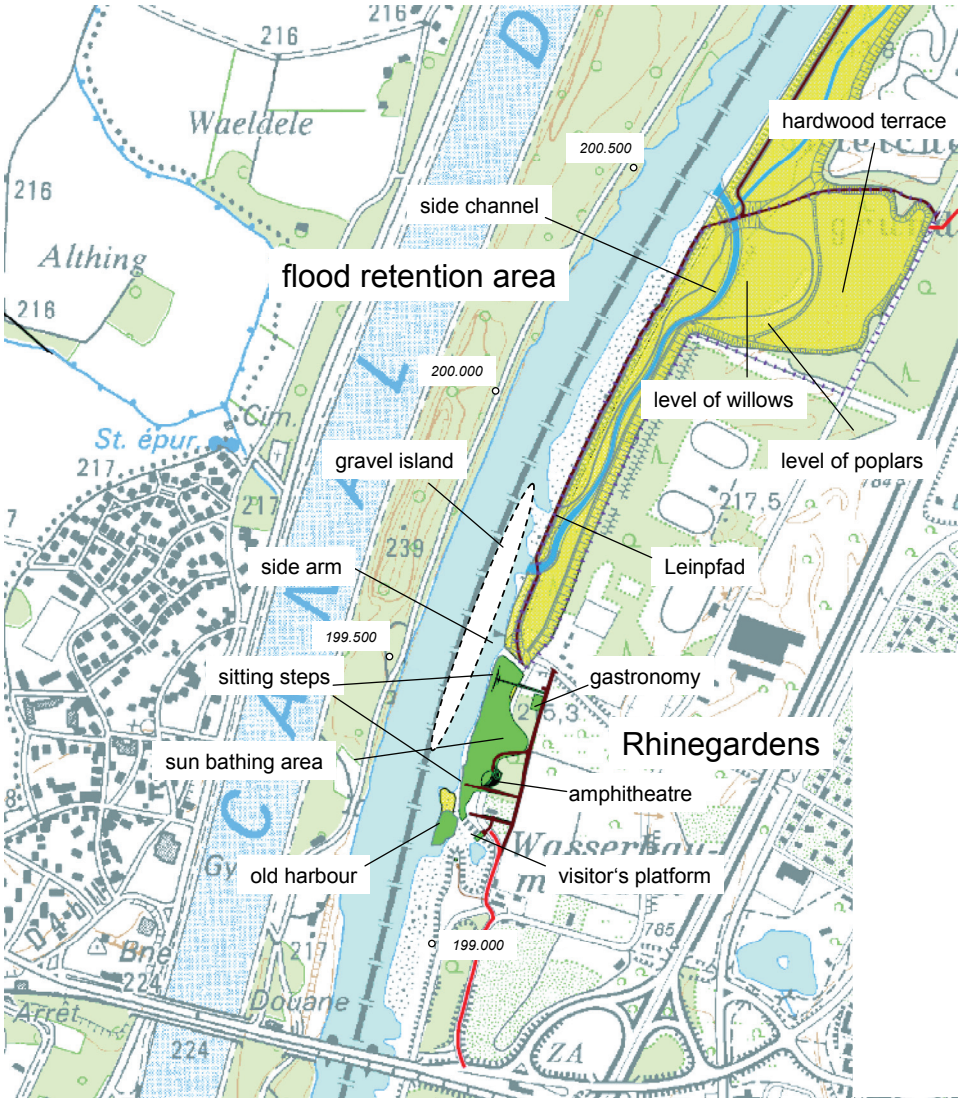

Figure 4.28: Overview of the measures in the river reach of Neuenburg in the planning state (Regierungspräsidium Freiburg, 2008).

Table 4-3: Topography and geometry of the flood retention area and the side channel (Regierungspräsidium Freiburg, 2007).

area	topography [m above groundwater level]			width [m]
	level of excavation	sedimentation height	total level	
<u>lowering area</u>				
level of willows	0.5	1.0	1.5	
level of poplars	1.3	0.2	1.5	
level of hardwood forest	1.5	3.0 (supplementary layer)	4.5	
<u>side channel</u>				
bed	-1.0	0	-1.0	10.0
banks	0.5	0	0.5	5.5

measure. In order to estimate its sustainability and to further develop optimization strategies, the identification of morphodynamic hazards is carried out in Chapter 4.4.

- The second important project at the study area are recreation measures along the German Rhine banks (see also Figure 4.28) which have been planned by the municipality of Neuenburg in the framework of a new tourism concept for the city. The city of Neuenburg is an important location for economy and business with about 12,000 inhabitants and had been originally founded on the former banks of the Rhine terraces about more than 800 years ago. However, nowadays the Rhine bed is located several meters deeper due to the severe erosion processes. Subsequently, Neuenburg has been "cut off" from the river with a distance of more than 800 m and without direct view contact leading to the neglect as recreation area by local people and tourists. To improve the attraction of the River Rhine for leisure activities and tourism and to further strengthen the location for business and economy, the municipality of Neuenburg has planned a rehabilitation and recreation concept called "a city moves towards the Rhine" ("eine Stadt geht zum Rhein"). Within this concept, recreation plans called "Rhinegardens" ("Rheingärten") have been worked out which will be realized directly upstream of the flood retention area at Rhine-km 199.300 – 199.500. An overview of these measures is presented in Figure 4.29 and Figure 4.30 comprising

  - flattening and restoration of the steep Rhine banks along a width of 40 m and a length of 400 m
  - sunbathing areas and an adventure playground
  - an amphitheatre
  - promenades with restaurants and a fairground
  - a new pedestrian bridge crossing the federal highway
  - restoration and reinstallation of an historic old harbour (Rhine-km 199.200)
  - an existing gravel island (Rhine-km 199.330 – 199.750) as main attraction point

The heritage-protected historic harbour basin originally had a size of 70 x 30 m and was paved with sandstone (ILN, 2006). However, due to erosion of the Rhine bed, the ground of the harbour is located 2 – 3 m above the groundwater level, has been silted up and is covered with vegetation today (see Figure 4.26 and Figure 4.27). According to the recreation plans, the basin will be dredged out and restored to create a place for canoos and small boats as shown in Figure 4.29. Close to the restored harbour, a visitor platform should attract people with panorama view along the Rhine (Figure 4.29). Last but not least, the key role for the success of the recreation concept concerns the gravel island already existing in direct vicinity of the harbour (see Figure 4.28 and Figure 4.30). The gravel island should function as main attraction view point for tourists visiting the Rhinegardens on the German side (Figure 4.30).

So far, the recreation concept has been planned in accordance with flood risk and inundation plans. For example, the gastronomy area is planned on a sufficiently high topographic level so that it will not be inundated at a 200-years event in the planning state. But it is not clear whether the measures which directly affect fluvial morphology such as bank flattening, harbour restoration and the gravel island will develop as planned under the future flow conditions and whether costly maintenance activities will be required in order to sustain the desired situation in the long-term.

According to Höhl (2008) the investments for the Rhinegardens construction will reach a double-digit mio € sum plus private investments for gastronomy. As a consequence, in the case of the concept's failure, severe consequences are likely to occur which are not only limited to direct material losses but also related to indirected losses due a failed economy and tourism concept of the business location. In Chapter 4.4, the potential hazards which might be able to put the system at harm will be identified in detail.

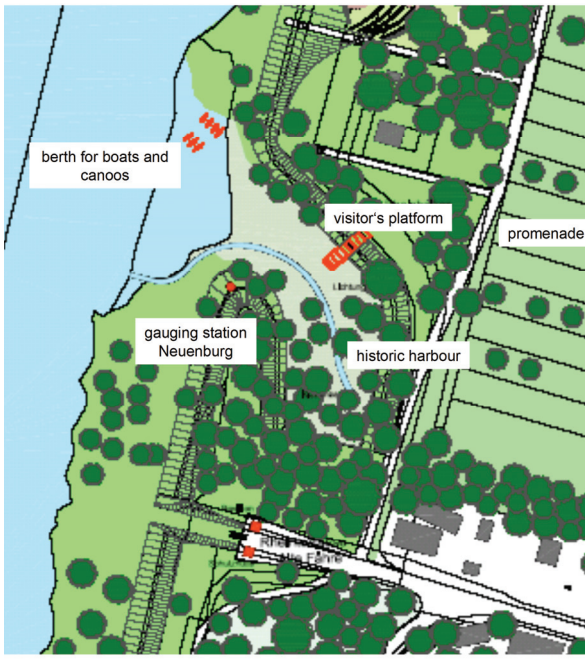

Figure 4.29: Municipality plans for the restoration of the historic harbour (provided by ILN, 2006).

Figure 4.30: Municipality plans for the recreation area "Rhinegardens" (provided by ILN, 2006).

4.3.3 Scenarios for the morphodynamic hazard analysis of the planning state Neuenburg

In order to adequately prognosticiate the morphodynamic hazards likely to occur in river restoration and flood protection projects, it is crucial to clearly define the hydromorphologic conditions which may govern in future. In the case the future conditions are not yet clear or the system is too complex to allow a reliable prognosis, the Hazard Analysis may be carried out based on scenarios. Those scenario conditions which are most likely in future can then be investigated separately. The analysis based on scenarios may allow to further enhance system understanding and to sketch the ranges of potential processes in the case the governing conditions change. It should be repetitively noted that this point is crucial for reliable estimation of fluvial morphodynamics due to the complexity of governing interrelationships among water flow, sediment and vegetation.

For the study site Neuenburg, it was decided to investigate two scenarios. For clarity, the boundary conditions defined for these planning state scenarios are listed in Table 4-4 and Table 4-5, respectively. As shown, the scenarios are identical concerning hydrological boundary conditions. This

is due to the fact that also in future the discharge regime will be ruled by concession concerning the weir operation Kembs. As a consequence, low water conditions will be apparent in future most time in the year until the discharge upstream of Kembs reaches the capacity of 1,400 m³/s. In the case of a flood however, the conditions change drastically because the flood protection plans envisage to convey the flood wave into the River Rhine completely with the consequence that the river measures should therefore be able to withstand high floods as well. Regarding morphology, the features and related properties in the planning state have been described in detail in the previous chapters and will be considered as being identical in both scenarios.

The scenarios differ concerning the sediment regime. In the first scenario, the sediment regime will be taken into account which is governing also the present day conditions: namely variable suspended load transport and negligible bed load transport. In the second scenario instead, the focus of interest is placed on the hypothesis that additional sediment transport is initiated as bed load from upstream. This scenario was chosen in order to detect how the system might react on larger amounts of sediments and

Table 4-4: Boundary conditions and related data for scenario A.

conditions	description	related data in Chapter 4
discharge regime	- frequently: low water 30 – 50 m³/s at appr. 300 days/a due to weir operation	- Figure 4.14
	- in the case of flood: flood wave completely diverted into the Rhine	- Figure 4.14
morphology	- bed/main channel: armour layer which remains stable until a high flood	- Figure 4.18, Figure 4.20, Table 4-2
	- German and French banks: fixed, stable at high floods	
	- groyne fields: bed material: fine sand, covered with floodplain forest, acc. to field observations stable at high floods	- Figure 4.23 - Figure 4.25
	- gravel island: gravel, reinforced by willow roots, covered with floodplain forest	- Figure 4.18, Figure 4.26, Figure 4.27, Table 4-2
	- Rhinegardens: covered with lawn and trees, acc. to municipality plans	- Figure 4.28, Figure 4.30
	- flood retention area: loose gravel reinforced by willow roots, covered with floodplain forest	- Figure 4.19, Figure 4.25, Table 4-2, Table 4-3, Figure 4.28
	- side channel/lowering area: loose gravel	- Figure 4.19, Table 4-2, Figure 4.28
	- ancient harbour, dredged, acc. to municipality plans	- Figure 4.29
sediment regime	- suspended sediment transport: natural concentrations, dependent on discharge dynamics	- Figure 4.15, Table 4-1
	- bed load transport: transport negligible from upstream due to barrages, armour layer, low-water conditions, fixed banks on the German and French Rhine side which do not release any material	- Figure 4.18, Table 4-2

whether this could affect the functionality of the river measures. As shown before, sediment transport might be occurring in the case of high flood when the weir sluices at Kembs are opened. Thus, sediment transport from upstream into the reach cannot be completely excluded and should be investigated as supplementary condition as well. The choice of this scenario was further enforced by intentions of the French company for electricity which regards additional river measures along the Rhine. The intention aims at improving the morphological situation concerning sediment transport mechanisms and the development of gravel bars by partly removing the embankments on the French side for the initiation of bank erosion upstream and downstream of the study section Neuenburg. As a consequence, the release of sediments from the French banks can have significant impact on the planning state: It is unclear to what extent this sediment supply might impact system behaviour, endanger the river measures for recreation and flood protection and, subsequently, increase risk. Thus, in order to detect potential cases of failure, it was decided to investigate this scenario in addition. In

Table 4-5: Boundary conditions and related information for scenario B.

conditions	description	related data in Chapter 4
discharge regime	- frequently: low water 30 – 50 m³/s at appr. 300 days/a due to weir operation	- Figure 4.14
	- in the case of flood: flood wave conveyed in the Rhine bed completely	- Figure 4.14
morphology	- bed/main channel: armour layer which remains stable until a high flood	- Figure 4.18, Figure 4.20,Table 4-2
	- German and French banks: fixed, stable at least until a high flood	
	- French banks upstream the study site: fully exposed to flow, without embankments	- Figure 4.19, Table 4-2
	- groyne fields: bed material: fine sand, covered with floodplain forest, acc. to field observations stable at least until a Q_{100}	- Figure 4.23 - Figure 4.25
	- gravel island: gravel, reinforced by willow roots, covered with floodplain forest	- Figure 4.18, Figure 4.26, Figure 4.27, Table 4-2
	- Rhinegardens: covered with lawn and trees, acc. to municipality plans	- Figure 4.28, Figure 4.30
	- flood retention area: loose gravel reinforced by willow roots, covered with floodplain forest	- Figure 4.19, Figure 4.25, Table 4-2, Table 4-3, Figure 4.28
	- side channel/lowering area: loose gravel	- Figure 4.19, Table 4-2, Figure 4.28
	- ancient harbour, dredged, acc. to municipality plans	- Figure 4.29
sediment regime	- suspended sediment transport: natural concentrations, dependent on discharge dynamics	- Figure 4.15, Table 4-1
	- bed load transport: transport into the study area from upstream initiated by weir operation or bank erosion on the French side	- Figure 4.18, Table 4-2

order to describe the properties of the potential eroded material from the French banks, the information available for loose bed material taken from the gravel pits can be used: It can be assumed that this sediment can well represent the material originally present on the floodplains and thus present also on the French side.

4.3.4 Identification of Elements at Risk

The System Definition carried out so far provides detailed insight into the hydromorphology of the river reach Neuenburg itself and upstream which have appeared in former times, today and which might be appearing in future. Based on this knowledge, it can now be defined which elements at the project site could be harmed by morphodynamic hazards within the two scenarios.

In a first step, the answer to this question is rather clear. Almost all morphological features at the project site Neuenburg might be affected by flood and morphodynamic hazards which might cause potential losses in some way. It should be noted that there are few exceptions comprising the banks on the German and French Rhine side on the one hand which are fixed nowadays and on the other hand the groyne field which are located close by. The major floods of 1999 and 2007 did not reveal any morphodynamic impact on the embankments. Thus, it can be concluded that they are negligibly vulnerable and are therefore defined as *EaNR*, Elements at No Risk.

In contrast, the bed of the main channel reaches a critical state of stability at high flood events (see e.g. Dittrich et al., 2005). It is therefore defined as EaR. The Elements of Risk (EaR) present in the river reach Neuenburg are listed as the following:

- main channel
- old harbour
- gravel island
- side arm (between gravel island and German banks)
- Rhinegardens
    a) sunbathing area (including playground, barbecue area)
    b) amphitheatre
    c) restaurants
- flood retention area
- side channel on the retention area including inlet and outlet

It has to be pointed out that the list above is an open list which must be updated consequently during the Risk Management chain. The hazards which might affect the EaRs are identified and discussed in the following chapter.

4.4 IDENTIFICATION OF POTENTIAL MORPHODYNAMIC HAZARDS AND POTENTIAL CONSEQUENCES IN THE PLANNING STATE

The prerequisite for reliable Risk Analysis and successful Risk Management is the identification of hazards and consequences likely to occur within the System under Analysis at the Elements at Risk. Without an accurate hazard listing, a sustainable river system that withstands the hazards cannot be

achieved. Thus, the second part of Risk Identification phase deals with the Hazard Identification for the case study region. In order to perform this second phase as accurately as possible, Chapter 4.2 and 4.3 are providing a detailed characterization of the system on the relevant temporal and spatial scales including original nature, historical development and present-day conditions. Moreover, further details for the study area Neuenburg are provided concerning the planned flood protection and recreation measures which will be in the further focus of this Hazard Analysis. Based on this information, important scenarios to be considered in the Risk Management chain and the Elements at Risk (EaR) which might be endangered in the scenarios by natural hazards have been clearly defined. With the system understanding gained so far, the following section now analyses *how* the functionality of the river design and the EaRs near Neuenburg can be affected. In other words, all sources and processes (*hazard*s) have to be detected which are potentially able to harm the planned flood protection and recreation measures. These hazards can be potential dangerous situations, events or sources of failure.

For the case of Neuenburg, it was decided to apply a simplified version of the Preliminary Hazard Analysis (PHA) methodology (see also Rausand, 2004; Faber, 2005) for hazard identification. The PHA is a qualitative or semi-quantitative approach for the purpose to identify major potential hazardous situations and related consequences. Due to its qualitative character, PHA is judged very useful for gaining a first overview of the risk conditions in the early stage of a project. Moreover, the procedure enables to systematically investigate which hazards and scenarios are relevant and which tools are appropriate in order to analyze them as reliably as possible. As the present study focuses on a semi-qualitative Risk Analysis, the PHA methodology is herein applied as an informative "brain storming" tool, as proposed also by Merz (2006), Rausand (2004) and Faber (2005): The PHA approach consists of a table where each hazard is listed together with its origin, hazardous processes, potential structural damages, consequences and severities (Rausand, 2004; Merz, 2006; Faber, 2005, Gowen et al., 1992).

The risk identification table derived for the river design Neuenburg is given in Table 4-6 which is valid for both the Scenario A (morphodynamic hazard analysis *without* sediment released from the upstream French banks; fixed embankments) and Scenario B (morphodynamic hazard analysis *with* sediment released from the French banks upstream) as for both scenarios, the same Elements at Risk, morphodynamic processes and consequences can be expected. Only the intensity of the morphodynamic hazard (sediment/bed load transport) might differ between the scenarios. First, Table 4-6 is listing the Elements at Risks and their planned functionality according to Chapter 4.2.2.2 and 4.3.2.3. The functionality of an EaR is described by the objective or purpose for which it is planned ("touristic" or "flood protection") and by the morphologic state which should be maintained according to the river plans. Furthermore, a qualitative definition of the accepted EaR's dynamics is provided:

It ranges from "no dynamics accepted" in the Rhinegardens (as here the measures are only successful if they are not affected by morphodynamics at all) to "moderate dynamics accepted" in the lowering area where natural floodplain processes are accepted and desired unless flood retention is not affected. Secondly, identifies which morphodynamic processes might harm the EaRs' functionality and what might be the structural damages likely to occur in the course of these processes. Finally, an overview about potential consequences related to the structural damages is provided. At this point it

Table 4-6: Table derived for preliminary hazard analysis for the case study region Neuenburg am Rhein.

Number	*Element at Risk*	planned functionality: purpose	planned functionality: state	planned functionality: accepted dynamics	hazards: morphodynamic processes	potential structural damages: description	potential consequences: CSH, economic, ecological - preliminary overview	severity
1	*old harbour*	touristic • place for boats	• open	moderate	• sedimentation of particles	• siltation of harbour	• cessation of touristic attraction: • losses due to lack of economic driver (sales, profits..) • costs of maintenance	moderate
2	*gravel island*	touristic • recreation, view	• vegetation • open gravel	moderate	• sedimentation of particles • erosion of vegetation • erosion of gravel	• siltation • destruction of willows • destruction of island	• cessation of touristic attraction: • losses due to lack of economic driver (sales, profits..) • costs of maintenance	high
3	*side arm*	touristic • recreation, bathing flood protection • location for inlet / EaR 6	• open • free flow	low	• sedimentation of particles	• siltation and drying of side arm • siltation of inlet of EaR 6 • damages see EaR 6	• cessation of touristic attraction: • losses due to lack of economic driver (sales, profits..) • costs of maintenance • costs of maintenance	moderate
4	*Rhinegardens* *sun bathing area* *theater* *restaurants*	touristic • recreation • recreation, cultural events • recreation	• as designed • as designed • as designed	no dynamics accepted	• erosion, sedimentation • inundation, erosion • inundation, erosion	• destruction or siltation of lawn • water damage, material destruction • water damage, material destruction	• cessation of touristic attraction: • stop of touristic attraction, also dependent on overall conditions • losses by lack of economic driver (sales, profits..), material losses • losses by lack of economic driver (sales, profits..), material losses eventually maintenance and reconstruction investments necessary	high
5	*lowering area*	flood protection • reduction of flood peak and floodwave velocity touristic • recreation	• floodplain forest	moderate	• sedimentation of particles • erosion of young vegetation in early project stage ↓ *can cause* • reduction of retention effect →	• siltation of lowering area • destruction of upcoming vegetation ↓ *can cause* • damages related to flooding	• costs of maintenance • costs of maintenance ↓ *and/or* • losses due to river flood disasters nearby and downstream	highest
6	*side channel*	flood protection • flush out of suspended sed. (sedimentation control) • connectivity main channel - flood plain - interstitial touristic • recreation	• open, free flow • crit. Q capacity met	moderate	• sedimentation of particles • sedimentation of particles • sedimentation of particles ↓ *can cause* • reduction of retention effect →	• siltation of side channel • siltation of in-/ outlets • inappropriate floodplain vegetation ↓ *can cause* • damages related to flooding	• costs of maintenance • costs of maintenance • costs of maintenance ↓ *and/or* • losses due to river flood disasters nearby and downstream	highest
7	*main channel*	flood protection flood discharge touristic • recreation	• open, free flow • crit. Q capacity met	low	• destabilization of armour layer, river bed erosion, initialization of bed load transport	• increase of sediment transport can lead to damages of EaR 1 - 6 (see EaR 1 - 6)	• costs of maintenance • losses due to damages at EaR 1 - 6 (see EaR 1 - 6)	very high

should be underlined that loss assessment is a very challenging task and requires a detailed analysis with expertise in economics and insurances. As the focus of the present study is placed on the Hazard Analysis of fluvial morphodynamics which represents a very complex field of research itself, an accurate loss listing cannot be claimed and is recommended to be carried out in separate studies in detail. Nevertheless, Table 4-6 is of great importance to give a first idea of consequences which are likely to occur in the case the river restoration project fails and to raise the awareness to the risk itself. This is further necessary in order to determine and understand the severity of morphodynamic hazards and related structural damages affecting the river design.

The EaRs are further classified in ranges of risk severity given that morphodynamic hazards affect them.[1] Highest risk severity, or in other words, highest priority for reliability, concern the measures for flood protection: lowering area and side channel: The failure of these flood protection measures affects the success of the Integrated Rhine Programme and must be prevented under all circumstances; e. g. structural damages such as severe sedimentation processes and a reduction in retention volume must be countered immediately by maintenance activities in order to avoid the occurrence of additional damages and consequences which are related to flood disasters.

Not less important is the morphodynamic state of the main channel. The river measures Neuenburg are based on the assumption of a stable armour layer and negligible bed load transport in the main channel as it is the case nowadays (Scenario A). The possibility that the EaRs 1 to 6 are affected by bed load is very low given a stable armour layer. However, in the case the armour layer reaches a critical state of stability which is likely to occur at high flood events (~ 3600 m^3/s or higher), coarse material can be released from the river bed initializing bed load transport. This can lead to widespread siltation processes and increased flow forces endangering the sustainability of all river measures.

High risk severity from the touristic point of view concern the EaR “gravel island” and “Rhinegardens”. The gravel island is supposed to be the main attraction point for recreation and touristic purposes. In the case of its erosion or its severe sedimentation, the region might be less frequented by people what, in turn, could endanger the success of the recreation project. Consequently, profits by the Rhinegardens and the municipality of Neuenburg might decrease dramatically leading to high financial economic losses. Given that Rhinegardens, its theatre and restaurants were directly affected by morphodynamics (inundation and erosion/destruction), high material losses would occur in addition. Costly maintenance and monitoring activities would be required in order to prevent the measures’ failure.

Moderate risk severity concerns the side arm between gravel island and Rhinegardens as well as the old harbour. On the one hand, both EaR are important for the overall success of the recreation measures. Moreover, the side arm is crucial for the flow connectivity between main channel and side channel/lowering area as the inlet of the side channel is located at its downstream end. On the other hand, losses related to structural damages are supposed to be lower in comparison to the lowering area, side channel and Rhinegardens.

[1] The term “risk severity” does not involve probabilities of occurrence at this early stage of the Risk Management framework. Probabilities are used in the risk ranking/evaluation phase only after the completion of the hazard assessment.

5 CASE STUDY UPPER RHINE: CALIBRATION OF THE HAZARD ANALYSIS APPROACH AND PLAUSIBILITY CHECKS

Based on the conducted System Definition and Hazard Identification, it is now aimed to apply and test the Hazard Analysis methodology as proposed in Chapter 3.4 and Figure 3.21 exemplarily on the case study region. A common shortcoming occurring in river modelling studies is lack of data which have to be overcome and completed. This problem is apparent also in the case study region. Therefore, a data generation procedure is derived at first in Chapter 5.1. Using the so enhanced data base, it is enabled to calibrate the new 1D/3D model approach with field data which is presented in the subsequent Chapter 5.2. Finally, prior to its application on the future river plannings, the calibrated approach must be extensively tested on its performance in order to assure that it can reflect the potential behaviour of natural, vegetated gravel-bed rivers sufficiently well. For this purpose, field measurements and observation of a recent flood event in the case study area are used. The plausibility check and the validation procedure are presented in Chapter 5.3.

5.1 AVAILABLE INFORMATION ON DISCHARGE AND TOPOGRAPHY AND RELATED PREPARATORY WORKS

5.1.1 Determination of morphodynamic relevant discharges

To estimate morphodynamic processes in the study area, it is required to investigate those discharges which are able to impact the morphology. Often not only the extreme discharge events are important for long-term fluvial development but much more events of mean magnitude occurring frequently during the year. A widely used concept is the channel-forming discharge concept (see Chapter 3.1.2.1). For rivers in equilibrium, the $Q_{c\text{-}f}$ is usually assumed to be around $Q_{1\text{-}2}$ or bankfull discharge, Q_b. However, this concept is not directly applicable to the morphodynamic analysis of the study reach Neuenburg. First of all, the parameter bankfull discharge ($Q_b \sim HQ_{1\text{-}2}$) cannot be taken into account since, due to the bed incision reported, the former floodplains are not inundated and the river discharges completely in the main channel until a 200 years' event. Secondly, the River Rhine exhibits low water conditions statistically at 300 days per year due to the weir operation Kembs. In combination with the regulated morphology, reduced sediment regime from upstream as well the armour layer which remains stable at mean and frequent discharges, this frequent discharge usually shows no impact on morphodynamics over this statistical period of 300 days. Thus, in order to guarantee the system's functionality over the long-term, the question must be answered whether higher and less frequent events are able to cause hazardous processes instead.

In the present case, a reasonable alternative to the use of a single $Q_{c\text{-}f}$ is the investigation of a range of discharges, e. g. from frequent mean yearly discharges towards moderate flood events and extreme events. This procedure allows to detect lower and upper boundaries of flow forces likely to occur in

the study reach and based on that, enables a more reliable estimation of potential hazards under the given conditions. However, the main limiting factor for the determination of morphodynamic relevant discharges is the data basis since only those discharges can be used for analysis which have been measured and documented. Field data are commonly scarce in fluvial analysis, so in the present study area where last field measurements have been carried out 10 years ago only. Discharge information is provided by the duration curve at the gauging station Hartheim (Rhine-km 214.0), see also Figure 4.14, water level information provided by GWD Südlicher Oberrhein (2000) based on the gauging stations Rheinweiler (Rhine-km 186.2) and Hartheim and as well as field observations documented by Regierungspräsidium Freiburg (2007) along the Rhine section Weil-Hartheim during the flood event of August 2007. Available water level information is listed in Table 5-1. Based on the foregoing discussion it was decided to use this information as follows:

Table 5-1: Available information on water levels for the study area Neuenburg/Upper Rhine.

Q [m³/s]	return period or flood magnitude	date	source	reference
671	9 days per year	2.11.1998	calibrated on measurements	GWD Südl.Oberrhein / Hochrhein, 2000
1587	1 year event	4.11.1998	calibrated on measurements	GWD Südl.Oberrhein / Hochrhein, 2000
2520	high flood with peak 3600 m³/s	14.05.1999	calibrated on measurements	GWD Südl.Oberrhein / Hochrhein, 2000
3040	high flood event	29.05.1994	calibrated on measurements	Dittrich et al., 2005
3300	high flood event	9.08.2007	field observations, no measurements	Regierungspräsidium Freiburg, 2007
4500	200 years event	hypothetical event	optimized estimation	Dittrich et al., 2005

The water level data of the discharges 671 m³/s (here named “Q1”), 1587 m³/s (“Q2”) and 4500 m³/s (“Q3”) are used for morphodynamic hazard analysis in order to cover the upper and lower boundaries of hydraulic forces from mean events (Q1) to a (hypothetical) extreme event (Q3). Since the events 2520 m³/s, 3040 m³/s and 3300 m³/s are well documented by water level measurements and field observations they will be explicitly used for model validation and plausibility checks and are therefore named “Q4”. Last but not least, the fact that low water conditions occur at 300 days a year resulting in mostly inactive morphodynamics during that period will be maintained as important background information.

5.1.2 Data availability and developed procedure for data generation

Before the Hazard Analysis, it must be taken into account that over the period for which data are available, the study area was subjected to morphological changes with impact on flow resistance: The gravel island which is located today at Rhine-km 199.330 – 199.750 did not exist in its current extent until the year 1998, but developed only during and after the flood of May 1999. After that, vegetation has grown up and willows are stabilizing the island until today. Therefore the water level and topography data was checked for consistency first, prior to the Hazard Analysis.

For the study area Neuenburg numerous data sets were available for the ancient, actual and planning state. The complete list of these data used is provided in Appendix A.2. For clarity, a summary and overview of available discharge and topography information is provided in Table 5-2. Table 5-2 reveals that the data sets are very heterogenous for the study site what makes both model calibration and use rather difficult. Data cover different time periods starting in the 90ies until the year 2004 while discharge information is not consistent with available topography data. Water level measurements only exist for the situation *before* the flood 1999 (without gravel island) but high-quality topography data is available only for the year 2004 via a high-resolution digital elevation model ("DEM2004"). In order to perform the Hazard Analysis for the planning state, the models must be calibrated for the complete area of investigation. Since neither the calibration and nor the hydrodynamic simulations cannot be performed directly with the available information due to inconsistency, a procedure was developed to use the available data and to generate new data via preliminary calculations. In addition to the treatment of data lacks, the 3D hydrodynamic model has some requirements to be considered during preprocessing, e. g. the boundary conditions provided by 1D water level calculations.

Table 5-2: Availability of data on topography and discharge and required data (grey) for Hazard Analysis (Q1 = 671 m³/s, Q2 = 1587 m³/s, Q3 = 4500 m³/s, Q4 = 3040 m³/s).

availability	topographical data and year of survey		discharge information	advantage	disadvantage
	site description	data format and geometry extent			
available	*prior to 1999* main channel without gravel island	cross-sectional profiles (resolution ~ 200 m, Rhine-km 198.000 – 201.000)	a) measurements (Q1, Q2, Q4) b) 1D calculations (Q3)	hydraulic data available	topographical information out of date, low resolution
available	*2004* main channel with gravel island with vegetation	digital elevation model (resolution ~ 1 m, Rhine-km 198.410 – 200.310)	no data	actual topography	no hydraulic data
available	*PLAN incomplete* main channel without gravel island without Rhinegardens with lowering area	cross-sectional profiles (resolution ~ 200 m, Rhine-km 198.000 – 201.000)	1D calculations (Q3)	hydraulic data available for Q3	a) topographical information out of date, low resolution b) Rhinegardens not included
required	*ACT*	extended DEM 2004 (Rhine-km 198.410 – 201.000)			
required	*PLAN* main channel with gravel island with vegetation with Rhinegardens with lowering area	DEM 2004 (Rhine-km 198.410 – 201.000) with gravel island with Rhinegardens with lowering area	a) start water levels (Q1, Q2) b) water levels (Q1, Q2, Q3)		

The procedure follows a stepwise calculation of cases according to the availability of data and complexity of the river reach. The cases, used input data, new generated data and related objectives are provided in Table 5-3. It was decided to produce one basic elevation grid for all 1D cases covering the area of both the actual state and the planning state: *Rhine-km 198.410 – 200.970*. In this way deviations and uncertainties in the results due to different grids and resolutions can be minimized. As

basic grid the digital elevation model 2004 was chosen. As it represents the actual state of the year 2004 (main channel with gravel island and vegetation) it must be modified for each case:

The first 1D case is called ACT1998 (actual state up to 1998). This case is used to calibrate the available discharge measurements for the topography present at the date of the measurements (1998 and before, main channel without gravel island). The topography of 1998 was gained by modification of the DEM2004 in two ways. First, the gravel island was deleted from the grid according to the old cross-sectional profiles. Second, this modified DEM was extended 680 m downstream from its original downstream end (Rhine-km 200.310, see Table 5-2) to the downstream end of the retention area in the planning state (Rhine-km 200.970). In this way, the grids cover the same area Rhine-km 198.410 – 200.970 in the actual state and the planning state. The second case (year 2000) represents the state ACT2000 comprising the stage of the Rhine channel directly after the gravel island has been deposited (non-vegetated gravel island). For this case it must be assumed due to data lacks that the topography of 2000 can be represented by the DEM2004 without modification. The used roughness has been gained by calibration in the first step (ACT1998). The third case (year 2004) covers the situation “main channel with vegetated gravel island” and is called ACT2004_1D. For this year, the actual topography is available (DEM2004). Information about vegetation cover on the island can be obtained by aerial photography of this year. The inundation zones and water levels calculated for this case are then used as input data for the 3D model.

Based on this preliminary work, the 3D calculations can be carried out for the actual state ACT2004_3D (gravel island with vegetation), see Table 5-3. To conduct the Hazard Analysis for the 3D planning state (PLAN3D), the planning stage is calculated as 1D case (PLAN1D) with HEC-RAS first, prior to the 3D model (PLAN3D). For details concerning the planning state please refer to Chapter 4.3.2.3.

Since each case requires preprocessing and postprocessing techniques, several steps are required in order to convert the modelling tools for their use in the Hazard Analysis. Table A.3.1, Appendix summarizes the preprocessing and simulation tools used per case.

Table 5-3: Data generation procedure: white – preliminary calculations for data base improvement, grey – originally intended calculations for Hazard Anaylsis.

step	case	site description	topographical data	modelling approach	hydraulic input data Q1 = 671 m³/s, Q2 = 1587 m³/s Q3 = 4500 m³/s, Q4 = 3040 m³/s	information about roughness and resistance	objectives
1	ACT1998	main channel without gravel island	extended DEM2004 without gravel island	1D	start water levels Q1, Q2, Q3, Q4 Dittrich et al. (2005)	via calibration	calculations and calibration 1D model
2	ACT2000	main channel with gravel island	extended DEM2004	1D	start water levels Q1, Q2, Q3, Q4 Dittrich et al. (2005)	roughness of 1), look-up tables	estimation hydraulic impact of gravel island
3a	ACT2004 1D	main channel with gravel island with vegetation	extended DEM2004	1D	start water levels Q1, Q2, Q3, Q4 Dittrich et al. (2005)	roughness of 1), look-up tables	a) estimation hydraulic impact gravel island with vegetation b) calculation of water levels as input data for 3D case 3b
3b	ACT2004 3D	main channel with gravel island with vegetation	extended DEM2004	3D	Q3, Q4 water levels of 3a)	via calibration, vegetation parameter Dittrich et al. (2005)	calibration, validation and quality check
4a	PLAN1D	main channel with gravel island with vegetation with Rhinegardens with lowering area	modified DEM2004 (extended DEM2004 with gravel island with Rhinegardens with lowering area)	1D	a) start water levels of planning stage, Q3, Dittrich et al. (2005) b) start water levels for Q1 and Q2 not available	roughness of 1), look-up tables	calculation of water levels Q1, Q2 and Q3 as input data for 3D case 4b
4b	PLAN3D	main channel with gravel island with vegetation with Rhinegardens with lowering area	modified DEM2004 (extended DEM2004 with gravel island with Rhinegardens with lowering area)	3D	a) start water levels of planning stage for Q3 Dittrich et al. (2005) b) start water levels for Q1 and Q2 to take from 4a)	see 3b), chosen acc. to plannings, look-up tables	Hazard Analysis

5.2 CALIBRATION PROCEDURE

The present chapter introduces the two models used and reports the calibration procedure and obtained results for the 1D model (Chapter 5.2.1) and for the 3D model (5.3.2). Furthermore, stability approaches are chosen according to the properties of each EaR in Chapter 5.2.3.

5.2.1 Calibration of the 1D model and preliminary calculations

5.2.1.1 Introduction and model description

The 1D water level calculations for the cases ACT1998, ACT2000, ACT2004_1D and PLAN1D are performed with the modelling tool HEC-RAS 3.1.3 (USACE, 2005). HEC-RAS 3.1.3 supports one-dimensional steady and unsteady hydraulic calculations for natural and constructed channels. The steady hydraulic calculations which are performed in the present study are based on the solution of the one-dimensional energy-equation (see Eq. 5-1) combined with the iterative procedure called the standard-step method. Energy losses are evaluated by friction losses and contraction/expansion losses.

$$h_2 + z_2 + \frac{\alpha_2 \cdot u_2^2}{2g} = h_1 + z_1 + \frac{\alpha_1 \cdot u_1^2}{2g} + h_e \qquad 5\text{-}1$$

with h_1, h_2 = water depth at cross section, z_1, z_2 = elevation of the main channel bed, α_1, α_2 = velocity weighting coefficients, u_1, u_2 = flow velocities, h_e = energy head loss.

In HEC-RAS, roughness is quantified by the Manning's equation as bulk approach with the consequence that Manning's n summarizes the roughness effects caused by several features in one single parameter, for example surface roughness (bed and bank material), form roughness by macrostructures, size and shape of the channel and vegetation. In HEC-RAS 3.1.3 it is possible to vary the Manning's coefficient within a cross-section in the horizontal direction and between each cross-section. This is necessary to indicate roughness variations due to bank vegetation or vegetated islands. The selection of an appropriate value for n is very significant for the accuracy of the computed water surface profiles. Usually, the Manning's values are determined via calibration and via look-up tables.

In the present study, the case ACT1998 is used for model calibration since water level measurements are only available for this topographical state (see Table 5-2). However, Manning's roughness can vary distinctly according to the water level and discharge, respectively. Therefore, calibration is performed for each discharge event Q1, Q2, Q3 and Q4 separately. The roughness calibrated in ACT1998 for each discharge is then transferred to ACT2000, ACT2004_1D and corresponding areas in PLAN1D. Since these latter cases exhibit additional roughness pattern caused by the gravel island, the related Manning's values must be estimated via literature tables and the available aerial photographs. Regarding Table A.4.1 (Appendix), a wide range of Manning's values can be used for a given river section leading to large variations in water level calculations. In the present study, a range of reasonable Manning's n values was estimated for each discharge and case according to Table 5-4, called n_{min} and n_{max} in order to show the range of possible water surface elevations and to reveal potential uncertainties.

To enable water surface calculations with HEC-RAS, the elevation data of the actual and the planning state need to be converted into a HEC-RAS friendly format. The cross-sections for the programme are generated with the GIS tool ArcView 3.2a (ESRI, 2000) and the HEC-RAS extension HEC-GeoRAS 3.1 (USACE, 2002) with a resolution of about 10 m spacing between the cross-sections. For the actual and planning state the same spacing and location of the cross-sections are chosen in order to minimize deviations und uncertainties due to the different data base.

5.2.1.2 Results of 1D calibration

The Manning's n values calibrated for the study area Neuenburg and ACT1998 from Rhine-km 198.410 – 200.970 as well as the start water levels for the four discharges are listed in Table 5-4. Furthermore, Table 5-4 presents the range of the calibrated Manning's values as well as the mean value for the river course. A comparison between the calibrated roughness and the look-up table (Table A.4.1, Appendix) shows that the calibrated roughness is in a reasonable order of magnitude for the given river morphology, bed structure, vegetation types and vegetation distribution.

Table 5-4: Calibrated Manning's roughness coefficients for the case ACT1998 (without gravel island) and used start water levels for the simulations (source: **) optimized estimation of Dittrich et al., 2005).

Q [m³/s]	start water level [m a. s. l.]	calibrated Manning's n [s/m$^{1/3}$]			
		main channel		left and right banks	
	Rhine-km 200.970	mean	range	mean	range
671	207.09	0.024	0.02 – 0.035	0.024	0.02 – 0.035
1587	208.95	0.025	0.02 – 0.036	0.027	0.02 – 0.036
3040	211.45	0.032	0.027 – 0.04	0.034	0.024 – 0.04
4500	213.73**)	0.036	0.029 – 0.05	0.046	0.041 – 0.05

Figure 5.1 shows the results of the calibrated 1D calculations versus the measured values (Q1 = 671 m³/s, Q2 = 1587 m³/s, Q4 = 3040 m³/s) and the 1D calculations of Dittrich et al. (2005) for Q3 = 4500 m³/s, respectively. It can be observed that the calibrated water levels match the measured values well, the deviations are in an acceptable range. The differences between calibration values and calculated values reach 1 – 3 cm for Q1, 1 cm for Q2, 0 – 5 cm for Q3 and 0 – 2 cm for Q4.

Moreover, the calibration process reveals as expected that the roughness impact changes distinctly with discharge and water level. For Q1, the best fit of measured and calculated water levels is obtained for a constant roughness over the cross-section while roughness increases with rising discharge and differences of n between banks and bed occur. This outcome is supported by Figure 5.2 which shows the calculated 1D water levels and inundated areas exemplarily for Q1, Q2 and Q3. Apparently, the influence of the vegetated banks is low at Q1 but increases with water level: the higher the water level, the more vegetated areas including groyne fields and banks are flooded. This relationship is in close agreement with field observations.

Given these outcomes, it can be concluded that the calibration of the 1D model was performed to a satisfying degree. The topography data and roughness chosen for the study area can reflect the current

morphologic situation adequately and the calibrated Manning's values are in a reasonable order of magnitude.

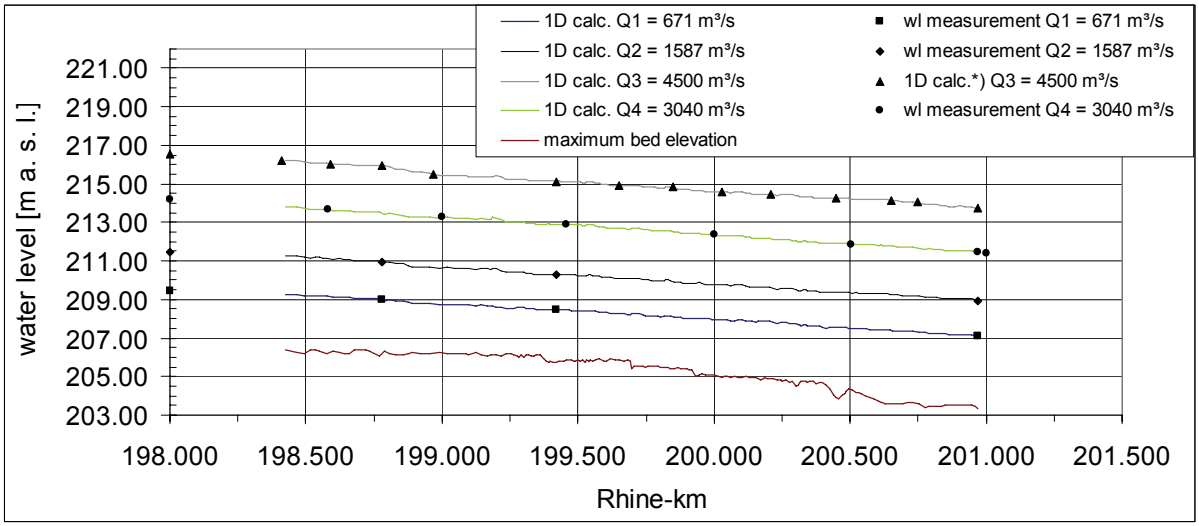

Figure 5.1: Calibrated water levels for the discharges of investigations and measured water levels for the case ACT1998 (without gravel island) and measured water levels.

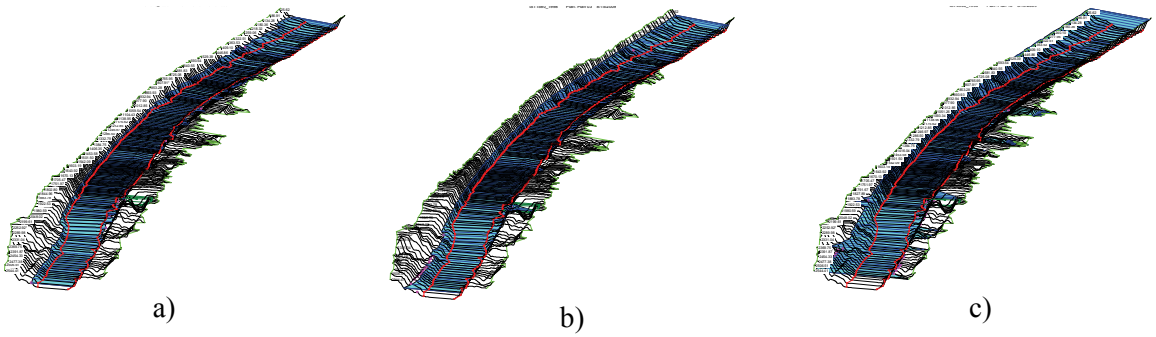

Figure 5.2: 3D view of the water table elevation computed with the 1D model for a) Q1 = 671 m³/s, b) Q2 = 1587 m³/s, c) Q3 = 4500 m³/s.

5.2.1.3 Preliminary 1D calculations for input data generation

1D calculations for the case "main channel, non-vegetated gravel island" (ACT 2000)

In this chapter the results of the 1D calculations for the case "Rhine with gravel island without vegetation" (ACT2000) are presented. The start water levels at the downstream end and the Manning's roughness used for this case are listed in Table 5-5. Start water levels and the roughnesses for the main channel and the vegetated banks are provided by the calibration case ACT1998. ACT2000 is investigated to quantify the roughness impact of the gravel island on the water level for the 1D calculations, 3D model calibration and validation, respectively. As afore mentioned, lower and upper boundaries of Manning's n are applied for each discharge in order to indicate the scatter and outer boundaries of water levels likely to appear in the study section dependent on the chosen roughnesses. The lower boundary is determined by the case "n_{min}". Here, the roughness is kept stable throughout the river bed / main channel and the roughness impact of the gravel island is assumed to be determined only by its geometry. Subsequently no further form roughness is added. The upper boundary is determined by the case "n_{max}" which considers an additional form roughness for the gravel island. The roughness values are estimated according to the look-up table (Table A.4.1, Appendix) and were kept constant for the four discharges in a first assumption.

Table 5-5: Manning's roughness coefficients for the case ACT2000 (with gravel island) with n_{min} and n_{max} selected as outer boundaries for the non-vegetated gravel island.

Q [m³/s]	Manning's n [s/m$^{1/3}$]			
	main channel	left and right banks	gravel island (Rhine-km 199.330 – 199.750)	
	mean	Mean	n_{min}	n_{max}
671	0.024	0.024	0.024	0.04
1587	0.025	0.027	0.025	0.04
3040	0.032	0.034	0.032	0.04
4500	0.036	0.046	0.036	0.04

The results of the water surface calculations are shown in Figure 5.3 and Figure 5.4 exemplarily for Q1 = 671 m³/s and Q3 = 4500 m³/s (for Q2 and Q4 please refer to Appendix A.5). For the smaller discharges Q1 and Q2, the gradient is more or less constant given that the geometry variation is rather low along the river course and roughness features do not explicitly vary for theses discharges. The calculations for the extreme event Q3 show steeper gradients in the upstream and the downstream part of the study area and moderate values in the middle section. It can be assumed that the lower gradient in the middle part is caused by additional inundated floodplain areas with higher roughness due to vegetation. The cross-sectional variations in combination with additional vegetation resistance lead to decreasing flow velocities and to lower gradients.

A comparison of the water levels for n_{max} and n_{min} shows that the choice of the Manning's value for the gravel island (Rhine-km 199.330 – 199.750) influence the calculated water levels only marginally.

Only slight water level rises can be observed for n_{max} yielding a maximum increase of 2 cm locally. This is reasonable since water depths in the main channel reach 2.5 m (at Q1) up to more than 9 m at the extreme event Q3 to the effect that hydraulic influence of the island becomes negligible.

However, it turns out that the 1D model HEC-RAS calculates rapid and not fully reasonable changes in the water table along the river course, see Figure 5.3 and Figure 5.4. Since the geometry is quite homogenous, the 1D model should be capable to perform sufficiently well. The reason for these water level changes is assumed to be found in the small cross-section distances in the HEC-RAS geometry of around 10 m which have been chosen to achieve a detailed representation of the channel geometry. Especially in the vicinity of the old harbour (Rhine-km 198.180) where the cross-sectional widening with vegetation is represented in detail in the grid, strong water level changes can be

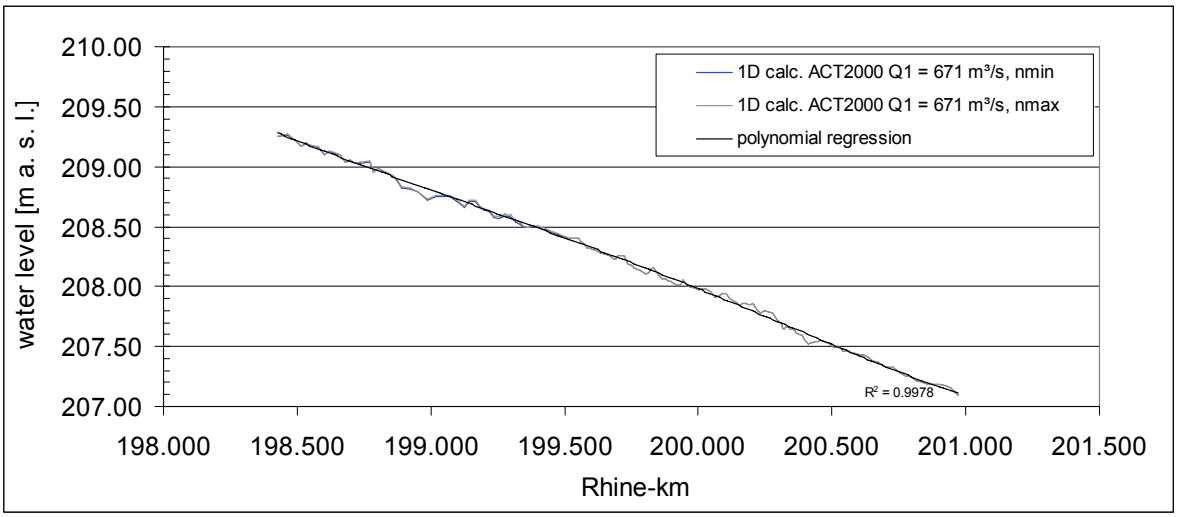

Figure 5.3: Calculated water levels for Q1 = 671 m³/s for the case ACT2000 with n_{min} and n_{max} selected as outer boundaries for the non-vegetated gravel island.

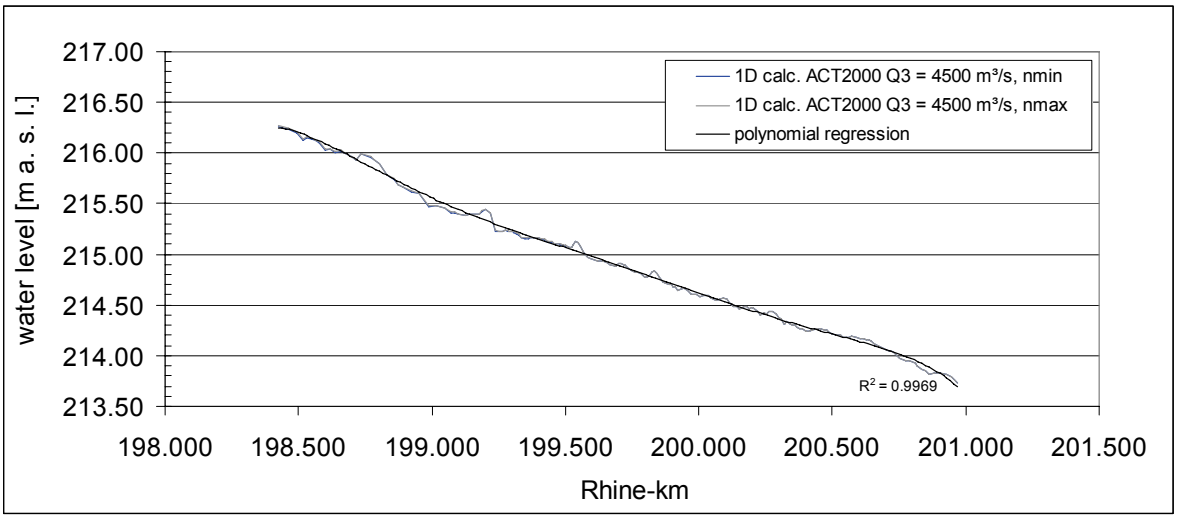

Figure 5.4: Calculated water levels for Q3 = 4500 m³/s for the case ACT2000 with n_{min} and n_{max} selected as outer boundaries for the non-vegetated gravel island.

observed. However, it appears that the 1D model cannot in detail predict the water level at this high geometrical resolution. This assumption was supported by test calculations with a coarser grid carried out in this study that provoked a water level smoothening. Therefore, a partial regression line was calculated for each water level to smoothen the water level graphs. The regression lines and corresponding coefficients of determination are provided for each 1D water level graph throughout the thesis.

1D calculations for the case "main channel with vegetated gravel island" (ACT 2004)

In this chapter, the results of the 1D calculations for the River section with gravel island and vegetation are exemplarily presented for Q1 = 671 m³/s and Q3 = 4500 m³/s, respectively (for Q2 and Q4 please refer to Appendix A.5). The roughness values for the river bed and the banks have been taken from the calibration case ACT1998. Moreover, a range of realistic Manning's values has been estimated from look-up tables to evaluate the roughness of the gravel island with willow stands as reliably as possible. The case n_{min} takes the lower boundary roughness for willows into account while the case n_{max} takes the upper boundary roughness for willows into account. Concerning n_{max}, it was assumed that the gravel island is totally covered by dense willows. The expansion of the vegetated surface was estimated by the topography data as well as by the aerial photographs of the year 2004. The Manning's values for the calculations are shown in Table 5-6, the results of the 1D calculations for Q1 and Q3 in Figure 5.5 and Figure 5.6.

The shapes of the water level distributions are comparable to the case ACT2000: For the smaller discharges, the gradient remains more or less constant along the river course while the water level of the extreme event shows a steeper gradient in the upstream and the downstream part of the study area and moderate values in the middle section. This likely due to several inundated areas with higher roughnesses (vegetated banks) and more cross-sectional variations at this discharge which cause decreasing flow velocities and lower gradients.

Moreover, as similar to the previous case, the choice of Manning's roughness for the vegetated gravel island seems to be relatively small for all discharges. The water level for n_{max} ("upper boundary for willows", see Table appendix) rises in comparison to the case n_{min} ("normal stand of willows") up to 2 cm near the gravel island and upstream. As for the case ACT2000, rapid water level changes have been calculated by the 1D model so that partial regression lines for water surface smoothening have been computed in addition.

Table 5-6: Manning's roughness coefficients for the case ACT2004 (with vegetated gravel island) with n_{min} and n_{max} selected as outer boundaries for the vegetated gravel island.

Q [m³/s]	Manning's n [s/m$^{1/3}$]			
	main channel	left and right banks	gravel island (Rhine-km 199.330 – 199.750)	
	Mean	mean	n_{min}	n_{max}
671	0.024	0.024	0.06	0.12
1587	0.025	0.027	0.06	0.12
3040	0.032	0.034	0.06	0.12
4500	0.036	0.046	0.06	0.12

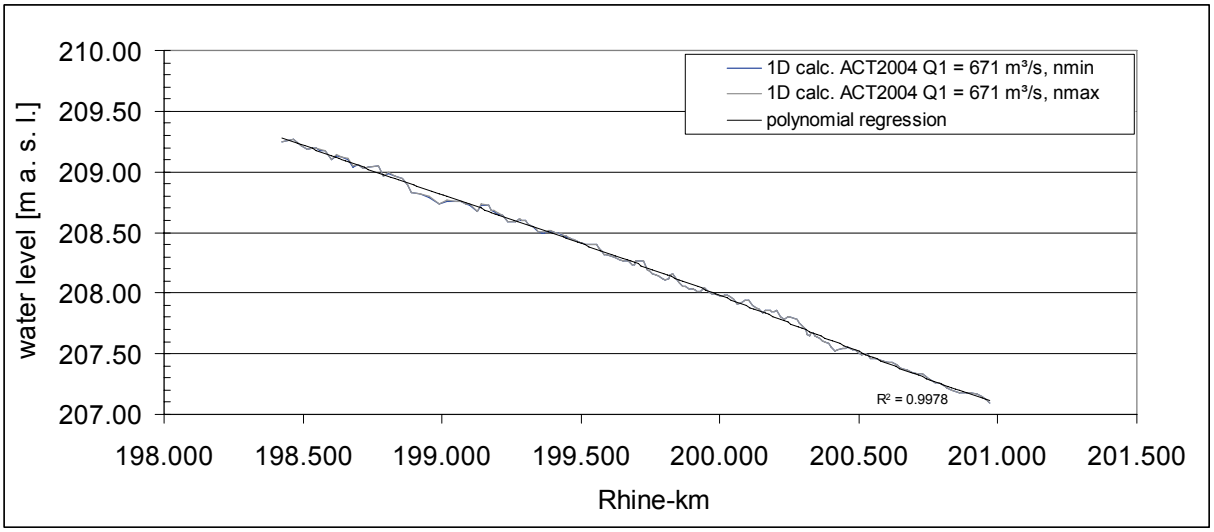

Figure 5.5: Calculated water levels for Q1 = 671 m³/s for the case ACT2004 with two roughness values indicating the outer boundaries for the vegetated gravel island.

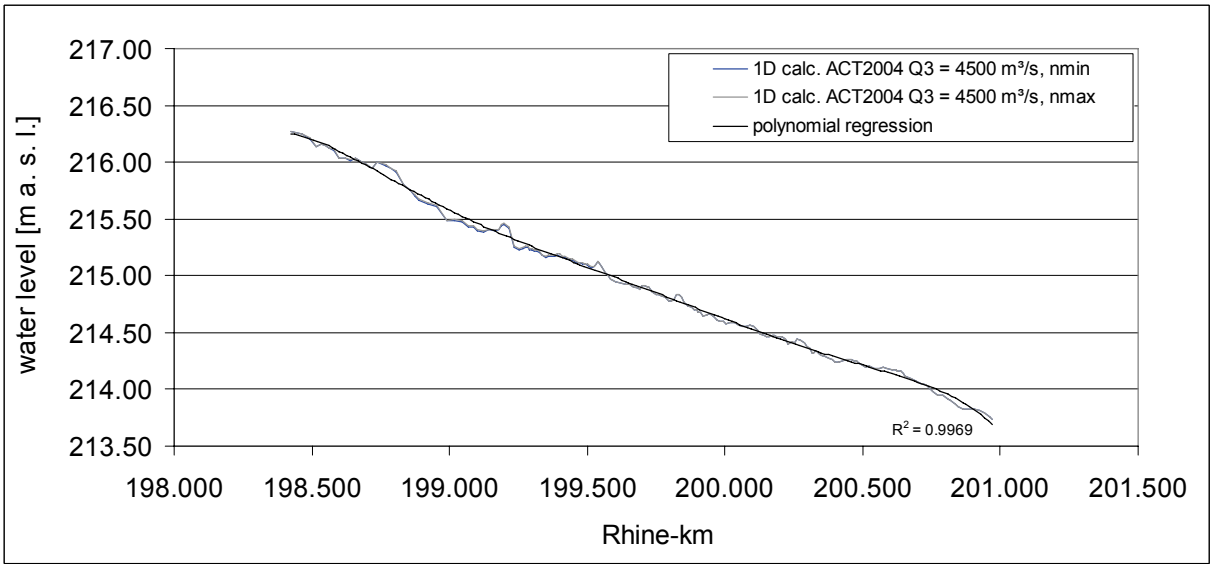

Figure 5.6: Calculated water levels for Q3 = 4500 m³/s for the case ACT2004 with two roughness values indicating the outer boundaries for the vegetated gravel island.

5.2.2 Calibration of the 3D model

The present chapter presents the results of the calibration of the 3D numerical model from Rhine-km 198.410 – 200.910 in the actual state ACT2004. First the grid which is used for the 3D simulations is described. Afterwards, the parameters of roughness and vegetation resistance required for the 1D water level and the 3D calculations are presented. In the last chapter, the results of the simulations are visualized and discussed in detail. The extreme event Q3= 4500 m³/s was chosen for calibration since for this discharge detailed data are available in literature. Dittrich et al. (2005) performed 1D hydrodynamic numerical modelling for water level estimations and further reported flow velocities, water depths and bed shear stresses for the Q_{200} = 4500 m³/s along the channelized river section Weil-Breisach in the actual state. This information can well indicate orders of magnitude of flow forces likely to occur in the study reach and was therefore selected for calibration of the present 3D model.

5.2.2.1 Introduction and model description

In the present study, the 3D numerical model SSIIM 2.0 (Olsen, 2008) is used for the estimation of morphodynamic development in the river reach Neuenburg. This 3D model SSIIM (Sediment Movement in Intakes with Multi-Block option) has been developed at the Norwegian University of Science and Technology in Trondheim mainly for river/environmental/hydraulic/sedimentation engineering. The programme solves the RANS equations (see Eq. 3-7, 3-8) with the k-ε model (see Eq. 3-10) and the three constants recommended by Rodi (1984) for turbulence closure on a three-dimensional non-orthogonal grid. SSIIM uses the wall law (Schlichting, 1979) for rough boundaries according to Eq. 3-11. For discretization the finite volume method is used in combination with the power-law scheme or the second order upwind scheme. The SIMPLE method is used for pressure coupling and an implicit solver is calculating the velocity field within the geometry.

The main strength of SSIIM compared to other tools used in river engineering is the capability of modelling the flow field in three dimensions including a physically based approach for the flow resistance due to vegetation. The vegetation is considered as vertical stems producing a form drag calculated by the classical drag force formula for flow around a cylinder, see Eq. 3-31. The drag force is introduced as sink term into the RANS equations. Moreover, a wetting and drying-algorithm is implemented in the version SSIIM 2.0. Using this algorithm the grid can adapt to water level changes automatically which is required for example in time-dependent calculations and scenario calculations where several discharges are investigated. An unstructured grid is used in combination with the wetting-drying algorithm which enables the modelling of high complex geometries. However as aforementioned, free-surface calculations together with wetting-and-drying-algorithms on an unstructured grid in three dimensions for natural river sections with vegetation are still a field research. To improve numeric stability, a fixed water level boundary condition is used in the present study which requires a first approximation of the water level in advance. The water level of each case is pre-estimated with the 1D model HEC-RAS 3.1.3.

5.2.2.2 Preprocessing and grid generation

Generating an unstructural grid which guarantees numerical stability is a complex task. The model SSIIM requires information about topography, water levels, maximal flood inundation extent, roughness and vegetation distribution in a SSIIM friendly format. To achieve these requirements,

preprocessing procedures have been developed in the present study. Both the development of the procedure as well as first 3D test calculations have been carried out during a research period at the Norwegian University of Science and Technology in Trondheim.

Thanks to the wetting-drying algorithm, the model only needs one numerical grid with topographical information for all discharges of interest. This numerical unstructured grid must comprise the area of maximum inundation of these discharges (in the present study the inundation area of Q3 = 4500 m³/s). It is generated in several steps as shown in Figure 5.7: The maximum inundation area is gained by the 1D calculation of Q3 with HEC-RAS. It is then transformed into a SSIIM friendly geodata ASCII file via a GIS system (ArcView 3.2a plus extension HEC-GeoRAS 3.1). Two further programmes Gridmeister (Bihs, 2007) and AutoCAD (Autodesk, 2002) are used to convert the geodata file and to generate the numerical grid for SSIIM. As the grid in this stage is still a structured

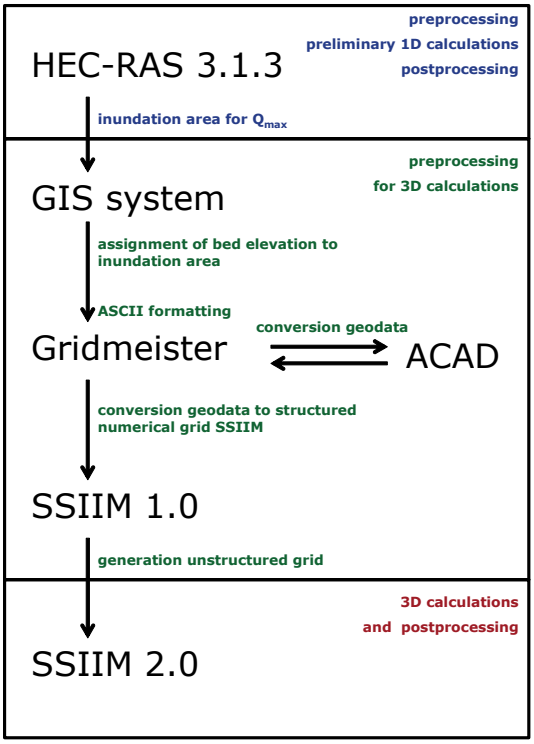

Figure 5.7: Procedure for the generation of the numerical unstructured grid according to the available data base.

one and cannot be used for wetting-and drying calculations, the conversion to the unstructured grid is necessary and performed within the 3D numerical programme.

During test calculations it turned out that the numerical grid from Rhine-km 198.410 – 200.910 was too short for the numerical evolution of the flow. The 3D model SSIIM 2.0 required a distance of several hundreds of grid cells to evolve the boundary conditions at the inflow cross section into a hydraulically reasonable flow field. To reach a hydraulically reasonable flow field in the inflow section at Rhine-km 198.410, it was necessary to extend the numerical grid in the upstream direction. The grid extension was carried out by copying the topographical data of the section 198.410 ~ 198.780 upstream (in front of) the original grid repetitively. In this way, it was assured that the flow field developed according to the topography present in the upstream Rhine section. The grid prolongation covers approximately 750 Rhine-meters. The maximum number of grid cells from Rhine-km

198.410 – 200.910 plus grid prolongation as well as the grid resolution are shown in Table 5-7 yielding a maximum number of 918,000 cells for the computational grid.

Table 5-7: Maximum number of cells in the computational grid and resolution.

direction	maximum number of grid cells	approx. resolution [m]
longitudinal (flow direction)	1020	3.2
horizontal (cross-section)	100	1.5
vertical (depth)	9	1

5.2.2.3 Calibration procedure for bed roughness and vegetation parameters

The 1D model HEC-RAS 3.1.3 uses the Manning's n approach for roughness of banks, bed and vegetation. In the previous part of this study, two water level calculations were carried out per discharge with different vegetation roughnesses on the gravel island to show the range of likely water levels, namely n_{min} and n_{max}. For the calibration case ACT2004_3D it was decided to use the 1D water level calculated for the vegetation density n_{max} in order to take the upper boundary for the water level with vegetated gravel island into account. In contrast to the 1D model in which a bulk roughness approach is used, SSIIM considers the roughness impact by bed material and vegetation separately. The bed roughness is implemented as equivalent sand-grain roughness k_s. For this scenario, k_s was gained by calibration of the 3D model on the 1D water level calculations ACT2004_1D which yields a best fit of bed shear stresses for $k_s = 0.32$ m. This value is in good agreement with the bed roughnesses obtained by Dittrich et al. (2005) for the Rhine section ($k_s = 0.27 – 0.35$ m).

As mentioned above, the flow resistance due to vegetation is modelled separately in the 3D model by means of the drag force approach. To calculate the drag force, SSIIM needs information about the vegetation present in the system, namely the vegetation density (distances between the stems or number of stems per square meter) and the stem diameter. Dittrich et al. (2005) performed 3D hydrodynamic calculations with a similar 3D model for several Rhine sections upstream and downstream of the study reach including lowering areas with floodplain forest in the succession stage. The vegetation parameters were obtained by calibration, sensitivity analysis and field data of detailed vegetation mapping. Since the vegetation structures are representative for the Rhine section area, the vegetation parameters are well suited for the Hazard Analysis of the present study. It is assumed that the vegetation on the French banks can be represented by a natural willow poplar forest in a mature forest stage, see also Figure 4.25. The vegetation on the German banks is represented by a thinned poplar hardwood forest (small pole stage forest, depicted in Figure 4.24). The dense vegetation near the ground of both the German and French banks was considered by increasing vegetation density in the first cell above the bed. Moreover, it is assumed that the vegetation on the gravel island is similar to the vegetation on the French banks which has evolved due to natural succession. The vegetation parameters used in the present study for the river banks and the gravel island as well as the calibrated bed roughness are listed in Table 5-8.

Table 5-8: Vegetation parameters used for the case study sites as well as calibrated bed roughnesses (3D model).

area	resistance and roughness parameters
vegetation	a_x [m] / a_y [m] / d_p [m] / c_{WR} [-]
German banks (Dittrich et al., 2005)	
near bed	3.0 / 3.0 / 1.0 / 1.5
Else	6.0 / 6.0 / 0.5 / 1.0
French banks (Dittrich et al., 2005)	
near bed	3.0 / 3.0 / 1.0 / 1.5
else	6.0 / 10.0 / 1.0 / 1.0
gravel island (present study)	
constant over depth	6.0 / 10.0 / 1.0 / 1.0
bed (present study)	0.32 / sand-grain roughness k_s [m]

5.2.2.4 Calibration results for bed roughness and vegetation parameters

In the following, the calibration results for the combined modelling approach achieved with the values in Table 5-8 are presented and based on the case ACT2004_3D (main channel and gravel island covered with vegetation, Q3 = 4500 m³/s) and the 1D water level ACT2004_1D as boundary condition. The results are compared for plausibility with a study of Dittrich et al. (2005) where the 1D model STAU was used including the vegetation resistance approach of Lindner (1982). Furthermore the stability approaches for the bed and vegetated areas are selected and evaluated.

At first, the depth-averaged velocities u_m computed for the river reach Neuenburg in the present study are compared to the flow velocities (1D) computed by Dittrich et al. (2005). u_m calculated for Neuenburg and the discharge Q3 = 4500 m³/s are shown in Figure 5.8. Mean flow velocities in the main channel yield approximately 3 – 4 m/s and increase up to 5 m/s in the west of the gravel island. The results are in good agreement with the outcomes of Dittrich et al. (2005) who yielded mean velocities of 3.40 m/s for the main channel without gravel island. Apparently, the island represents an obstacle in the flow to the effect that the flow is divided and directed towards the left banks leading to rising flow velocities locally. On the vegetated gravel island and the groyne fields instead, vegetation resistance delays the flow distinctly down to 0.5 – 1 m/s and 0.5 m/s, respectively. Figure 5.9 shows the water depths for the same event calculated with the combined modelling approach. Water depths range from 5 – 6.5 m on the groyne fields and up to 9 – 9.5 m in the main channel. On the gravel island the water depth decreases down to 8.40 m. The old harbour is completely flooded, water depths range between 5 m near the borders and 8.7 m in the lowest areas. Compared to the results of the 1D calculation carried out by Dittrich et al. (2005), the calculations are in a reasonable order of

magnitude: An average water depth for the main channel in this reach of 9.80 m were obtained, however with a different elevation data base.

In addition to the depth-averaged flow field, the 3D approach enables to visualize the depth-dependency of the flow field. The near-bed velocities (flow velocities in the nearest bed cell) computed are subsequently presented in Figure 5.10. It becomes evident that flow velocity is plausibly reduced near the bed in the area of the main channel down to values of 2.5 – 3.0 m/s while in the vegetated areas in comparison to the main channel, near-bed flow velocity decreases only by 0.2 m/s down to 0.4 – 0.7 m/s due to the more uniform vertical velocity distribution apparent in zones with rigid vegetation.

In the 3D approach, the 3D turbulent flow pattern is further used to derive the local bed shear stresses τ_0 in the river which are an important parameter for the prognosis of morphodynamic development and bed stability. The results of these calculations for the extreme event Q3 = 4500 m/s are shown in Figure 5.11 and Figure 5.12. The spatial distribution of bed shear stresses achieved in the present study are clearly visible. In the main channel, bed shear stresses range from 50 to 90 N/m² while near the gravel island where the flow is concentrated bed shear stresses increase up to 110 N/m². In the old harbour, bed shear stresses slow down to values lower than 0.1 N/m². Dittrich et al. (2005) estimated the bed shear stresses for this river reach (without gravel island) based on STAU and analytical formula. They obtained values of 54 – 95 N/m² for this study area. Due to the reported uncertainties related to 1D bed shear stress calculations on the local scale both data sets should only be compared regarding the order of magnitude since the 1D model cannot account for local distribution of bed shear stresses with vegetation in contrast the multidimensional approach. But in any case, the 1D model can provide a good approximation of averaged bed shear stresses for this homogenous geometry. Bearing this in mind, it can be concluded that the outcomes of this study obtained with the 1D/3D method are in a reasonable order of magnitude. A more detailed view of the location Neuenburg is shown in Figure 5.12 where the computed bed shear stresses are plotted together with the flow field. Here, the potential of the combined modelling approach including a fully 3D model compared to a low-dimensional method is visible because a detailed investigation of the local flow field and of related bed shear stress distributions is possible: The simulations show that the flow is divided at the upstream end of the island due to vegetation resistance which leads to flow concentration with increasing stream forces on the bed towards the French river side. Bed shear stresses on the gravel island and the groyne fields are much lower with τ_0 values of 5 to 20 N/m² and 6 to 10 N/m², respectively.

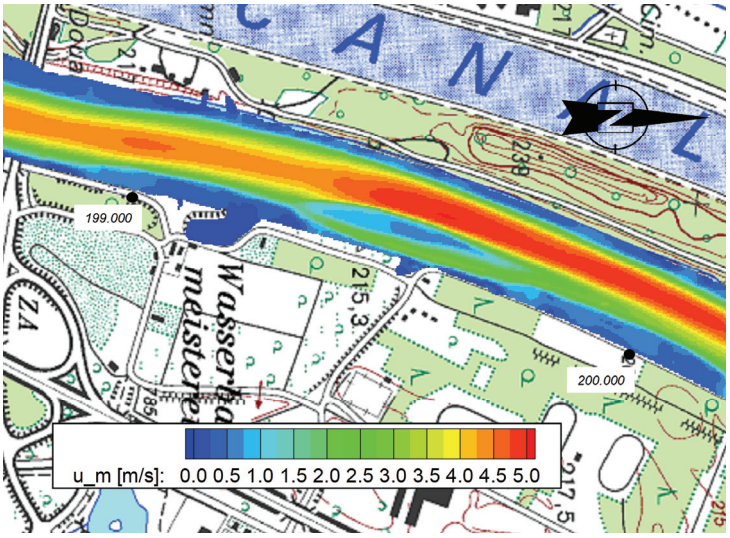

Figure 5.8: Calculated depth-averaged velocities for Q3 = 4500 m³/s (ACT2004).

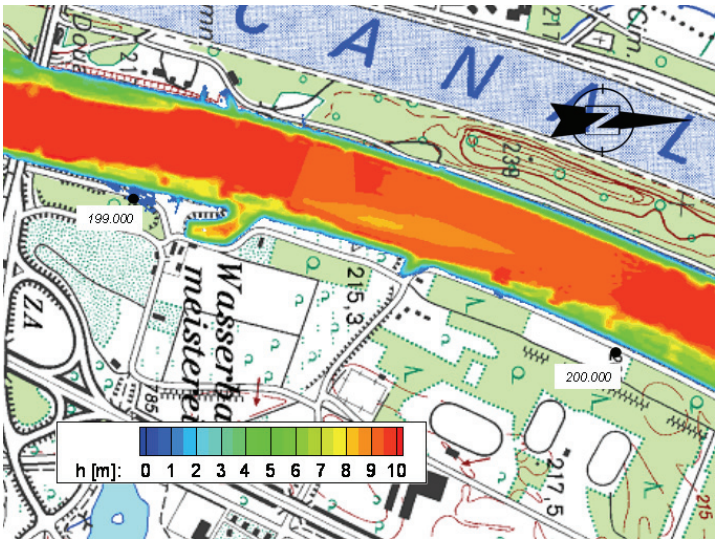

Figure 5.9: Calculated water depths for Q3 = 4500 m³/s (ACT2004).

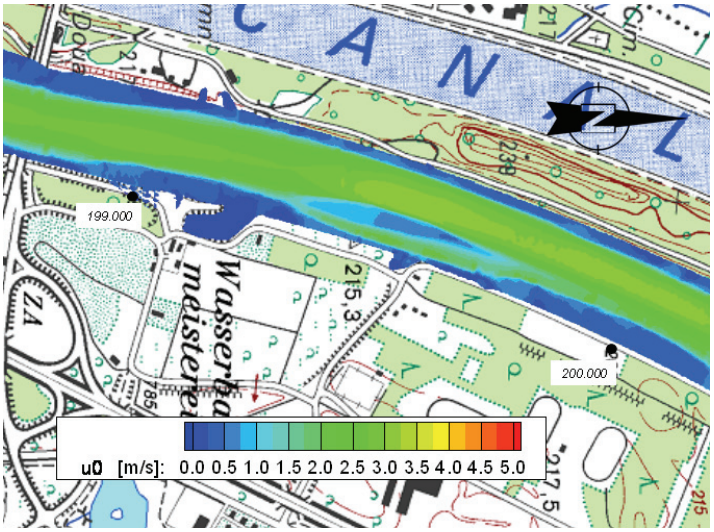

Figure 5.10: Calculated near-bed velocity for Q3 = 4500 m³/s (ACT2004).

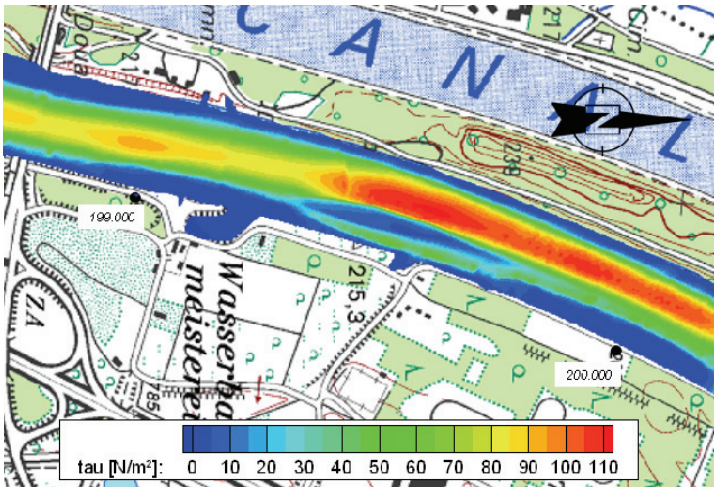

Figure 5.11: Calculated bed shear stresses for Q3 = 4500 m³/s (ACT2004).

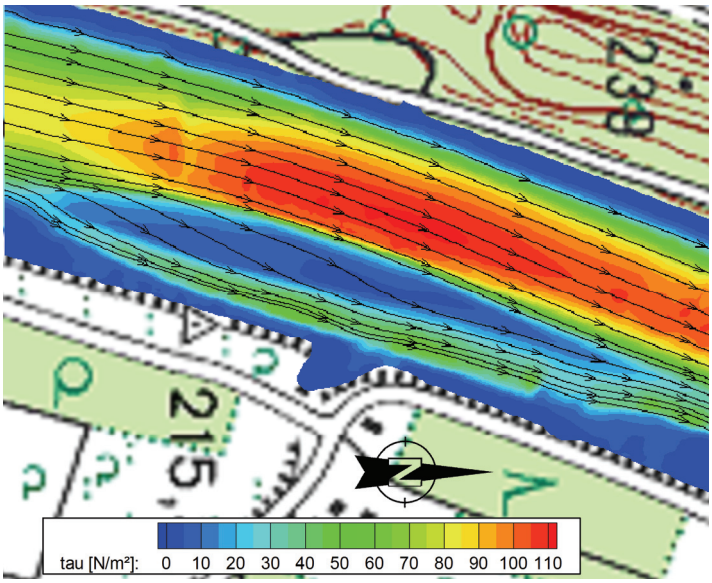

Figure 5.12: Calculated bed shear stresses near the gravel island for Q3 = 4500 m³/s (ACT2004).

5.2.3 Selection of stability approaches

5.2.3.1 Stability approaches for the river bed

Based on the foregoing computations, approaches for the stability of river bed and vegetated areas are selected and tested for the extreme event Q3 = 4500 m³/s. Bed stability can be estimated by comparing the bed shear stresses τ_0 of the water flow with the critical shear stress τ_{0c} of the material. As reported in Chapter 3.2.3.1, numerous formulas for τ_{0c} have been developed for various bed material and river types. But it should be noted that it is still common in practice to conduct stability assessments with standard formulas while disregarding the boundary conditions present in the river system. As a consequence, large scatter and uncertainties can occur in the case the approaches are not applied in close regard to the system's properties. The present study alternatively proposes a calibration and validation of the stability approaches based on field data prior to their application.

The bed shear stresses due to water flow τ_0 are provided by the computations of the 3D numerical model while τ_{0c} of the bed material can be derived by sediment samples and corresponding grain size distributions samples. As reported, the bed of the River Rhine consists of an armour layer which has developed in the course of selective erosion processes within the last century. The upper armour layer is covering a lower layer of finer material. In order to estimate the river bed stability or in other words its tendency of erosion, the approach of Günter (1971) for armour layers in a critical state of stability is selected. The Günter formula is based on laboratory experiments with different sediment samples (d_{max} = 6 mm, d_m = 1.32 – 2.62, slope 1.4 – 5.5 ‰) with the aim to determine the critical bed shear stress of river beds of maximum stability with non-homogenous material. The formula of Günter (1971) yields:

$$\tau_{0c} = \lambda \cdot \tau_{c[E]} = \lambda \cdot 0.047 \cdot (\rho_S - \rho_W) \cdot g \cdot d_{max} \qquad 5\text{-}2$$

with $\tau_{c[E]}$ equal to τ_{0c} of a reference bed with homogenous material and grain d_{max} of the original non-homogenous bed.

The factor λ is dependent on the armour layer and the original sediment sample and determines the constitution and density of the grains with d_{max} of an armour layer in the critical state of stability, s. Eq. **5-3**. The relevant grain diameter d_{rA} of the armour layer is obtained from the original sample and is further calculated via a distribution function (for details please refer to e. g. Dittrich, 1998).

$$\lambda = \left(\frac{d_{rA}}{d_{max}}\right)^{0.64} \cdot \left(\frac{d_{rO}}{d_{max}}\right)^{0.33} \qquad 5\text{-}3$$

d_{rA} – relevant grain diameter of armour layer [m], d_{rO} – grain diameter of original sample [m]

In order to investigate the suitability of the above mentioned approach for the study region, a sieve curve is calculated for a typical armour layer in a critical state of stability as it would theoretically occur in the Rhine reach and then compared with the grain size distribution of the present material. For this objective, sediment samples had been taken from several gravel banks and locations in the main channel along the river section Weil-Breisach. Both the sampling and sieve curve analyses had been conducted by the Leichtweiss-Institute for Hydraulic Engineering (LWI). Based on these samples, a mean maximum grain diameter has been calculated yielding $d_{max,m}$ = 168.8 mm. Examples of typical grain size distributions of the armour layer (upper layer) and the lower layer at Rhine-km 210.50 are shown repetitively in Figure 5.13. In addition to this typical bed material of the Rhine, the theoretical sieve curve computed with the approach of Günter (1971) is depicted in Figure 5.13 as well. It turns out that the sieve curve according to Günter (1971) and the sieve curve of the armour layer material exemplarily shown for Rhine-km 210.50 are very similar. Thus, the conclusion can be drawn that the stability conditions of the main channel in the study site can be well approximated by the Günter approach in a first assumption. As quality check, this approach is tested and validated with field data prior to the application to the area Neuenburg in Chapter 5.3.

Based on the outcomes, Eq. 5-3 may be further used to derive the critical shear stress τ_{0c} for the armour layer of the River Rhine. The values obtained for τ_{0c} form the fundamental basis for the determination of present and potential stability conditions. For the gravel bank at Rhine-km 210.50, τ_{0c} = 75 N/m² is obtained with the Günter formula while the sediment samples of the Rhine bed

provided by LWI exhibit τ_{0c} = 64 N/m² which shows the range of critical shear stresses present in the reach.

These values can be used to derive the stability conditions for the case study ACT2004_3D presented in Figure 5.11 and Figure 5.12. Comparing the τ_{0c} values of 64 – 75 N/m² to the calculated bed shear stresses with SSIIM 2.0 for the study site Neuenburg, it turns out that in many areas, the critical

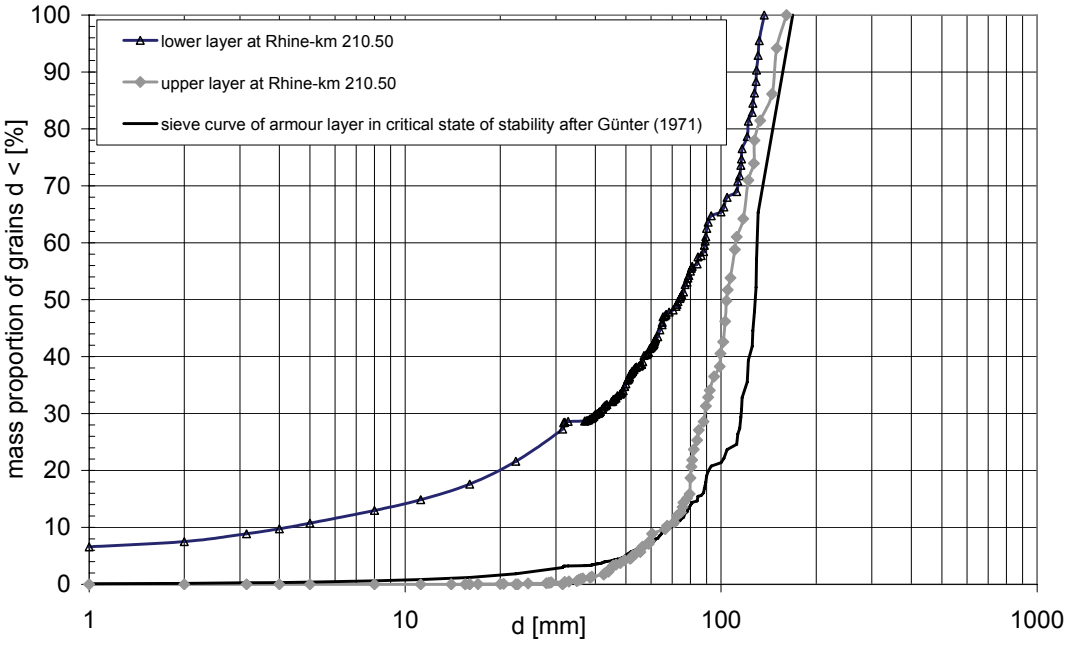

Figure 5.13: Sieve curves of the upper layer (armoured) and the lower layer taken from a gravel bank at Rhine-km 210.5 and derived theoretical sieve curve for an armour layer in a critical state of stability with the formula of Günter (1971).

shear stress of the bed material is exceeded by τ_0 of the flow which reaches values up to 90 N/m². This leads to the conclusion that the main channel of the River Rhine is in a critical state of stability at the extreme event Q3 = 4500 m³/s and hazardous erosion processes would be likely to occur along the river bed. It is important to underline that this outcome is in close agreement with the study of Dittrich et al (2005). They concluded for the extreme event 4500 m³/s that the Rhine bed would be unstable in many areas and that widespread destruction of the armour layer could be expected.

5.2.3.2 Stability approaches for vegetation

However, the stability of the gravel island and the groyne fields may differ significantly from the stability of the armour layer / main channel due to its vegetation cover. Figure 5.14 shows exemplarily for the Rhine section that the roots of the willows reinforce and fix the loose gravel which in turn enhances the stability of the bed material. Therefore, the stability approach for armour layers of Günter (1971) is not applicable here and another method is required in order to estimate the stability of vegetation in natural gravel-bed rivers as reliably as possible. Due to missing mathematical approaches, it was decided to use literature values for the scope of the present study. Information on vegetation stability in bioengineering structures is provided by e. g. Dittrich (1995) for several

vegetation types. He reports τ_c for lawn ranging from 15 – 30 N/m² depending on inundation time, for upcoming lawn on gravel τ_c < 30 N/m² and for roots of willows and earls ranging τ_c = 60 – 140 N/m².

Apparently, willow and earl roots are able to stabilize the gravel bed significantly reaching and even exceeding the critical shear stresses of the armour layer. Comparing τ_c of willows and earls to the τ_0 computed with the 3D model for Q3 in Figure 5.12, it turns out that τ_c of the vegetation and τ_0 due to water flow reach the same order of magnitude. According to these data, the conclusion can be drawn that parts of the gravel island would be both partly eroded and partly remain stable even at the extreme event.

Figure 5.14: Pioneer vegetation growing on bare gravel in the Rhine section Weil-Breisach (provided by ILN).

At this point it should be remarked that the applicability of these literature values for vegetation stability will be further validated in Chapter 5.3 based on field data prior to its application to the area Neuenburg.

5.2.3.3 Stability approaches for loose bed material

Furthermore, a stability approach for the loose sediment is chosen in order to estimate the erosion tendency of the side channel on the future lowering areas. This is required since fully moveable material will be present in the side channel whose discharge capacity must be sustained in order to transport fine suspended sediment off the area. As a consequence, the lowering area might be subjected to hazardous sedimentation processes more easily which in turn may affect the functionality of flood protection and the safety of adjacent areas. In contrast, it is further assumed that the vegetated zones on the retention area are not subjected to erosive processes due to stabilization by tree roots (see Chapter 5.2.3.2).

Information about the behaviour of loose gravel on the future retention area can be obtained by sediment samples available for the gravel pits of Grissheim (Rhine-km 207), Bremgarten (Rhine-km 211) and Hartheim (Rhine-km 216) in the vicinity of Neuenburg, see Chapter 4.3.2.1. Table 3-3 has highlighted a variety of formulas available for initiation of motion. Among these the approach of Wilcock et al. (1996) yields satisfying results for loose coarse material as concluded by Koll and Dittrich (1998) and Dittrich (1999). The formula of Wilcock et al. (1996) for non-homogenous material (0.2 -110 mm) follows:

$$\tau_{0c} = 0.035 \cdot (\rho_S - \rho_W) \cdot g \cdot d_{50} \qquad 5\text{-}4$$

Since the equation has been obtained by field studies with conditions similar to those of the future side channel, it was chosen for the stability estimations in the present study. Based on Eq. 5-4, the critical bed shear stress of the side channel was derived by the mean sieve curve computed for the three gravel pits and the corresponding d_{50}. Table 5-9 lists the characteristic grain sizes and the range of critical shear stresses obtained for the study area while Table 5-10 finally summarizes the critical shear stresses selected for the case study region.

Table 5-9: Characteristic grain diameter of loose gravel taken from the gravel pits as well as computed critical bed shear stress with the approach of Wilcock et al. (1996).

d_{ch} [mm]	Grissheim (min)	mean	Hartheim (max)
d_{50}	18.0	25.3	35.0
d_m	30.3	36.7	49.0
d_{max}	130.0	131.0	153.0
τ_{c0} [N/m²]	10.2	14.3	19.8

Table 5-10: Overview of critical shear stresses derived for the case study.

critical shear stress [N/m²]	sediments		vegetation			
	main channel (armour layer)	loose gravel	lawn (briefly flooded)	lawn (long-term flooded)	upcoming lawn on gravel	roots of willows and earls
τ_c	64 – 75	10 – 20	15	30	< 30	60 – 140

5.3 VALIDATION AND QUALITY CHECK

For the validation of the proposed methodology, three discharges events have been chosen in combination. These comprise high floods of similar magnitudes: the event 1994 (3040 m³/s), the event of 2007 (3300 m³/s) and the event of 1999 (3600 m³/s peak discharge). These floods have been selected because of the sound data basis allowing an accurate model evaluation. The data basis covers field information on water level, velocities and morphodynamic development: Water levels measurements have been carried out in the years 1994 and 1999. In addition, mean flow velocities apparent in the vegetated groyne fields were measured in 1999 via tracer injection. It is important to remark that in the year 1999, measurements were conducted not at the flood peak but at the decrease of the peak flood wave: Water level was measured at Q = 2520 m³/s while flow velocities were measured at 2000 m³/s. Last but not least, the event 2007 was documented by Regierungspräsidium Freiburg (2008) which provide field observations along the Rhine section Weil-Breisach including

photo and video documentation. Although the data correspond to three different events, their magnitudes and related processes are approximately comparable. Subsequently, the data of these three discharges were used in combination as the following: The combined modelling tool was tested and validated on the event of 1994, Q4 = 3040 m³/s in the way that the water levels and the 3D flow field were computed with the 1D/3D models and the morphodynamic development was derived with the proposed approaches. The events 1999 and 2007 were then taken into account to assess the outcomes' plausibility based on field observations. The results are shown in the following.

The water level calculated for Q4 = 3040 m³/s is repetitively presented in Figure 5.15. Figure 5.16 shows the 3D depth-averaged (mean) flow velocities of the study area Neuenburg computed with SSIIM 2.0 for Q4. In the main channel, mean flow velocities range from 2.5 – 3.0 m/s in areas with relative wide cross-section (e. g. Rhine-km 199.500) and reach 3.5 – 4 m/s in areas where the cross

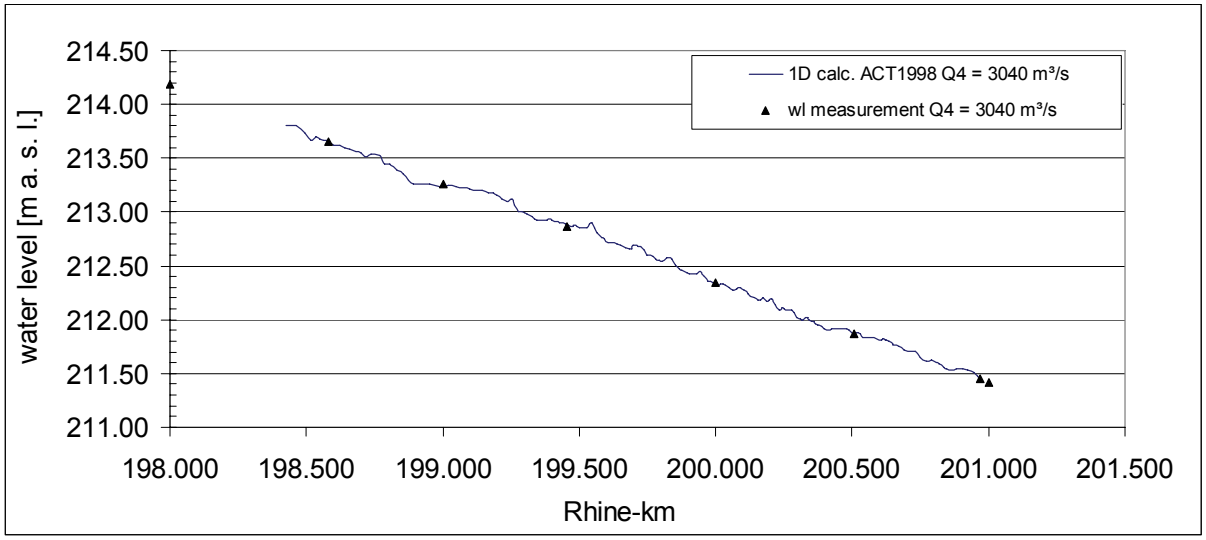

Figure 5.15: Calculated water level for Q4 = 3040 m³/s for the case ACT1998 (without gravel island) and measured water level.

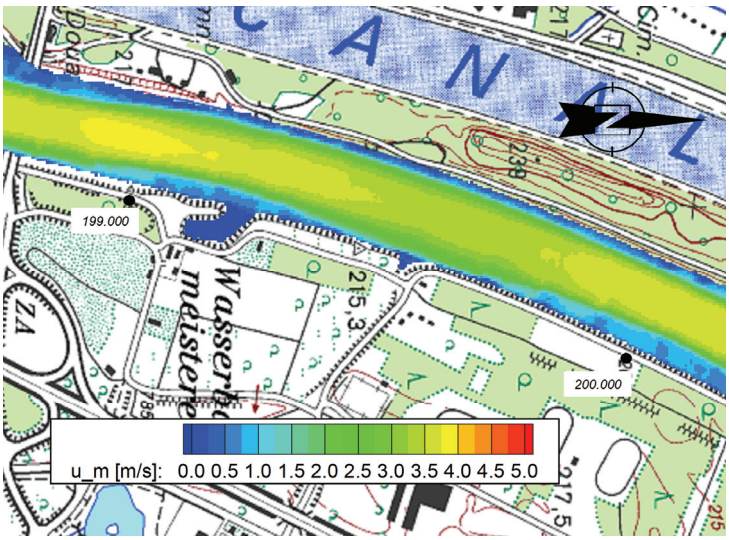

Figure 5.16: Calculated depth-averaged flow velocities for Q4 = 3040 m³/s (ACT1998).

sections are narrowed by the groyne fields (e.g. Rhine-km 198.9 or 200.250). In the harbour, flow velocities are close to zero which enfavours sedimentation processes. This outcome is consistent with field observations revealing siltation of the basin throughout the last decades.

As afore mentioned, field measurements were taken from the literature in order to assess the flow velocity computations. During the flood event 1999, Hartmann et al. (2000) conducted tracer measurements in the vegetated groyne fields at Rhine-km 191.30 (Bad Bellingen, German side) yielding mean flow velocities of 1.1 m/s. A photo of the measurement campaign is depicted in Figure 5.17. It must be taken into account that these measurements only reflect local conditions with bended vegetation and cannot be directly transferred to the study site Neuenburg. But in any case, they can give a rough idea of typical flow velocities under comparable conditions. Comparing these field data with the mean flow velocities obtained with the 3D model and rigid vegetation as illustrated in Figure 5.16, it can be shown that the simulations match the order of magnitude of the measurements well: Simulated u_m values range between 1 – 1.5 m/s on the groyne fields of the study site Neuenburg.

Furthermore, the information on the flood events 1999 and 2007 is considered to assess the stability approaches chosen for the present study, namely the approach of Günter (1971) for armour layers in a critical state of stability as well as the literature data for critical shear stresses of vegetation. The simulated bed shear stresses obtained for the event Q4 are presented in Figure 5.18. Bed shear stresses in the non-vegetated main channel reach 65 – 75 N/m² in the narrow sections of the site (e.g. Rhine-km 198.9 or 200.250) and decrease down to 45 – 65 N/m² in the wider areas which are not restricted by groyne fields (e. g. Rhine-km 199.500). Comparing these values with the critical shear stresses obtained with the Günter formula - 64 – 75 N/m² - it is revealed that the river bed Neuenburg remains stable in many areas at Q4 but that local erosion processes are likely to occur since the critical values are partly reached or even partly exceeded by the water flow. This outcome is confirmed by the studies

Figure 5.17: Measurement campaign for flow velocities with tracers at the 1999 event (Hartmann et al., 2000).

of Hartmann et al. (2000). They report for the flood of 1999 that erosion processes as well as deposition phenomena could have been observed along the river section Weil-Breisach while mass balance was apparently maintained constant. For example, the armour layer at Rhine-km 184 – 186 was widely destructed while the river bed at Rhine-km 199 – 208 has remained relatively stable. The

latter area includes the site Neuenburg revealing that the present outcomes reflect the conditions sufficiently well.

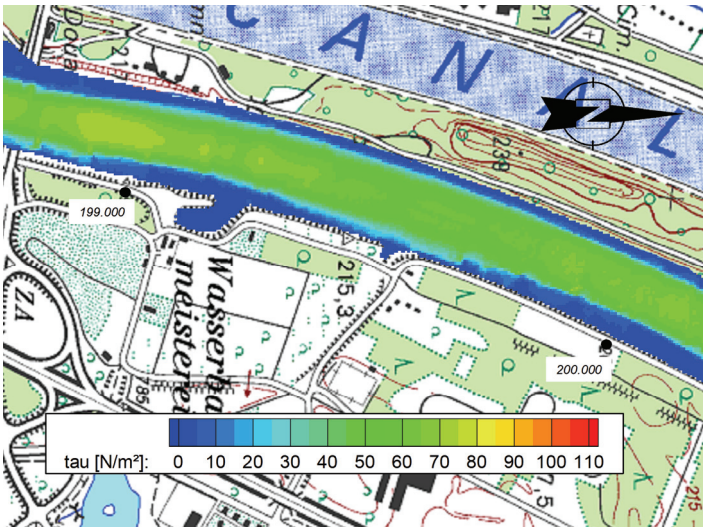

Figure 5.18: Calculated bed shear stresses for Q4 = 3040 m³/s (ACT1998).

The plausibility of bed shear stresses obtained with SSIIM is additionally underlined by further calculations reported in the above mentioned study. Dittrich et al. (2005) calculated τ_0 based on the mean water depth (averaged over the cross-section) and based on R, respectively, for the flood peak Q = 3600 m³/s along the Rhine section Weil-Breisach. Their results are illustrated in Figure 5.19. The calculated bed shear stresses range from 56 – 83 N/m² for Rhine-km 198 – 210. These values exhibit the same order of magnitude, but are slightly higher than the values obtained in the present study but in any case, this outcome is reasonable given the higher discharge considered in the the other study.

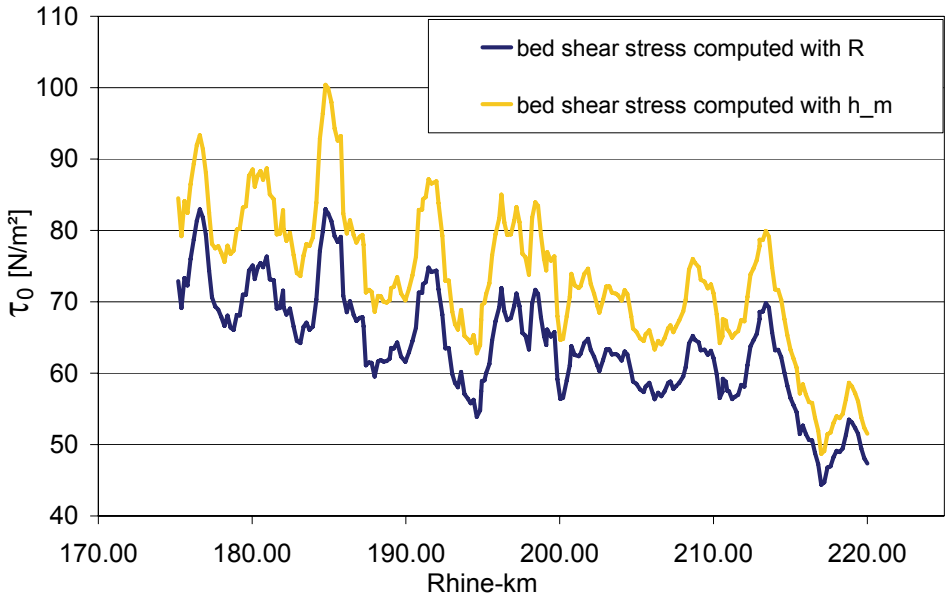

Figure 5.19: Bed shear stresses computed by Dittrich et al. (2005) for the peak discharge of 1999 (3600 m³/s).

The good performance of the calibrated 3D model can also be confirmed by a comparison of the simulations with field observations during the flood 2007. During this event with a peak discharge of 3300 m³/s, the gravel island remained stable. But it is observed that, since then, the side arm between gravel island and German Rhine bank has stopped conveying water and remains dry at normal (low) water conditions (30 – 50 m³/s). Field observations revealed that the bed material present in the side arm consists of coarse stabilized gravel of high stability, obviously the original, non-affected armour layer of the river bed. Thus, first of all, siltation of the side arm was excluded as a possible reason for the dry up. In order to test whether the Hazard Analysis approach is capable to deliver new findings for this event, it was used to carry out simulations for the case which corresponds best to the conditions of 2007: Q4 and ACT2004 (gravel island with vegetation) as it was present in 2007 and today. Figure 5.20 presents the computed mean (depth-averaged) velocities at the study site with vegetated gravel island for Q4 while Figure 5.21 presents the corresponding bed shear stresses. Figure 5.22 finally provides a closer look on the situation at the gravel island for the bed shear stresses including stream traces. The pictures reveal that the flow situation upstream of the harbour is similar to the flow situation of the case ACT1998. Subsequently, flow velocities range between 3 – 4 m/s and corresponding bed shear stresses range between 50 – 70 N/m² in the main channel. In contrast, near the gravel island towards the French side, u_m rises up to more than 4 m/s with bed shear stresses reaching 70 – 85 N/m². As already reported for Q3 and ACT2004, the vegetated island obviously forms an obstacle to the flow. Stream traces show that the flow is concentrated in the west part of the channel due to the flow resistance of the vegetation. Here, in the area of stream concentration, the critical shear stresses are exceeded by shear stresses of the flow indicating initiation of motion and erosion processes. Instead, the side arm is only moderately affected:

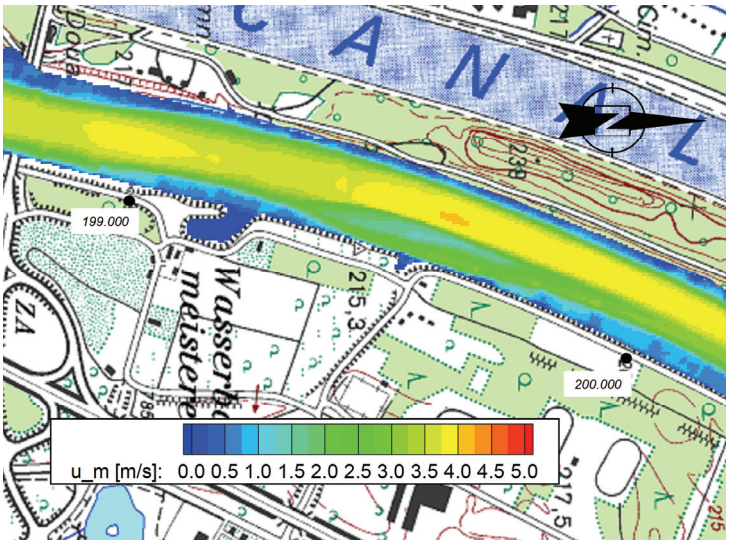

Figure 5.20: Calculated depth-averaged flow velocities for Q4 = 3040 m³/s (ACT2004, actual state with vegetated gravel island).

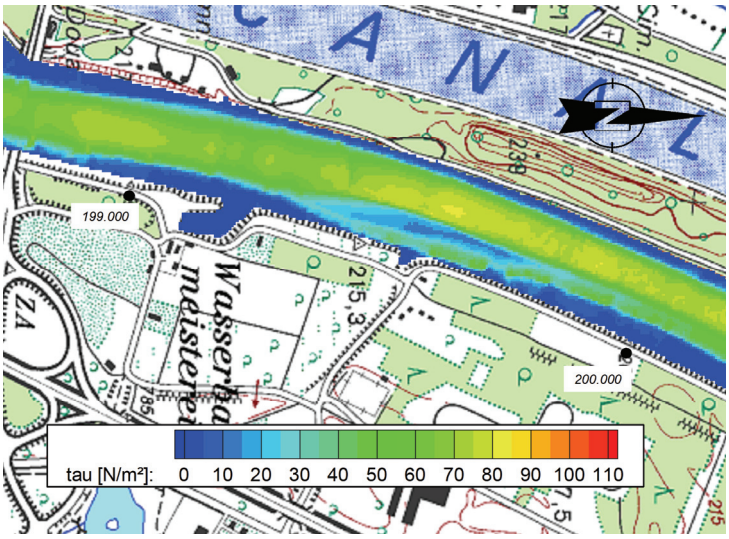

Figure 5.21: Calculated bed shear stresses for Q4 = 3040 m³/s (ACT2004).

Bed shear stresses reach 30 – 45 N/m² and are clearly lower than the critical shear stresses of the river bed but still high enough to inhibit fine material deposition. These outcomes confirm the field observations of Regierungspräsidium Freiburg (2007) and ILN (2008) that apparently the flow concentration has provoked erosion and bed incision between the island and French banks. This may have led to a local decrease of the water level near the gravel island with the effect that the side arm is now located above the low water table and dries up frequently during the year.

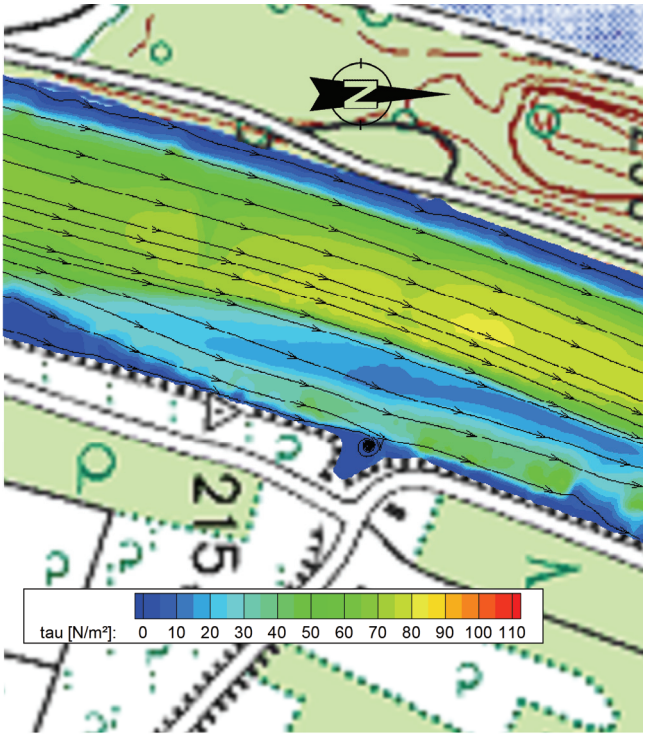

Figure 5.22: Calculated bed shear stresses for Q4 = 3040 m³/s near the gravel island and stream traces (ACT2004).

Finally, it is worth noting that the plausibility of simulated bed shear stresses on the vegetated areas can be confirmed once again with the simulations of the event 2007: According to the present study, the flow is slowing down due to the resistance in the vegetated areas, especially on the gravel island. Mean flow velocities decrease to 0.7 – 1.5 m/s and 1.0 – 2.0 m/s on the island, respectively. As shown, these values are in agreement with the field measurements of 1999 (~ 1.1 m/s) keeping in mind that the measurements were carried out at a lower discharge (~ 2000 m³/s). Furthermore, critical bed shear stresses are not reached on the gravel island with maximum values of 30 N/m². These results indicate that the vegetated gravel island remains widely stable at a high flood event. This is consistent with field observation of 2007 as well.

Besides simulations, field measurements are of fundamental importance for system understanding and morphodynamic estimations of future states and should always be processed in parallel to theoretical considerations. Thus, in future, new geodetic measurements will be carried out along the River Rhine which will help to gain new insights.

The outcomes of the validation and plausibility check reveal that the novel 1D/3D model approach derived in the present thesis is capable to deliver a reasonable estimation of morphodynamic processes in gravel-bed rivers with vegetation on the local scale. Calibrated coefficients of roughness and flow resistance, grid resolution as well as stability values chosen from the literature can reflect the conditions at Neuenburg of the actual state adequately. Based on this, the 1D /3D model approach is applied to the study site Neuenburg for the analysis of morphodynamic hazards in the planning state.

6 CASE STUDY UPPER RHINE: APPLICATION OF THE HAZARD ANALYSIS APPROACH TO THE PLANNED FLOOD PROTECTION AND RESTORATION MEASURES

The present chapter reports the application of the new concept to the planning state of the study area Neuenburg based on the calibration and validation procedure carried out in the previous sections. In order to assure a sound basis of input data as well as accurate computational grids, several preparatory working steps had to be conducted prior to the simulations. In the first part of this chapter, this working procedure is described concerning grid generation (Chapter 6.1) as well as roughness and vegetation resistance for the planning study area (Chapter 6.2). In Chapter 6.3, it is aimed at conducting the analysis of morphodynamic hazards in the study site for the planned flood protection measures with the new approach and at revealing potential needs for planning optimization.

6.1 PREPROCESSING AND RELATED PREPARATORY WORKS

6.1.1 Preprocessing and data generation

In order to perform the hydrodynamic numerical calculations for the planning state, several steps have to be carried out before. The used methodology and input data are briefly described in the following, see Table 6-1. The preparatory working steps cover 1) the 1D roughness calibration of the

Table 6-1: Generation of hydrologic input data (white) for the hydrodynamic calculation of the planning state (grey).

step	state	description	tool	input data		
				topography	discharge information	roughness
0	actual state	calibration km 198.410 - 200.970 for Q1, Q2, Q3	1D model HECRAS 3.1.3	extended DEM	water levels ACT1998 (Dittrich et al., 2005)	calibration for bed and banks
1	planning state	calibration of Manning's roughness for lowering area/German side	Schluess	DEM PLAN	water level PLAN Q3 (Dittrich et al., 2005)	for bed and banks see step 0
2		determination of start water levels for the planning state for Q1 and Q2	Schluess	DEM PLAN	to be determined	a) bed, banks, see step 0 b) lowering area, see step 1
3		1D calculations planning state for Q1, Q2, Q3	1D model HECRAS 3.1.3	DEM PLAN	start water levels, see step 2	see step 2
4		3D calculations planning state for Q1, Q2, Q3	3D model SSIIM 2.0	DEM PLAN	1D water levels see step 3	see step 2

lowering area (planning state) and 2) the generation of start water levels for the planning state required for the 1D and 3D calculations.

Step 0 in Table 6-1 which has been performed in the previous chapter has comprised the 1D calibration on the actual state of 1998. This successful calibration procedure allows to transfer the roughness values to the corresponding areas in the planning state (main channel and vegetated banks). It must be noted that, until now, the roughness of the future areas of the planning state, namely flood retention area and Rhinegardens are unknown and that as a consequence, the 1D calculations cannot be carried out reliably yet. Hence, step 1) comprises the determination of the Manning's roughness for the lowering area. In order to select the Manning's roughness as accurately as possible, the roughness was calibrated on literature data available for this Rhine section (Dittrich et al., 2005). The authors investigated potential water level changes due to the planned retention areas along the Rhine section Weil-Breisach in the framework of the Integrated Rhine Programme. Vegetation resistance was derived from vegetation mapping in the field, calibration and sensitivity analysis in close cooperation with biologists and foresters in order to achieve a reliably prognosis of vegetation development on the future lowering areas. The studies revealed that natural willow poplar forest is very likely to develop on the retention area approximately 50 years after lowering due to natural succession and thus will develop simultaneously to the natural vegetation structure on the French groyne fields (ILN, 2006, 2007). Based on these data, Dittrich et al. (2005) conducted 1D water level calculations for a state with retention areas for the hypothetical extreme event Q_{200} = 4500 m³/s with the programme STAU and the approach of Lindner (1982) for vegetation resistance. These 1D water levels are judged to be very suitable for the river site Neuenburg. In order to ensure that the 1D model used in the present study can reflect the vegetation resistance on the future lowering area adequately, the water levels of the aforementioned study have been used to calibrate the Manning's value for the lowering area for the HEC-RAS model.

Furthermore, reliable start water levels for the planning state must be derived for the downstream cross-section. This demand is followed in step 2. Here, the calibrated roughness of main channel, vegetated banks and lowering area were used to calculate the start water levels for Q1 = 671 m³/s and Q2 = 1587 m³/s by means of a h-Q relationship via the routine Schluess (provided by Koll). With this procedure, it can be achieved that start water levels correspond closely to the system behaviour of the study area. With completion of step 2, all relevant hydrologic input data for model forcing are generated.

6.1.2 Grid generation for the planning state

The simulation of the planning state requires a new elevation grid incorporating the new design. As basic grid the extended DEM2004 is chosen which represents the main channel in the actual state including the gravel island from Rhine-km 198.410 – 200.910 (see also Chapter 3.1). As presented in detail in the Risk Identification phase, the future design covers the restoration and dredging of the harbour basin, the flattening of the harbour banks and a visitor's platform at the basin. Downstream of the harbour, in front of the gravel island the river plans comprise the recreation area "Rhinegardens" including the flattening of the banks, the construction of an amphitheater, sitting places, sun bathing area, a fairground, an adventure playground and gastronomy. Further downstream, the flood protection

area will be built at the downstream end of the gravel island in the framework of the Integrated Rhine Programme.

For the Hazard Analysis of the planning state, a new topography data base has been developed which incorporates all relevant measures with high resolution. A challenge which is related to the estimation of future river sites and their development is to achieve data consistency. It must be assured that the additional morphological features are well incorporated in the topography and are in accordance with grid resolution and resistance pattern already provided by the calibrated actual state model. More than 30 different sources, mostly consisting of analogue plans, photos, technical data and drawings were available and had to be considered in the topography. In order to generate a reliable data base, it was decided to modify the extended digital elevation model DEM2004 and to digitize the new features and elevations manually into the DEM. This work was performed in a GIS system (ArcGIS 9.1, ESRI, 2005) on the DEM2004 in TIN format comprising more than 3000 single points to guarantee accuracy. Figure 6.1 shows the working procedure on the DEM2004 with the digitized data as single points extracted from the analogue plans and entered into the TIN.

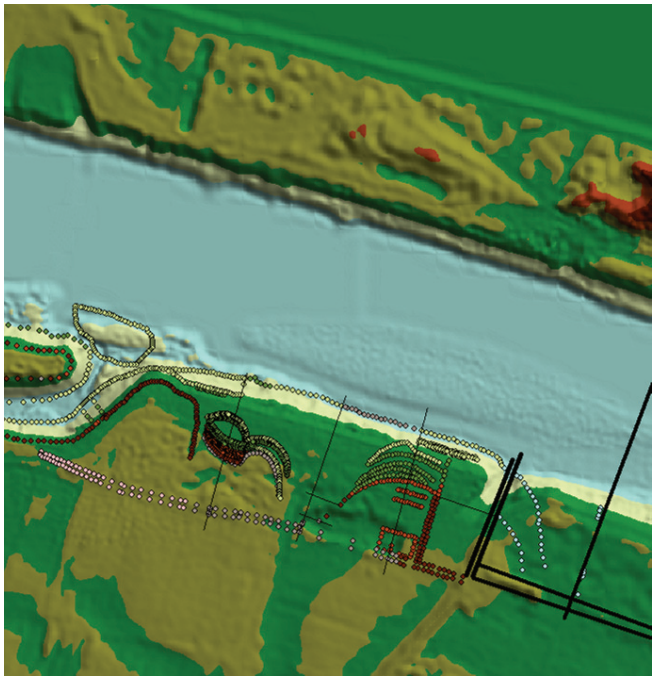

Figure 6.1 Manual modification of the TIN digital elevation model according to the municipality and technical plans in ArcGIS 9.1 (ESRI, 2005) (data source: provided by ILN, 2006).

Figure 6.2 finally presents the completed digital elevation model PLAN modified for the planning state. The resolution is 1m x 1 m in horizontal and longitudinal direction. Dregded harbour, gravel island, Rhinegardens with theatre, sun bathing area etc. as well as the flood retention area including hardwood terrace and side channel are accurately incorporated.

This generated digital elevation model for the planning state (called “DEM PLAN”) is the basis for both the 1D water level calculations and the 3D hydrodynamic calculations as decribed in Table 6-1. It is worth noting that the preprocessing and conversion procedures which have been developed in Chapter 5.2.2.2 can directly be applied. For reasons of consistency, the grid resolution chosen in the actual state of both the HEC-RAS geometry and the 3D model, respectively, are maintained in the final geometry of the planning state. Similar to the actual state, the 3D grid had to be extended in the

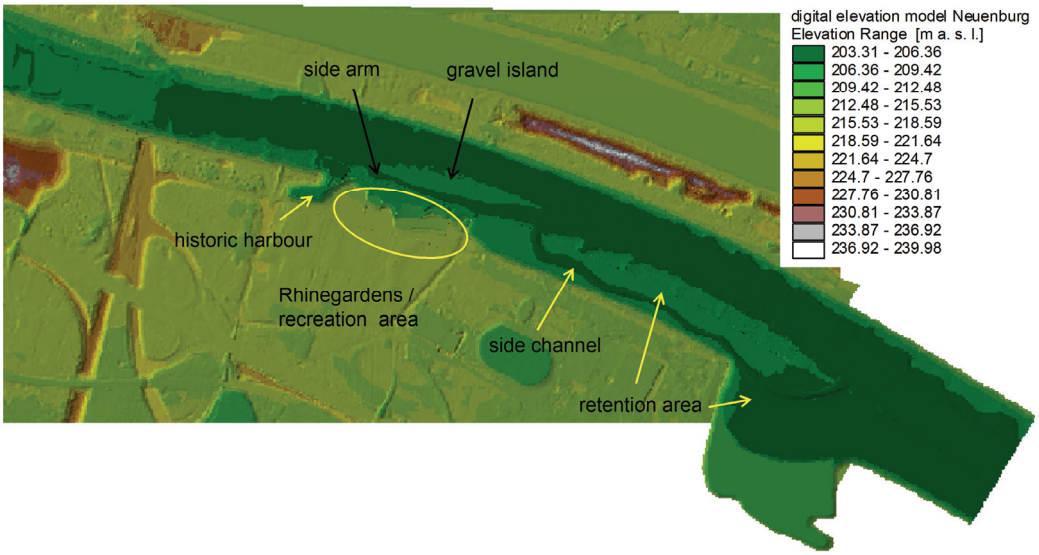

Figure 6.2: Digital elevation model of the planning state generated in this study (resolution 1x1m).

upstream direction for the numerical evolution of the flow field. The maximum cell number of the 3D grid including the grid prolongation as well as the grid resolution are repetitively provided in Table 6-2 yielding a maximum number of 918,000 cells for the computational grid in the planning state.

Table 6-2: Number of cells and spatial resolution of the numerical grid for the 3D simulations of the planning state.

direction	maximum number of grid cells	approx. resolution [m]
longitudinal (flow direction)	1020	3.2
horizontal (cross-section)	100	1.5
vertical (depth)	9	1

6.2 INFORMATION ON ROUGHNESS AND VEGETATION RESISTANCE IN THE PLANNING STATE

6.2.1 Information on roughness for the 1D calculations of the planning state

The roughness data of the channel and the vegetation used for the 1D calculation of the planning state are listed in Table 6-3. The roughness values for the retention area were obtained via calibration in step 1 during preprocessing (see also Table 6-1) to n = 0.12 s/m$^{1/3}$. It turns out that this value is identical with the Manning's n value which has been selected as upper roughness boundary for the vegetated gravel island n_{max} in the case ACT2004. This correspondence underlines that the vegetation resistances are in a reasonable order of magnitude and can be supposed as representative for the vegetation structure in the study site. Consequently, also the vegetation resistance of the gravel island was set to n = 0.12 s/m$^{1/3}$ since it may be similar to the French floodplain forest. Moreover, it is assumed that the roughness of the Rhinegardens and the flattened banks on the German side can be approximated by the roughness calibrated for the banks in the actual state. This assumption is well justified as 1D test calculations showed that variations in the Manning's values at these small locations did not have any significant influence on the calculated water levels.

Table 6-3: Calibrated Manning's roughness for the 1D calculations of the planning state.

Q [m³/s]	Manning's n [s/m$^{1/3}$]			
	main channel	left and right banks	gravel island	retention area
	mean	mean		
671	0.024	0.024	0.12	0.12
1587	0.025	0.027	0.12	0.12
4500	0.036	0.046	0.12	0.12

6.2.2 Information on roughness for the 3D calculations of the planning state

6.2.2.1 Selection of the equivalent sand-grain roughness k_s for the bed

In contrast to the 1D model, SSIIM 2.0 implements the equivalent sand-grain roughness for surface resistance representation. The k_s values used in the 3D model for the EaRs are listed in Table 6-4. For the main channel and banks, k_s was set to 0.32 m according to the calibration in the actual state. It is worth noting that the same value can also be used for the bed roughness of the retention area in a first assumption: On the retention area, the total roughness is composed on the one hand of the surface roughness of the bed and on the other hand of the flow resistance due to floodplain forest with

increased vegetation density (bushes) close to the bed (see Figure 4.25). It is evident that the surface roughness of the bed material is negligible compared to the flow resistance due to drag force exhibited by bushes and trees. Therefore, the k_s value chosen for the bed may not significantly contribute to the overall resistance and the k_s value calibrated for the main channel can be applied.

In contrast, the total roughness of the EaR side channel on the lowering area is determined *only* by its surface/bed resistance exerted by non-vegetated, loose gravel. As a consequence, the use of the k_s value which has been selected for the retention area would not be correct. Thus, the roughness of the side channel was explicitly determined by sediment samples of the gravel pits since they represent typical grain size distributions of loose gravel originally present in the floodplains and likely to be apparent on the retention area after excavation.

Finally, k_s values had to be chosen for the EaR Rhinegardens. In order to reflect the properties in the planned design adequately, the information of the municipality plans and drawings (see Appendix A2) were used for the determination of bed roughness and vegetation parameters. Since the Rhinegardens will exhibit large areas with lawn (e. g. on the sunbathing areas) the corresponding bed roughness value was chosen from literature (USACE, 2005) while for the Leinpfad, the equivalent sand-grain roughness of fine gravel was assumed.

Table 6-4: Equivalent sand-grain roughness used for the 3D calculations of the planning state.

area or EaR	k_s [m]
main channel	0.32
left and right banks	
lowering area	
Leinpfad	0.01
Rhinegardens	0.06
side channel	
else	

6.2.2.2 Selection of parameters for vegetation resistance

Vegetation parameters for the 3D simulations are listed in Table 6-5. The parameters for the EaNR German and French banks have been taken from the calibration of the actual state. The vegetation types of the EaRs Rhinegardens, the sunbathing area etc. are determined in accordance with the available data base listed in Appendix A.2 such as municipality plans, technical plans and the FaF movie (www.freudeamflussmovie.org). In order to reliably predict the vegetation structure on the future retention area, the above mentioned study (Chapter 6.1.1) on future vegetation development was taken into account. Since the vegetation structure on the retention area as well as on the gravel island may be similar to the French groyne fields today (ILN, 2006, 2007) it was decided to transfer the vegetation parameters of the French groyne field to both the retention area and the gravel island. This assumption is in close accordance with the 1D Manning's roughness calibrated for the retention area with n = 0.12 s/m$^{1/3}$: According to literature, this n-value reflects natural floodplains and dense willow stands with bushes (see Appendix Table A.4.1).

Figure 6.3 illustrates the spatial vegetation distribution as selected for the study reach Neuenburg in the planning state according to Table 6-5. The generation of data and preprocessing for the 3D model was performed with the GIS system ArcView 3.2a.

Table 6-5: Vegetation parameter per vegetation type used in the 3D calculations of the planning state.

Location	vegetation type	vertical distribution	a_x [m]	a_y [m]	d_p [m]	c_W [-]
German banks	thinned poplar hardwood floodplain forest with undergrowth	near bed	3.0	3.0	1.0	1.5
		else	6.0	6.0	0.5	1.0
banks harbour peninsula harbour gastronomy	thinned poplar hardwood floodplain forest	constant over depth	6.0	6.0	0.5	1.0
French banks	natural willow poplar forest (mature forest stage)	near bed	3.0	3.0	1.0	1.5
retention area		else	6.0	10.0	1.0	1.0
gravel island	natural willow poplar forest (mature forest stage)	constant over depth	6.0	10.0	1.0	1.0
flattened German banks	low plant density		10.0	10.0	1.0	1.0
plateau	high plant density		4.0	5.0	0.7	1.0
sunbathing area	few trees		20.0	20.0	1.0	1.0

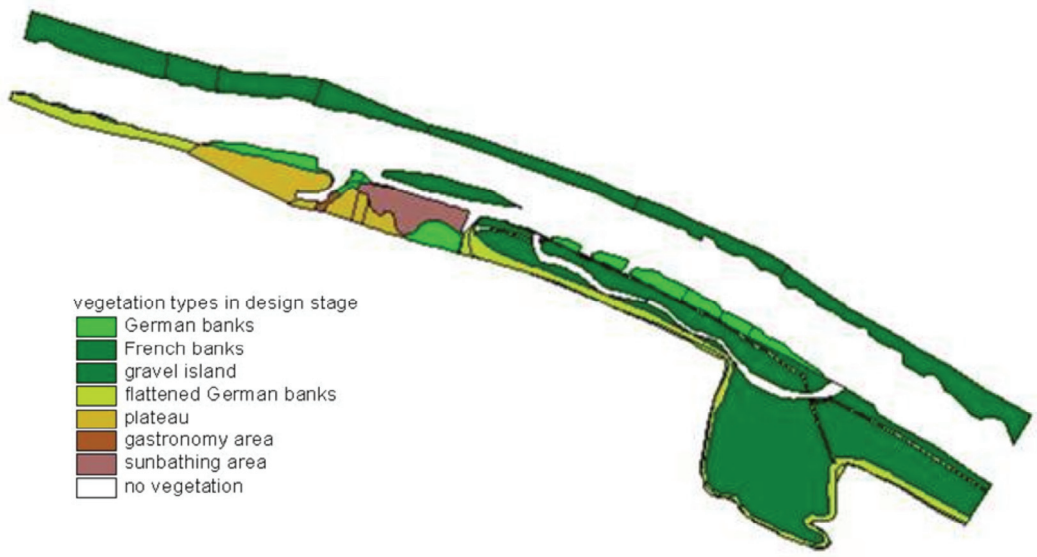

Figure 6.3: Distribution of vegetation types used in the 3D calculations of the planning state.

6.3 RESULTS OF THE 1D AND 3D CALCULATIONS FOR THE PLANNING STATE AND PROGNOSIS OF HAZARDOUS MORPHODYNAMIC PROCESSES

In this chapter, the results of the Hazard Analysis are presented for the case study reach in the planning state. According to Figure 6.4, the novel approach comprises the step A where the driving flow characteristics likely to occur in the planning state are computed by 1D/3D numerical simulations for the three discharges of interest. In the consecutive step B, the morphodynamic hazards endangering the river reach and the EaRs are derived based on the outcomes of step A.

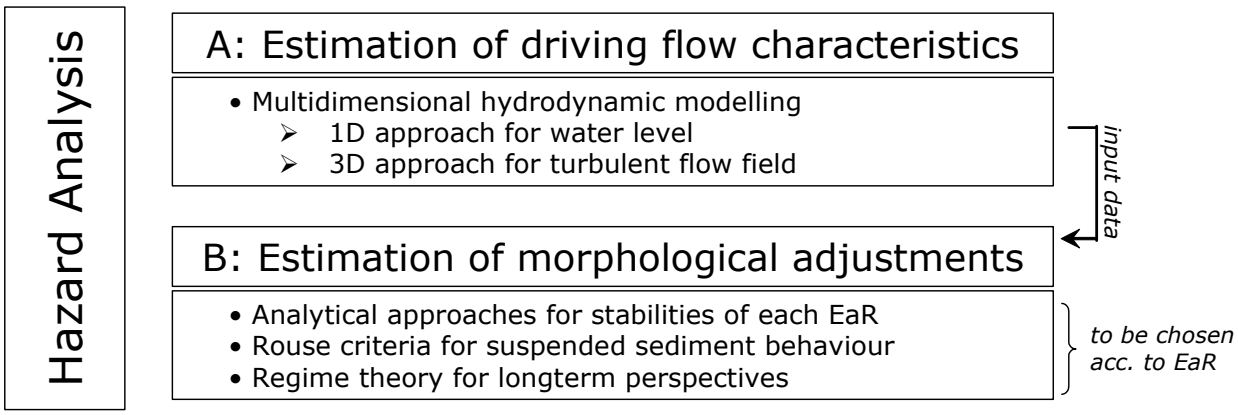

Figure 6.4: New approach of Hazard Analysis of morphodynamic processes in river restoration and flood measures.

The present chapter is structured as followed: In the first part, the computed depth-averaged velocities and water depths are shown and discussed together with the water levels calculated with the 1D model HEC-RAS 3.1.3. Based on this overview, the morphodynamic development and potential hazards in the study site are deducted by means of bed shear stresses and the 3D flow field obtained with the 3D model and by analytical formulas for the two scenarios in Chapter 6.3.2 and 6.3.3, respectively.

Finally, the new approach will be used to investigate to what extent e.g. the vegetation cover on the gravel island may affect the 3D flow field and related morphodynamic hazards. This allows to detect the upper and lower boundaries of flow forces likely to occur in the vicinity of the EaR dependent on the vegetation density. Last but not least, it is attempted to find indications for the long-term morphodynamic development of the main channel in the case of additional bed load transport (scenario B).

6.3.1 Water levels, water depths and flow field for all discharges

In the following, the 1D water level calculations of the planning state are presented for the three discharges Q1= 671 m³/s, Q2 = 1587 m³/s and Q3 = 4500 m³/s and are discussed together with the depth-averaged velocities and water depths calculated with the 3D numerical model SSIIM 2.0 for the planning state. In order to reveal the impact of the lowering area on the water level in comparison to the *actual* state (without lowering area), the water level of the *actual* state is depicted as well. Finally,

it is shown to what extent an existing vegetation cover on the gravel island might affect the water level in comparison to the gravel island without vegetation cover. Hence, in order to detect the lower boundaries of water level to occur, 1D water levels have been supplementarily computed for the planning state and the gravel island *without* vegetation.

The start water levels of the planning state for the three discharges of interest at the downstream cross-section Rhine-km 200.970 are listed in Table 6-6. It turns out that, at the most downstream location, the influence of the lowering area on the water table is increasing with discharge. While at Q1, a water level decrease of few centimeters is observed, the water level decreases by 18 cm at Q2 and by 60 cm for the extreme event Q3. This outcome can be explained by the circumstance that the cross-sectional flow area increases relatively to the increase of discharge. At Q3, a higher partition of discharge is conveyed via the floodplain and the full cross-sectional extent of the retention area is flooded. At the smaller discharges instead, the major partition of discharge is still conveyed in the main channel while only few parts of the retention area are flooded which leads to a relatively smaller cross-sectional flow area compared to Q3. As a consequence, the impact of the flood protection measure on the water level decrease is less evident.

Table 6-6: Start water levels for the actual and planning state at Rhine-km 200.970.

Q	start water level	
	actual state	planning state (*) Dittrich et al., 2005)
[m³/s]	[m above sea level]	[m above sea level]
671	207.09	207.01
1587	208.95	208.77
4500	213.73	*) 213.12

6.3.1.1 Water levels, water depths and flow field for Q1 = 671 m³/s

Figure 6.5 shows the depth-averaged velocities calculated for Q1 with vegetation on the gravel island. As aforementioned, it can be observed that the area is not completely flooded. It turns out that neither the groyne fields at Rhine-km 200.000 nor the hardwood terrace at Rhine-km 200.450 are inundated yet. Moreover, the EaR Rhinegardens are not affected by inundation. Apparently, the potential hazards according to Table 4-6 are not likely to occur at this event. The flow velocities in the main channel range from 2 – 3 m/s upstream the lowering area. They maximize in the narrow cross-sections at Rhine-km 199.000 and near the gravel island and minimize in the wide section near the retention area down to 1.5 m/s. On the retention area, the effect on flow resistance due to vegetation is clearly evident. Here, the depth-averaged velocities are low and reach values of 0.5 m/s due to the vegetation cover and the cross-sectional widening. In contrast to this, they are higher, up to 1.5 m/s, in the side channel which is free of vegetation. The effect of vegetation resistance is also visible on the EaR gravel island. In that area, the vegetation slows down the flow velocities drastically from values of 2.8 m/s in the main channel to 1.2 m/s on the island. The water depths (Figure 6.6) range between 1 – 1.5 m on the lowering area and 2 – 3 m in the main channel.

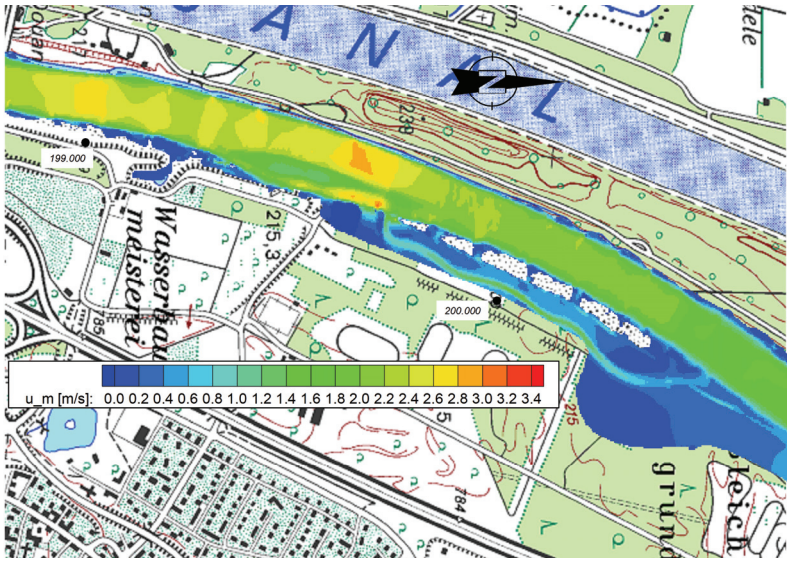

Figure 6.5: Calculated depth-averaged velocities (3D) for Q1 = 671 m³/s with SSIIM 2.0 (planning state).

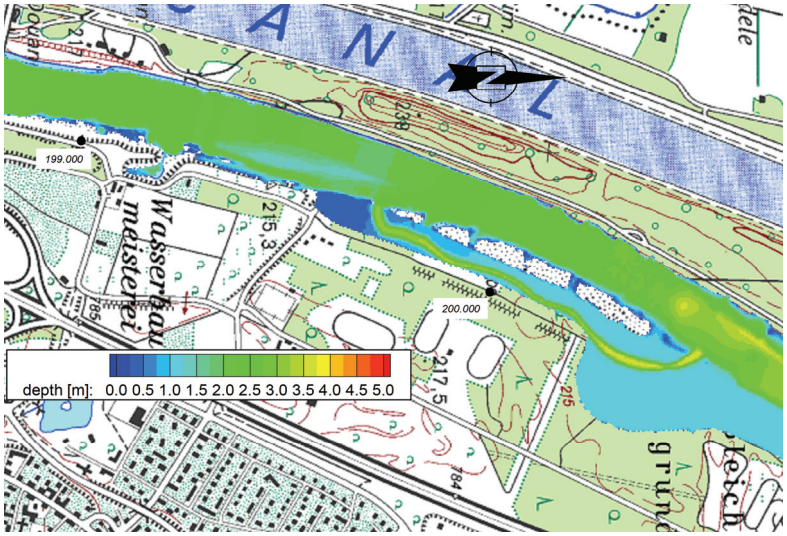

Figure 6.6: Calculated water depths for Q1 = 671 m³/s with SSIIM 2.0 (planning state).

Figure 6.7 shows three different 1D water levels for the discharges Q1. The blue line represents the corresponding water level for Figure 6.5 and Figure 6.6 with vegetation on the island in the planning state. The orange line represents the water level calculated for the gravel island *without* vegetation to investigate whether vegetation on the gravel island has major influence on the water level. Finally, the green line represents the water level for the *actual* state.

Also here, it turns out that the 1D model HEC-RAS is not fully capable of calculating the water levels for the given complex topography. The variations in cross-sectional area and roughness which are apparent in the planning state lead to rapid and not fully reasonable changes in the water table. However, this is not surprising because the cross-sectional spacing chosen for the actual state was maintained in the planning state for reasons of comparability. Simultaneously to the computation of the actual state, a fitting curve was generated for smoothing the water level according to the calculated water table shape. This curve is shown in Figure 6.7 as black line.

The water level gradient is plausibly changing according to the flow field and the topographical variations. The gradient is decreasing in the section of the retention area at Rhine-km 199.600 – 200.500 due to lower flow velocities and the increase of cross-sectional area. Compared to the water level for the *actual* state, the water level in the planning state decreases down to 34 cm maximum. The new approach shows that the flood protection measure might be capable to significantly mitigate the flood situation in the study reach as desired in the IRP.

Moreover, the Hazard Analysis reveals that similar to the actual state, the impact of the vegetation cover on the gravel island on the water level is moderate. This can be shown by comparing the orange line with the blue line. The differences are limited to the area close to the gravel island and further upstream and decrease few centimetres for the situation *without* gravel island.

Furthermore, the new approach enables to investigate to what extent the vegetation cover on the gravel island may alter the 3D flow field as shown in Chapter 6.3.3.6.

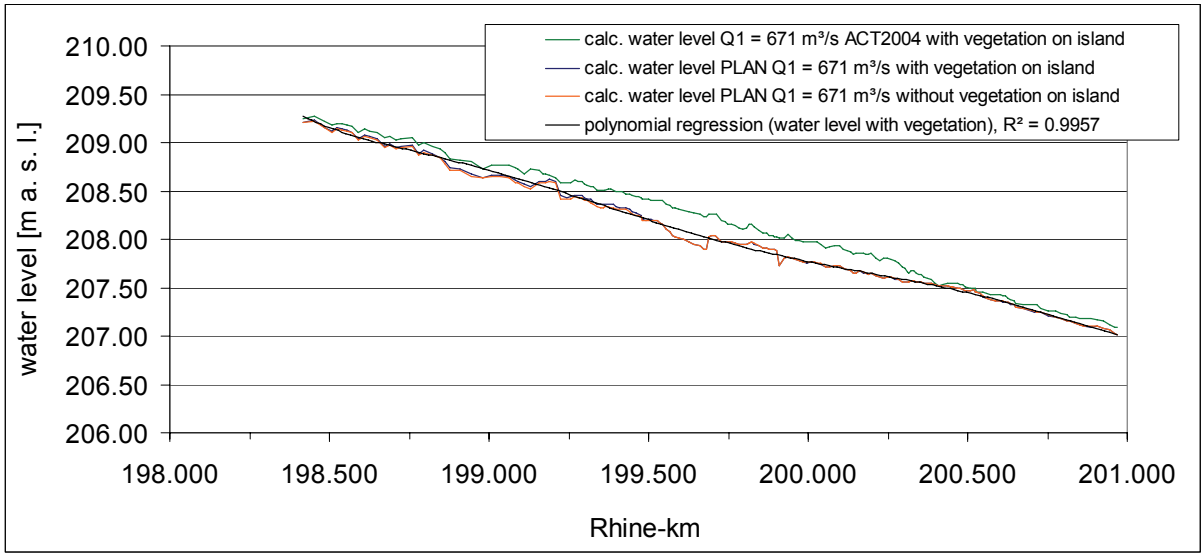

Figure 6.7: Calculated 1D water levels for Q1= 671 m³/s with HEC-RAS 3.1.3 (planning state).

6.3.1.2 Water levels, water depths and flow field for Q2 = 1587 m³/s

The depth-averaged velocities, the water depths as well as 1D water levels for the discharge of Q2 are shown in Figure 6.8 - Figure 6.10. At this discharge, the groyne fields at Rhine-km 199.500 are flooded as well as the sunbathing area and sitting steps of the EaR Rhinegardens. Compared to the discharge Q1, the depth-averaged velocities are increasing up to 3 m/s in the EaR main channel with a maximum of 3.5 m/s in the cross-sectional narrowings near the EaR gravel island as well as near the groyne fields at 199.000. Moreover, the new approach plausibly underlines the impact of both the cross-sectional widening and the vegetation resistance on the flow field: In the main channel in the vicinity of the lowering area, the velocities go down to 2.5 m/s. On the vegetated gravel island, mean flow velocities decrease down to 1.4 m/s while on the lowering area itself, flow velocities decrease down to 0.5 – 0.7 m/s due to the cross-sectional widening and vegetation resistance. They are plausibly higher in the non-vegetated side channel (1.8 m/s). In sum, the mean flow velocities on the lowering area computed for Q2 are comparable with the flow velocities calculated for the lower discharge Q1.

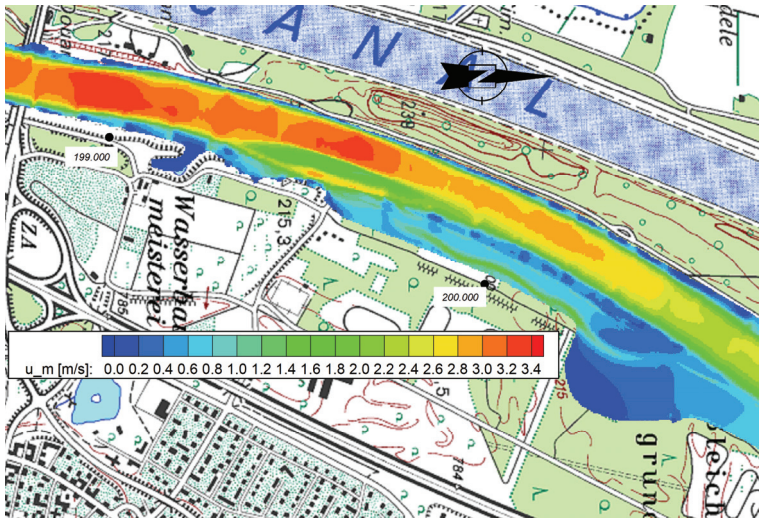

Figure 6.8: Calculated depth-averaged velocities (3D) for Q2 = 1587 m³/s (planning state).

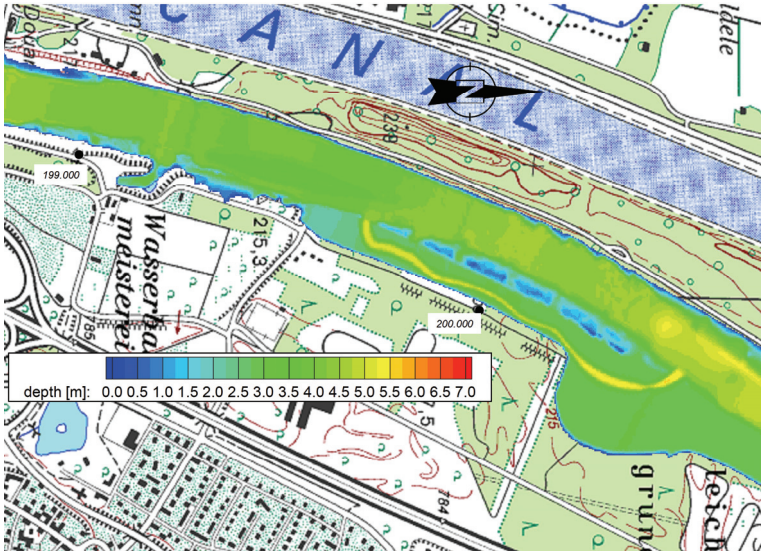

Figure 6.9: Calculated water depths for Q2 = 1587 m³/s (planning state).

Figure 6.10 presents the 1D water levels for the discharge Q2. The blue line represents the water level for the situation *with* vegetation on the gravel island (used as input data for the 3D calculations of velocities and water depths), with the black line as the corresponding regression curve. The orange line shows the water level for the planning situation *without* vegetation on the island. The green line represents the *actual* state. The positive impact of the lowering area on the water table compared to the actual state is clearly evident. The water level decreases by 28 cm which leads to a significiant mitigation of flood water level. Furthermore, the water level gradient is relatively uniform along the river section. It is higher in the upstream section where the discharge is concentrated in the main channel and decreases in the downstream direction near the cross-sectional widening of the retention area.

Comparing the blue line (vegetation cover on the island) with the orange line (no vegetation on the island) is turns out that the impact of the vegetation is relatively low and similar to the lower discharge of Q1 = 671 m³/s. The increase of the water level for the situation with vegetation compared to the situation without vegetation is locally limited and reaches few centimetres. In Chapter 6.3.3.6, the new

approach is further used to analyse whether the vegetation cover on the gravel island may impact the 3D flow field in addition to the water level.

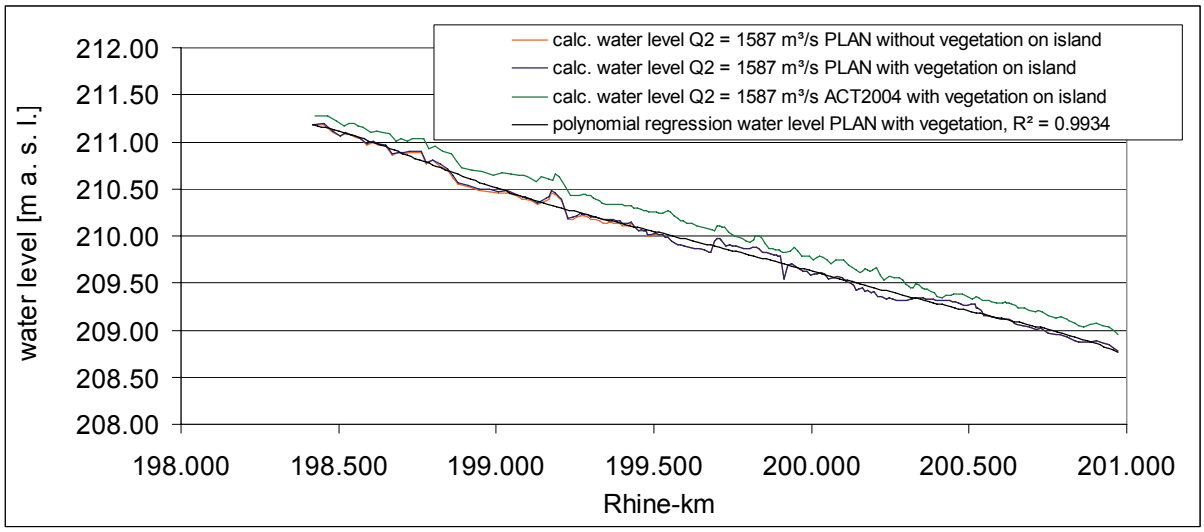

Figure 6.10: Calculated 1D water levels for Q2 = 1587 m³/s (planning state).

6.3.1.3 Water levels, water depths and flow field for Q3 = 4500 m³/s

In the following, the results for the discharge Q3 are presented. The depth-averaged velocities and the water depths are shown in Figure 6.11 and Figure 6.12. The 1D water levels are shown in Figure 6.13. The new approach is capable to reveal in detail how the extreme event would affect the EaRs in the study area: The Rhinegardens including sunbathing area, sitting steps and amphitheatre as well as the lowering area are now completely flooded with water depths of 3 – 5 m and 7.5 m, respectively. As expected for the extreme event, also the flow velocities are significantly increased with values up to 5 m/s in the main channel near the EaR gravel island. It should be noted that the flow field exhibits similar characteristics as plausibly computed for Q1 and Q2: In the vicinity of the cross-sectional widening, flow velocities decrease significantly in the EaR main channel. On the lowering area and in the EaR side channel, flow velocities exhibit the order of magnitude as the flow velocities calculated for the two lower discharges. As aforementioned, this might be due to the fact that the cross-sectional area at Q3 is relatively large compared to Q1 and Q2. This leads to a relative decrease in τ_0 for the extreme event Q3 compared to the two lower discharges.

The 1D water levels are shown in Figure 6.13. The blue line represents the corresponding water level to Figure 6.11 and Figure 6.12 (with the black line as regression curve). Similar to the smaller discharges, the gradient is highest in the upstream section where the impact of the lowering area is lowest. It decreases significantly in downstream direction due to the cross-sectional widening and the flow resistance of the vegetation on the lowering area.

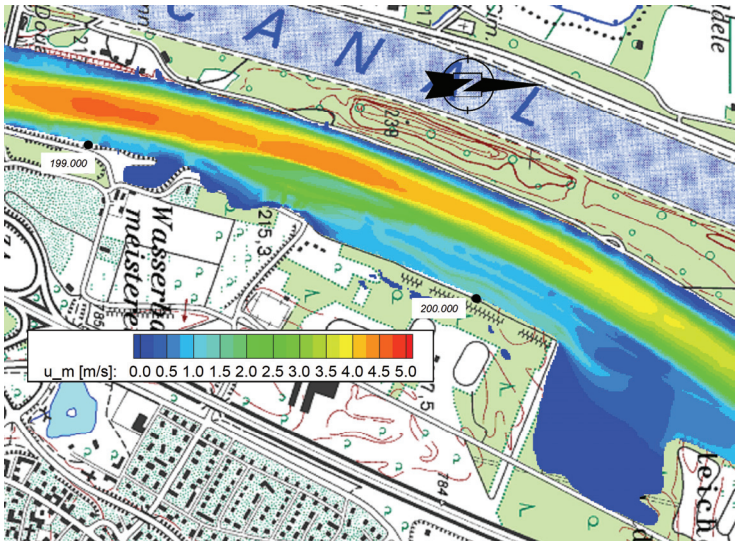

Figure 6.11: Calculated depth-averaged velocities (3D) for Q3 = 4500 m³/s with SSIIM 2.0 (planning state).

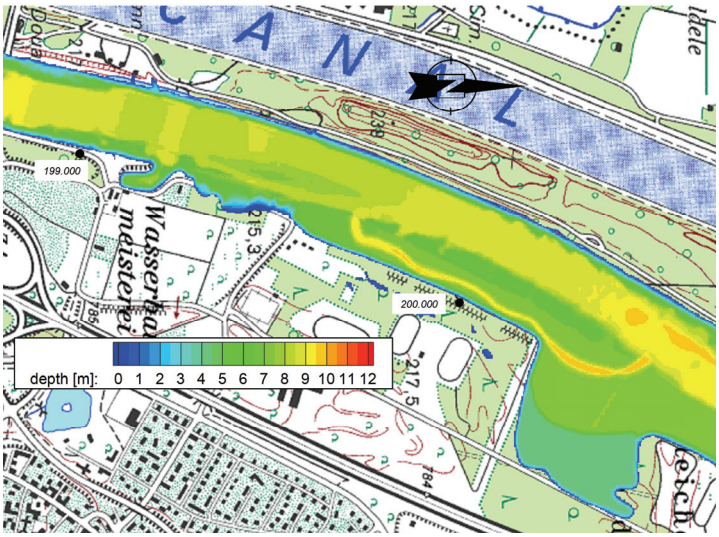

Figure 6.12: Calculated water depths for Q3 = 4500 m³/s with SSIIM 2.0 (planning state).

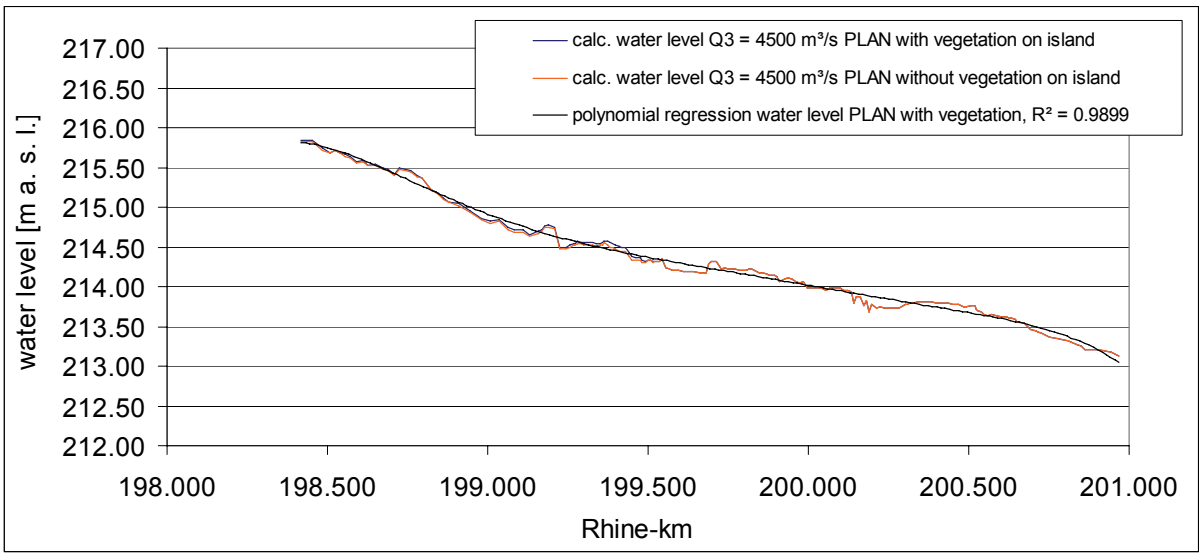

Figure 6.13: Calculated 1D water levels for Q3 = 4500 m³/s with HEC-RAS 3.1.3 (planning state).

6.3.2 Potential morphodynamic hazards without supplementary bed load transport from upstream into the project reach – scenario A

In the aforementioned chapters, the water levels calculated with the 1D programme as well as the water depths and depth-averaged velocities calculated with the 3D programme for the three discharges of interest were presented. Based on this overview, it is now aimed at determining morphodynamic hazards likely to occur in the River section in the planning state for each EaR in detail. The present chapter is discussing the potential hazards for the main channel, the Rhinegardens, the vegetated gravel island, for the side arm between island and German banks, for the retention area and the side channel as well as for the old harbour.

6.3.2.1 Morphodynamic hazards for the EaR *main channel*

According to the PHA Table 4-6, a potential hazard which could endanger the recreation and flood protection measures is the destabilization of the armour layer together with severe erosion, sediment transport and deposition phenomena. In order to estimate the stability of the main channel for the range of discharges, bed shear stresses τ which have been calculated with the 3D model are compared with the critical shear stresses τ_c of the bed material. As aforementioned, the critical shear stresses of the main channel are relatively high due to the armour layer exhibiting values of 64 – 75 N/m². If these values are reached by the bed shear stresses of the flow, erosion processes will be likely to occur. The bed shear stresses of the Rhine section Neuenburg are provided in Figure 6.14 - Figure 6.16 for Q3.

The advantages of the novel methodology are clearly shown. Also here, it is possible to investigate the local flow characteristics and bed shear stresses in detail. The approach reasonably reveals how the flow field and the bed shear stresses derived by the 3D flow field close to the bed and a physically based approach for vegetation resistance are distributed throughout the study area in dependency of geometry and flow resistance and that they exhibit plausible orders of magnitude. The shear stresses are highest in the upstream part of the Rhine section where the flow is concentrated in the main channel and decrease significantly with the cross-sectional widening of the lowering area. Comparing the τ-values to the critical shear stresses, it is indicated that the EaR main channel apparently remains stable for the two smaller discharges Q1 and Q2. Especially in the vicinity of the lowering area, the bed shear stresses are lower than the critical values. Instabilities are only likely to occur in the sections between gravel island and French banks and further upstream. Here, shear stresses close to the critical values are possible. For the extreme event Q3, it must be pointed out that widespread erosion processes must be expected in the main channel along the total River section. The bed shear stresses are significantly higher than the critical values of the main channel material.

6.3.2.2 Morphodynamic hazards for the EaRs *gravel island* and *Rhinegardens*

In the following, the new approach is used to analyse whether and in which way the EaRs gravel island and Rhine gardens might be affected by morphodynamic hazards. As noted in Table 4-6, no morphodynamics are accepted for these EaRs since their functionality is strictly ruled by the municipality plans and recreation concept. Regarding the gravel island, losses could be evoked by erosion of gravel or vegetation cover or by severe sedimentation processes. Regarding the Rhinegardens, water damages due to inundation as well as material destruction by flow forces should be inhibited. Here, losses would consists of e.g. maintenance activities or in the worst case of total

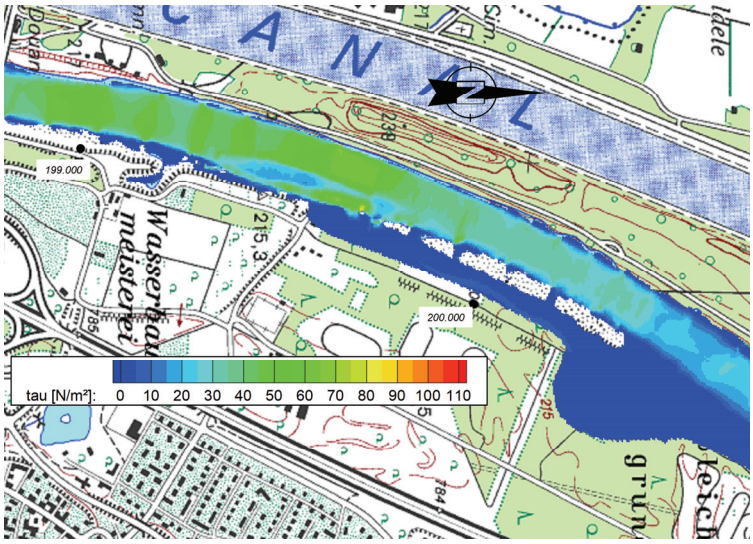

Figure 6.14: Calculated bed shear stresses (3D) for Q1 = 671 m³/s (planning state).

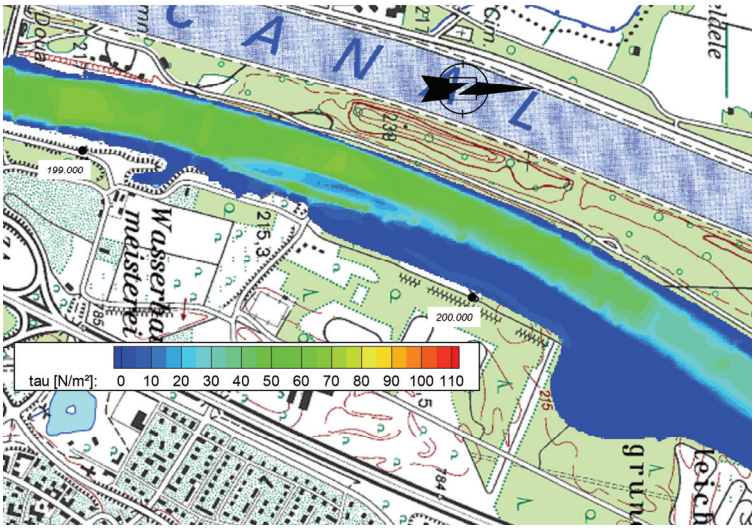

Figure 6.15: Calculated bed shear stresses (3D) for Q2 = 1587 m³/s (planning state).

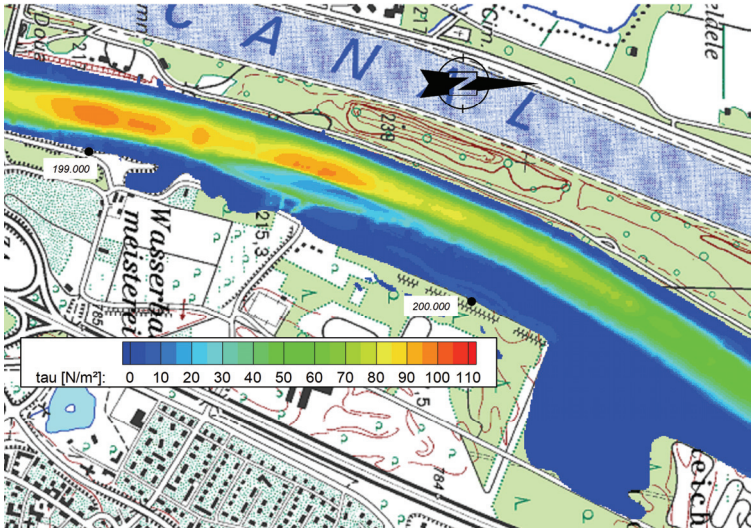

Figure 6.16: Calculated bed shear stresses (3D) for Q3 = 4500 m³/s (planning state).

failure of the recreation concept. A detailed view of the bed shear stresses at the gravel island and Rhinegardens calculated with the 3D model is given in Figure 6.17 - Figure 6.19. In order to visualize

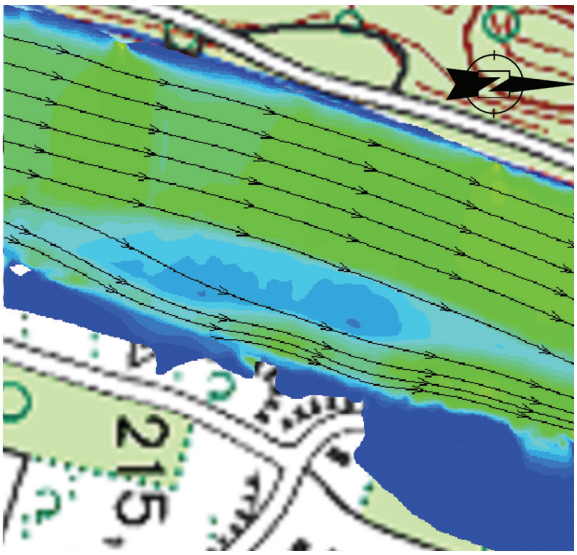

Figure 6.17: Bed shear stresses (3D) for Q1 = 671 m³/s near the gravel island (planning state).

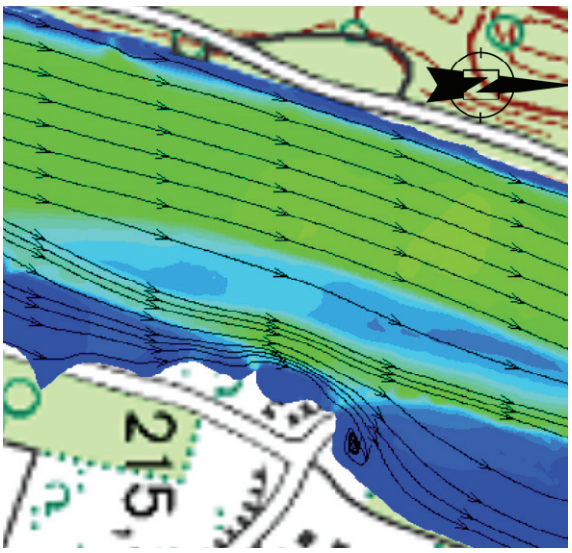

Figure 6.18: Bed shear stresses (3D) for Q2 = 1587 m³/s near the gravel island (planning state).

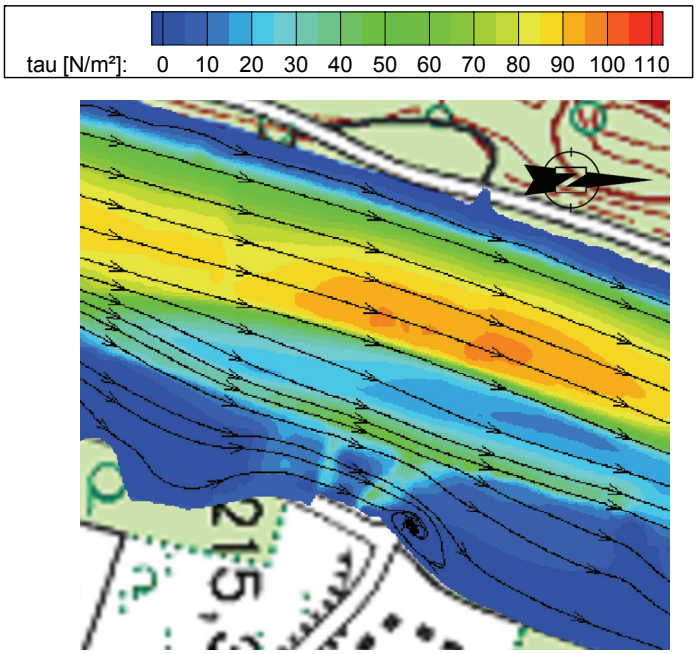

Figure 6.19 Bed shear stresses (3D) for Q3 = 4500 m³/s near the gravel island (planning state).

the governing flow field in detail, the mean flow direction is indicated by streamtraces. The pictures reveal that as already shown for the actual state, the gravel island is acting as an obstruction to the flow: The Hazard Analysis method indicates how the shear stress is reduced on the island due to the vegetation, and concentrated in the main channel between the French banks and the island. This stream concentration is leading to high bed shear stresses which reach the critical values to the effect that here, erosion processes are there likely to occur. Furthermore, bed shear stresses are lower in the side arm between gravel island and Rhinegardens with values of 20 – 50 N/m². It should be underlined that this prognosis is supported by observations made during the flood of 2007 which has been discussed in

detail in Chapter 5.3. Based on these observations, it can be confirmed that maintenance activities may be required at higher flood events in order to maintain water conveyance in the side arm as envisaged in the municipality plans. Concerning the EaRs Rhinegardens, the computations show moderate shear stresses which are supposed to be mainly due to the soft bank flattening and the local cross-sectional widening. In sum, it turns out that the bed shear stresses on gravel island, side arm/German side and Rhinegardens do not differ significantly among the three discharges.

The critical shear stresses for the EaRs main channel, the gravel island and Rhinegardens are summarized for clarity repetitively in Table 6-7. It turns out that according to the 3D calculations and the analytical approaches both the gravel island and the Rhinegardens remain stable at all discharges. Apparently, erosive processes do not play a major hazardous role in these locations.

Table 6-7: Critical shear stresses of morphological features in the planning state.

critical shear stress [N/m²]	Elements at Risk			
	main channel (armour layer)	side channel (loose gravel)	Rhinegardens (lawn)	retention area, gravel island (roots of willows and earls)
τ_c	64 – 75	10 – 20	15 – 30	60 – 140

6.3.2.3 Morphodynamic hazards for the EaR *side channel* on the *lowering area*

In the scenario A which is in the focus of the present section, bed load transport can be neglected in the study site due to the reduced discharge dynamics, the weir operation at Kembs upstream of the reach, fixed river banks and the relatively stable bed of the main channel. But it must be emphasized that suspended sediment is transported with the flow into the river section and can therefore have a significant impact on morphodynamics via deposition and siltation in areas of low flow as well as via filtering by vegetation. On the one hand, the deposition of this fine material is required for the development of the floodplain forest on the lowering area. On the other hand, however, an enhanced sedimentation can influence the retention volume. In order to control sedimentation, the side channel is planned on the lowering area which is desired to provoke a flush out of the fine sediment at all discharge conditions. The functionality of the side channel can be assessed by the investigation of the flow velocities and bed shear stresses obtained with the Hazard Analysis tool.

It turns out that mean flow velocities are in the same order of magnitude for all three discharges. Figure 6.20 - Figure 6.23 provide a detailed view of the flow field (depth-averaged velocities) in the side channel and on the lowering area exemplarily for Q1 and Q2.

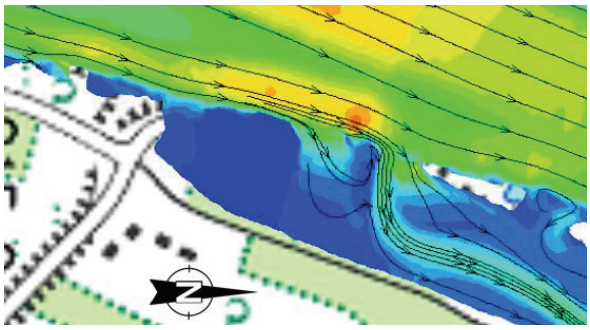

Figure 6.20: Depth-averaged velocities (3D) for Q1 = 671 m³/s near the inlet of the side channel and gravel island (planning state).

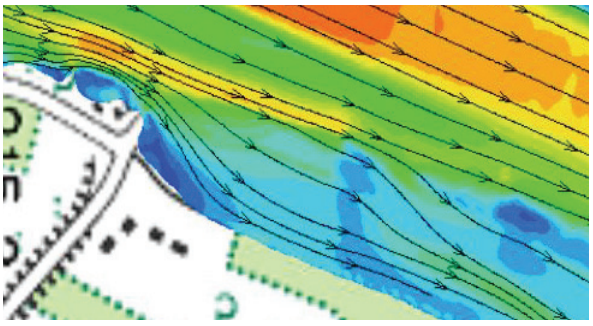

Figure 6.21: Depth-averaged velocities (3D) for Q2 = 1587 m³/s near the inlet of the side channel and gravel island (planning state).

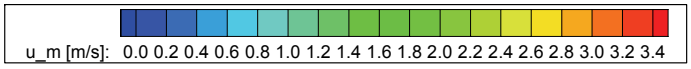

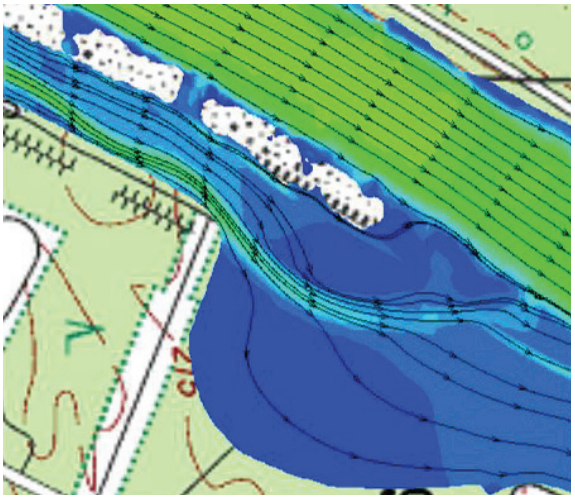

Figure 6.22: Depth-averaged velocities (3D) for Q1 = 671 m³/s on the lowering area (planning state).

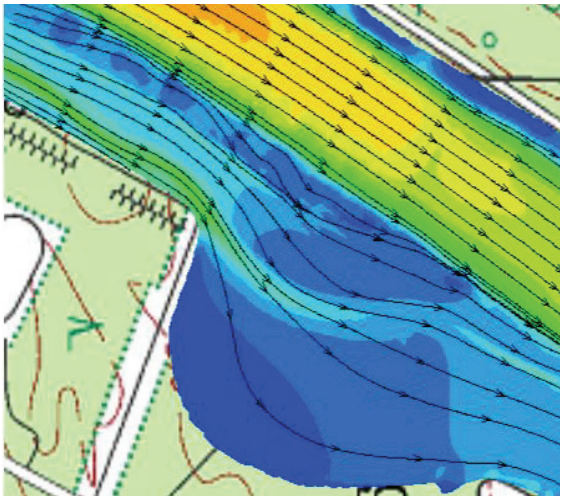

Figure 6.23: Depth-averaged velocities (3D) for Q2 = 1587 m³/s near the outlet of the side channel (planning state).

The new approach enables to detect in detail that the flow field is well developed in accordance with the plans. As desired, the non-vegetated side channel exhibits significantly higher mean flow velocities (up to 1.8 m/s) in comparison with the vegetated floodplain. Obviously, neither the discharge capacity nor the free flow are affected. A comparison of the flow field in the inlet of the side channels for both discharges reveals that the inlet is more active for Q1 than for Q2. Apparently, at Q1, water is conveyed into the channel more easily and more directly than at Q2. At Q2, water is directed parallel to the inlet due to the higher inundation extent. This aspect may show that the proper functioning is well assured also for low and frequent discharges. In order to investigate this further, the extent of hazardous sedimentation in the side channel as well as the sedimentation behaviour of transported fine particles in the side channel shall be roughly assessed with the Rouse approach (Wang and Dittrich, 1992). The smaller the Rouse number z, the higher the probability that the sediment is transported through the channel without forming layers of deposition. If bed material is destabilized and $z > 5$, the material is transported along the river bed as bed load. If z is in the range $0.1 < z < 3$, the sediment is kept in suspension and transported through the channel with almost no contact with the river bed. If z decreases to $z < 0.06$, no contact exists with the river bed and the sediment is washed out of the channel. The sink velocity of the fine material in suspension can be well approximated by

the sediment of the groyne fields. With the approach of Zanke (1977) and the grain size distribution of the aforementioned material, a sink velocity of u_s = 0.014 m/s is obtained. Taken the range of the bed shear stresses in the side channel into account (3 – 10 N/m²) the Rouse number is calculated to 0.35 – 0.64. Evidently, these values are well in the range of suspended sediment transport. Thus, it can be concluded that the fine sediment particles are kept in suspension and are to a high percentage transported out of the side channel at all investigated discharges.

Further it shall be analysed whether hazardous channel shifting or transport processes in the side channel can be expected. Since the river plans envisage to pave both the inlet and outlet to prevent severe erosion, these areas may be neglected in the following. For the aforementioned objective, the bed shear stresses in the side channel computed with the 3D numerical model (3 – 10 N/m²) and the critical shear stresses of the loose gravel (10 – 20 N/m²) are compared. It turns out that sediment transport might be locally initiated in the side channel. Moreover, these eroded particles may be deposited further downstream and near the outlet of the side channel since here, bed shear stresses decrease and might even fall below the critical shear stresses of loose gravel. As a result, sedimentation cannot be excluded. In order to assure the functionality of this important EaR, monitoring and maintenance activities may be required. But it is worth noting that given the dense vegetation cover on the banks reinforcing the material, severe channel shifting may not to be expected.

In the case local dredging activities are carried out accordingly, the functionality of the side channel is apparently assured in the light of the considered boundary conditions.

6.3.2.4 Morphodynamic hazards for the EaR *flood retention area*

In this section, the focus is placed on the morphodynamic processes affecting the lowering area at the relevant discharges. The PHA underlines that main hazards would be related to the retention effect and the retention volume since both are of fundamental importance for reliability of the flood protection and must be inhibited under all circumstances. Morphodynamic hazards in this sense consist of severe sedimentation of the lowering area as well as of erosion of the floodplain forest. At this point it should be emphasized that also the proper development of young willows and pioneer vegetation might play a significant role for morphodynamics of the retention area directly after excavation. As this aspect however, goes beyond the scope of the present study, it should be in the focus of further research as it is the basis for a proper development of the floodplain forest and subsequently of reliable flood protection.

For the present analysis, Figure 6.14 - Figure 6.16 may be considered once again showing the bed shear stresses in the floodplain for the discharges of interest. It turns out that bed shear stresses do not significantly vary for the three flow events, only the inundation extent changes. Figure 6.24 and Figure 6.25 give a more detailed view of the bed shear stresses and mean flow velocities exemplarily for the extreme event Q3. Also here, the potential of the new Hazard Analysis tool becomes evident. The flow velocities and bed shear stresses are rather low due to the vegetation resistance and hardly reach values of 0.1 m/s and 2.5 N/m², higher values can be found only in the non-vegetated side channel. It can be concluded that the erosion of mature floodplain forest event for the extreme event is not likely and therefore could be judged as of minor importance for risk management. Nevertheless, these low u_m and τ_0 can distinctly enfavour sedimentation processes on the retention area with all consequences as listed in the PHA Table 4-6.

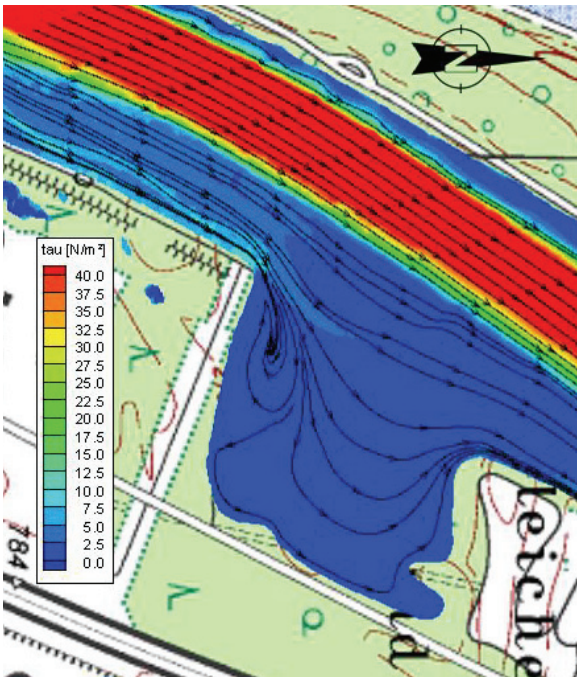

Figure 6.24: Bed shear stresses (3D) computed on the lowering area exemplarily for Q3 = 4500 m³/s.

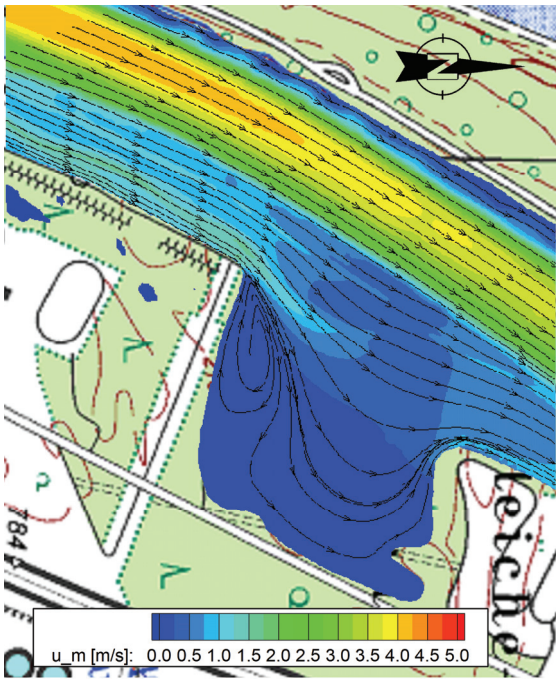

Figure 6.25: Depth-averaged flow velocities (3D) computed on the lowering area exemplarily for Q3 = 4500 m³/s.

At this point, an important remark has to be made. It must be expected that after the peak discharge - or in other words with decreasing flood wave - shear stresses decrease beyond those τ_0 showed in Figure 6.24. Consequently, sedimentation processes might be initiated as widely observed on the vegetated groyne fields today. Given the high severity regarding the proper functionality of the retention area, sedimentation processes should always be accurately monitored in the field to be on the safe side. This recommendation is underlined by the subsequent Chapter.

6.3.2.5 Morphodynamic hazards for the EaR *old harbour*

An important question for the planners concerns the morphodynamic development of the ancient harbour. The old harbour is located upstream of the Rhinegardens and the gravel island. In the planning state, the harbour is dredged out in order to provide a place for small boats and canoos. However, it is not clear up to now whether the harbour design is sustainable or whether the probability of silting is so high that maintenance work is required. Figure 6.26 and Figure 6.27 show the near-bed and depth-averaged velocities for the old harbour and the streamtraces exemplarily for the discharge Q2. The advantages of the novel Hazard Analysis tools are repetitively confirmed. The computations reveal in detail that flow velocities are very low in the harbour basin. The flow circulates with values < 0.5 m/s for all discharges. The situation is similar to the flow field at the actual state. Given this, a slow siltation of the harbour is likely to occur under the present boundary conditions with the consequence that losses due to maintenance must be expected in order to meet the desired functionality of a berth as touristic attraction. This fine suspended material can be transported via the secondary currents into the basin where it may be trapped and deposited due to low flow velocities. This development has already been observed in the old harbour up to now since it has been silted up in the course of the last decades.

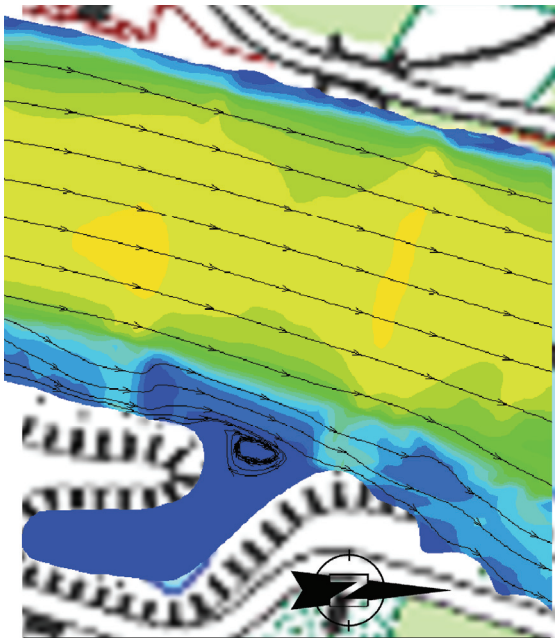

Figure 6.26: Near-bed velocities for Q2 = 1587 m³/s at the old harbour (planning state).

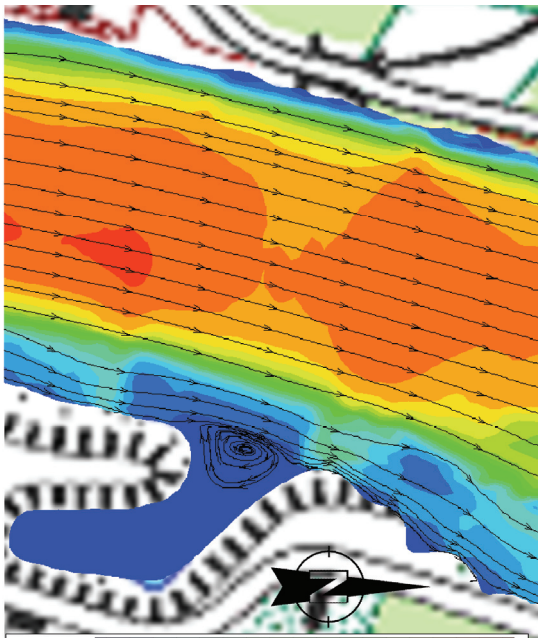

Figure 6.27: Depth-averaged velocities (3D) for Q2 = 1587 m³/s at the old harbour (planning state).

6.3.2.6 Summary scenario A

It could be shown in the last sections that by means of the novel Hazard Analysis method it is possible to plausibly estimate morphodynamic hazards for restoration and flood protection projects of natural gravel-bed rivers with vegetated areas. The outcomes show reasonable orders of magnitude concerning water levels, hydraulic flow field and bed shear stresses and could be further confirmed by field observations.

In order to systematically continue in the Risk Management framework, the outcomes of the previous sections must be clearly documented. For this objective, it was decided to pick up the original PHA table and continue it in a modified version, see Table 6-8. For each EaR, the potential morphodynamic hazards are repeated once again. Based on the results, it is further summarized whether or not these hazards are likely to occur at the investigated discharges.

But before working with Table 6-8, an important remark should be made. The Hazard Analysis has investigated peak discharges for a range of typical events. The range of discharges is able to indicate and cover the outer boundaries of processes which might occur at the study site. But of course, a flood event does not consist of a peak only, but is time-variant with a part of rising discharge and a tail of decreasing discharge and numerous sequences of those. As a consequence, also the occurrence of morphodynamics hazards varies accordingly. Due to the high complexity among discharge dynamics, sediment transport and vegetation, morphodynamics of natural rivers with vegetation cannot be forecasted in hard figures up to now (see also Chapter 3.2). A detailed prognosis is therefore not reliable and is not claimed in the present study. Hence, it should be emphasized that Table 6-8 does not provide probability of occurrences for the hazards but provides plausible tendencies based on physically based approaches and 3D scales which could be repetitively confirmed and validated by

field data and observations. The new method might help to improve the system understanding, to gain new important insights, and as a consequence to sensibilize for potential hazards.

Table 6-8: Summary of morphodynamic processes for each EaR detected with the Hazard Analysis tool and the scenario A.

Number	Element at Risk	hazards morphodynamic processes	occurrence at Q1	occurrence at Q2	occurrence at Q3	severity
1	old harbour	• sedimentation of particles	yes	yes	Yes	moderate
		• sedimentation of particles	no	no	No	high
2	gravel island	• erosion of vegetation	no	no	No	high
		• erosion of gravel	no	no	No	high
3	side arm	• sedimentation of suspended particles	no	no	No	moderate
4	Rhinegardens					
	sunbathing area	• erosion, sedimentation	no	no	No	high
		• inundation	no	yes	Yes	high
	theater	• inundation/erosion	no	no	yes/no	high
	restaurants	• inundation, erosion	no	no	No	high
5	lowering area	• sedimentation of particles	yes	yes	Yes	highest
		• erosion of vegetation	no	no	No	highest
6	side channel					
	inlet	• sedimentation of particles	no	no	No	highest
	reach	• sedimentation of particles	no	no	No	highest
		• erosion of gravel	yes	yes	Yes	highest
	outlet/widening	• sedimentation of particles	yes	yes	Yes	highest
7	main channel					
	near gravel island	• destabilization of armour layer, river bed erosion, initialization of bed load transport	no	yes	Yes	very high
	else	• destabilization of armour layer, river bed erosion, initialization of bed load transport	no	no	Yes	very high

It turns out that the Hazard Analysis has revealed some new aspects which have not been evident at the beginning. For example, some morphodynamic processes which had been expected to be harming in the Risk Identification phase could be classified as less hazardous or less likely (such as erosion of vegetation on the gravel island and on the retention area or the destruction of the sunbathing area). Nevertheless, the Hazard Analysis has confirmed some morphodynamic processes as hazardous (e.g. the siltation of the harbour). Furthermore, the spatial distributions of bed shear stresses and the 3D flow field obtained with the Hazard Analysis technique shifted additional processes in the focus of

further Risk Management which have not been evident before. These are e.g. the outlet of the side channel as well as the destabilization of the main channel at high discharges near the gravel island. In sum, it can be concluded that Table 6-8 well indicates hot spots of morphodynamic hazards which might support the development of optimization already in the planning state.

6.3.3 Potential morphodynamic hazards considering supplementary bed load transported from upstream

In the last chapter the morphodynamic development of the River section Neuenburg was estimated and assessed for the scenario A with boundary conditions which are apparent in the river section nowadays. Morphodynamics are restricted in the actual state due to the low discharge dynamics, the fixed banks and the stable Rhine bed. In the following, the scenario B is in the focus of interest. Scenario B aims at prognosticating how the river reach would develop in the case that bed load transport was initialized upstream. The question must be answered because additional sediment transport and associated sedimentation processes might affect the functionality of all river measures planned in the study reach under the flow conditions. As reported previously, bed load cannot be completely excluded. Coarse gravel might be transported into the Rhine section Weil-Breisach in the case of a large flood event given that the sluices at weir Kembs are lowered to unload the Canal d'Alsace. Moreover, the investigation of scenario B is necessitated by additional restoration plans in France. The French electricity company which is responsible for the power generation at the barrage Kembs envisages local bank erosion sites on the French Rhine side upstream and downstream of the study reach in order to improve the morphodynamic situation and biodiversity in the main channel.

In the present chapter, it is being analysed whether and how material that is transported into the study site Neuenburg might impact the morphodynamic situation of the river Rhine in the planning state. The boundary conditions have been clearly defined in Chapter 4.3.3 and Table 4-5. The detection of morphodynamic hazards is following the procedure applied in the previous chapter based on the 1D/3D hydrodynamic calculations for the three discharges Q1 = 671 m³/s, Q2 = 1587 m³/s and Q3 = 4500 m³/s. The simulation results are interpreted in the now well-known way such that the critical shear stresses of potentially transported bed load sediments are compared to the bed shear stresses and the flow field. Consequently, potential areas of sedimentation can be identified and the further development of the reach can be prognosticated.

6.3.3.1 Characterization of sediments potentially transported as bed load from upstream

Prior to the interpretation of the simulations, the material which might be transported into the case study Rhine-section 198.410 – 200.970 must be accurately characterized. As aforementioned, field data and grain size distribution of loose gravel originating from upstream or the French banks are not available. But it can be assumed that the sediments which are potentially eroded by the banks and/or transported can be represented by the grain size distributions of the loose gravel present in the gravel pits Bremgarten, Grissheim and Hartheim. The loose material typical for the Upper Rhine is repetitively presented in Figure 6.28 showing the sieve curve of both gravel pits Grißheim and Hartheim as well as the mean sieve curves for all three gravel pits. Also regarding Chapter 3, it must be underlined that the approaches for transport and sedimentation behaviour and, thus, for critical

shear stresses are among others, highly dependent on the chosen grain diameter. In order to estimate the transport behaviour in the Rhine section as accurately as possible, the sieve curve is therefore divided into fractions as shown in Figure 6.28 and as listed in Table 6-9. Hence, the heterogenity of the material can be considered and the transport behaviour can be estimated in more detail. Each fraction in Figure 6.28 covers a limited range of grain diameters for which a d_{50} is determined. The d_{50} is then used to calculate the critical shear stress per fraction with the approach of Wilcock et al. (1996). Furthermore, a mass proportion can be assigned to each fraction. This methodology enables a rough estimation of how much is transported or sedimentated of each fraction relatively to the total mass.

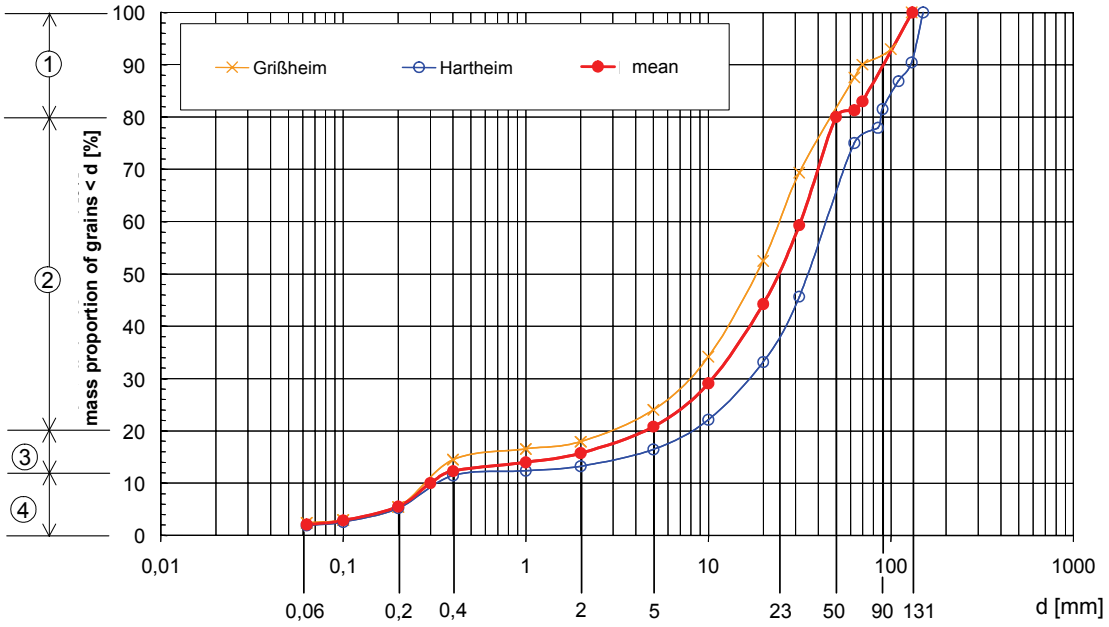

Figure 6.28: Sieve curves of loose bed material and classified grain fractions for two gravel pits on the German Rhine side.

Table 6-9: Grain fractions and characteristic grain parameters of the loose bed material (see Figure 6.28).

fraction	mass proportion of grains [%]	grain fractions [mm]	d_{50} [mm]	τ_c Wilcock et al. (1991) [N/m²]
1	20	50 - 131	90	51
2	60	5 - 50	23	13
3	8	0.4 - 5	2	1
4	12	0.06 - 0.4	0.2	0.1

Moreover, it must be pointed out that the amount and the grain sizes of the sediment which is released from the river banks and transported through the channel are highly dependent on the discharge dynamics, the local flow field and the interaction between sediment and vegetation upstream of the investigated Rhine section. Up to now, these interactions cannot be quantified due to their high complexity and remain a field of research. Nevertheless, the present study provides an appropriate tool to estimate the morphodynamic hazards of the study section as accurately as possible according to the latest status of science. This methodology is now applied to prognosticiate morphodynamic hazards

for the major EaRs in the planning state: the gravel island, the recreation area Rhinegardens, the side channel on the retention area and the old harbour.

6.3.3.2 Impact of additional sediments on the EaRs *gravel island*, the *Rhinegardens* and the *side channel*

To estimate the development of the recreation area, the bed shear stresses calculated with the novel approach are compared to the critical shear stresses of the loose bed material, see Figure 6.29 and Table 6-9, respectively. As shown previously, the flow field at the Rhinegardens, gravel island and the side channel inlet on the lowering area does not differ significantly among the three discharges. Therefore, Figure 6.29 presents the bed shear stresses and streamtraces computed for this section exemplarily for the discharge Q2= 1587 m³/s.

It turns out that additional sediment input might impact the morphology and therefore the sustainability of the planned measures in this area to a large extent. Comparing the bed shear stresses caused by the flow with the critical shear stresses of the loose bed material, three critical zones can be identified (highlighted in Figure 6.29 with circles).

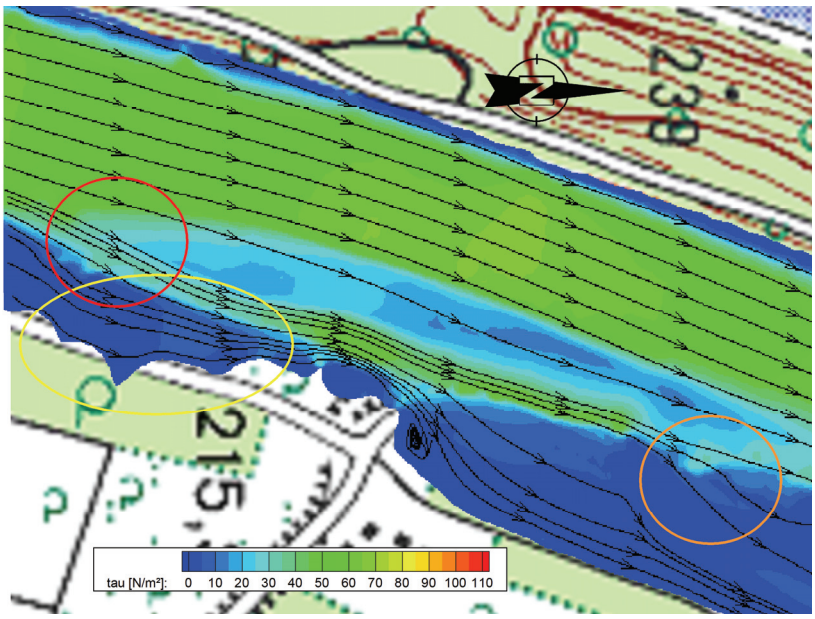

Figure 6.29: Bed shear stresses (3D) for Q2 = 1587 m³/s near the gravel island and critical locations of deposition (planning state).

The EaRs gravel island as well as the side arm between the gravel island and the Rhinegardens (indicated in red) show relatively low bed shear stresses (around 30 N/m²). Regarding Table 6-9, it can be concluded that larger grain sizes (fraction 1) are likely to be deposited in this area which in turn could cause zones of sedimentation in the side arm. The bed shear stresses in the EaR Rhinegardens (indicated in yellow) are lower with values < 5 N/m² with the consequence that sandy fractions may be deposited there. Thus, also this zone apparently would require regular maintenance. At lower discharges which appear almost all year long (≤Q1 = 671 m³/s), the Rhinegardens are not flooded and are therefore not directly affected.

The orange circle indicates the inlet of the side channel / lowering area. Also this indicated zone is at high possibility of deposition in the case that additional sediments are transported into the study

section from upstream. The bed shear stresses calculated with the 3D model are low for all discharges (~ 5 N/m²) so that sedimentation processes are likely to occur. To assure the functionality of the side channel, regular maintenance work would be expected.

6.3.3.3 Impact of additional sediments on the EaR *old harbour*

Chapter 5.3 and Chapter 6.3.2.5 show that the old harbour has a high probability of siltation with suspended sediment at all investigated discharges. The bed shear stresses and depth-averaged velocities calculated by the 3D model as well as the streamtraces are shown again exemplarily for Q2 = 1587 m³/s in Figure 6.30 and Figure 6.31. By comparing the bed shear stresses with those reported in Table 6-9, it turns out that both the flow velocities and bed shear stresses are high enough to transport finer fractions of the bank material towards the basin following secondary currents. It should be further noted, that in addition to the deposition of suspended sediment, the deposition of fine bed load is likely to occur at all discharges as well. The results show that the harbour might have an enhanced probability of silting by both suspended sediment and bed load material. Subsequently, consequences in terms of e. g. maintenance work can be expected to be required at least in order to ensure the use of the basin for touristic purposes in the long-term.

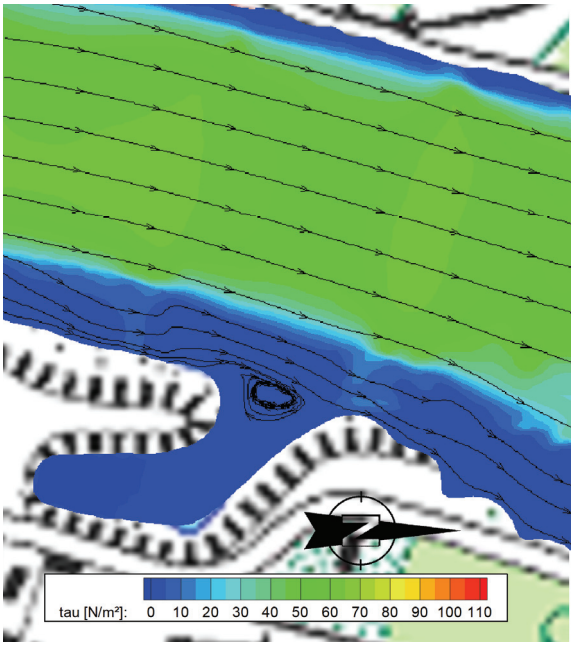

Figure 6.30: Bed shear stresses (3D) for Q2 = 1587 m³/s at the old harbour (planning state).

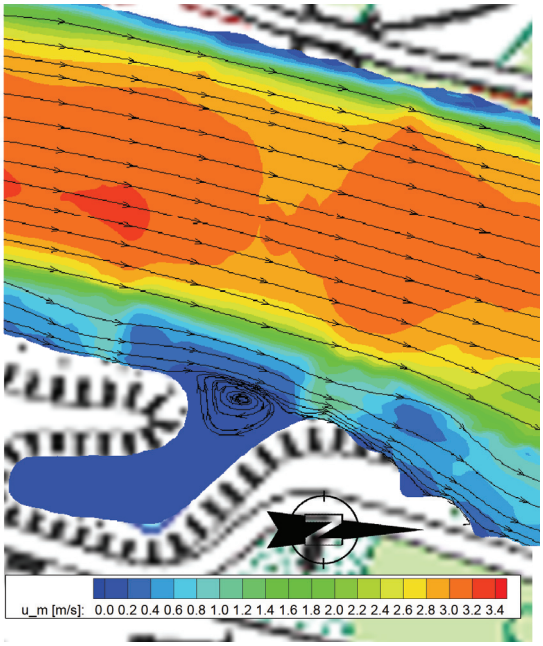

Figure 6.31: Depth-averaged velocities (3D) for Q2 = 1587 m³/s at the old harbour (planning state).

6.3.3.4 Impact of additional sediments on the EaR *main channel*

Nowadays, the river Rhine at Neuenburg is more or less an uniform channel with few sediment dynamics and low biodiversity due to the reasons mentioned above. However, additional sediments released from the French banks can have a significant impact on the morphology of the main channel. In this section, it is discussed whether in the long-term, bed load transport could lead to morphodynamic hazards in the main channel. For this task, the critical shear stresses of the loose bed material listed in Table 6-9 are compared to the bed shear stresses of the main channel calculated with

the 3D programme. As the long-term morphodynamic development is mostly predominated by the discharges which appear more frequently (1 – 2 years' events), the present chapter refers to the bed shear stresses of Q1 and Q2 (period of occurrence 9 days/year and 1day/year, respectively). They are shown in Figure 6.32 and Figure 6.33 repetitively. At both discharges, the bed shear stresses are relatively high in the upstream part due to the concentration of flow in the main channel. They are decreasing in the downstream direction reaching values lower than the critical shear stress of the larger and mean grain fractions (see Table 15). It can be concluded that almost all fractions likely to be transported into the reach are transported further through the channel until the bed shear stresses decrease in the cross-sectional widening of the lowering area. There, most of the transported material is likely to be deposited (indicated in red), especially at the discharge Q1. At the higher discharge Q2, the calculated bed shear stresses reach again the critical values of about 70 % of the loose bed material. Thus, the conclusion can be drawn that sediment dynamics with re-erosion and re-deposition of sediment could be enabled along the main channel during the year. It should be emphasized that the impact of bed load transport on the discharge capacity of the main channel cannot be forecasted in hard figures herein because of the large complexity involved and because the amount of transported sediments is not yet clear. In any case it can be stated, that sedimentation phenomena would be likely to appear in the cross-sectional widening which may require monitoring programmes or maintenance activities. In the case the French plans with bank erosion upstream sites will be concretized, an additional Hazard Analysis would be necessitated using an enhanced data basis and more detailed information on boundary conditions for this scenario. It should be kept in mind, that however, deposition features can initiate and amplify morphodynamics further by directing the flow towards the river banks potentially leading to severe consequences as it is well-known for e.g. alternate bars (Solari, 2005; Zarn, 2008). Although the river banks on the French side are widely protected by embankments as well as the German side by the Leinpfad in the earlier stage of the project, these processes should not be neglected but accounted for in the planning procedure.

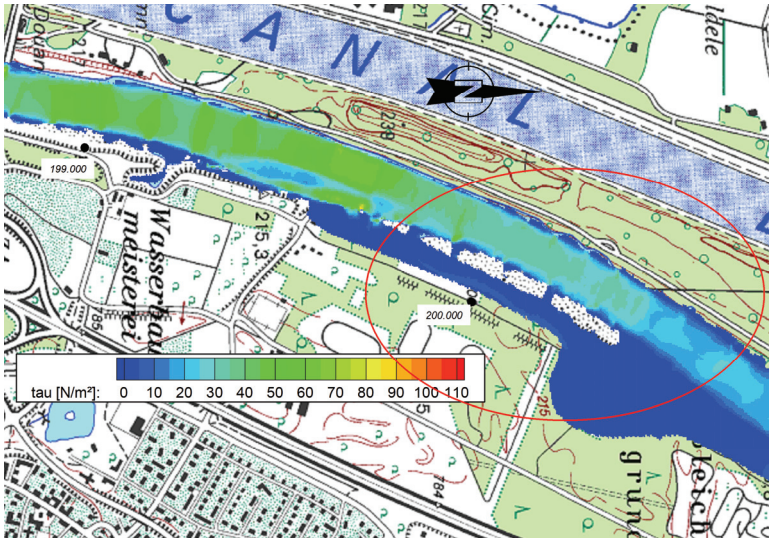

Figure 6.32: Bed shear stresses (3D) for Q1 = 671 m³/s and critical locations of deposition (planning state).

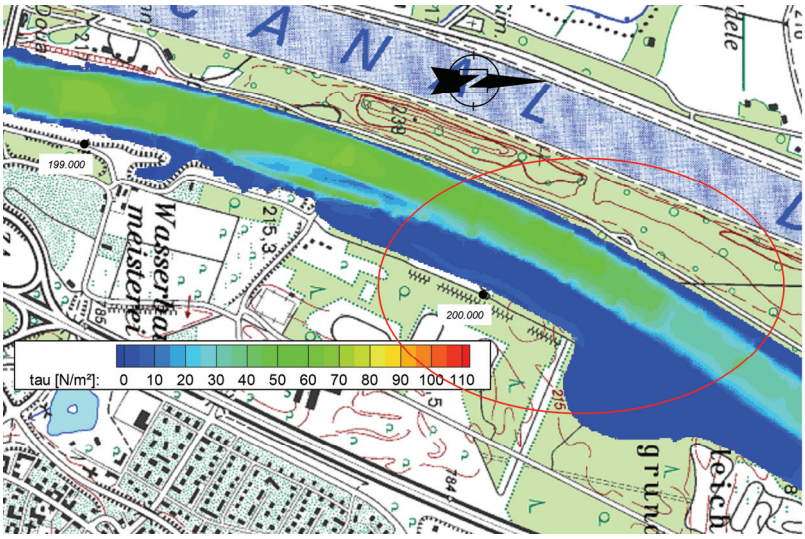

Figure 6.33: Bed shear stresses (3D) for Q2 = 1587 m³/s and critical locations of deposition (planning state).

6.3.3.5 Summary scenario B

In the following, the outcomes of the Hazard Analysis / scenario B are summarized so that they can be used for the consecutive steps of the Risk Management framework. The modified PHA table for scenario B is indicated in Table 6-10. Based on the results, it is further summarized whether or not these hazards are likely to occur at the investigated discharges. Here, the reader may remember the important remarks stated for scenario A: Due to the high complexity among discharge dynamics, sediment transport and vegetation, morphodynamics of natural rivers with vegetation cannot be predicted in hard figures up to now. A detailed forecast is therefore not reliable and is not claimed in the present study. But Table 6-10 enables to reveal reasonable tendencies of morphodynamic hazards which have been derived with a sound data basis, detailed calibration and verification techniques and physically based approaches on 3D scales. As a conclusion, it can be shown that the new methodology might help to reveal and identify risk on local scales and might sensibilize for potential hazards which is crucial for the reliability and sustainability of river projects.

Comparing this scenario B with scenario A it is evident that initiated bed load transport may change the morphodynamic features significantly. Widespread sedimentation processes can be expected which may require maintenance activities or/and monitoring programmes. One example is the old harbour. Here, sedimentation processes of fine suspended material are likely to occur frequently, see also scenario A. However, in the case additional coarse sediments are transported into the reach, siltation may be accelerated and related damages even more severe. Second, the area near the side arm between gravel island and Rhinegardens was identified as second hot spot of morphodynamic hazards. In the side arm, τ_0 are so low that coarse and sandy fractions may be deposited. As a consequence, dredging activitivies may be required to sustain the situation as desired in the recreation plans, namely the side arm should be open for conveying water. Also the sunbathing area might be put at harm since the area is flooded at higher discharges and sedimentation of mainly sandy fractions are likely. In sum, it can be concluded from the results that initiated bed load transport may significantly affect the scenery of the recreation area. Finally, the analysis revealed that also the

Table 6-10: Summary of morphodynamic processes for each EaR detected with the Hazard Analysis tool and the scenario B.

Number	Element at Risk	hazards morphodynamic processes	occurrence at Q1	Q2	Q3	severity
1	old harbour	• sedimentation of particles	yes	yes	yes	moderate
		• sedimentation of particles	yes	yes	yes	high
2	gravel island	• erosion of vegetation	no	no	no	high
		• erosion of gravel	no	no	no	high
3	side arm	• sedimentation of suspended particles	yes	yes	yes	moderate
4	Rhinegardens					
	area	• erosion	no	no	no	high
		• inundation, sedimentation	no	yes	yes	high
	theater	• inundation/erosion	no	no	yes/no	high
	restaurants	• inundation, erosion	no	no	no	high
5	lowering area	• sedimentation of particles	yes	yes	yes	highest
		• erosion of vegetation	no	no	no	highest
6	side channel					
	inlet	• sedimentation of particles	yes	yes	yes	highest
	reach	• sedimentation of particles	yes	yes	yes	highest
		• erosion of gravel	yes	yes	yes	highest
	outlet/widening	• sedimentation of particles	yes	yes	yes	highest
7	main channel					
	near gravel island	• destabilization of armour layer	no	yes	yes	very high
		• sedimentation	no	no	no	very high
	else	• destabilization of armour layer	no	no	yes	very high
		• sedimentation	yes	yes	no	very high

inlet of the side channel might be a critical location of sedimentation with all consequences related to a proper functionality of the flood retention area. Although the river project envisages the inlet to be located several decimetres above the main channel bed to prevent deposition phenomena, it cannot be completely excluded. Given the high priority of reliability, the flood retention area and side channel should be monitored frequently.

6.3.3.6 Additional aspects on morphodynamic hazards initiated by vegetation cover and by supplementary sediment input

The impact of the vegetation cover on the gravel island on morphodynamics

In this Chapter, the new Hazard Analysis approach is used to investigate how vegetation may influence the local hydraulic flow field and subsequently morphodynamic hazards in the planning state. In the focus of interest is the EaR vegetated gravel island at Rhine-km 199.500 as an example. The following analysis can further support and complete system understanding and might help to detect the range of τ_0 which are possible to appear in the study site under the given boundary conditions.

The 1D/3D approach has been used to calculate water level and the driving flow characteristics for the situation with vegetation on the island and without vegetation cover in the planning state. The

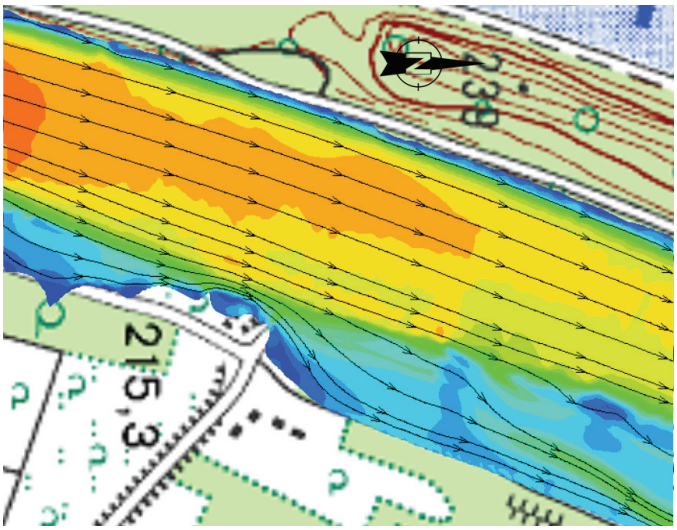

Figure 6.34: Depth-averaged velocities (3D) for Q2 = 1587 m³/s near the gravel island without vegetation cover (planning state).

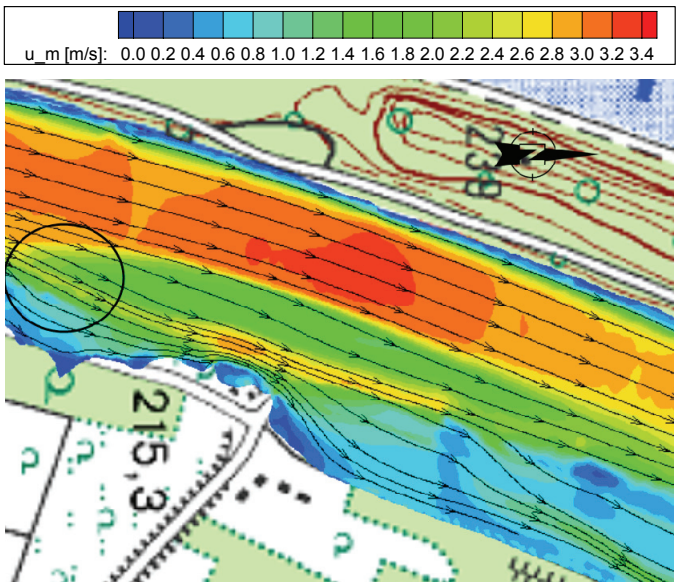

Figure 6.35: Depth-averaged velocities (3D) for Q2 = 1587 m³/s near the gravel island with vegetation cover and indicated hazardous location (planning state).

computed depth-averaged velocities and streamtraces are shown in detail in Figure 6.34 for the situation *without* vegetation on the gravel island while Figure 6.35 presents the situation *with* vegetation. As the flow field at this location does not differ significantly among the three discharges, Figure 6.34 and Figure 6.35 only present the results for the discharge Q2 = 1587 m³/s exemplarily.

It turns out that the flow resistance of vegetation has a significant impact on the flow field. As aforementioned, the vegetation cover acts as an obstacle in the flow leading to a local stream concentration in the main channel near the gravel island and the French bank. Without vegetation cover, the flow field is more uniform in the main channel. The peak and minimum depth-averaged velocities are lower and the velocity distribution is less heterogeneous. The uniformity of the flow may lead to two consequences concerning morphodynamic development. On the one hand, the bed shear stresses near the gravel island and the French bank (see Figure 6.37) are lower compared to the situation with vegetation (Figure 6.36). This may enhance stability and reduce bed dynamics of the main channel bed for the more frequent discharges Q1 and Q2. On the other hand, the impact of sediment transport enabled by erosion of the French banks may change. Bed load material of certain grain sizes may not be deposited in the side arm between gravel island and Rhinegardens (in Figure 6.35 and Figure 6.37 indicated with black circle). Consequently, the probability of deposition in the side arm may be reduced. This would imply less maintenance required for sustainability of the planned measures.

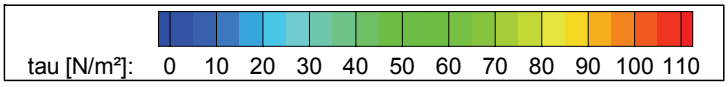

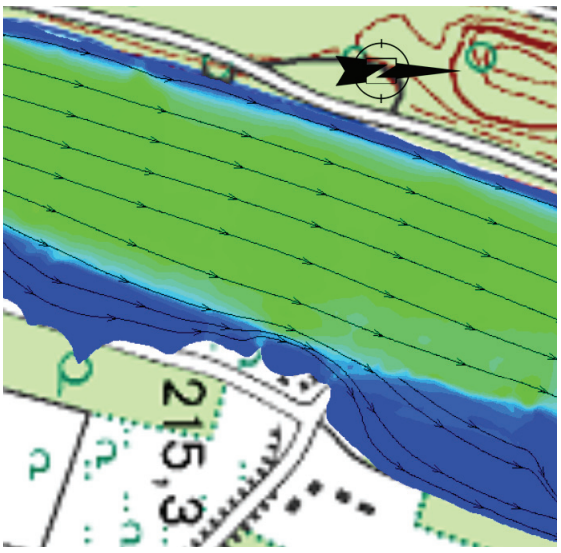

Figure 6.36: Bed shear stresses (3D) for Q2 = 1587 m³/s near the gravel island without vegetation cover (planning state).

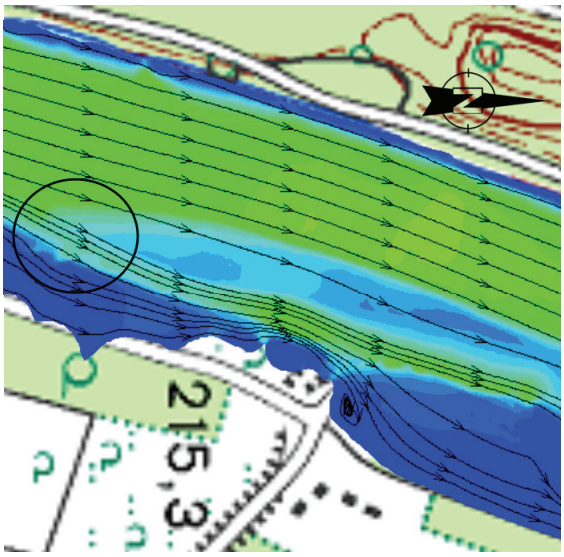

Figure 6.37: Bed shear stresses (3D) for Q2 = 1587 m³/s near the gravel island with vegetation cover and indicated hazardous location (planning state).

An attempt of estimating the potential for long-term rehabilitation of the main channel by additional sediment input

In order to get a first idea whether rehabilitation including sediment dynamics and the generation of gravel bars would be possible in the main channel as desired, it must be once again remarked that the

formation of morphological features is directly related to the amount and the type of transported sediment, to discharge dynamics and to the interaction among flow, sediment and vegetation. So far, there are no approved approaches available to quantify these complex interactions in detail. A detailed prognosis of the amount of bed load, erosion and deposition phenomena is therefore not reliable and is not conducted in the present study. But it could be interesting to gain at least a first impression of the morphology likely to appear in the main channel with additional sediment input. For this objective, the regime theory is suitable. Prior to the application, it should be noted that natural rivers do not follow regime relationships strictly as indicated in Figure 6.38. Moreover, as a matter of fact, it must be considered that the conditions of fully moveable bed on which the regime theory is based, are not satisfied in the main channel of the River Rhine due to the armour layer. Thus, the results should be interpreted as a first estimation of potential behaviour only.

In order to find out how the future morphology in the main channel might be in the case bed load transport is initiated from upstream, the regime approaches of Zarn (1997) and da Silva (1991) are used. The well-known relationship is repetitively presented in Figure 6.38. According to Zarn (1997) and da Silva (1991) the morphology of the river bed is mainly determined by the bed width, water

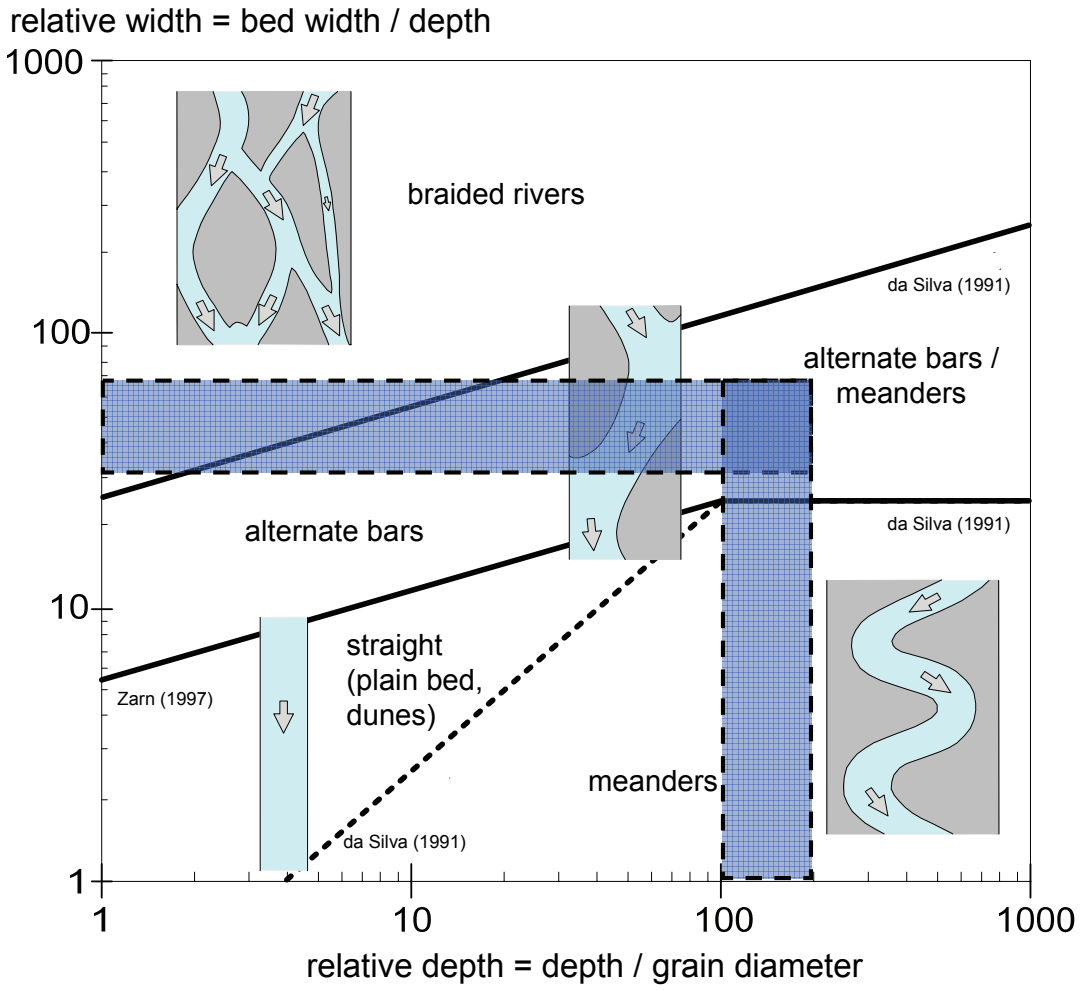

Figure 6.38: Potential morphology of the study site under the conditions of scenario B derived with the approaches of Zarn (1997) and da Silva (1991).

depth and grain diameter of the bed material expressed by the two parameters relative width w_{rel} and relative depth h_{rel} according to Eqs. 6.1. and 6.2.

$$w_{rel} = w/h \quad 6\text{-}1$$

$$h_{rel} = h/d \quad 6\text{-}2$$

These relationships are applied to the main channel of the River Rhine at Neuenburg with the following data which have been generated by the 1D/3D approach:

- water depth h: 2.5 m (Q1, Figure 6.6) – 4.5 m (Q2, Figure 6.9)
- characteristic grain diameter d_{50} (loose bed material, Figure 4.19): 0.023 m
- bed width w_{rel}: 150 m

With the these data, the parameter h_{rel} is calculated to 109 – 196 while the parameter w_{rel} is calculated to 33 – 60. Using Figure 6.38, it can be assumed that the most likely morphodynamic features for the given conditions and the discharges investigated is the formation of alternating bars. However, the dynamics and flexibility of the alternating bars are dependent, among many others, on discharge dynamics. For example, if higher flood events are missing throughout a year, pioneer vegetation will grow up on the bars very fast which in turn fixes the loose bank material and enhance their stability. In this way, sediment dynamics in the main channel can be limited again. Thus, instead of open alternating gravel banks with high mobility, relatively stable gravel islands with vegetation cover can develop such as the gravel island Neuenburg at Rhine-km 199.500. At this point, the concern of Chapter 3.1.2.3 shall be remembered which stated that alternate bars might also initiate and amplify hazardous processes such as bank erosion which in turn must be clearly accounted for.

7 EVALUATION OF THE PROPOSED MODELLING APPROACH BY A COMPARISON WITH A STANDARD 2D MODEL

7.1 INTRODUCTION

Due to the reported high physical complexity concerning flow and sediment transport through vegetation, damage measures such as “erosion rates” or deposition rates” cannot be clearly quantified in vegetated areas until today. The present dissertation developed an alternative approach combined of high-resolution 3D hydraulic modelling to quantify the flow field adequately and a semi-qualitative approach via stability assessment. The validation and plausibility check carried out with field data confirmed that this concept is capable of providing helpful information on potential morphodynamic hazards and their possible location. Fluvial modelling is, however, related to large uncertainties that should to be kept in mind for risk management. It is not possible in the framework of this thesis to conduct a stochastic uncertainty assessment of the input data and modelling tools used, but may be recommended in future. Instead, it is attempted to show the scatter of potential processes as well as possible alternatively with the calibrated model, e.g. via investigating a range of relevant discharges from a low discharge event up to an extreme flood event or by considering sediment characteristics from various samples gained near the study site. Moreover, the impact of chosen roughness coefficients for vegetation on the water level was assessed by selecting a lower and an upper value in the 1D model (n_{min}, n_{max}) and the impact of vegetation cover on the 3D flow field was investigated for different cases.

In the following, the performance of the combined 1D-3D modelling approach shall be briefly assessed by a comparison with a standard 2D model. This evaluation is carried out in two ways. First, the standard 2D model will be used to calculate the water level exemplarily for one discharge. Then, the 2D water level will be implemented in the 3D model as boundary condition and the hydraulic flow field will be computed (so-called 2D-3D approach). The outcome will be compared to the results obtained with the proposed 1D-3D approach and differences will be discussed and evaluated. Secondly, the results of bed shear stresses obtained solely with the 2D models will be presented and compared to the bed shear stresses obtained with the 1D-3D approach.

As 2D approach, the model Hydro2dE is used (Beffa and Connell, 2001; www.fluvial.ch). It solves the 2D, depth-averaged shallow water equations with an explicit Finite-Volume-approach on unstructured meshs using a wetting-and-drying algorithm, a zero-equation turbulence model and the hydrostatic pressure approach. For bed friction the Manning-Strickler-formula is implemented while vegetation resistance is modelled by the approach of Lindner (1982) for rigid stems. The Manning’s formula and the approach of Lindner are used in combination. The total bed shear stress is the sum of the bed shear stress due to bed friction and drag from vegetation elements.

7.2 CALIBRATION, RESULTS AND DISCUSSION

The calibration of the 2D model was carried out for Q1 = 671 m³/s and Q3 = 4500 m³/s to obtain the Strickler values for surface roughness of bed and banks in the actual state. Vegetation parameters were taken from Table 5-8 in a first assumption. Start water levels for actual and planning state were taken from Table 6-6. K_{St} values ranging from 28 – 48 $m^{1/3}/s$ for the bed and 20 $m^{1/3}/s$ for the banks yielded the best results. The calibrated water levels are shown in Appendix, Figure A.6.1. It turned out that calibration was not as successful as for the 1D model. Deviations between measured values and computations reached +6 – -7 cm for Q1 while for Q3, deviations reached +6 – -5 cm with -18 cm locally. Since only a first comparison between the 1D-3D concept and the 2D model regarding the orders of magnitudes was envisaged, the calibration results were assumed to be acceptable for the scope of the present study. For model forcing of the planning state, the calibrated Strickler values were used as well as the vegetation parameters according to Table 6-5.

The water level in the planning state computed with the 2D model is presented exemplarily for Q3 in Figure 7.1. The 2D model is capable of computing the spatial distribution of water levels along the vegetated stream reasonably well with differences in the vegetated retention area compared to the main channel. A water level gradient is visible in the cross-sectional (lateral) direction caused by flow acceleration near the French banks due to the curvature and the increased flow resistance on the German banks. These features cannot be visualized with a 1D model which supports the use of a 2D model for inundation studies alone, satisfactory calibration implied.

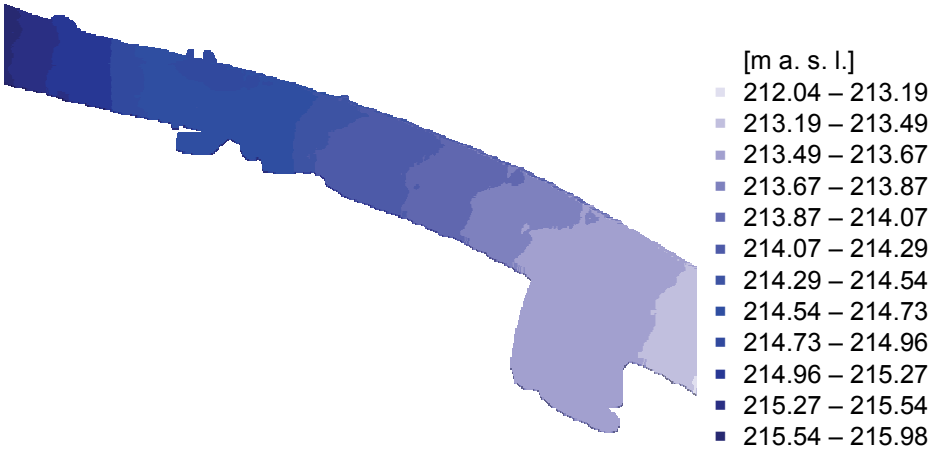

Figure 7.1: Water levels for Q3 = 4500 m³/s computed with the 2D model (planning state).

Figure 7.2 and Figure A.6.2 (Appendix) present the bed shear stresses as well as the depth-averaged flow velocities computed with the 2D model exemplarily for the Rhine section 199 – 200. Flow velocities are comparable with the flow velocities obtained with the 3D model ranging from 4 m/s up to 5 m/s in the main channel and 0.5 – 1.5 m/s in the vegetated areas and groyne fields. In contrast to its overall good performance in inundation modelling, the 2D model reveals significant shortcomings if the detailed flow field in vegetated areas is of interest. Bed shear stresses are strongly overestimated in the vegetated areas exceeding 100 N/m². In particular, bed shear stresses reached values up to 300 N/m² on the vegetated gravel island and the transition zone between main channel and vegetated areas. In the main channel and the non-vegetated side-channel instead, bed shear

stresses are much lower with 50 – 70 N/m² and 20 – 30 N/m², respectively. These exaggerated values cannot be explained by the weaker calibration results but reveal a systematic problem. On the one hand, it is possible that resistance coefficients have to be adopted. On the other hand, also the simplified representation of energy losses due to turbulence in the 2D model can lead to strongly exaggerated bed shear values in vegetation as reported in other studies, see van den Bosch (2003), Baptist (2005) and Lane et al. (1999). Given these shear stresses, the vegetated areas would be subjected to severe erosion at high flood events in the actual state which is, however, disproved by field observations which showed that the gravel island and the banks remained widely stable until today.

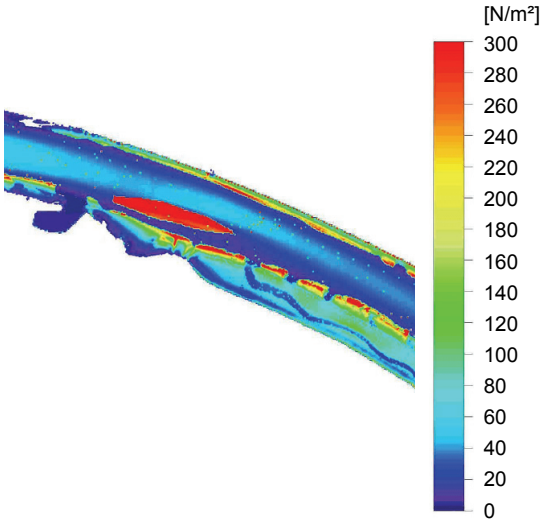

Figure 7.2: Bed shear stresses for Q3 = 4500 m³/s and Rhine-km 198.800 – 200.00 computed with the 2D model (planning state).

Finally, it is investigated how a 2D-3D approach (the 2D water levels inserted in the 3D model as boundary condition) might perform in comparison to the 1D-3D concept proposed in the Hazard Analysis herein. Figure 7.3 shows the bed shear stresses computed with the 2D-3D approach for Q3. It turns out that they are comparable with the values of the 1D-3D approach (see Figure 6.16), both exhibit very similar orders of magnitudes as well as very similar spatial distributions. Apparently, the

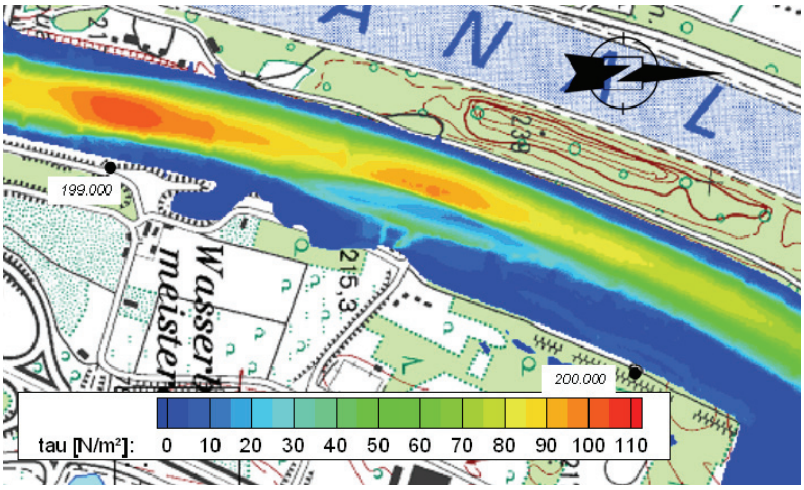

Figure 7.3: Bed shear stresses for Q3 = 4500 m³/s computed with the 3D model and the 2D water levels as boundary conditions (planning state).

detailed water level distribution obtained with the 2D model does not lead to significantly ameliorated results compared to the 1D water levels of the 1D-3D approach. This outcome is underlined by bed shear stresses computed for Q1 and the planning state, compare Figure A.6.3 Appendix and Figure 6.14.

8 SYNOPSIS

8.1 SUMMARY AND CONCLUSIONS

In the last years, the number of floods has increased significantly worldwide leading to over one-third of total costs of natural disasters. Disastrous inundations caused hundreds fatalities, millions of people evacuated and economic losses yielding billions of € in the last 15 years in Central Europe alone. Subsequently, also in the course of river regulation, climate change and the realization of the EU Water Framework Directive, new sustainable flood protection measures are developed which go hand in hand with natural river behaviour and ecological demands. Among others, the creation of inundation space has gained importance comprising e.g. the reactivation of former floodplains, dike relocation and the creation of flood retention areas. However, inundation hazards are often accompanied by morphological response of the river which can cause severe consequences in addition. These morphodynamic hazards are of major concern for the success of river restoration measures and might provoke exceptional damages and losses in the case of the measures' failure. As a consequence, sustainable nature-close flood risk management calls for explicit consideration of fluvial dynamics in addition to inundation studies alone. However, it is until today not possible to estimate the feasibility and sustainability of these kinds of projects a priori in the planning state reliably.

The present dissertation aims at developing a new concept for identification and analysis of local morphodynamic hazards which can be used for planning optimization of nature-close flood protection measures. As fluvial behaviour is dependent on numerous, the river's own properties such as bed and bank material, valley width and slope etc., the thesis is focussing on one representative river type in the actual state and the planned restored state, namely regulated gravel-bed rivers with variable geometry, floodplains as well as macrostructures such as vegetation and gravel islands. In order to facilitate the implementation in available flood risk management strategies, the morphodynamic hazard concept is embedded in the Risk chain as standardized e.g. within the International Graduate College 802.

In Chapter 2, the overall Risk Management framework was presented. Based on this overview, a strategy for identification, analysis and preliminary assessment of morphodynamic risk was derived using the source-pathway-receptor-consequences-concept (SPRC). The method was concretized in Chapter 3 based on the state of the art in science and modelling of morphodynamic hazards. The state of the art underlined the complex three-dimensional interactions among river geometry, flow, sediment transport and vegetation. It was shown that there is no reliable tool available which could be used to prognosticate the local morphodynamic development on high resolution adequately. In order to tackle these shortcomings, an alternative concept was proposed as follows.

The main contribution consists of a new stepwise methodology for the *Risk and Hazard Identification* as well as the *Hazard Analysis* of morphodynamic processes in natural gravel-bed rivers with vegetation. The *Risk Identification* procedure accounts for the special characteristics of the river in question by defining the system and the governing hydromorphological boundary conditions on the

relevant spatial and temporal scales. For *Hazard Identification*, a version of the Preliminary Hazard Analysis (PHA) table was developed which lists the Elements at Risk in the river reach, their desired functionality in the project, potential hazards which might endanger their functionality as well as related potential consequences and the hazards' severity.

Since morphodynamic processes in natural rivers are highly complex, it is not possible to predict the interaction among flow, vegetation and sediment in hard figures. As a consequence, the Hazard Analysis could not be based on process-based considerations alone, but demand a phenomenological, qualitative approach in addition. Thus, the *Hazard Analysis* method derived herein consists of two steps: A) the computation of the three-dimensional hydraulic flow field in the river reach and B) the semi-qualitative prognosis of the fluvial morphological response on the flow field. In step A, a combined-modelling approach was developed. In contrast to current modelling tools, the present thesis proposed the use of a fully 3D model with an unstructured, non-orthogonal grid. The three-dimensional flow field is computed including a physically based approach of flow resistance due to vegetation in order to account for the complex mass and impulse transfer accurately. Moreover, the literature review confirmed that 1D models yield good approximations of water levels despite their poor performance when detailed flow pattern are of interest. Thus, in order to facilitate the use of the 3D model for practical applications, it was further combined with a straightforward 1D model which is used to pre-estimate the water level. Step B of the Hazard Analysis comprised the estimation of morphodynamic behaviour as reaction of the driving forces simulated in step A by means of analytical stability approaches and a new approach for sediment transport behaviour. For the estimation of long-term morphodynamic processes the use of adequate regime equations was suggested. To support model outcomes and the applicability of the analytical approaches for the river reach, the concept includes the demand for a sound calibration and validation with field data and observation as well as permanent checks for plausibility.

In the second part of the dissertation – Chapters 4, 5 and 6 – the concept was applied on a case study area to test its performance. The area is located in the Upper Rhine north of Basel/CH in the vicinity of the municipality Neuenburg. Here, numerous river restoration projects and a large flood retention area are planned along the regulated stream. In the case of failure, losses with magnitudes of several million € are likely locally. The new method was used to evaluate the feasibility and sustainability of the rehabilitation plans and to reveal needs for optimization.

In Chapter 4, the *Risk Identification* was carried out together with the generation of a data base for the Hazard Analysis. The suggested procedure generated a detailed understanding of the fluvial system by regarding its historical development, actual state and trends for the river catchment, for the river reach to be restored and the future design. The method including the Preliminary Hazard Analysis (PHA) table permitted to systematically identify potential Elements at Risks (EaR) and hazardous processes likely to endanger the river measures.

In Chapter 5, the combined modelling concept was successfully calibrated with field data while the analytical approaches were explicitly selected for each EaR according to their properties. Plausibility check and validation were carried out for a recent flood event by means of field observations. The validation confirmed that by means of the combined modelling approach it was possible to achieve promising and plausible results for the detailed hydraulic flow field with vegetation, complex geometry and at the same time, to minimize problems related with numerical stability and extensive

computational time. The advantages of the 3D model became obvious: The distribution of the 3D flow field and bed shear stresses showed reasonable orders of magnitudes and could, in combination with the analytical approaches, reflect the morphodynamic behaviour of the river reach in the actual state very well. The model coupling as well as pre- and postprocessing were facilitated by the consecutive use of several softwares chosen for the scope of the study. Moreover, the *Hazard Analysis* concept enabled to overcome data lack which is however a well-know problem in river studies. It became evident that used as preliminary calculation tool, the 1D model can supplementarily provide helpful information regarding the system's behaviour at various boundary conditions in addition to the detailed 3D calculations which are performed for a limited number of explicit cases only.

In Chapter 6, the calibrated and validated methodology was used to prognosticate potential morphodynamic hazards for the case study region in the planning state with river measures. It turned out that the *Hazard Analysis* concept allowed to investigate morphodynamic processes in complex vegetated rivers in high spatial resolution adequately. Potential hazards could be detected for each EaR in detail and further needs for planning optimization could be plausibly uncovered.

Due to the high complexity of the interactions among flow, vegetation and sediment, it is not reliable to predict – in terms of forecasting – the amount of sediment transport, erosion and deposition rates and it is therefore not claimed in the present study. Alternatively, the thesis aims at revealing upper and lower boundaries of processes by varying conditions and model parameters, e.g. by investigating a range of relevant discharges, grain sizes, bed load transport conditions or a range of roughness coefficients likely for vegetation. Finally, Chapter 7 aimed at evaluating the performance of the new approach by a comparison with a standard 2D model exemplarily for one discharge event. The 2D model exhibited both disadvantages and advantages. Given that calibration of the 2D model is performed satisfactorily, the 2D model yielded, as well known, a better spatial distribution of water levels compared to the 1D model which enfavours its use for inundation studies alone. Comparing the quality of the proposed 1D-3D approach with a 2D-3D approach (using the 2D water level as boundary condition for the 3D model), it turned out that both approaches yielded very similar results. Apparently, given high water depths, the 1D-3D method performs as well as a more sophisticated 2D-3D approach. Together with the validation and plausibility check carried out before, this allowed the conclusion that the proposed Hazard Analysis concept can prognosticate morphodynamic hazards sufficiently well. It should be pointed out that further statistically-based uncertainty analysis is recommended in order to determine model sensitivity on e.g. roughness coeffients and grid resolution. Chapter 7 further evaluated the bed shear stresses directly computed with the 2D model for the study reach. It was underlined that by means of a standard 2D model a plausible computation of bed shear stresses in vegetated areas is not possible. Bed shear stresses were severely overestimated reaching values of more than 300 N/m² locally.

A final remark should be made. As modelling concepts cannot reflect the fluvial behaviour to its full extent, the obtained results should be checked in any case against field observations and field measurements. Furthermore, monitoring campaigns should be carried out frequently after the implementation of the river measures to further improve system understanding. Laboratory experiments could help to confirm or improve model results in addition.

8.2 OUTLOOK FOR FURTHER RESEARCH

Modelling of morphodynamic hazards in natural rivers with vegetation is a strongly multidisciplinary task covering physics, biology, mathematics and informatics and in a wider sense hydrology and meteorology. As a consequence, further research is required in many of the aforementioned disciplines, in particular in the course of climate change. Examples concerning hydraulic modelling are given in the following.

Basic research is distinctly demanded concerning the physical processes which govern the interaction vegetation, sediment and flow in order to enable the quantification of morphodynamics to its full extent, i. e. rates of erosion, deposition and sediment transport. The concept derived in the present thesis showed good performance for floodplain forest approximated by cylindric, stiff roughness elements. In order to estimate morphodynamic behaviour on floodplains for different succession stages which is of fundamental importance for long-term development of nature-close flood protection measures, the parametrization of different vegetation types including stiffness and foliage pattern and related transport processes is required. Basic research is further needed regarding the understanding and modelling of bank erosion rates on the local scale as they are the result of various interdepencies such as discharge magnitude, vegetation, material, porosity and soil water content to name only a few.

Further progress is needed in performing instationary simulations in order to be able to prognosticate morphodynamics for a complete flood event in addition to peak discharge investigations carried out in the present thesis. Last but not least, morphodynamic modelling on larger temporal scales e.g. years or decades may be helpful for sustainable risk management supplemenatrily to the investigation of single discharge events.

9 LIST OF SYMBOLS

a	[-]	constant Regime variable
A	[m]	meander amplitude
A	[m²]	base area
A	[m²]	cross-sectional flow area
A_P	[m²]	projected area of plant to the flow
a_x, a_y	[m]	distance in x and y direction
B	[-]	term of channel form in Colebrook-White formula
c	[g/m³]	suspended sediment concentration
c	[-]	constant Regime variable
c_f	[-]	friction parameter
c_μ	[-]	constant
C	[$m^{1/2}$/s]	Chézy roughness
c_D	[-]	drag coefficient
c_v	[1/m]	vegetation factor
d	[m]	grain diameter
d_{ch}	[m]	characteristic grain diameter
d_m	[m]	mean grain diameter
d_{max}	[m]	maximum grain diameter
d_{rA}	[m]	relevant grain diameter of armour layer
d_{rO}	[m]	relevant grain diameter of original sample
d_{50}	[m]	grain diameter with d < 50% of total sample
d_{90}	[m]	grain diameter with d < 90% of total sample
d_P	[m]	
D	[damage measure]	damage at a given hazard intensity
f	[-]	friction factor
f_P	[-]	form resistance coefficient of the plant
f_S	[-]	surface resistance coefficient of the bed
F	[N]	external forces
F_D	[N]	drag force
Fr^*	[-]	Shields parameter
Fr^*_c	[-]	critical Shields parameter
$Fr^*_{c,m}$	[-]	critical Shields parameter of the river bed with d_m
$Fr^*_{c,0}$	[-]	critical Shields parameter of the river bed
$Fr^*_{c,\beta}$	[-]	critical Shields parameter of the river bank
g	[m/s²]	acceleration of gravity
h	[m]	water depth
h_b	[m]	bankfull water depth

h_c	[m]	critical water depth
h_e	[m]	energy head loss
h_m	[m]	mean water depth
I_0	[-]	bed slope
I_E	[-]	energy slope
I_r	[-]	friction slope
k	[m²/s²]	turbulent kinetic energy
K	[-]	ratio
k_m	[-]	velocity correction factor
k_r	[$m^{1/3}$/s]	grain Strickler roughness
k_s	[m]	equivalent sand-grain roughness
k_{St}	[$m^{1/3}$/s]	Strickler roughness
L	[monetary value]	loss
m_B	[kg/m/s]	bed load transport rate
m_S	[kg/m/s]	suspended load transport rate
n	[s/$m^{1/3}$]	Manning's roughness
P	[-]	probability of occurrence for a hazard of a certain intensity
P	[N/m²]	pressure
P	[m]	wetted perimeter
q	[m³/s]	discharge
Q	[m³/s]	discharge
Q_b	[m³/s]	bankfull discharge
Q_{bed}	[m³/s]	part of discharge forcing the bed
$Q_{c\text{-}f}$	[m³/s]	channel-forming discharge
Q_n	[m³/s]	discharge with a return interval of n years
r	[m]	meander radius
R	[m]	hydraulic radius
R_b	[m]	hydraulic radius of the bed
Re^*	[-]	grain Reynolds number
R_L	[loss value/time value]	total risk
R_S	[damage value/time value]	structural risk
s	[m]	longitudinal river length
t	[s]	time
u_0	[m/s]	near-bed flow velocity
u_0^*	[m/s]	near-bed shear velocity
u_i	[m/s]	flow velocity
u_m	[m/s]	mean flow velocity
u_{ref}	[m/s]	reference velocity
u_S	[m/s]	settling velocity
u_S^*	[m/s]	shear stress velocity
U	[m/s]	averaged flow velocity

w	[m]	bed width
w_b	[m]	bankfull width
wl	[m]	water level
w_m	[m]	mean bed width
x	[m]	spatial geometric scale
y	[m]	distance from wall
Y		dependent Regime variable
z	[m]	depth, vertical direction
z_c	[m]	critical sedimentation height
z_{WL}	[m]	depth at water level
Z	[-]	Rouse number

α	[°]	meander angle
α	[-]	velocity weighing coefficient
β	[°]	friction angle
β	[-]	reciprocal turbulent Schmidt number
δ	[-]	Kronecker delta
ε	[m²/s²]	dissipation rate of turbulent kinetic energy
φ	[°]	bank slope
κ	[-]	von Kármán constant, 0.4
λ	[m]	meander wave length
λ	[-]	Günter factor for bed constitution
ν	[m²/s]	kinematic viscosity
ν_T	[m²/s]	turbulent viscosity
ρ_W	[kg/m³]	water density
ρ_S	[kg/m³]	sediment density
ρ'	[-]	relative density (ρ_W-ρ_S/ρ_W)
τ	[N/m²]	shear stress
τ_0	[N/m²]	bed shear stress
τ_c	[N/m²]	critical shear stress
τ_{0c}	[N/m²]	critical shear stress of the bed
τ_{0P}	[N/m²]	shear stress exerted by plant
τ_{0S}	[N/m²]	shear stress exerted by bed
$€_c$	[€]	critical loss

10 REFERENCES

Abad, J. D., Buscaglia, G. C., Garcia, M. (2008): *2D stream hydrodynamic, sediment transport and bed morphology model for engineering applications.* Hydrol. Proc., Vol. 22, pp. 1443–1459, doi:10.1002/hyp.6697.

Ahnert, F. (1973): *Inhalt und Stellung der funktionalen Methode in der Geomorphologie.* Geogr. Z., No. 33, pp. 105–113.

Alkema, D., Cavallin, A. (2003): *Geomorphic risk assessment for EIA*. Studi Trentini di Scienze Naturali – Acta Geologica, Vol. 78, pp.139–145.

Alsace Nature, BASNU, BUND, BBU, Regiowasser (2003): *La seconde jeunesse du Vieux-Rhin - Die zweite Jugend des Restrheins.* Strasbourg.

Andrews, E. D. (1984): *Bed-material entrainment and hydraulic geometry of gravel-bed rivers in Colorado.* Bulletin of the Geol. Soc. of America, Vol. 95, pp. 371–378.

Anable, W. K. (1996): *Database of morphological characteristics of watercourses in Southern Ontario.* Ontario.

Armanini, A., Righetti, M., Grisenti, P. (2005): *Direct measurement of vegetation resistance in prototype scale.* J. Hydraul. Res., Vol. 43, No. 5, pp. 481–487.

Armbruster, J., Muley Fritze, A., Pfarr, U., Rhodius, R., Siepmann-Schinker, D., Sittler, B., Späth, V., Tremolieres M., Rennenberg H., Kreuzwieser J. (2006): *FOWARA Forested Water Retention areas - Guideline for decision makers, forest managers and land owners. The Fowara Project.* University of Freiburg. portal.uni-freiburg.de/ifp/news-de/fowara/download.

Autodesk (2002): *AutoCAD*.

Baptist, M. J. (2005): *Modelling floodplain biogeomorphology.* Dissertation. Technical University of Delft, Delft.

Baptist, M. J., Babovic, V., Rodríguez Uthurburu, J., Keijzer, M., Uittenbogaard, R. E., Mynett, A., Verwey, A. (2007): *On inducing equations for vegetation resistance.* J. Hydraul. Res., Vol. 45, No. 4, pp. 435–450.

Bates, P. D., de Roo, A. P. J. (2000): *A simple raster-based model for flood inundation simulation.* J. Hydrol., Vol. 236, pp. 54–77.

BAFU - Bundesamt für Umwelt (2008): *Hydrologisches Jahrbuch der Schweiz 2007.* Umwelt-Wissen, No. 0824, Bern.

BAW - Bundesanstalt für Wasserbau (2004): *Grundlagen zur Bemessung von Böschungs- und Sohlensicherungen an Binnenwasserstraßen.* Mitteilungsblatt der Bundesanstalt für Wasserbau, No. 87, Karlsruhe.

Beffa, C., Connell, R. J. (2001): *Two-dimensional flood plain flow - I: Model description.* J. Hydraul. Eng., Vol. 6, No. 5, pp. 397–405.

Bennett S. J., Simon, A. (Eds.) (2004): *Riparian vegetation and fluvial geomorphology.* American Geophysical Union, Washington.

Bennett, S. J., Wu, W., Alonso, C. V., Wang, S. (2008): *Modeling fluvial response to in-stream woody vegetation: implications for stream corridor restoration.* Earth Surf. Process. Landforms, Vol. 33, pp. 890–909, doi:10.1002/esp.1581.

Bertoldi, W., Ashmore, P., Tubino, M. (2009): *A method for estimating the mean bed load flux in braided rivers.* Geomorphology, Vol. 103, No. 3, pp. 330–340.

Bihs, H. (2007): *Gridmeister*. http://folk.ntnuno./bihs/downloads_de.html.

Blackwell, M. S. A., Maltby, E. (2005): *Ecoflood guidelines: How to use floodplains for flood reduction - The Ecoflood Project.* http://levis.sggw.waw.pl/ecoflood/.

Bölscher, J., Ergenzinger, P. Obenauf, P. J. (2005): *Hydraulic, sedimentological and ecological problems of multi-functional riparian forest management - RIPFOR - The scientific report.* Berliner Geographische Abhandlungen, No. 65.

Bund-Länder-Arbeitsgruppe (1995): *Hochwassergefährdung am Ober- und Mittelrhein.* via Regierungspräsidium Freiburg, Germany.

Caporali, E., Rinaldi, M., Casagli, N. (2005): *The Arno river floods.* Giornale di Geologia Applicata, pp.177–192.

Caruso, B. (2006): *Effectiveness of braided, gravel-bed river restoration in the Upper Waitaki Basin, New Zealand.* River Res. Applic., Vol. 22, pp. 905–922.

Catella, M., Paris, E., Solari, L. (2005): *1D morphodynamic model for natural rivers.* In: G. Parker & M. Garcia (Eds.): *River, coastal and estuarine morphodynamics: RCEM 2005.* Taylor & Francis Group, London.

Charlton, F. G., Brown, P. M., Benson, R. W. (1978): *The hydraulic geometry of some gravel rivers in Britain.* Hydraulics Research Station, Report IT 180. Wallingford.

Chatterjee, C., Förster, S., Bronstert, A. (2008): *Comparison of hydrodynamic models of different complexities to model floods with emergency storage areas.* Hydrol. Proc., Vol. 22, pp. 4695–4709, doi:10.1002/hyp.7079.

Chin, C. O. (1985): *Stream bed armouring.* School of Engineering, Report No. 403, University of Auckland, New Zealand.

Choi, S. S., Kang, H. (2006): *Numerical investigations of mean flow and turbulence structures of partly-vegetated open-channel flows using the Reynolds stress model.* J. Hydraul. Res., Vol. 44, No. 2, pp. 203–217.

Chorley, R. J., Kennedy, B. A. (1971): *Physical geography - A systems approach.* Prentice Hall Int. Incl., London.

Chow, V. T. (1959): *Open channel hydraulics.* McGraw Hill, New York.

Church, M., Hassan, M. A. (1992): *Size and distance of travel of unconstrained clasts on a streambed*. Wat. Resour. Res., Vol. 28.

Colebrook, C. F., White C. M. (1937): *Experiments with fluid friction in roughened pipes.* Proc. of the Royal Society of London, Vol. 161, Series A, pp. 367–387.

Copeland, R. R., McComas, D. N., Thorne, C. R., Soar, P. J., Jonas, M. M., Fripp, J. B. (2001): *Hydraulic design of stream restoration projects.* U.S. Army Engineer Research and Development Center, Coastal and Hydraulics Laboratory. No. Report ERDC/CHL TR-01-28, Vicksburg. http://www.dtic.mil/cgi-bin/GetTRDoc?AD=ADA400662&Location=U2&doc=GetTRDoc.pdf.

Cowan, W. L. (1956): *Estimating hydraulic roughness coefficients.* Agr. Eng., Vol. 37, pp. 473–475.

Crowder, D. W., Diplas, P. (2000): *Using two-dimensional hydrodynamic models at scales of ecological importance.* J. Hydrol., Vol. 230, pp. 172–191.

Da Silva, A. M. A. F. (1991): *Alternate bars and related alluvial processes.* M. Th. Queen's University, Kingston, Ontario.

Daly, E., Porporato, A. (2005): *Some self-similar solutions in river morphodynamics.* Wat. Resour. Res., Vol. 41, doi:10.1029/2005WR004488.

De Moor, J. J. W., van Balen, R. T., Kasse, C. (2007): *Simulating meander evolution of the Geul River (the Netherlands) using a topographic steering model.* Earth Surf. Process. Landforms, Vol. 32, pp. 1077–1093, doi:10.1002/esp.1466.

DIN EN IEC 60812:2006: *Analysis techniques for system reliability - Procedure for failure mode and effects analysis (FMEA) (*11.2006).

Dittrich, A. (1995): *Hydraulische Belastbarkeit ingenieurbiologischer Bauweisen.* Status report 1994/1995, WBW-Fortbildungsgesellschaft für Gewässerentwicklung mbH, Heidelberg.

Dittrich, A. (1998): *Wechselwirkung Morphologie/Strömung naturnaher Fließgewässer.* Mitteil. d. Inst. f. Wasserwirtschaft und Kulturtechnik, No. 198, Karlsruhe.

Dittrich, A. (1999): *Sohlenstabilität naturnaher Fließgewässer.* in: *Gewässernachbarschaften in Baden-Württemberg*. Status report 1998/1999, WBW-Fortbildungsgesellschaft für Gewässerentwicklung mbH, pp. 42–49, Heidelberg.

Dittrich, A., Järvelä, J. (2005): *Flow-vegetation-sediment interaction.* Wat. Eng. Research, Vol. 6, No. 3, pp. 123–130.

Dittrich, A., Marek, M., Specht, F.-J., Dippe, D. (2005): *Hydraulische Berechnungen und morphodynamische Entwicklung für den Rhein zwischen Märkt und Breisach*. Bericht d. Leichtweiss-Instituts für Wasserbau, Abteilung Wasserbau, No. 904, Braunschweig. (unpubl.)

Dittrich, A., Schulte-Rentrop, A., Marek, M., Späth, V. (2007): *Morphological development of the retention basin "Hartheim" - A case study.* Acta Geophysica Polonica, Vol. 55, No. 1, pp. 33–46, doi:10.2478/s11600-006-0045-4.

Dittrich, A. (2007): *Wasserbau und Wasserwirtschaft II.* Lecture notes. Leichtweiß-Institut für Wasserbau, Braunschweig.

Dittrich, A. (2008): *Personal communication.*

Downs, P. W., Thorne, C. R. (1998): *Design principles and suitability testing for rehabilitation in a food defence channel the River Idle, Nottinghamshire, UK.* Aquatic conservation, Vol. 8, No. 1, pp. 17–38.

Downs, P. W., Thorne, C. R. (2000): *Rehabilitation of a lowland river: Reconciling flood defence with habitat diversity and geomorphological sustainability.* J. Environm. Manag., Vol. 58, pp. 249–268, doi:10.1006/jema.2000.0327.

Duan, J. G. (2005): *Analytical approach to calculate rate of bank erosion.* J. Hydraul. Eng., Vol. 131, No. 11, pp. 980–990.

Dunn, C., Lopez, F., Garcia, M. (1996): *Mean flow and turbulence in a laboratory channel with simulated vegetation.* Civil Engineering Studies Hydraulic Engineering Studies, No. 51, Hydrosystems Laboratory, Urbana-Champaign.

Dury, G. H. (1965): *Theoretical implications of underfit streams.* U. S. Geol. Survey Prof. Paper, No. 452-C, p. 44.

DVWK - Deutscher Verband für Wasserwirtschaft und Kulturbau e. V. (1990): *Hydraulische Methoden zur Erfassung von Rauheiten.* Schriftenreihe des Dt. Verb. für Wasserwirtschaft u. Kulturbau e. V., No. 92, Parey, Hamburg.

DVWK - Deutscher Verband für Wasserwirtschaft und Kulturbau e. V. (1991): *Hydraulische Berechnung von Fließgewässern.* Merkblätter zur Wasserwirtschaft, No. 220, Parey, Hamburg.

DVWK - Deutscher Verband für Wasserwirtschaft und Kulturbau e. V. (1994): *Hydraulisch-sedimentologische Berechnungen naturnah gestalteter Fließgewässer. Berechnungsverfahren für die Ingenieurspraxis. DVWK-Mitteil.*, No. 25/1994, Wirtschafts- und Verlagsgesellschaft Gas und Wasser mbH, Bonn.

DVWK - Deutscher Verband für Wasserwirtschaft und Kulturbau e. V. (1999): *Numerische Modelle von Flüssen, Seen und Küstengewässern.* Wirtschafts- und Verlagsgesellschaft Gas und Wasser mbH, Bonn.

Edgecombe, A. R. B. (Ed.) (1941): *Annual report (technical) of the Central Board of Irrigation, India, 1939-40.* Central Board of Irrigation, India.

Einstein, H. A., Horton, R. (1933): *Separate roughness coefficients for channel bottom and sides.* Engineering Record, Vol. 111, No. 22.

Emmett, W. W. (1972): *The hydraulic geometry of some Alaskan streams south of the Yukon River.* U.S. Geol. Survey, pp. 72–108.

Emmett, W. W. (1975): *The channels and waters of the upper Salmon River, Idaho.* Geolog. Survey Prof. Paper, No. 870-A.

ESRI (2000): *ArcView 3.2a*.

ESRI (2005): *ArcGIS 9.1*.

Faber, M. H. (2005): *Risk and safety in civil, surveying and environmental engineering.* Lecture notes. Eidgen. Techn. Hochsch. Zürich, Zurich.

Faulhaber, K., Riehl, K. (2000): *Geschiebezugabe an der Elbe*. Proceedings Gewässermorphologisches Kolloquium, Bundesanstalt für Gewässerkunde, Koblenz.

Felkel, K. (1960): *Gemessene Abflüsse in Gerinnen mit Weidenbewuchs.* Mitteilungsblatt der Bundesanstalt für Wasserbau, No. 15, Karlsruhe.

Fischenich, C., Morrow, J. V. (2000): *Reconnection of floodplains with incised channels.* EMRRP Technical Notes collection, No. TN-EMRRP-SR-09, Vicksburg, MS. www.wes.army.mil/el/emrrp.

Fischer-Antze, T. (2005): *Assessing river bed changes by morphological and numerical analysis.* Dissertation. Vienna University of Technology, Vienna.

FISRWG (2001): *Stream corridor restoration - Principles, processes, and practices.* Stream Restoration Working Group. http://www.nrcs.usda.gov/.

Floodsite (2008): *Task 3 - Contributing to european flood hazard atlas.* The Floodsite Project - Integrated flood risk analysis and management methodologies. http://www.floodsite.net/.

Gautier, J. N. (2004): *Personal communication.*

Gebler, R.-J. (1992): *Aktionsprogramm Rhein 2000 - Potentielle Laichplätze für Kieslaicher und Wanderungshindernisse im Oberrhein*. Ingenieurbüro Dr.-Ing. Rolf-Jürgen Gebler, Walzbachtal.

Geerling, G. W. (2008): *Changing rivers - Analysing fluvial landscape dynamics using remote sensing.* Dissertation. Radboud University, Nijmegen.

Gessler, J. (1965): *Der Geschiebetriebbeginn bei Mischungen untersucht an natürlichen Abpflasterungserscheinungen in Kanälen.* Dissertation. No. 3711, Eidgen. Techn. Hochsch. Zürich, Zurich.

GWD - Gewässerdirektion Südlicher Oberrhein/Hochrhein (1997): *The Integrated Rhine Programm - Flood control and restoration of former flood plains on the Upper Rhine.* Lahr.

GWD - Gewässerdirektion Südlicher Oberrhein/Hochrhein (2000): *Personal communication*.

Gilvear, D. J. (1999): *Fluvial geomorphology and river engineering: future roles utilizing a fluvial hydrosystem framework*. Geomorphology, Vol. 31, pp.229–245.

Gölz, E., Trompeter, U. (2000): *Transport und Verteilung von Zugabematerial, Feststoffeintrag, Laufentwicklung und Transportprozesse in schiffbaren Flüssen*. Proceedings Gewässermorphologisches Kolloquium, Bundesanstalt für Gewässerkunde, Koblenz.

Gouldby, B., Samuels, P. (2005): *Language of risk - Project definitions - The Floodsite Project - Integrated flood risk analysis and management methodologies.* Technical Report, No. T32-04-01. http://www.floodsite.net/html/publications2.asp?documentType=1&Submit=View.

Gowen, L. D., Collofello, J. S., Calliss, F. W. (1992): *Preliminary hazard analysis for safety-critical software systems.* Eleventh Annual International Phoenix Conference on Computers and Communications, Proceedings, Scottsdale.

Griffiths, G. A. (1981): *Flow resistance in coarse gravel bed rivers.* J. Hydraul. Div., Vol. 107, No. 7, p. 899.

Günter, A. (1971): *Die kritische mittlere Sohlenschubspannung bei Geschiebemischungen unter Berücksichtigung der Deckschichtbildung und der turbulenzbedingten Sohlenschubspannungsschwankungen.* Dissertation. No. 4649, Eidgen. Techn. Hochsch. Zürich, Zurich.

Hartmann, G., Dittrich, A. (1995): *Abschätzung der Sohlstabilität des Retentionsraumes südlich des Kulturwehres Breisach.* Internal report. Karlsruhe.

Hartmann, G., Dittrich, A., Träbing, K. (1998): *Untersuchungen zum Vorlandabtrag zwischen Märkt und Karpfenhod.* Internal Report. Inst. f. Wasserwirtschaft und Kulturtechnik, Karlsruhe.

Hartmann, G., Träbing, K., Dittrich, A., Stoesser, T. (2000): *Rückhalteraum südlich des Kulturwehres Breisach - Wasserspiegellagenberechnungen von Märkt bis Breisach.* Internal Report. Inst. f. Wasserwirtschaft und Kulturtechnik, Karlsruhe.

Hey, R. D., Bathurst, J. C., Thorne, C. R. (Eds.) (1982): *Gravel-bed rivers.* Wiley, Chichester.

Hey, R. D., Thorne, C. R. (1986): *Stable channels with mobile gravelbeds.* J. Hydraul. Eng., Vol. 112, No. 6, pp. 671–689.

Höhl, S. (2008): *Vorwärts in die Vergangenheit.* Badische Zeitung, 14.11.2008.

Hughes, F. (2003): *The Flooded Forest – Guidance for policy makers and river managers in Europe on the restoration of floodplain forests - The FLOBAR2 Project.* Department of Geography, University of Cambridge. http://www.geog.cam.ac.uk/research/projects/flobar2/reports/final/flobar2.pdf.

Hunziker, R. P. (1995): *Flussaufweitungen - Morphologie, Geschiebehaushalt und Grundsätze zur Bemessung.* Dissertation. Mitteil. der Versuchsanstalt für Wasserbau, Hydrologie und Glaziologie, No. 11037, Eidgen. Techn. Hochsch. Zürich, Zurich.

Hupp, C. R.; Rinaldi, M. (2007): *Riparian vegetation patterns in relation to fluvial landforms and channel evolution along selected rivers of Tuscany (Central Italy).* Annals of the Association of American Geographers, Vol. 97, No. 1, pp. 12 – 30.

Hütte, M. (1994): *Die Bedeutung der Wasserfassung für die Ökologie eines alpinen Baches.* Dissertation. Institut für Zoologie und Limnologie, Universität Innsbruck, Innsbruck.

IHP/OHP - Deutsches Nationalkomittee für das Internationale Hydrologische Programm der UNESCO (IHP) und das Operationelle Hydrologische Programm der WMO (OHP) (1996): *The River Rhine - Development and management.* Special Issue. BfG, Koblenz.

Ikeda, S., Parker, G. (1989): *River meandering.* American Geophysical Union, Washington, D.C.

IKSR - Internationale Kommission zum Schutz des Rheins (2003): *Gewässerstrukturkarte Rhein - Begleitbericht.* Koblenz.

IKSR - Internationale Kommission zum Schutz des Rheins (2005): *Internationale Flussgebietseinheit Rhein - Merkmale, Überprüfung der Umweltauswirkungen menschlicher Tätigkeiten und wirtschaftliche Analyse der Wassernutzung - Teil A.* CC, No. 02-05d, Germany.

ILN - Institut für Landschaftsökologie und Naturschutz im NABU (2004): *Personal communication.*

ILN - Institut für Landschaftsökologie und Naturschutz im NABU (2006): *Personal communication.*

ILN - Institut für Landschaftsökologie und Naturschutz im NABU (2007): *Personal communication.*

ILN - Institut für Landschaftsökologie und Naturschutz im NABU (2008): *Personal communication.*

Inglis, C. C. (1941): *Digest of answers to the Central Board of irrigation questionaire on meandering of rivers with comments on factors controlling meandering and suggestions for future action.* In: A. R. B. Edgecombe (Ed.): *Annual report (technical) of the Central Board of Irrigation, India, 1939-40.* Central Board of Irrigation, IndiaVol. 24, pp. 100–114.

Integriertes Rheinprogramm (1996): *Rahmenkonzept des Landes Baden-Württemberg zur Umsetzung des Integrierten Rheinprogramms.* No. 7, Karlsruhe.

Jäggi, M. (1983): *Alternierende Kiesbänke - Untersuchungen über ihr Auftreten, den Zusammenhang mit der Bildung von Sohlenformen im allgemeinen, sowie ihre Auswirkungen auf Ufererosion und Fliesswiderstand.* Dissertation. Mitteil. der Versuchsanstalt für Wasserbau, Hydrologie und Glaziologie, No. 62, Eidgen. Techn. Hochsch. Zürich, Zurich.

James, C. S., Birkhead, A. L., Jordanova, A. A., O'Sullivan, J. J. (2004): *Flow resistance of emergent vegetation.* J. Hydraul. Res., Vol. 42, No. 4, pp. 390–398.

Järvelä, J. (2004): *Determination of flow resistance caused by non-submerged woody vegetation.* Int. J. River Basin Manag., Vol. 2, No. 1, pp. 61–70.

Julian, J. P., Torres, R. (2006): *Hydraulic erosion of cohesive riverbanks*. Geomorphology, Vol. 76, pp. 193–206.

Jun, B. H., Lee, S. I., Seo, I. W., Choi, G. W. (Eds.) (2005): *Water engineering for the future - Choices and challenges.* XXXI IAHR Congress, Seoul.

Kellerhals, R. (1967): *Stable channels with gravel-paved beds.* J. Waterw. Harb. Div., pp. 63–84.

Kern, K. (1994): *Grundlagen naturnaher Gewässergestaltung - Geomorphologische Entwicklung von Fließgewässern.* Springer, Berlin.

Kidson, R. L., Richards, K. S., Carling, P. A. (2006): *Hydraulic model calibration for extreme floods in bedrock-confined channels: A case study from northern Thailand.* Hydrol. Proc., Vol. 20, pp. 329–344.

Knight, D. W., Omran, M., Tang, X. (2007): *Modeling depth-averaged velocity and boundary shear in trapezoidal channels with secondary flows.* J. Hydraul. Eng., Vol. 133, No. 1, pp. 39–47.

Knighton, D. (1996): *Fluvial forms and processes,* 9th ed, Arnold, London.

Koll, K., Dittrich, A. (1998): *Validation of incipient motion formulas with field data.* Int. Symposium on River Sedimentation, Hong Kong.

Kortenhaus, A. (2006): *Coastal floods - Concept for risk evaluation and management.* International Doctoral Course on Risk Management, International Graduate College 802, Braunschweig.

Kouwen, N., Unny, T. E., Hill, H. M. (1969): *Flow retardance in vegetated channels.* J. of the Irrigation and Drainage Div., Vol. 95, No. IR2, pp. 329–342.

Kovacs, A., Parker, G. (1994): *A new vectorial bedload formulation and its application to the time evolution of straight river channels.* J. Fluid Mech., Vol. 264, pp. 153–183.

Kowalski, R. L., Schröder, M., Kaluza, T. (2006): *Pflanzen in der 2D Simulation von Flüssen.* Wasserbaukolloqium 2006, Dresdener Wasserbaul. Mitt., No. 32, Dresden.

Lacey, G. (1930): *Stable channels in alluvium.* Minutes of Proc. of the Inst. For Civil Eng., Vol. 229, No. 4736.

Landesanstalt für Umweltschutz (2006): *Deutsches Gewässerkundliches Jahrbuch 2003 - Rheingebiet, Teil I, Hoch- und Oberrhein.* Karlsruhe.

Landesanstalt für Umweltschutz (2007): *Deutsches Gewässerkundliches Jahrbuch 2004 - Rheingebiet, Teil I, Hoch- und Oberrhein.* Karlsruhe.

Lane, S. N. (1998): *Hydraulic modelling in hydrology and geomorphology - A review of high resolution approaches.* Hydrol. Proc., Vol. 12, pp. 1131–1150.

Lane, S. N., Bradbook, K. F., Richards, K. S., Biron, P. A., Royer A.G. (1999): *The application of computational fluid dynamics to natural river channels: Three-dimensional versus two-dimensional approaches.* Geomorphology, Vol. 29, pp. 1–20.

Leopold, L. B., Wolman, R. G. (1957): *River channel patterns - Braided, meandering and straight.* Geolog. Survey Prof. Paper, 282-B, pp. 45–62.

Leopold, L. B., Wolman, R. G., Miller, J. G. (1964): *Fluvial processes in geomorphology.* W.H. Freeman, San Francisco.

Li, C. W., Zeng, C. (2009): *3D numerical modelling of flow divisions at open channel junctions with or without vegetation.* Adv. Wat. Resour., Vol. 32, pp. 49–60, doi:10.1016/j.advwatres.2008.09.005.

Li, R. M., Shen, H. W. (1973): *Effect of tall vegetations on flow and sediment.* J. Hydraul. Div., Vol. 99, No. 5, pp. 793–814.

Li, S. S., Millar, R. G. (2007): *Simulating bed-load transport in a complex gravel-bed river.* Technical Notes. J. Hydraul. Eng., Vol. 133, No. 3, pp. 323–328.

Lindner, K. (1982): *Der Strömungswiderstand von Pflanzenbeständen.* Mitteil. d. Leichtweiß-Instituts für Wasserbau der TU Braunschweig, No. 25, Braunschweig.

Ljubomirova, K. S., Seveleva, G. G. (1968): in: Stelczer, K. (1981).

López-Avilés, A. (2007): *Flash flooding in Spain: Geomorphological approaches supporting flood frequency analysis, and the implications for the design of structures.* Wat. Environm. J., Vol. 21, No. 3, pp. 217–226, doi:10.1111/j.1747-6593.2006.00063.x.

Mackin, J. H. (1948): *Concept of the graded river.* Bulletin of the Geol. Soc. of America, Vol. 59, pp. 463–512.

Mahdi, T. (2007): *Pairing geotechnics and fluvial hydraulics for the prediction of the hazard zones of an exceptional flooding.* Nat. Hazards, Vol. 42, No. 1, pp. 225–236, doi:10.1007/s11069-006-9096-8.

Malcherek, A. (2009): *Sedimenttransport und Morphodynamik.* Manuscript. Universität der Bundeswehr München, Munich.

Mc Ewan, I. K., Habersack H. M., Heald J. G. C. (2000): *Discrete particle modelling and active tracers: New techniques for studying sediment transport as a langragian phenomenon.* Gravel Bed Rivers, 2000.

McMillan, H. K., Brasington, J. (2007): *Reduced complexity strategies for modelling urban floodplain inundation.* Geomorphology, Vol. 90, pp. 226–243.

Meixner, H., Schnauder, I., Bölscher, J. (2003): *Riparian Forest Management - Guidelines for End-Users.* RipFor-Team, 1st ed, Vienna.

Mertens, W. (1995): *Zur Wahl geeigneter Sedimenttransportformeln.* Wasserwirtschaft, Vol. 85, No. 10,

Mertens, W. (2006): *Hydraulisch-sedimentologische Berechnungen naturnah gestalteter Fließgewässer - Berechnungsverfahren für die Ingenieurpraxis,* 2nd ed, Deutsche Vereinigung für Wasserwirtschaft Abwasser und Abfall, Hennef.

Merz, B. (2006): *Hochwasserrisiken - Grenzen und Möglichkeiten der Risikoabschätzung; mit 33 Tabellen.* Schweizerbart, Stuttgart.

Meyer-Peter, E., Müller, R. (1949): *Eine Formel zur Berechnung des Geschiebetriebs.* Schweiz. Bauzeitung, Vol. 67, No. 3.

Micheli, E. R., Kirchner, J. W., Larsen, E. W. (2004): *Quantifying the effect of riparian forest versus agricultural vegetation on river meander migration rates, Central Sacramento River, California, USA.* River Res. Appl., Vol. 20, pp. 537–548.

Millar, R. G. (2005): *Theoretical regime equations for mobile gravel-bed rivers with stable banks.* Geomorphology, Vol. 64, pp. 207–220.

Minh Duc, B., Bernhart, H. H., Kleemeier, H. (2005): *Morphological numerical simulation of flood situations in the Danube River.* Int. J. River Basin Manag., Vol. 3, No. 4, pp. 283–293.

Minh Thu, P. T. (2002): *A hydrodynamic-numerical model of the River Rhine.* Dissertation. Mitteil. d. Inst. f. Wasserwirtschaft und Kulturtechnik, No. 213, Karlsruhe.

Nepf, H. M. (1999): *Drag, turbulence, and diffusion in flow through emergent vegetation.* Wat. Resour. Res., Vol. 35, No. 2, pp. 479–489.

Nezu, I., Nakagawa, H. (1993): *Turbulence in open-channel flows.* IAHR Monograph Series, A. A. Balkema, Rotterdam.

Nixon, M. (1959): *A study of bankfull discharges of rivers in England and Wales.* Proceedings of the Institution of Civil Engineers, Vol. 12, pp. 157–175.

Olsen, N. R. B. (2004a): *Hydroinformatics, fluvial hydraulics and limnology,* 4th ed, Department of Hydraulic and Environmental Engineering, Norwegian University of Science and Technology, Trondheim.

Olsen, N. R. B. (2004b): *SSIIM user's manual - Version 2004.* Norwegian University of Science and Technology, Trondheim.

Olsen, N. R. B. (2006): *SSIIM user's manual - Version 2006.* Norwegian University of Science and Technology, Trondheim.

Olsen, N. R. B. (2008): *SSIIM 2.0 - Version 2008.* Norwegian University of Science and Technology, Trondheim.

Palmer, V. J. (1945): *A method for designing vegetated waterways.* Agr. Eng., Vol. 26, No. 12, pp. 512–520.

Parker, G., Klingeman, P. C. (1982): *On why gravel bed streams are paved.* Wat. Res. Res., Vol. 18, No. HY9, pp. 1409 -1423.

Parker, G., Garcia, M. (Eds.) (2005): *River, coastal and estuarine morphodynamics: RCEM 2005.* Taylor & Francis Group, London.

Pasche, E., Rouvé, G. (1985): *Overbank flow with vegetatively roughened flood plains.* J. Hydraul. Eng., Vol. 111, No. 9, pp. 1262–1278.

Pasternack, G. B., Lau Wang, C., Merz, J. E. (2004): *Application of a 2D hydrodynamic model to design of reach-scale spawning gravel replenishment on the Mokelumne River, California.* River Res. Applic., Vol. 20, pp. 205–225.

Patt, H., Jürging, P., Kraus, W. (1998): *Naturnaher Wasserbau - Entwicklung und Gestaltung von Fließgewässern.* Springer, Berlin.

Perucca, E., Camporeale, C., Ridolfi, L. (2009): *Estimation of the dispersion coefficient in rivers with riparian vegetation.* Adv. Wat. Resour., Vol. 32, pp. 78–87, doi:10.1016/j.advwatres.2008.10.007.

Petryk, S., Bosmajian, G. (1975): *Analysis of flow through vegetation.* J. Hydraul. Div., Vol. 101, No. 7, pp. 871–884.

Piégay, H., Darby, S. E., Mosselman, E., Surian, N. (2005): *A review of techniques available for delimiting the erodible river corridor: A sustainable approach to managing bank erosion.* River Res. Appl., Vol. 21, pp. 773–789.

Plate, E. (2001): *Naturkatastrophen - Herausforderung an Wissenschaft und Gesellschaft.* In: E. Plate & B. Merz (Eds.): *Naturkatastrophen.* Schweizerbart, Stuttgart, pp. 1–45.

Plate, E., Merz, B. (Eds.) (2001): *Naturkatastrophen.* Schweizerbart, Stuttgart.

Pliefke, T., Sperbeck, S. T., Urban, M. (2006): *The probabilistic risk management chain - General concepts and definitions.* Internal discussion paper. International Graduate College 802. www.grk802.tu-braunschweig.de/Links/PliefkeSperbeckUrban2006_RMpaper_V3.pdf.

Pliefke, T., Sperbeck, S. T., Urban, M., Peil, U., Budelmann H. (2007): *A standardized method for managing disaster risk - An attempt to remove ambiguity.* 5th International Probabilistic Workshop, Ghent.

Prandtl, L., Oswatitsch, K., Wieghardt, K. (1969): *Führer durch die Strömungslehre,* 7th ed, Vieweg, Braunschweig.

Proske, D. (2004): *Katalog der Risiken - Risiken und ihre Darstellung.* Eigenverlag, Dresden.

Pruijssen, H. (1999): *Working Together with Nature in the River Regions*. Dienst Landeliyk Gebied, Arnheim, ISBN 90-802342-4-9.

Rausand, M. (2004): *System reliability theory - Preliminary hazard analysis,* 2nd ed., Wiley, Chichester.

Reed, S., Thorne, C. R., Doornkamp, J. C. (1994): *Bank erosion on navigable waterways.* R&D Project, No. 336, NRA - National River Authority, Bristol.

Regierungspräsidium Baden-Württemberg (2005): *EG-Wasserrahmenrichtlinie - Bericht zur Bestandsaufnahme, Bearbeitungsgebiet Oberrhein, Teil Baden-Württemberg.* Karlsruhe.

Regierungspräsidium Freiburg (2007): *Personal communication.*

Regierungspräsidium Freiburg (2008): *http://www.rp.baden-wuerttemberg.de/servlet/PB/menu/125415 /index.html.*

Regierungspräsidium Freiburg (2009): *Hochwasser-Rückhalteraum Weil-Breisach.* Brochure, Freiburg.

Rhee, D. S., Woo, H., Kwon, B. A., Ahn, H. K. (2008): *Hydraulic resistance of some selected vegetation in open channel flows.* River Res. Applic., Vol. 24, pp. 673–687.

Richards, K. S. (1982): *Rivers: Form and process in alluvial channels.* Methuen, London.

Rickert, K. (1986): *Der Einfluss von Gehölzen auf die Lichtverhältnisse und das Abflussverhalten in Fließgewässern.* Mitteil. d. Inst. f. Wasserwirtschaft, Hydrologie und Landwirtschaftlichen Wasserbau der Universität Hannover, No. 61, Hannover.

Rodi, W. (1984): *Turbulence models and their application in hydraulic,* 2nd ed., IAHR, Delft.

Rosgen, D. (1996): *Applied river morphology.* Wildland Hydrology Books, Pagosa Springs, Colorado.

Rosgen, D. (2001): *A stream channel stability assessment methodology.* Proceedings of the Seventh Federal Interagency Sedimentation Conference, No. 2, pp. 18–26, doi:http://www.wildlandhydrology.com.

Rother, K.-H. (2002): *Der Rhein – Europäische Wasserstraße mit Zukunft.* Symposium of 4th Sept. 2001, Bundesministerium für Verkehr, Bau- und Wohnungswesen, pp. 43–49, Koblenz, ISBN 3-9800835-8-6.

Rouse, H. (1938): *Fluid mechanics for Hydraulic Engineers*. McGraw Hill, New York.

Rouvé, G. (1987): *Hydraulische Probleme beim naturnahen Gewässerausbau.* VCH Verlagsgesellschaft, Weinheim.

RRC - the River Restoration Centre (2002): *Manual of techniques.* Arca Press Ltd., Cranfield, UK.

Rüther, N. (2006): *Computational fluid dynamics in fluvial sedimentation engineering.* Dissertation. Department of Hydraulic and Environmental Engineering, Norwegian University of Science and Technology, Trondheim.

Rutherfurd, I. D., Jerie, K., Marsh N. (2000): *A rehabilitation manual for australian streams - Vol. 1+2.* LWRRDC and CRCCH, Canberra, Clayton.

Salant, N. L., Renshaw, C. E., Magilligan, F. J. (2006): *Short and long-term changes to bed mobility and bed composition under altered sediment regimes.* Geomorphology, Vol. 76, No. 1-2, pp. 43–53, doi:10.1016/j.geomorph.2005.09.003.

Salvatori, L. (2008): *Assessment and mitigation of wind risk of suspended-span bridges.* Dissertation. Technische Universität Braunschweig, Braunschweig.

Schälchli, Abegg + Hunzinger, IWK - Institut für Wasserwirtschaft und Kulturtechnik (2000): *Geschiebehaushalt Hochrhein.* Zürich, Karlsruhe.

Scherle, J. (1999): *Entwicklung naturnaher Gewässerstrukturen - Grundlagen, Leitbilder, Planung.* Mitteil. d. Inst. f. Wasserwirtschaft und Kulturtechnik, No. 199, Technische Hochschule Karlsruhe, Karlsruhe.

Schindler, M. (2008): *Grundlagen morphodynamischer Phänomene in Fließgewässern - Ufertypen und Rehnen.* LWI Kolloqium, Leichtweiß-Institut für Wasserbau, Braunschweig.

Schlichting, H. (1979): *Boundary layer theory.* McGraw Hill, New York.

Schmautz, M. (2003): *Eigendynamische Aufweitung in einer geraden Gewässerstrecke - Entwicklung und Untersuchung an einem numerischen Modell.* Dissertation. Berichte des Lehrstuhls und der Versuchsanstalt f. Wasserbau und Wasserwirtschaft, No. 96, Münich.

Schnauder, I. (2004): *Strömungsstruktur und Impulsaustausch in gegliederten Gerinnen mit Vorlandvegetation*. Dissertation. Mitteil. d. Inst. f. Wasserwirtschaft und Kulturtechnik, No. 224, Technische Hochschule Karlsruhe, Karlsruhe.

Schöberl, F. (1979): *Zur Frage der Gefällsausbildung beim Selbststabilisierungsprozess von erodierenden Flussstrecken.* Dissertation, Institut f. Konstruktiven Wasser- und Tunnelbau, Universität Innsbruck, Innsbruck.

Schöberl, F. (1991): Prediction methods für grain size distribution and armour layer stability. Proc. Int. Grain Sorting Seminar, Ascona, Switzerland, Mittl. D. VAW Zürich, Zurich.

Schoneboom, T., Aberle, J., Wilson, C. A. M. E., Dittrich, A. (2008): *Drag force measurements of vegetation elements.* Proceedings of 8th Int. Conference on HydroScience and Engineering, Nagoya, Japan.

Schulte-Rentrop, A., Koll, K., Aberle, J., Dittrich, A. (2005): *Sediment budget of a heathland sand-bed river.* Acta Geophysica Polonica, Vol. 53, No. 4, pp. 553–565.

Schulte-Rentrop, A., Dittrich, A. (2007): *Abschätzung der morphodynamischen Auswirkungen von Hochwasserabflüssen am Beispiel des Oberrheins.* Wasserbaukolloqium 2007; Dresdener Wasserbaul. Mitt., No. 35, Dresden.

Schweizer, S., Borsuk, M. E., Reichert, P. (2007): *Predicting the morphological and hydraulic consequences of river rehabilitation.* River Res. Applic., Vol. 23, pp. 303–322, doi:10.1002/rra.981.

Sear, D. A., Newson, M. D., Thorne, C. R. (2003): *Guidebook of applied geomorphology.* R&D Technical Report, No. FD1914, DEFRA/Enviroment Agency, London. http://www.defra.gov.uk/science/project_data/DocumentLibrary/FD1914/FD1914_1147_TRP.pdf.

Shen, Y., Diplas, P. (2008): *Application of two- and three-dimensional computational fluid dynamics models to complex ecological stream flows.* J. Hydrol., Vol. 348, pp. 195–214, doi:10.1016/j.jhydrol.2007.09.060.

Shields, A. (1936): *Anwendung der Ähnlichkeitsmechanik und der Turbulenzforschung auf die Geschiebebewegung.* Mitteil. d. Preußisch. Versuchsanstalt f. Wasser-, Erd- und Schiffbau, No. 26, Berlin.

Shields, F. D., Copeland, R. R., Klingeman, P. C., Doyle, M. W., Simon, A. (2003): *Design for stream restoration.* J. Hydraul. Eng., Vol. 129, No. 8, pp. 575–584, doi:10.1061/(ASCE)0733-9429(2003)129:8(575).

Shiono, K., Knight, D. W. (1991): *Turbulent open-channel flows with variable depth across the channel*. J. Fluid Mech., Vol. 222, pp. 617–646.

Simons D. B., Albertson M. L. (1960): *Uniform water conveyance channels in alluvial material.* Proceedings ASCE J. Hydraul. Div., Vol. 86, No. HY5, pp. 33–71.

Singh, V. P. (2003): *On the theories of hydraulic geometry.* Int. J. Sed. Res., Vol. 18, No. 3, pp. 196–218.

Solari, L., Seminara, G. (2005): *On width variations in meandering rivers.* In: G. Parker & M. Garcia (Eds.): *River, coastal and estuarine morphodynamics: RCEM 2005.* Taylor & Francis Group, London.

Solari, L. (2005): *Hydraulic risk*. Lectures in the framework of the International Graduate College 802, Università di Firenze, Florence.

Specht, F. J. (2002): *Influence of channel width and bank vegetation on the flow resistance and the sediment transport of renaturated rivers (in German).* Dissertation. Mitteil. d. Leichtweiß-Instituts für Wasserbau der TU Braunschweig, No. 153, Braunschweig. http://www.digibib.tu-bs.de/?docid=00001336.

State Ministry of the Environment Baden-Württemberg (2007): *The Integrated Rhine Programme – Flood control and restoration of former floodplains along the Upper Rhine*. Stuttgart.

Steiger, J., Tabacchi, E., Dufour, S., Corenblit, D., Peiry, J. L. (2005): *Hydrogeomorphic processes affecting riparian habitat within alluvial channel-floodplain river systems - A review for the temperate zone.* River Res. Applic., No. 21, pp. 719–737, doi:10.1002/rra.879.

Stelczer, K. (1981): *Bed-load transport, theory and practice*. Water Resources Publications, UK. ISBN 0-918334-39.

Stoesser, T., Wilson, C. A. M. E., Bates, P. D., Dittrich, A. (2003): *Application of a 3D numerical model to a river with vegetated floodplains.* J. Hydroinformatics, Vol. 5, No. 2, pp. 99–112.

Stoesser, T., Dittrich, A. (2007): *Qualitätssicherung bei der Verwendung mehrdimensionaler Strömungsmodelle in der wasserbaulichen Praxis.* Wasserwirtschaft, No. 7-8, pp. 26–31.

Tang, X., Knight, D. W. (2008): *A general model of lateral depth-averaged velocity distributions for open channel flows.* Adv. Wat. Resour., Vol. 31, pp. 846–857, doi:10.1016/j.advwatres.2008.02.002.

Thomas, H., Nisbet, T. R. (2006): *An assessment of the impact of floodplain woodland on flood flows.* Wat. Environm. J., Vol. 21, pp. 114–126, doi:10.1111/j.1747-6593.2006.00056.x.

Thompson, A., Clayton J.: (2002): *The role of geomorphology in flood risk assessment*. Civil Engineering, Vol. 150, pp. 25–29.

Thorne, C. R. (1982): *Processes and mechanismen of river bank erosion.* In: R. D. Hey, J. C. Bathurst, C. R. Thorne (Eds.): *Gravel-bed rivers.* Wiley, Chichester, pp. 227–271.

Thorne, C. R. (1997): *Channel types and morphological classification.* In: C. R. Thorne, R. D. Hey, M. D. Newson (Eds.): *Applied fluvial geomorphology for river engineering and management.* Wiley, Chichester, pp. 175–222.

Thorne, C. R., Hey, R. D., Newson, M. D. (Eds.) (1997): *Applied fluvial geomorphology for river engineering and management.* Wiley, Chichester.

Thorne, C. R., Tovey, N. K. (1981): *Stability of composite river banks.* Earth Surf. Process. Landforms, Vol. 6, pp. 469–484.

Toda, Y., Ikeda, S., Kumagai, K., Asano, T. (2005): *Effects of flood flow on flood plain soil and riparian vegetation in a gravel river.* J. Hydraul. Eng., Vol. 131, No. 11, pp. 950–960.

Umweltbüro Essen (2004): *Entwicklung einer (Abschnitts-) Typologie für den natürlichen Rheinstrom - Endbericht.* Report, No. 146d, Essen.

University of Freiburg (2007): Auenvegetation. http://www.silviculture.uni-freiburg.de/Download/pdf/451a_auen_oek_ws07.pdf.

Urban, M. (2007): *Earthquake risk assessment of historical structures.* Dissertation. Institut für Stahlbau, Technische Universität Braunschweig, Braunschweig.

USACE - United States Army Corps of Engineers (2000): *Determination of resistance due to shrubs and woody vegetation.* ERDC/CHL, No. TR-00-25, Washington.

USACE - United States Army Corps of Engineers (2002): *HEC-GeoRAS 3.1 – An extension for support of HEC-RAS using ArcView.* Davis.

USACE - United States Army Corps of Engineers (2005): *HEC-RAS River Analysis System - User's Manual, Version 3.1.3.* Report, No. CPC-68, Davis.

Van den Bosch, L. (2003): *Influence of vegetation on flow and morphology in the river Allier, France.* M.Th. Technical University of Delft, Delft.

Van Rijn, L. C. (1984a): *Sediment pick-up functions.* J. Hydraul. Eng., Vol. 110, No. 10, pp. 1494–1502.

Van Rijn, L. C. (1984b): *Sediment transport Part II: Suspended load transport.* J. Hydraul. Eng., Vol. 110, No. 11, pp. 1613–1641.

VANR - Vermont Agency of Natural Resources (2008): *Municipality guide to fluvial erosion hazard mitigation.* http://www.anr.state.vt.us/dec//waterq/rivers/docs/rv_municipalguide.pdf.

Verhaar, P. M., Biron, P. M., Ferguson, R. I., Hoey, T. B. (2008): *A modified morphodynamic model for investigating the response of rivers to short-term climate change.* Geomorphology, Vol. 101, No. 4, pp. 674–682, doi:10.1016/j.geomorph.2008.03.010.

Vischer, D., Oplatka, M. (1998): *Der Strömungswiderstand eines flexiblen Ufer- und Vorlandbewuchs.* Wasserwirtschaft, Vol. 88, No. 6, pp. 284–288.

Wallick, J. R., Lancaster, S. T., Bolte, J. P. (2006): *Determination of bank erodibility for natural and anthropogenic bank materials using a model of lateral migration and observed erosion along the Willamette River, Oregon, USA*. River Res. Appl., Vol. 22, pp. 631–649.

Wang, Z., Dittrich, A. (1992): *A study on problems in suspended sediment transportation.* Proc. of 2nd Intern. Confer. on Hydraulic and Environmental Modelling of Coastal, Estuaring and River Waters, Vol. 2, pp. 467–478.

Wilcock, P. R., Barta, A. F., Shea, C. C., Kondolf, G. M., Matthews, W. V. G., Pitlick, J. (1996): *Observations of flow and sediment entrainment on a large gravel-bed river.* Wat. Res. Res., Vol. 32, No. 9, pp. 2897 – 2909.

Williams, G. P. (1978): *Bankfull discharge of rivers.* Wat. Res. Res., Vol. 14, No. 6, pp. 1141–1154.

Wilson, C. A. M. E., Schnauder, I., Mas, J., Hoyt, J. (2005): *Measuring the drag force of vegetation.* In: B. H. Jun, S. I. Lee, I. W. Seo, G. W. Choi (Eds.): *Water engineering for the future - Choices and challenges.* Seoul, pp. 2142–2151.

Wilson, C. A. M. E., Yagci, O., Rauch, H. P., Stoesser, T. (2006): *Application of the drag force approach to model the flow-interaction of natural vegetation.* Int. J. River Basin Manag., Vol. 4, No. 2, pp. 137–146.

Wolman, M. G. (1955): *The natural channel of Brandywine Creek Pennsylvania.* Geolog. Survey Prof. Paper, Vol. 271.

Wolman, M. G., Miller, J. G. (1960): *Magnitude and frequency of forces in geomorphic processes.* J. Geol., Vol. 68, pp. 54–74.

Wolters, H. A., Platteeuw, M., Schoor, M. M. (2001): *Guidelines for rehabilitation and management of floodplains - Ecology and safety combined.* RIZA report, NCR-Publications, the Netherlands.

Wu, W., Shields, F., Bennet, S., Wang, S. (2004): *A depth-averaged two dimensional model for flow, sediment transport in open channels with vegetation.* In: Bennett S. J. & A. Simon (Eds.): *Riparian vegetation and fluvial geomorphology.* American Geophysical Union, Washington, pp. 267–282.

Wu, W., Shields, F., Bennett, S. J., Wang, S. (2005): *A depth-averaged two dimensional model for flow, sediment transport, and bed topography in curved channels with riparian vegetation.* Wat. Resour. Res., Vol. 41, No. 3, doi:10.1029/2004WR003730.

Wynn, T. M., Mostaghimi, S. (2006): Effects of riparian vegetation on streambank subaerial processes in southwestern Virginia, USA. Earth Surf. Process. Landforms, Vol. 31, pp. 399–413.

Yalin, M. S. (1992): *River mechanics,* 1st ed, Pergamon Press, Oxford.

Yalin, M. S., Scheuerlein, H. (1988): *Friction factors in alluvial rivers.* Inst. f. Wasserbau und Wassermengenwirtschaft, Oskar von Müller-Inst., Obernach.

Yen, B. C. (2002): *Open channel flow resistance.* J. Hydraul. Eng., Vol. 128, No. 1, pp. 20–39.

Yoshida, H., Dittrich, A. (2002): *1D unsteady-state flow simulation of a section of the Upper Rhine.* J. Hydrol., Vol. 269, pp. 79–88.

Yu, D., Lane, S. N. (2006a): *Urban fluvial flood modelling using a two-dimensional diffusion-wave treatment - Part 1: Mesh resolution effects.* Hydrol. Proc., Vol. 20, pp. 1541–1565.

Yu, D., Lane S. N. (2006b): *Urban fluvial flood modelling using a two-dimensional diffusion-wave treatment - Part 2: development of a sub-grid-scale treatment.* Hydrol. Proc., Vol. 20, pp. 1567–1583.

Zanke, U. (1977): *Berechnung der Sinkgeschwindigkeiten von Sedimenten.* Mitt. d. Franzius-Instituts für Wasserbau der Technischen Universität Hannover, No. 46, p. 243.

Zanke, U. (1982): *Grundlagen der Sedimentbewegung.* Springer, Berlin.

Zarn, B. (1997): *Einfluß der Flussbettbreite auf die Wechselwirkung zwischen Abfluss, Morphologie und Geschiebetransportkapazität.* Dissertation. Mitteil. der Versuchsanstalt für Wasserbau, Hydrologie und Glaziologie, No. 154, Eidgen. Techn. Hochsch. Zürich, Zurich.

Zarn, B. (2008): *Grundlagen morphodynamischer Phänomene in Fließgewässern - Laufformen.* LWI Kolloquium, Leichtweiß-Institut für Wasserbau, Braunschweig.

Zinke, P., Olsen, N. R. B. (2007): *Modeling of sediment deposition in a partly vegetated open channel.* Proceedings of the 32nd IAHR Congress, Venice.

APPENDIX

A.1 SAMPLING LOCATIONS OF SEDIMENTS IN THE STUDY AREA

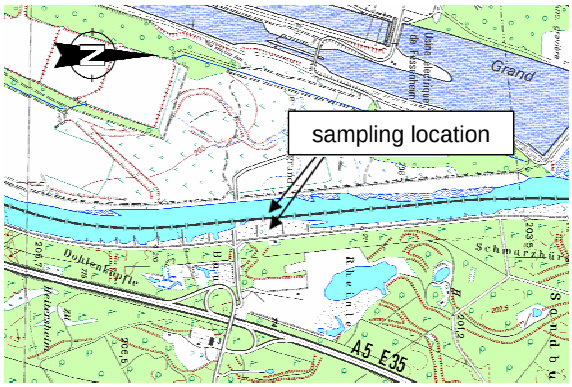

sampling location

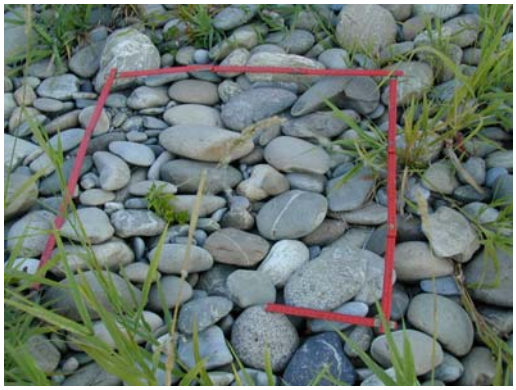

armour layer

lower layer

Figure A.1.1: Sampling location gravel bank Rhine-km 210.50 – armoured material (upper and lower layer).

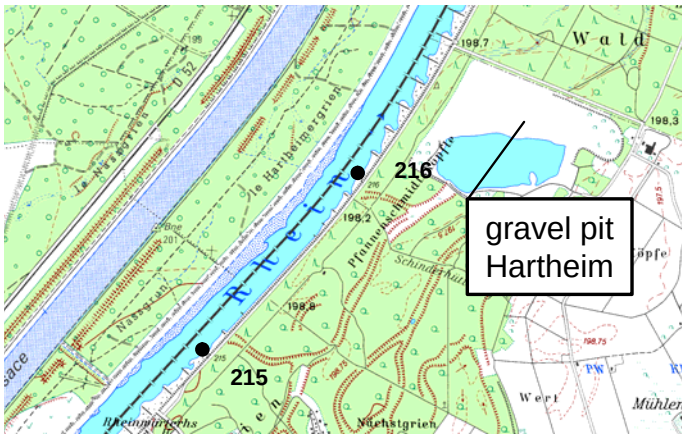

Figure A.1.2: Sampling location Hartheim – loose bed material.

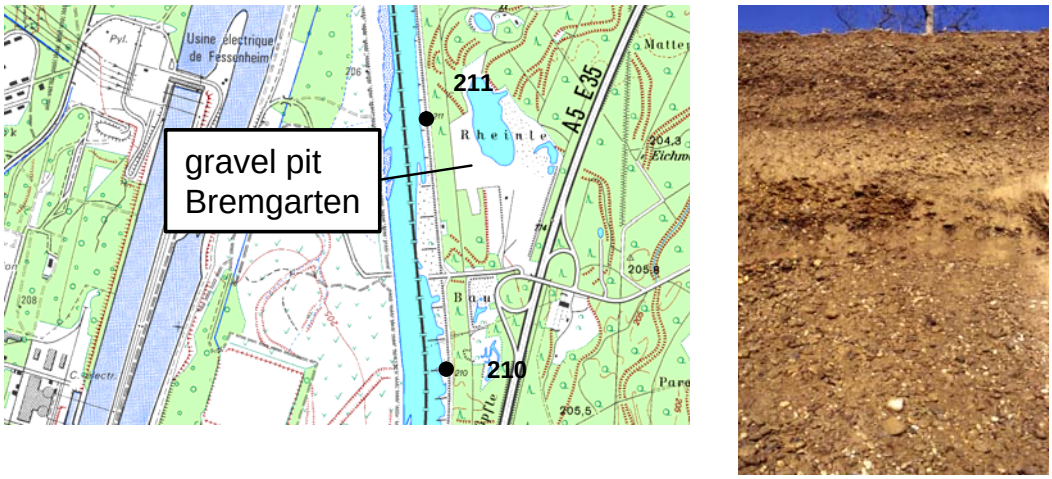

Figure A.1.3: Sampling location Bremgarten – loose bed material.

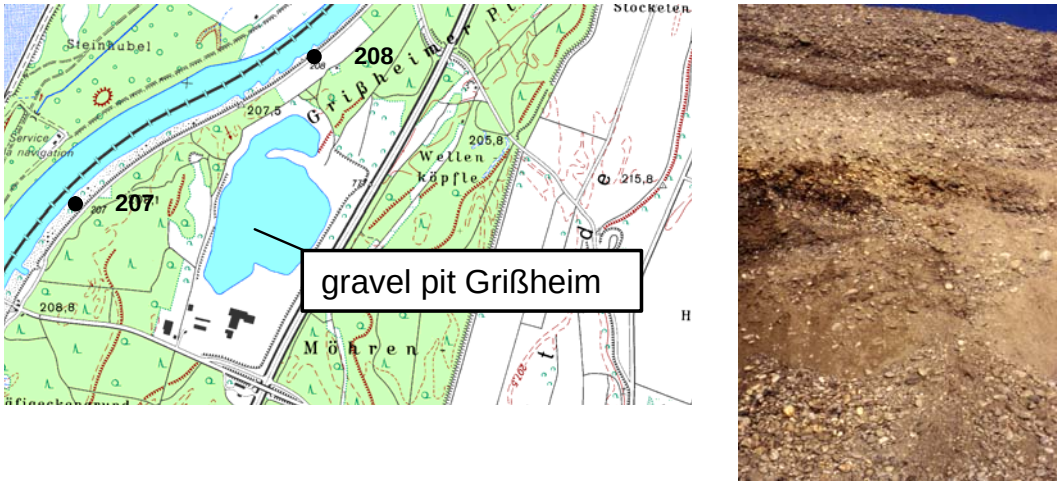

Figure A.1.4: Sampling location Grißheim – loose bed material

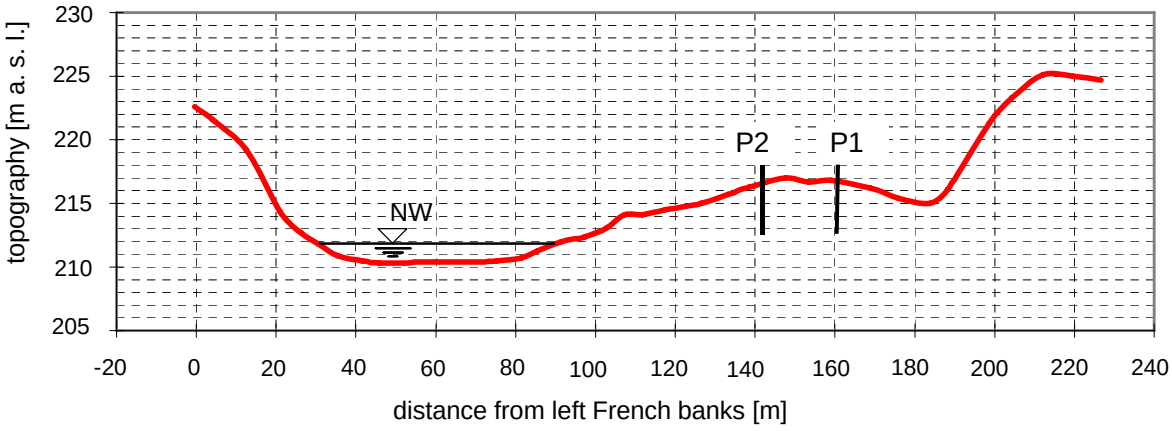

Figure A.1.5: Sampling location on the groyne field Hartheim, Rhine-km 191.300 NW = low water level (Hartmann et al. 1998).

A.2 AVAILABLE DATA ON TOPOGRAPHY AND HYDROMORPHOLOGY FOR THE STUDY AREA (ALL PLANS ARE ANALOGUE, EXCEPT FOR *)

a) Rhine "main channel" (states of 1993, 2000 and 2004)
- *)Digital elevation model of the year 2004 for Rhine-km 198+410 – 200+317 horizontal resolution 1m * 1m, Gauss-Krüger-coordinates lower left corner: 3391000 / 5298000, upper right corner: 3392000 / 5300000; derived from laser scanning data, provided by ILN, 2006
- Cross-sectional profiles from Rhine-km 198+410 – 200+970; irregular resolution, (tens up to hundreds of meters), Dittrich et al., 2005
  - of the year 1993: Rhine-kms 198+410, 198+590, 198+780, 198+970, 199+180, 199+420, 199+850 – 200+970
  - of the year 2000: Rhine-kms 199+125, 199+650
- 12 aerial photographs of the Rhine section Neuenburg from Rhine-km 198 – 200 taken on 18/08/2004, provided by ILN, 2006

b) Topography "Rhinegardens" (planning state)
- Site plan Rhinegardens „Städtebauliches Entwicklungskonzept 2025 Neuenburg am Rhein; Plandaten"; Fahle Stadtplaner, scale 1:2000, provided by ILN, 2006
- Site plan of "Lowering area 12 Neuenburg", provided by ILN, 2006
- Municipality plan "Rhinegardens", provided by ILN, 2006
- Municipality plan "Old harbour", provided by ILN, 2006
- Technical site plan of Rhinegardens including 3 cross-sectional profiles (Rhine-km 199+339.75, 199+414.75, 199+489.75), edited by Rapp Regioplan, provided by ILN, 2006
- *)Digital site plan Rhinegardens in ACAD dxf-format, georeferenced, provided by ILN, 2007
- Technical plans (cross-sections and groundplan) of "visitors platform" scale 1:200, edited by Rapp Regioplan, provided by ILN, 2007
- Movie "Freude am Fluss" and related design plans, www.freudeamflussmovie.org

c) Topography "lowering area" (planning state)
- Cross-sectional profiles of the lowering area 12 Neuenburg, Rhine-kms 199+650, 199+850, 200+030, 200+210, 200+450, scale 1:500, edited by Rapp Regioplan, July 2006, provided by ILN, 2007
- Cross-sectional profiles of the lowering area 12 Neuenburg, Rhine-kms 200+650, 200+750, 200+970, scale 1:500, edited by Rapp Regioplan, July 2006, provided by Regierungspräsidium Freiburg, 2007
- Site plan of the lowering area 12 Neuenburg, provided by ILN, 2006
- Technical plan of the lowering area 12 Neuenburg, scale, 1:2500, edited by Rapp Regioplan, July 2006, provided by Regierungspräsidium Freiburg, 2007

- Detailed design of lowering area 12, scale 1.100/1:50, edited by Rapp Regioplan, July 2006, provided by Regierungspräsidium Freiburg, 2007
- Design of bridge and passage above side channel on lowering area 12, scale 1.100/1:50, edited by Rapp Regioplan, July 2006, provided by Regierungspräsidium Freiburg, 2007
- Movie "Freude am Fluss" and related design plans, www.freudeamflussmovie.org

A.3 TOOLS USED IN THE PRESENT STUDY

Table A.3-1: Used tools in the stepwise data generation procedure and referring chapters in the present thesis; white – preliminary calculations for data base improvement, grey – originally intended calculations for Hazard Anaylsis.

step	case	site description	modelling approach	preprocessing tools	simulation tools	chapter
1	ACT1998	main channel without gravel island	1D	ArcView 3.2a HEC-GeoRAS 3.1	HEC-RAS 3.1.3	5.2.1.
2	ACT2000	main channel with gravel island	1D	not required	HEC-RAS 3.1.3	5.2.1.
3a	ACT2004 1D	main channel with gravel island with vegetation	1D	not required	HEC-RAS 3.1.3	5.2.1.
3b	ACT2004 3D	main channel with gravel island with vegetation	3D	ArcView 3.2a HEC-GeoRAS 3.1 AutoCAD Gridmeister SSIIM 1.0	SSIIM 2.0	5.2.2
4a	PLAN1D	main channel with gravel island with vegetation with Rhinegardens with lowering area	1D	ArcView 3.2a HEC-GeoRAS 3.1 ArcGIS 9.1 AutoCAD Schluess	HEC-RAS 3.1.3	6
4b	PLAN3D	main channel with gravel island with vegetation with Rhinegardens with lowering area	3D	ArcGIS 9.1 ArcView 3.2a HEC-GeoRAS 3.1 AutoCAD Gridmeister SSIIM 1.0	SSIIM 2.0	6

A.4 TABLE WITH ROUGHNESS COEFFICIENTS FOR DIFFERENT CHANNEL TYPES

Table A.4-1: Manning values for various channel types (USACE, 2005).

Type of Channel and Description	Minimum	Normal	Maximum
A. *Natural Streams*			
1. Main Channels			
a. Clean, straight, full, no rifts or deep pools	0.025	0.030	0.033
b. Same as above, but more stones and weeds	0.030	0.035	0.040
c. Clean, winding, some pools and shoals	0.033	0.040	0.045
d. Same as above, but some weeds and stones	0.035	0.045	0.050
e. Same as above, lower stages, more ineffective slopes and sections	0.040	0.048	0.055
f. Same as "d" but more stones	0.045	0.050	0.060
g. Sluggish reaches, weedy. deep pools	0.050	0.070	0.080
h. Very weedy reaches, deep pools, or floodways with heavy stands of timber and brush	0.070	0.100	0.150
2. Flood Plains			
a. Pasture no brush			
1. Short grass	0.025	0.030	0.035
2. High grass	0.030	0.035	0.050
b. Cultivated areas			
1. No crop	0.020	0.030	0.040
2. Mature row crops	0.025	0.035	0.045
3. Mature field crops	0.030	0.040	0.050
c. Brush			
1. Scattered brush, heavy weeds	0.035	0.050	0.070
2. Light brush and trees, in winter	0.035	0.050	0.060
3. Light brush and trees, in summer	0.040	0.060	0.080
4. Medium to dense brush, in winter	0.045	0.070	0.110
5. Medium to dense brush, in summer	0.070	0.100	0.160
d. Trees			
1. Cleared land with tree stumps, no sprouts	0.030	0.040	0.050
2. Same as above, but heavy sprouts	0.050	0.060	0.080
3. Heavy stand of timber, few down trees, little undergrowth, flow below branches	0.080	0.100	0.120
4. Same as above, but with flow into branches	0.100	0.120	0.160
5. Dense willows, summer, straight	0.110	0.150	0.200
3. Mountain Streams, no vegetation in channel, banks usually steep, with trees and brush on banks submerged			
a. Bottom: gravels, cobbles, and few boulders	0.030	0.040	0.050
b. Bottom: cobbles with large boulders	0.040	0.050	0.070

A.5 PREPARATORY 1D WATER LEVEL CALCULATIONS

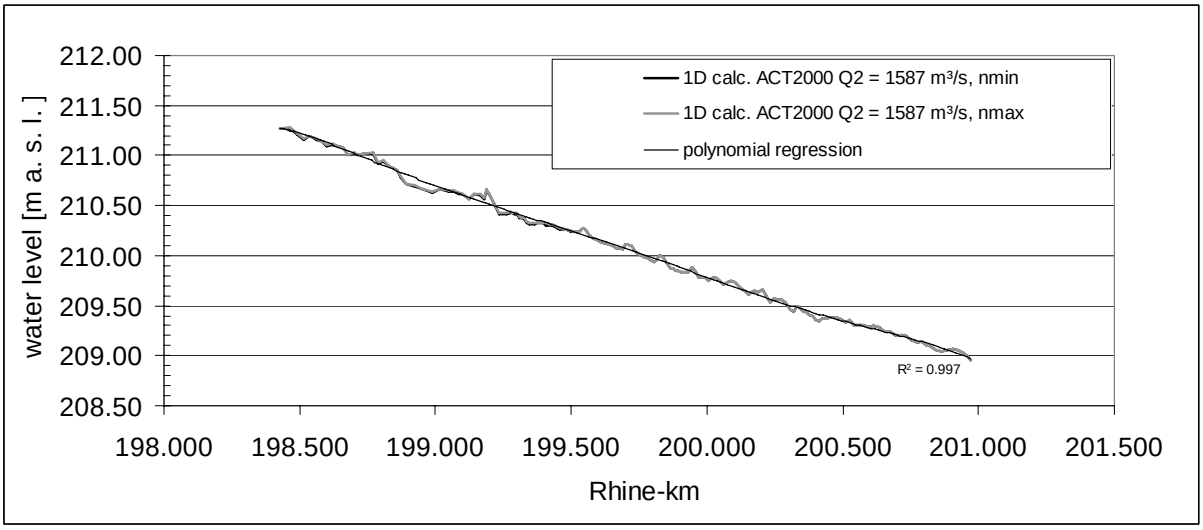

Figure A.5.1: 1D water level calculations for Q2 = 1587 m³/s, ACT2000.

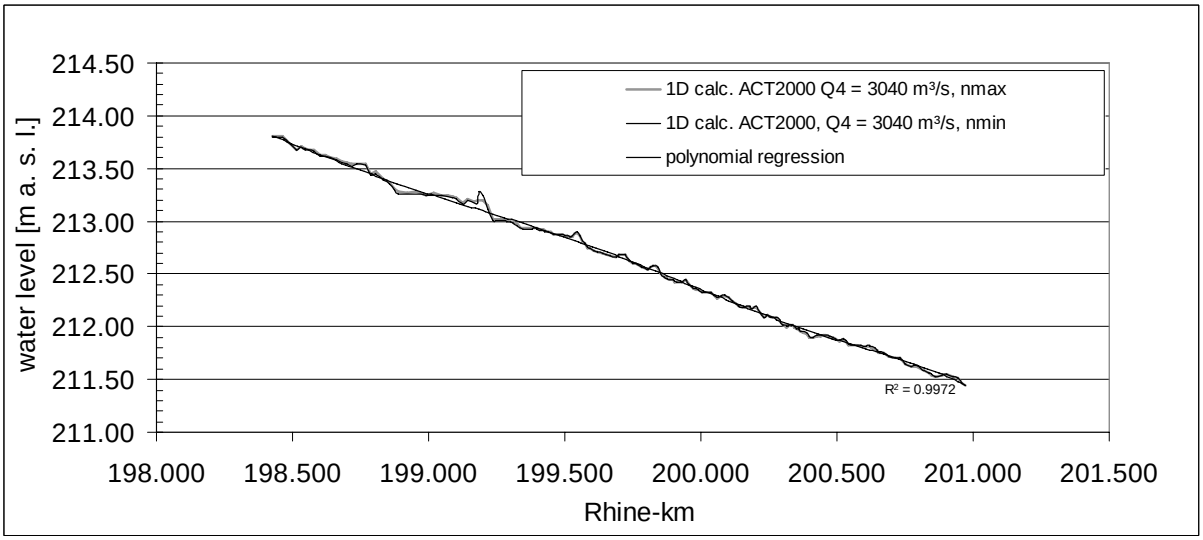

Figure A.5.2: 1D water level calculations for Q4= 3040 m³/s, ACT2000.

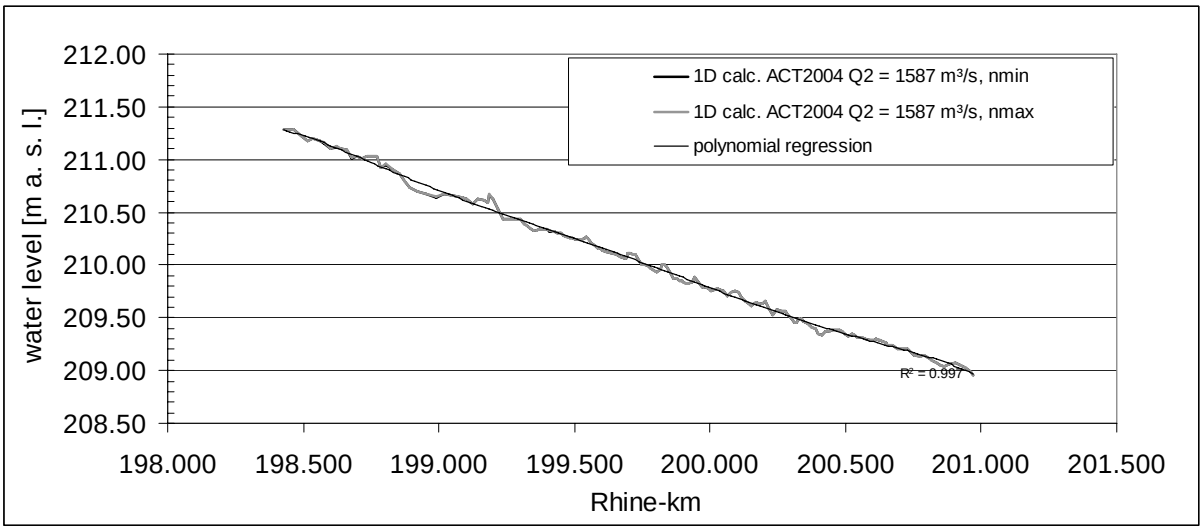

Figure A.5.3: 1D water level calculations for Q2 = 1587 m³/s, ACT2004.

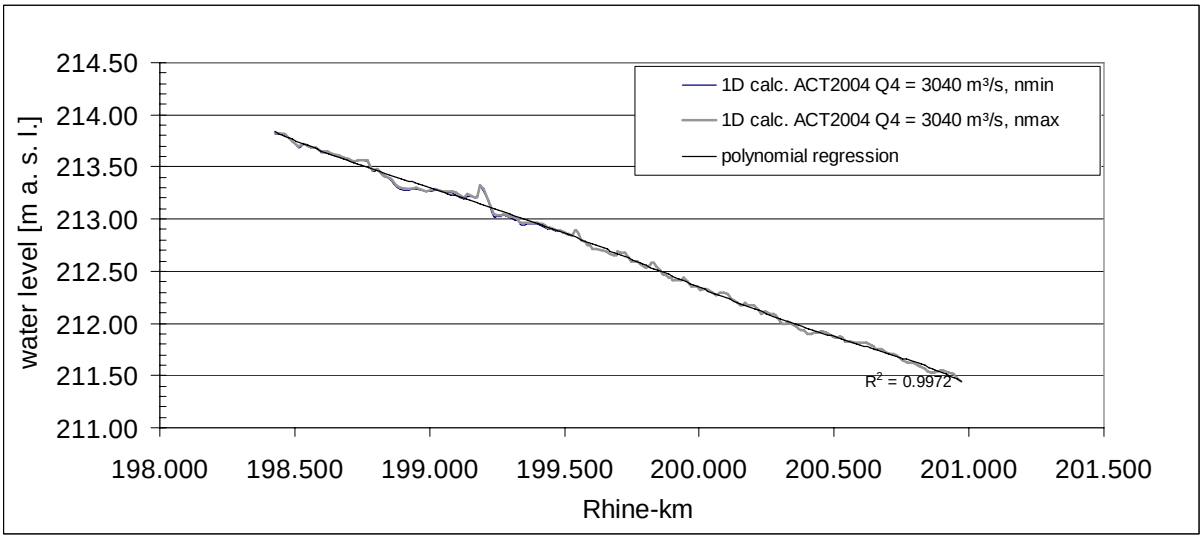

Figure A.5.4: 1D water level calculations for Q4 = 3040 m³/s, ACT2004.

A.6 TEST RESULTS OBTAINED WITH THE 2D MODEL AND THE 2D-3D APPROACH

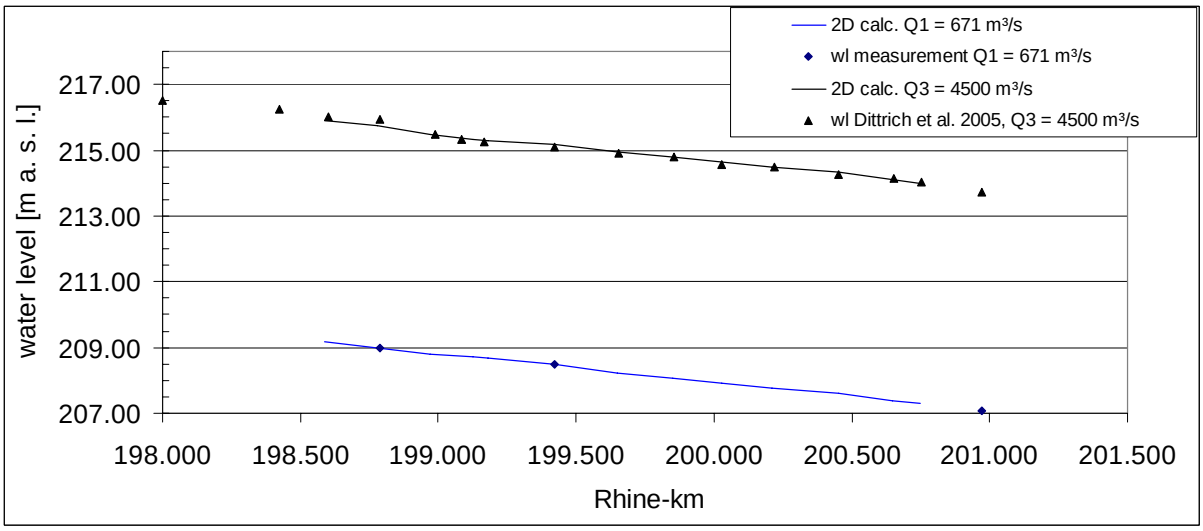

Figure A.6.1: Calibrated water levels for the 2D model und water level measurements for Q1 = 671 m³/s and Q3 = 4500 m³/s.

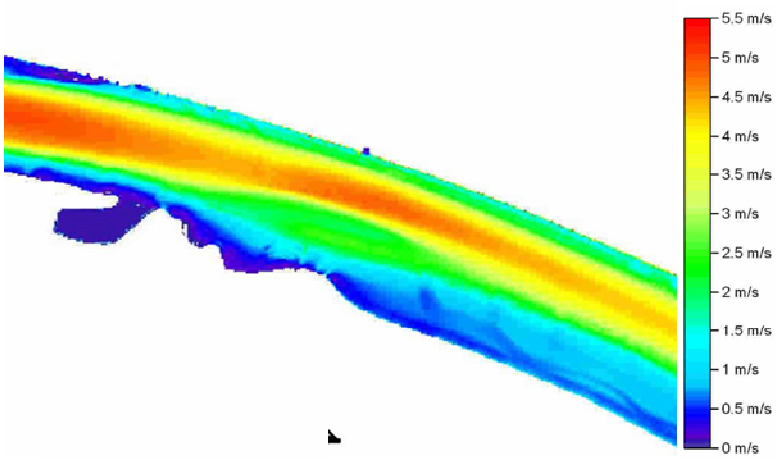

Figure A.6.2: Depth-averaged flow velocities for Q3 = 4500 m³/s for Rhine-km 199.8 – 200.000 computed with the 2D model (planning state).

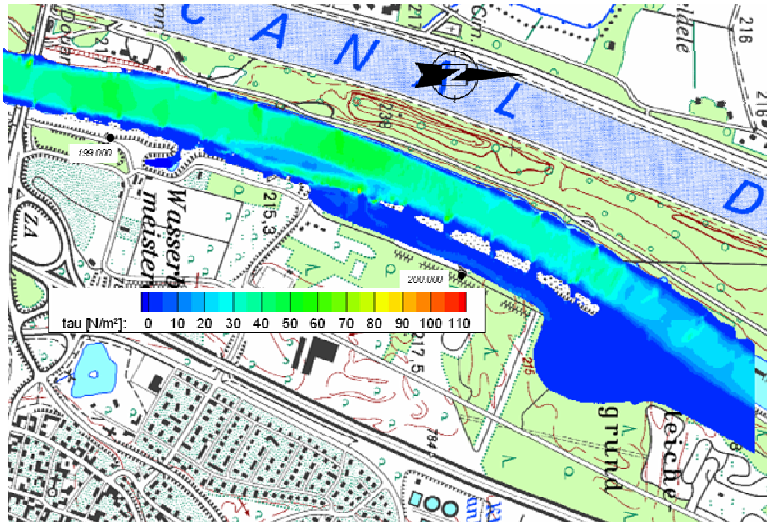

Figure A.6.3: Bed shear stresses for Q1 = 671 m³/s computed with the 3D model and with 2D water levels as boundary conditions (planning state).